

Analyses of miRNA let-7 and its targets in canine neoplasias as model for human counterparts

Von der Naturwissenschaftlichen Fakultät der
Gottfried Wilhelm Leibniz Universität Hannover

zur Erlangung des Grades
Doktor der Naturwissenschaften
Dr. rer. nat.

genehmigte Dissertation
von

Dipl. -Biol. Siegfried Wagner
geboren am 24.03.1981 in Omsk/Russland

2015

Referent: Prof. Dr. Anaclet Ngezahayo

Korreferent: Dr. rer. nat. habil. Hugo Murua Escobar

Tag der Promotion: 17.12.2014

Contents

Abbreviations.....5

Zusammenfassung.....8

Abstract..... 10

1. Introduction 12

 1.1. Cancer..... 12

 1.1.1. Prostate cancer..... 13

 1.1.2. Lymphoma..... 14

 1.1.3. miRNA biogenesis and function..... 15

 1.1.4. miRNA *let-7* and associated genes..... 17

 1.2. Model organism dog..... 19

2. Aims of the thesis.....21

 2.1.1. Expression analyses.....21

 2.1.2. Structural and functional *HMGA* analyses21

 2.1.3. Tools for modification and detection of gene expression21

3. Selected list of publications22

 3.1. Published manuscripts22

 3.2. Manuscripts in preparation for submission23

4. Results 24

 4.1. Gene expression analyses 24

 4.1.1. Prostate cancer.....24

 4.1.2. Lymphoma.....68

 4.1.3. Comparison of non-coding RNAs in human and canine cancer.....80

 4.2. Structural and functional *HMGA* analyses91

 4.2.1. HMGA protein impact analyses on stem cells..... 116

 4.3. Tools for modification and detection of gene expression..... 129

 4.3.1. Generation of miRNA *let-7* constructs 129

4.3.2. AAV genome isolation for quantification by absolute real-time PCR...	131
4.3.3. AuNP based laser-transfection	148
4.3.4. Verification of a canine PSMA (FolH1) antibody	165
5. Discussion.....	169
5.1. Gene expression analyses	169
5.1.1. Prostate cancer.....	169
5.1.2. Lymphoma.....	171
5.1.3. Comparison of non-coding RNAs in human and canine cancer.....	172
5.2. Structural and functional <i>HMGA</i> analyses	173
5.3. Tools for modification and detection of gene expression.....	178
5.3.1. Generation of miRNA let-7 constructs	179
5.3.2. rAAV genome isolation for quantification by absolute real-time PCR .	179
5.3.3. AuNP based laser-transfection	180
5.3.4. Verification of a canine PSMA (FolH1) antibody	180
6. Outlook.....	182
7. References.....	183
8. Publications.....	195
8.1. All Published manuscripts in reverse chronological order	195
8.2. Manuscripts in preparation for submission	196
8.3. Oral presentations	197
8.4. Poster presentations	197
9. Schulischer / Wissenschaftlicher Werdegang	198
10. Erklärung zur Dissertation.....	199
11. Danksagung.....	200

Abbreviations

%	Percent
≈	Approximately
°C	Degree Celsius
μg	Microgram
μl	Microlitre
aa	Amino acid
AAV	Adeno-associated virus
ACTB	β-Actin
ADMSC	Adipose-tissue derived mesenchymal stem cells
AP	Alkaline phosphatase
AR	Androgen receptor
AuNP	Gold nano particle
BMSC	Bone marrow mesenchymal stem cells
bp	Base pairs
CCND2	Cyclin D2
CDH1	E-cadherin
CDS	Coding sequence
c-Myc	Myc
CSC	Cancer stem cells
C _T	Cycle threshold
DNA	Deoxyribonucleic acid
DNase	Deoxyribonucelase
EGFP	Eukaryotic green fluorescent protein
EMT	Epithelial-to-mesenchymal transition
FCS	Fetal calf serum
Fig.	Figure
FolH1	Folate hydrolase 1
g	G-force
h	Hour
HIPK2	Homeodomain-interacting protein kinase 2
HMGA	High mobility group A
HMGA1	High mobility group AT-Hook 1

Abbreviations

HMGA2	High mobility group AT-Hook 2
HMGB1	High mobility group Box 1
HPRT1	Hypoxanthine guanine phosphoribosyltransferase 1
HRAS	V-HA-RAS Harvey rat sarcoma viral oncogene homolog
IARC	International Agency for Research on Cancer
IL6	Interleukin 6
kDa	Kilo Dalton
Klf4	Kruppel-like factor factor 4
KRAS	V-KI-RAS2 Kirsten rat sarcoma viral oncogene homolog
let-7	Lethal-7
MAPK	Mitogen-activated protein kinase
min	Minute
miRNA	Micro RNA
mRNA	Messenger RNA
MSC	Mesenchymal stem cells
NFκB	Nuclear factor kappa-B
ng	Nanogram
NHL	Non-Hodgkin lymphoma
NRAS	Neuroblastoma ras viral oncogene homolog
nt	Nucleotide
p53	Tumor protein p53
PC	Prostate cancer
PCR	Polymerase chain reaction
PI3KCA	Phosphatidylinositol 3-kinase, catalytic, alpha
PIN	Prostatic intraepithelial neoplasias
PSA	Kallikrein-related peptidase 3
PSMA	Prostate specific membrane antigen
PTEN	Phosphatase and tensin homolog
PTGS	Post-transcriptional gene silencing
qRT-PCR	Quantitative real-time PCR
rAAV	Recombinant adeno-associated virus
RAGE	Advanced glycosylation end product-specific receptor
RISC	RNA induced silencing complex

Abbreviations

rpm	Revolutions per minute
SDS-PAG	Sodium dodecyl sulfate polyacrylamide gel
SDS-PAGE	Sodium dodecyl sulfate polyacrylamide gel electrophoresis
siRNA	Short interfering RNA
SNAI1	Snail
SNAI2	Slug
Tab.	Table
TLR	Toll-like receptor
T _M	Annealing temperature
UN	United nations
US	United States
UTR	Untranslated region
VG	Viral genome
WB	Western Blot
WHO	World Health Organisation

Zusammenfassung

Die Entwicklung von neuen Diagnose- und Therapieverfahren gegen Tumorerkrankungen hängt in hohem Maße von einem detaillierten Verständnis der molekularbiologischen Veränderungen, die zur Entstehung und zum Fortschreiten von malignen Tumoren beitragen, ab. In diesem Zusammenhang hat sich der Hund als geeignetes Großtiermodell für verschiedene Erkrankungen des Menschen etabliert, da zahlreiche Tumoren, die beim Menschen eine Rolle spielen, auch beim Hund spontan auftreten.

In der vorliegenden Arbeit wurden Expressionsanalysen von mehreren in humanen Neoplasien deregulierten Genen am Modell Hund untersucht. Hierbei stand einerseits die miRNA *let-7*, aber auch die *let-7* regulierten Gene *HMGA1* und *HMGA2* im Fokus. Zusätzlich wurde die Expression von weiteren direkt von *let-7* regulierten und assoziierten Genen analysiert.

Die *let-7* Genfamilie gehört zu den miRNAs die während der embryonalen Entwicklung und in Stammzellen kaum exprimiert werden. Erst mit der fortschreitenden Entwicklung des Organismus nimmt die *let-7* Expression stetig zu und erreicht ein relativ hohes Niveau in ausdifferenzierten Zellen. Eine Abnahme der *let-7* Expression hat zur Folge, dass die von *let-7* negativ regulierten Gene zunehmend exprimiert werden, wie es in zahlreichen malignen Neoplasien beobachtet wurde.

Hierzu wurde die Expression von *let-7a* und der *let-7* assoziierten Gene *CCND2*, *c-Myc*, *FoI1*, *HMGA1*, *HMGA2*, *HMGB1*, *IL6*, *Klf4*, *MAPK1*, *NRAS*, *PTEN*, und *PI3K* in caninen Prostataprobe untersucht. Dabei zeigte sich sowohl die *let-7a* als auch die *HMGA2*-Transkriptzahl in hyperplastischem und malignem Prostatagewebe sowie in mehreren untersuchten prostatistischen Zelllinien signifikant erhöht. Zusätzlich war die Expression der *HMGB1*- und *MAPK1*-Gene deutlich niedriger in malignen neoplastischen Geweben verglichen mit gesundem Prostatagewebe.

Außerdem wurde die *HMGA1*- und *HMGA2*-Genexpression in caninen Lymphomen analysiert. Dabei war die *HMGA1*-Transkriptzahl in B-Zell-, aber nicht in T-Zell-Lymphomen des Hundes erhöht. Die *HMGA2*-Expression wies ein zu *HMGA1* reziprokes Profil auf, sie war in den T-Zell-Lymphomen erhöht und in den B-Zell-Lymphomen sehr niedrig.

Weiterhin wurden strukturelle und funktionelle Untersuchungen an den *HMGA*-Genen und deren Produkten durchgeführt, welche eine große Ähnlichkeit zu den humanen Molekülen in Genstruktur und Proteinfunktion offenbarten.

Da der nächste Schritt nach der Identifizierung und Charakterisierung von potentiellen Tumormarkern die gezielte Modifikation der jeweiligen Geneexpression ist, wurden mehrere *let-7* kodierende Plasmide konstruiert, die auch zur Produktion von adeno-assoziierten Viren geeignet sind.

Zusätzlich wurde ein neues Protokoll zur Isolierung von Genomen adeno-assoziiierter Viren etabliert, welches die nachfolgende reproduzierbare und genaue Quantifizierung der Virengenome ermöglicht.

Für *in vitro* Anwendungen wurde eine neue, Gold-Nanopartikel-basierte Methode zur effizienten und zellschonenden Transfektion von unterschiedlichen Zelltypen entwickelt.

Schließlich wurde die Kreuzreaktivität eines PSMA Antikörpers mit dem caninen PSMA Protein evaluiert, welcher vergleichende Proteinanalysen zwischen Mensch und Hund ermöglicht.

Schlagerworte: Vergleichende Onkologie, Expressionsanalysen, molekulare Marker

Abstract

The development of diagnostic and therapeutic modalities depends highly on the understanding of the genetic and epigenetic alterations which favor cancer. In this regard the domesticated dog qualifies as a potent large animal model for many human cancer entities, as these occur spontaneously in man and dog.

In the present thesis expression analyses of tumor associated genes were carried out paying particular attention to the miRNA *let-7* family and its direct target genes *HMGA1* and *HMGA2*. Furthermore, additional directly by *let-7* regulated targets as well as associated genes were analyzed.

The miRNA *let-7* gene family is barely expressed during embryogenesis but increases constantly during organismal development. Interestingly, several members of the miRNA *let-7* family were found to be down regulated in various cancer entities.

Owing to that the expression of *let-7a* and of the *let-7* associated genes *CCND2*, *c-Myc*, *FoIH1*, *HMGA1*, *HMGA2*, *HMGB1*, *IL6*, *Kif4*, *MAPK1*, *NRAS*, *PTEN*, and *PI3K*, which have also been described to be deregulated in a variety of human neoplasias, was analyzed in canine prostate cancer. The analyses revealed elevated *let-7a* and *HMGA2* levels in canine hyperplastic and malignant prostatic tissues as well as in three analyzed prostate cancer cell lines. Additionally a significant *HMGB1* and *MAPK1* down-regulation was found in the cancerous prostatic tissues.

Furthermore, *HMGA1* and *HMGA2* expression was investigated in canine healthy and diseased lymph node samples, presenting elevated *HMGA1* levels in B-cell lymphomas and increased *HMGA2* levels in T-cell lymphomas.

The knowledge of the target expression, structure and function is important for the successful engagement of *let-7* based therapeutics. Owing to that structural and functional analyses of the canine *HMGA* genes were carried out, revealing a similar *HMGA1* gene structure. The analyses of the HMGA protein activity and impact on gene expression and cell growth showed as well high similarities between human and canine protein homologs.

As the next step after successful identification and characterization of potential molecular tumor markers is the modification of gene expression, various *let-7* encoding expression plasmids were constructed. Some of these plasmids are as

well suitable for the production of adeno-associated viruses for therapeutic approaches.

For *in vivo* cell modifications viruses are still the most potent vehicles, but depend highly on pure and exactly titered vectors. Thus a novel viral genome isolation protocol was evaluated allowing a more accurate and highly reproducible viral genome quantification by subsequent real-time PCR.

Additionally a new nanoparticle mediated laser transfection method was established enabling efficient, up-scalable modification of different cell types *in vitro*.

Finally, cross-reactivity of a human PSMA (FolH1) specific antibody was evaluated for the canine homolog enabling ongoing comparative cancer research between man and dog.

Keywords: Comparative oncology, gene expression analyses, molecular marker

1. Introduction

1.1. Cancer

Cancer is a major global health burden of mankind, worldwide it is one of the leading causes of death especially in economically developed countries (Ferlay *et al.*, 2010). In December 2013, the specialized cancer agency of the World Health Organization (WHO), the International Agency for Research on Cancer (IARC) published the latest data set on cancer incidence and mortality (<http://www.uicc.org>) (Fig. 1), according to which the IARC estimates a rising of the global burden of cancer to 14.1 million new cases and 8.2 million cancer deaths in 2012 (<http://globocan.iarc.fr>). These data indicate that lung, breast, colorectal and prostate cancers are among the most frequent malignant neoplasias worldwide followed by cancers of the stomach, liver, cervix uteri, bladder and many others (Fig. 1).

Compared to the IARC estimates for the year 2008 the number of cancer related deaths and diagnosed cases increased by $\approx 8\%$ and $\approx 11\%$ respectively (GLOBOCAN 2008 - GLOBOCAN 2012, IARC). In contrast, according to the UN World Population Prospects, the world population grew only by approximately 5% in this period (<http://esa.un.org>). The non-proportionally increasing numbers of new cancer cases and deaths compared to the world population highlight the need for better molecular diagnostic, prognostic and therapeutic approaches.

However, the detection of molecular cancer biomarkers and the development of more effective drugs are still hampered by the limited knowledge of the genetic and epigenetic factors implicated in cancer etiology and additionally by the great diversity of tumors.

Studies on model organisms greatly contribute to the deciphering of these factors and to the development of novel treatment modalities. However, the translation from bench-to-bedside is often hindered by the lack of appropriate *in vivo* animal models (Mitsiades *et al.*, 2003).

In this thesis analyses of the micro RNA (miRNA) *let-7* and several associated genes, which are commonly deregulated in human cancers, were performed. To achieve this goal the expression of these genes was analyzed exemplarily in two canine cancer entities: the prostate cancer and Non-Hodgkin lymphoma.

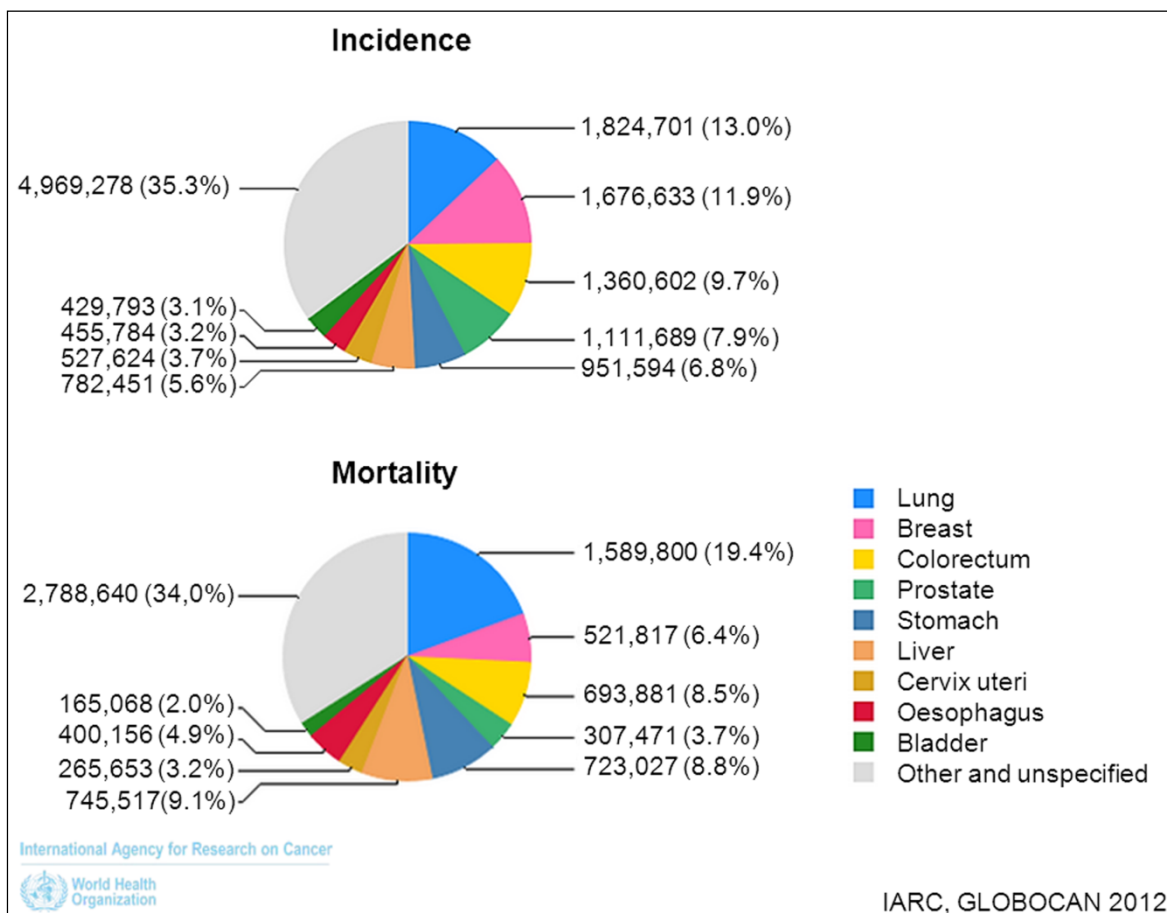


Figure 1 Estimated incidence and mortality rates in both sexes for the most common human cancer entities in 2012 (derived from <http://www.cancer.org>).

1.1.1. Prostate cancer

Prostate cancer (PC) is the 2nd most common cancerous disease in men (GLOBOCAN 2012, IARC), ranging from an asymptomatic to a rapid, fatal systemic malignancy (Kopper and Timar, 2005). In the year 2012 worldwide more than a million men were estimated to be diagnosed with this disorder and 307,471 died from it (GLOBOCAN 2012, IARC) (Fig. 1).

The development of PC is believed to be a multi-step process initiated by genetic and epigenetic alterations (Kopper and Timar, 2005). At early stage human PC is accepted to be an androgen dependent tumor (Kopper and Timar, 2005). Survival rates of advanced human PCs are very low (<http://www.cancer.org>) as these, treated according to the androgen deprivation therapy, become in the majority of patients resistant to castration (Divrik *et al.*, 2012).

Beside man, the dog is the only domesticated large mammal developing PC

spontaneously (Withrow and Vail, 2012). Remarkably, this disorder occurs more often in older individuals of both species (Waters *et al.*, 1996), shares many functional and morphological features (Leroy and Northrup, 2009) and shows similar clinical manifestations of advanced disease by spreading to lymph nodes, lungs, bones and liver (Leav and Ling, 1968; Cornell *et al.*, 2000). Like humans, dogs develop benign prostatic hyperplasia (Coffey and Walsh, 1990) and high-grade prostatic intraepithelial neoplasias (PIN). Notably, PINs are speculated to be a likely precursor of human PC (Waters *et al.*, 1997).

Opposing the situation in men, canine PC presents a natural incidence rate of less than 1 % (Withrow and Vail, 2012) but appears androgen-independent similarly to the human hormone refractory disease (Teske *et al.*, 2002; Kopper and Timar, 2005). As dogs are usually presented with clinically advanced disease, the treatment remains palliative (Waters *et al.*, 1998; Leroy and Northrup, 2009). Thus the understanding of the molecular changes contributing to canine PC and identification of molecular markers might not only improve treatment options for the canine patients, but also accelerate the establishment of preclinical approaches in human medicine using the dog as model.

1.1.2. Lymphoma

The second cancer entity investigated in this study are Non-Hodgkin lymphomas (NHL). NHL is a non-specific term that encompasses a wide variety of lymphoproliferative malignant diseases with varying clinical and histological appearances as well as incidence patterns (Evans and Hancock, 2003; Jemal *et al.*, 2011).

For the year 2012 it was estimated that 385,741 new NHL cases occurred worldwide and 199,630 people died from it (GLOBOCAN 2012, IARC).

Accounting for \approx 40% of all NHLs, B-cell lymphomas are most common in western countries (Alexander *et al.*, 2007). Similar to other types of cancer environmental factors, life style and genetic predisposition are discussed to promote NHL development (Boffetta, 2011).

As NHL etiology remains obscure and humans and canines present similar disease progression and response to chemotherapy-based regimen, the dog is a very important large animal model (Rowell *et al.*, 2011).

Canine lymphomas are estimated to occur in 13 to 24 cases per 100,000 dogs each year with rising up to 84 cases annually per 100,000 in the group of 10 to 11 years old animals (Withrow and Vail, 2012). According to a previous study, approximately 60 % of the canine lymphomas are B-cell lymphomas and one third is represented by T-cell lymphomas (Ponce *et al.*, 2010).

The value of the canine model depends on the possibility to discriminate between these spontaneously occurring lymphoma subgroups (Ponce *et al.*, 2010) thus identification of molecular markers is of great interest not only for veterinarians but also for research on comparative oncology.

1.1.3. miRNA biogenesis and function

Micro RNAs (miRNA) are small non-protein-coding endogenously expressed RNA molecules. The primary miRNA (pri-miRNA) transcripts form, owing to an intrinsic self-complementarity, a hairpin structure consisting of a “loop-” and a “stem”-region. The nuclear enzyme Drosha cuts the pri-miRNA precursor, which can be up to several kilo bases in length, between the flanking sequences and the “stem” (Fig. 2). The nascent precursor, the precursor-miRNA (pre-miRNA, approximately 70 nt in length) is exported by Exportin-5 into the cytoplasm where it is further processed by Dicer into the mature double-stranded miRNA (approximately 20 bp in length). The “guide strand” of the mature miRNA is loaded into the RNA induced silencing complex (RISC) which recognizes the 5’-, the 3’-untranslated region (UTR) or in some cases exon regions of the target mRNA leading to translational repression (Mondol and Pasquinelli, 2012). The second strand, the “passenger strand” is usually degraded (Filipowicz *et al.*, 2008) (Fig. 2).

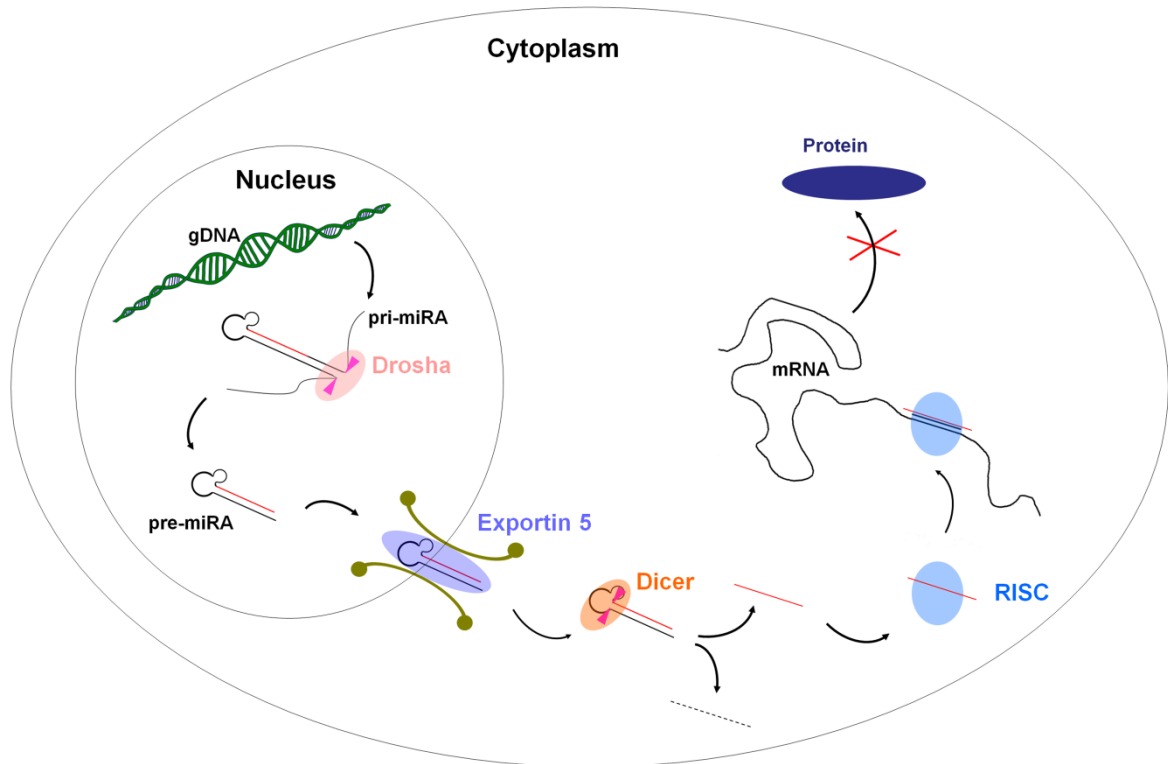


Figure 2 Schematic overview of the miRNA biogenesis and mode of action (Wagner *et al.*, 2014). The endogenous miRNA precursors form a hairpin structure due to the intrinsic self-complementarity. The nuclear enzyme Drosha cuts the hairpin between the “stem” and the flanking regions, the released precursor miRNA is transported by Exportin-5 into the cytoplasm. After export the precursor is further processed by Dicer into the mature double stranded miRNA consisting of a “guide” and “passenger” strand. In the following the “guide” strand is incorporated into RISC, the passenger strand is usually degraded. RISC recognizes with the incorporated miRNA strand the target mRNA and blocks its translation into the protein.

miRNAs regulate diverse biological processes such as development (Zhao *et al.*, 2005), differentiation (Kawasaki and Taira, 2003), proliferation (Viticchie *et al.*, 2011), apoptosis (Cimmino *et al.*, 2005), and stress response (Croce and Calin, 2005). It is remarkable that a single miRNA can orchestrate the expression of several genes as well as a single gene can be regulated by a set of different miRNAs (Reinhart *et al.*, 2000; Winter *et al.*, 2009; Chen *et al.*, 2011).

In the last decades numerous miRNA encoding genes were described, many of these were reported to be implicated in cardiovascular diseases (Filipowicz *et al.*, 2008; Creemers *et al.*, 2010), muscular disorders (Cacchiarelli *et al.*, 2010; Mizuno *et al.*, 2011), diabetes (Kantharidis *et al.*, 2011), renal fibrosis (Li *et al.*, 2013) and various cancer entities such as melanoma (Noguchi *et al.*, 2013), mammary cancer

(Boggs *et al.*, 2008), lymphoma (Di Lisio *et al.*, 2012) and prostate cancer (Kong *et al.*, 2012; Ru *et al.*, 2012).

1.1.4. miRNA *let-7* and associated genes

One of the large class of miRNAs is *let-7*, which was the second miRNA discovered and designated as *lethal-7* (*let-7*) according to the phenotype of a *let-7* deficient *C. elegans* mutant (Reinhart *et al.*, 2000). Soon thereafter, in a variety of species further *let-7* homologs were identified (Pasquinelli *et al.*, 2000).

Compared to “less complex” organisms such as worms, vertebrates possess a higher number of *let-7* isoforms (Mondol and Pasquinelli, 2012). Until now 13 human *let-7* family members were described (*let-7a-1*, *let-7a-2*, *let-7a-3*, *let-7b*, *let-7c*, *let-7d*, *let-7e*, *let-7f1*, *let-7f2*, *let-7g*, *let-7i*, *miR-98* and *mir-202*). These miRNA precursors code for 10 diverse mature *let-7* miRNAs (Wang *et al.*, 2012). Even though the role of the *let-7* family is still not fully deciphered yet, it is evident that these molecules have a distinct expression pattern in developmental processes of animals (Pasquinelli *et al.*, 2000). Being barely detectable at the embryonic stage, the *let-7* miRNAs present higher levels in differentiated adult tissues (Reinhart *et al.*, 2000; Thomson *et al.*, 2006).

An aberrant *let-7* expression was found in several malignant neoplasias such as lung cancer (Johnson *et al.*, 2007; Tay *et al.*, 2014), prostate cancer (Dong *et al.*, 2010; Liu *et al.*, 2012a; Nadiminty *et al.*, 2012b), lymphoma (Sampson *et al.*, 2007) and many more (Boyerinas *et al.*, 2010; Sterenczak *et al.*, 2014).

Remarkably, several of the direct *let-7* target genes such as *HMGA1* (Rahman *et al.*, 2009; Joetzke *et al.*, 2010; Schubert *et al.*, 2013), *HMGA2* (Mayr *et al.*, 2007; Winkler *et al.*, 2007; Joetzke *et al.*, 2010; Sterenczak *et al.*, 2014), *c-Myc* (Sampson *et al.*, 2007; Liu *et al.*, 2012b), *CCND2* (Dong *et al.*, 2010), *IL6* (Iliopoulos *et al.*, 2009) and *NRAS* (Gideon *et al.*, 1992; Johnson *et al.*, 2005; Fernandez-Medarde and Santos, 2011) are as well commonly deregulated or affected by mutations in a variety of human and canine cancers. These protein-encoding targets in turn spread the signal wave further on and modify the biogenesis and activity of other, often in cancer aberrantly expressed genes such as *AR* (Boonyaratanakornkit *et al.*, 1998; Attard *et al.*, 2009; Lyu *et al.*, 2013), *FoIH1* (Colombatti *et al.*, 2009; Bouchelouche *et al.*, 2010; Cho and Szabo, 2013), *HMGB1* (Pierantoni *et al.*, 2007; Tang *et al.*,

2010; Ueda and Yoshida, 2010), *Klf4* (Klaewsongkram *et al.*, 2007; Le Magnen *et al.*, 2012), *MAPK1* (Dhillon *et al.*, 2007; Gerits *et al.*, 2008), *PI3KCA* (Engelman *et al.*, 2006; Castellano and Downward, 2011), and *PTEN* (Ma *et al.*, 2009). Remarkably, all these genes are tightly interwoven with each other and the miRNA *let-7* family appears to be one of the major players in the controlled expression of these genes in healthy cells. For a better overview, the complex interactions are indicated in the figure 3.

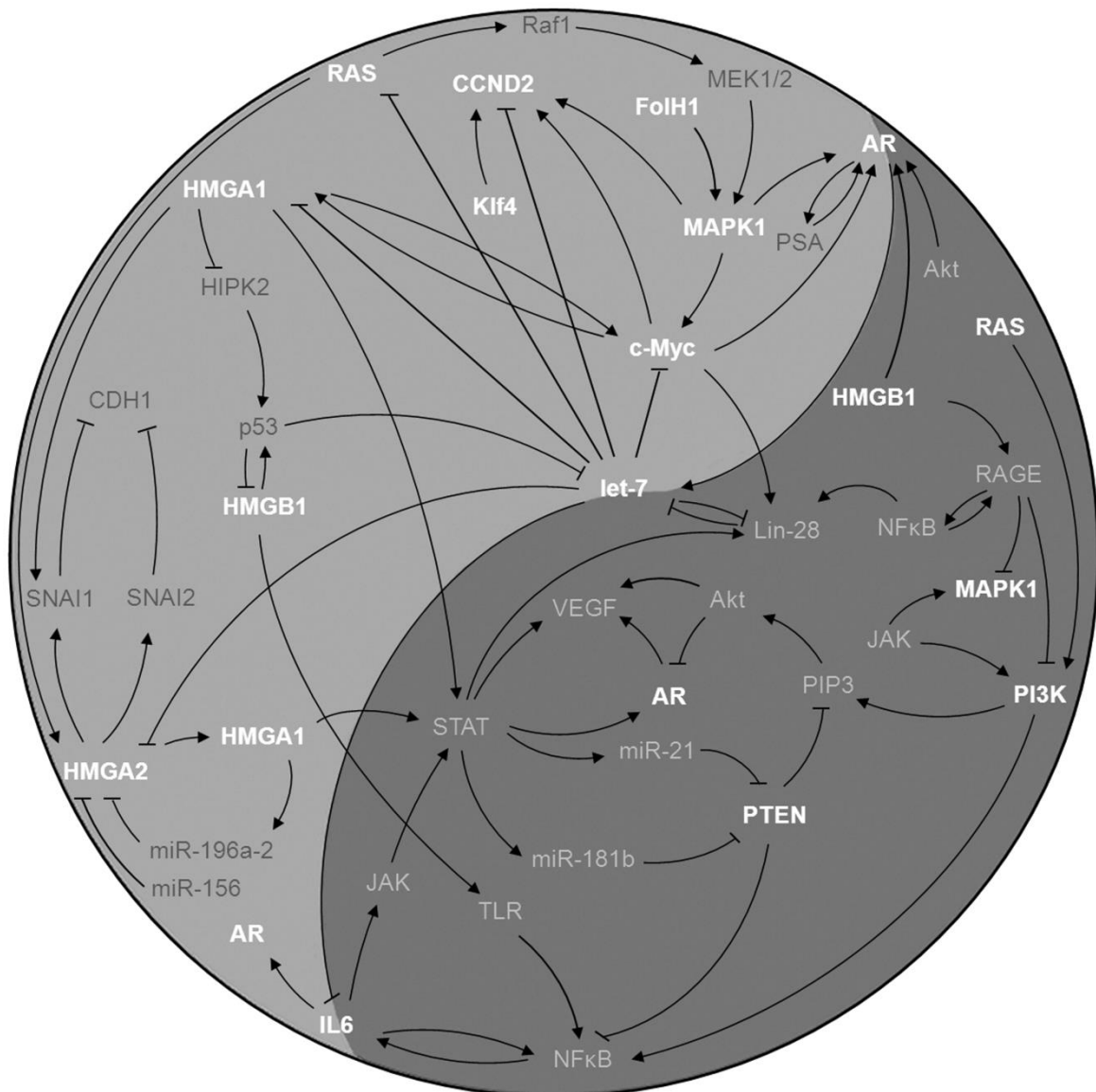


Figure 3 Schematic overview of the interactions of the miRNA *let-7* and its direct and downstream targets. All the shown genes are commonly deregulated in human cancers. The indicated interactions are on transcriptional, post-transcriptional or post-translational level (Wagner *et al.*, 2014). Targets which were analyzed within this thesis are depicted in white, bold typed letters.

1.2. Model organism dog

As mentioned before, deeper knowledge of the molecular processes in human and animal cells is important and would not only improve the choice of the best suited animal model for a certain kind of cancer but as well advance progress in the identification and evaluation of the most effective molecular drugs and targets.

Although the commonly used murine xenografts with induced tumors are a valuable model for cancer research, closing the missing link between cell culture experiments and studies on the canine model (Pinho *et al.*, 2012), they bear major limitations. Among these are the lacking influence of an intact immune system, tumor growth over long periods of time, the significant heterogeneity in tumor cell populations and the tumor microenvironment (Waters *et al.*, 1997; Leroy and Northrup, 2009; Pinho *et al.*, 2012).

In this regard, the domesticated dog qualifies as a large animal model for various human diseases (Eaton *et al.*, 1995; Lin *et al.*, 1999; Rofina *et al.*, 2003; Lohi *et al.*, 2005; Ionut *et al.*, 2008; Shan *et al.*, 2009; Mizuno *et al.*, 2011) including mammary cancer (Boggs *et al.*, 2008), osteosarcoma (Mueller *et al.*, 2007), melanoma (Noguchi *et al.*, 2011), prostate cancer (Cornell *et al.*, 2000; Winkler *et al.*, 2007) and lymphoma (Joetzke *et al.*, 2010; Sterenczak *et al.*, 2010; Uhl *et al.*, 2011). In this context it is remarkable that \approx 1 million pet dog cancer cases are diagnosed each year in the United States (Paoloni and Khanna, 2008). As dogs often live side by side with their owners and are part of the family (Rowell *et al.*, 2011) this offers a great number of patients with intensively monitored disease progression enabling comparative cancer studies.

Taken together, the dog shares many features with man, including tumor genetics, molecular targets, histological appearance, response to conventional therapies (Vail and MacEwen, 2000; Withrow and MacEwen, 2001; Paoloni and Khanna, 2008; Pinho *et al.*, 2012) and a similar clinical manifestation of many neoplasias (Ostrander *et al.*, 2000; Sutter and Ostrander, 2004; Ponce *et al.*, 2010). Additionally the mentioned *let-7* associated genes present high sequence homologies. The mature *let-7* miRNAs are even up to 100 % identical between man and dog.

Thus it is of major interest to decipher the role of the miRNA *let-7* family and associated genes, which will as well shed light on the situation in human neoplasias

and enable the development of novel more effective strategies to treat cancer in both species.

2. Aims of the thesis

The analysis of the canine miRNA *let-7* and its direct target genes, the *HMGAs* was the focus of the present thesis. For that purpose the expression pattern, structure and function of these genes and their products were investigated in the context of canine prostate cancer, lymphomas and stem cells.

In addition, based on the notion that these genes were found to be deregulated in various cancer entities, several tools/methods were constructed/established to modify their expression *in vitro* and *in vivo*. Finally, tools for target expression analyses were evaluated.

2.1.1. Expression analyses

- Identification of potential molecular tumor markers for canine prostate cancer
- Quantitative analyses of the *HMGA1* and *HMGA2* genes in canine B-cell and T-cell lymphomas

2.1.2. Structural and functional *HMGA* analyses

- Characterization of the canine *HMGA1* gene structure
- Analysis of the *HMGA2* impact on *HMGA2/let-7* axis on cell growth in prostate cancer
- Investigation of the *HMGA1* and *HMGA2* protein impact on adipose-derived mesenchymal stem cells

2.1.3. Tools for modification and detection of gene expression

- Construction of *let-7* encoding vectors for modification of gene expression
- Establishment of an adeno-associated virus (AAV) genome purification protocol for subsequent accurate AAV quantification
- Evaluation of a gold-nanoparticle mediated laser-transfection method for *in vitro* approaches
- PSMA antibody (clone YPSMA-1) evaluation for cross-reactivity with the canine protein homolog in WB and target verification by mass spectrometry

3. Selected list of publications

3.1. Published manuscripts

- I. Role of miRNA let-7 and its major targets in prostate cancer. Wagner S., Ngezahayo A., Murua Escobar H., Nolte I.. Biomed Res Int. 2014;2014:376326. Epub 2014 Sep 3.
- II. Generation and Characterisation of a Canine EGFP-HMGA2 Prostate Cancer In Vitro Model. Willenbrock S., Wagner S., Reimann-Berg N., Moulay M., Hewicker-Trautwein M., Nolte I., Murua Escobar H.. PLoS One. 2014 Jun 10;9(6):e98788. doi: 10.1371/journal.pone.0098788. eCollection 2014.
- III. Comparison of non-coding RNAs in human and canine cancer. Wagner S., Willenbrock S., Nolte I., Murua Escobar H.. Front Genet. 2013; 4: 46. Front Genet. 2013 Apr 8;4:46. doi: 10.3389/fgene.2013.00046. eCollection 2013.
- IV. Effects of High-Mobility Group A Protein Application on Canine Adipose-Derived Mesenchymal Stem Cells In Vitro. Ismail A.A., Wagner S., Murua Escobar H., Willenbrock S., Sterenczak K. A., Samy M. T., Abd El-Aal A. M., Nolte I., Wefstaedt P.. Vet Med Int. 2012;2012:752083. doi: 10.1155/2012/752083. Epub 2012 Feb 8.
- V. Expression of the high mobility group A1 (HMGA1) and A2 (HMGA2) genes in canine lymphoma: analysis of 23 cases and comparison to control cases. Joetzke A. E., Sterenczak K. A., Eberle N., Wagner S., Soller J. T., Nolte I., Bullerdiek J., Murua Escobar H., Simon D.. Vet Comp Oncol. 2010 Jun;8(2):87-95. doi: 10.1111/j.1476-5829.2010.00207.x.
- VI. Genomic characterisation, chromosomal assignment and in vivo localisation of the canine high mobility group A1 (HMGA1) gene. Beuing C., Soller J. T., Muth M., Wagner S., Dolf G., Schelling C., Richter A., Willenbrock S., Reimann-Berg N., Winkler S., Nolte I., Bullerdiek J., Murua Escobar H.. BMC Genet. 2008 Jul 23;9:49. doi: 10.1186/1471-2156-9-49.

VII. Characterization of Nanoparticle Mediated Lasertransfection by Femtosecond Laser Pulses for Applications in Molecular Medicine. Schomaker M., Heinemann D., Kalies S., Willenbrock S., Wagner S., Nolte I., Ripken T., Murua Escobar H., Meyer H., Heisterkamp A.. J Nanobiotechnology. 2015; 13: 10. Published online 2015 February 3. doi: 10.1186/s12951-014-0057-1

VIII. Verification of a canine PSMA (FolH1) antibody. Wagner S., Maibaum D., Pich A., Nolte I., Murua Escobar H.. Anticancer Res. 2015 Jan;35(1):145-8.

3.2. Manuscripts in preparation for submission

IX. Let-7 and associated genes in canine prostate cancer. Wagner S., Eberle N., Ngezahayo A., Murua Escobar H., Nolte I..

X. Improved rAAV genome isolation for quantification by absolute real-time PCR. Wagner S., Ngezahayo A., Murua Escobar H., Nolte I..

4. Results

4.1. Gene expression analyses

4.1.1. Prostate cancer

Human PC is accepted to be a hormone dependent tumor. The androgen deprivation therapy is thus the standard palliative treatment modality of primary advanced tumors. Nevertheless, the majority of the patients relapse subsequently due to castration resistance (Divrik *et al.*, 2012).

Although much progress in diagnosis and therapy of PC has been made there are still many men with potentially indolent disease being treated. On the other hand this malignancy contributed to approximately 310,000 cases of cancer-related deaths in 2012 (GLOBOCAN 2012, IARC) highlighting the importance of molecular PC markers.

As PC occurs spontaneously in human and dog (Withrow and Vail, 2012) and additionally shares many functional and morphological features (Leroy and Northrup, 2009) the following section deals with the analyses of gene expression in canine PC.

To provide an overview about the genes involved in PC the first review article in this section highlights the role of the miRNA *let-7* and associated genes in the human malignancy. In the second experimental study the expression of several genes deregulated in human PC and other neoplasias was analyzed in canine prostatic samples.

I. Role of miRNA *let-7* and its major targets in prostate cancer.

Wagner *et al.*, Biomed Research International, 2014

In the following review article the molecular interactions between the miRNA *let-7* family members, its direct targets and regulators *HMGA1*, *HMGA2*, *CCND2*, *IL6*, *AR* and *RAS* as well as the downstream target *HMGB1*, which is implicated in all proposed hallmarks of cancer, were described. The role of these genes, which were previously shown to be deregulated in a variety of human malignant neoplasias was

Results

critically reviewed in the context of prostate cancer etiology with miRNA *let-7* being the central point.

I.

Role of miRNA let-7 and its major targets in prostate cancer

Siegfried Wagner, Anaclet Ngezahayo, Hugo Murua Escobar, Ingo Nolte

Hindawi, Biomed Research International, 2014

Own contribution:

- Literature search and data analyses
- Partial manuscript drafting
- Preparation of all figures

Review Article

Role of miRNA *Let-7* and Its Major Targets in Prostate Cancer

Siegfried Wagner,^{1,2} Anacleto Ngezahayo,² Hugo Murua Escobar,^{1,3} and Ingo Nolte¹

¹ *Small Animal Clinic, University of Veterinary Medicine Hannover, 30559 Hannover, Germany*

² *Institute of Biophysics, University Hannover, 30419 Hannover, Germany*

³ *Division of Medicine, Department of Haematology/Oncology, University of Rostock, 18057 Rostock, Germany*

Correspondence should be addressed to Ingo Nolte; ingo.nolte@tiho-hannover.de

Received 16 April 2014; Revised 11 August 2014; Accepted 18 August 2014; Published 3 September 2014

Academic Editor: Andreas Doll

Copyright © 2014 Siegfried Wagner et al. This is an open access article distributed under the Creative Commons Attribution License, which permits unrestricted use, distribution, and reproduction in any medium, provided the original work is properly cited.

Prostate cancer is worldwide the sixth leading cause of cancer related death in men thus early detection and successful treatment are still of major interest. The commonly performed screening of the prostate-specific antigen (PSA) is controversially discussed, as in many patients the prostate-specific antigen levels are chronically elevated in the absence of cancer. Due to the unsatisfying efficiency of available prostate cancer screening markers and the current treatment outcome of the aggressive hormone refractory prostate cancer, the evaluation of novel molecular markers and targets is considered an issue of high importance. MicroRNAs are relatively stable in body fluids orchestrating simultaneously the expression of many genes. These molecules are currently discussed to bear a greater diagnostic potential than protein-coding genes, being additionally promising therapeutic drugs and/or targets. Herein we review the potential impact of the microRNA *let-7* family on prostate cancer and show how deregulation of several of its target genes could influence the cellular equilibrium in the prostate gland, promoting cancer development as they do in a variety of other human malignant neoplasias.

1. Introduction

Prostate cancer (PC) is a heterogeneous disease ranging from an asymptomatic to a fatal systemic malignancy [1]. According to the World Health Organization (WHO) 1,111,689 men were estimated to be diagnosed with PC in the year 2012 (<http://globocan.iarc.fr/>). Accounting worldwide for 6.6% (307,471) of all cancer death in men in 2012, PC is one of the most common malignant neoplasias and the sixth leading cause of cancer related death in men (<http://globocan.iarc.fr/>).

The development of PC is considered to be a multi-step process initiated by genetic and epigenetic changes [1]. Human PC is commonly accepted to be an androgen dependent malignancy.

An analysis of PC related metastatic pattern in 1,589 patients by Bubendorf et al. revealed that 35% of the analyzed tumors spread to other organs with preference to the bones (90%), lungs (46%), liver (25%), pleura (21%), and adrenals (13%) [2].

The androgen deprivation therapy is actually the most effective palliative standard treatment for primary advanced

PCs with bone metastasis (effective in up to ~90% of patients). However, the great majority of patients relapse subsequently due to the development of castration resistance [3].

Since the introduction of the prostate-specific antigen (PSA) test in the 1990s, the number of diagnosed cases has been rapidly rising being initially associated with a reduced mortality. However, the recent decline in PC related mortality rates is now being discussed to be partially explained by the improved treatment and earlier diagnosis due to a broad standard PSA screening in economically developed countries [4, 5]. As the standard PSA screening in the early diagnosis of human PC remains a very controversial issue, novel, reliable molecular PC markers are needed [6–8].

A promising marker candidate gene is the miRNA *let-7*, which was reported to be down regulated among others in human PC [9–11]. Further, the reconstitution of the *let-7* expression resulted in suppression of PC cell proliferation [10, 12]. In general a single miRNA is able to regulate a huge number of genes. Concerning *let-7* the respective acting ways are actually not entirely deciphered.

Nevertheless, it is to be expected that a deeper understanding of the molecular interactions of *let-7* and associated genes will significantly contribute to the development of novel diagnostic and therapeutic treatment modalities for PC.

Due to the complex regulation mechanisms of *let-7* and its potential role in PC development and relapse the present review highlights *let-7* and its direct and downstream targets in the context of PC.

2. Micro RNA *Let-7* Family

MicroRNAs (miRNAs) are small, non-protein-coding RNAs derived from long, endogenously expressed primary RNA (pri-miRNA) molecules. These pri-miRNAs are processed by the nuclear enzyme Drosha to precursor RNAs (pre-miRNAs), exported by Exportin-5 [13] and matured by the cytoplasmic enzyme Dicer [14]. Finally the guide strand of the mature miRNA is incorporated into the RNA-induced silencing complex (RISC), which blocks the translation of the target mRNA by binding to its 5'-, 3'-prime, or exon regions [15, 16]. The passenger strand is usually degraded [17] (Figure 1).

Mature miRNAs are known to be part of the gene expression regulating machinery at transcriptional [18, 19] and as well posttranscriptional level [13]. It was reported that a single miRNA can orchestrate the expression of several genes and a single gene can be regulated by a set of different miRNAs [20–22]. Several observations suggest that more than 60% of all protein coding genes are regulated by miRNAs [23].

One of the first described members of the large class of non-protein-coding RNAs is *let-7* which was the second miRNA discovered and designated as *lethal-7* (*let-7*) according to the phenotype of a *let-7* deficient *C. elegans* mutant [20]. Soon thereafter, further *let-7* homologs were identified in a variety of species ranging from vertebrates to mollusks [24].

In contrast to “less complex” organisms such as worms, vertebrates show a higher number of *let-7* isoforms coded by different genes [16]. In humans, 13 *let-7* family precursor miRNAs were described (*let-7a-1*, *let-7a-2*, *let-7a-3*, *let-7b*, *let-7c*, *let-7d*, *let-7e*, *let-7f*, *let-7g*, *let-7i*, *miR-98*, and *mir-202*) which code for 10 different mature *let-7* miRNA isoforms [25].

Although the role of *let-7* is still not fully understood, it is evident that the *let-7* family members have a distinct expression pattern in animal development [26]. In the embryonic stage the *let-7* miRNAs were found to be barely detectable, but having an increased expression in differentiated cells [20, 27]. Furthermore, aberrant *let-7* expression was associated with a variety of human diseases as, for example, cardiovascular diseases [28], liver fibrosis [29], lung diseases [30], and cancer [9–12, 26, 31–34]. Interestingly several *let-7* family members were found to be located at fragile sites of human chromosomes potentially contributing to aberrant *let-7* transcript levels [35].

Cancer initiation, progression, and aggressiveness are hypothesized to be driven by cancer stem cells (CSCs)

[36, 37]. Inflammatory microenvironment [38] as well as epithelial-to-mesenchymal transition (EMT), which is tightly linked with CSC biology [39], seems to play a substantial role in cancer etiology as well. Remarkably, a linkage between these factors is the *let-7* miRNA family. As described above *let-7* was shown to be downregulated in prostatic CSCs [36] whereas reconstitution of the *let-7* suppressed the growth of PC cells [10, 12]. Additionally, a direct causal link between cancer and inflammation is given by the association of *let-7*, IL6, and NFκB, which are major players involved in the epigenetic switch from inflammation to cell transformation [31]. The connection between EMT and *let-7* is represented by the *HMGA1* and *HMGA2* genes, which are directly regulated by *let-7* and were found to be implicated in EMT [40, 41].

Further, miRNAs of the *let-7* family were reported to directly, negatively regulate *IL6* [24], *NRAS* [42], *c-Myc*, *HMGA1* [43, 44], *HMGA2* [45], and *CCND2* [11]. Notably, these *let-7* targets are involved in a wide range of diverse cellular processes interwoven with *let-7* and each other in a fine balanced way (Figure 10).

The *c-Myc* protein regulates the biogenesis of *let-7* by stimulating *Lin28* [46], *Lin28* in turn blocks the maturation of *let-7* [47]. Additionally, *c-Myc* stimulates the expression of *HMGA1* [48], *AR* [12], and *IL6* [49]. *NRAS* is suggested to have an impact on *HMGA2* biogenesis [45]. *HMGA2* on the other hand influences *HMGA1*, its gene product in turn regulates the expression of *c-Myc* [50] and *HMGB1* [51]. *HMGB1* was found to bind the *AR* promoter [52], *AR* protein was described itself to stimulate *let-7* expression [53] (Figure 10).

Interestingly, the *let-7* family [10, 11] and some of its above mentioned targets were already found to be implicated in PC. As *let-7* is linked with all these protein-coding genes a deeper insight into these connections is of great interest. Thus, these interactions are reviewed more detailed in the following parts.

3. *HMGA1*

The high mobility group proteins (HMG) are chromatin associated nonhistone proteins constituting three superfamilies (*HMGA*, *HMGB*, and *HMGN*) which are classified by their characteristic functional DNA-binding motifs [54]. Expression of these proteins was described to be involved in a variety of biological processes as, for example, transcription, embryogenesis, differentiation, neoplastic transformation, apoptosis, and inflammation [52, 55, 56].

In human neoplasias the *HMGA* genes are among the most commonly rearranged genes [57]. Deregulation of the *HMGA1* expression was described in human PC [58, 59], lung cancer [60], and breast cancer cells [61]. Its oncogenic property is speculated to be partly mediated through the cytoplasmic relocalization of the *HIPK2* which is a proapoptotic activator of the tumor suppressor *p53* [51] (Figures 2 and 10). *HMGA1* was reported to enhance the proliferation rate and invasion of PC cells [62, 63] potentially through the implication in epithelial-to-mesenchymal transition (EMT) [61]. In line with this, *HMGA1* knock down in the human triple-negative breast cancer cell lines MDA-MB-231 and Hs578T

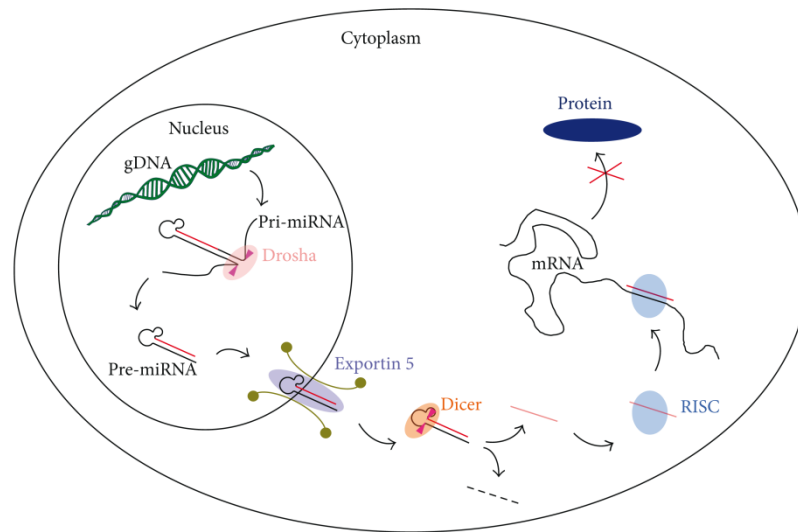


FIGURE 1: Schematic overview of the miRNA maturation and the way of function in eukaryotic cells. The endogenously expressed primary miRNA (pri-miRNA) is processed in the nucleus of a cell by the enzyme Drosha. The emerging precursor miRNA (pre-miRNA) product is exported into the cytoplasm by Exportin-5 and matured by Dicer. Finally the guide strand is incorporated into the RNA-induced silencing complex (RISC), which blocks the translation of the target mRNA.

repressed the mesenchymal gene *SNAIL* and stimulated *CDH1* expression [40] (Figures 2 and 10), both of which are involved in EMT [64, 65]. Furthermore, *HMGA1* was reported to drive tumor progression by reprogramming cells to a stem-cell-like state [40]. In accordance, Shah et al. reported in human embryonic stem cells (hESCs) a significant downregulation of the stemness-associated genes *OCT4*, *Sox2*, *Lin28*, and *c-Myc* 96 h after *HMGA1* repression [50]. Interestingly *HMGA1* is not only stimulating *c-Myc* expression [50] it was also reported to be itself induced by *c-Myc* [48] (Figures 2 and 10). It is remarkable that *HMGA1* is implicated in the upregulation of several miRNAs in murine embryonic fibroblasts. Among these miRNAs is the *miR-196a-2*, which in turn is predicted to target its sister gene *HMGA2* [66] (Figures 2 and 10). Furthermore, Hillion and colleagues reported a positive correlation between *HMGA1* and *STAT3* in a subset of primary human acute lymphoblastic leukemia samples [67]. In line with this, *HMGA1* was described to bind the *STAT3* promoter and to upregulate its expression in malignant human hematopoietic cells [67] (Figures 2 and 10). The transcription factor *STAT3* mediates uncontrolled growth, angiogenesis, and survival of cells and has a great potential as target in cancer therapies [68]. Remarkably, Iliopoulos et al. identified *STAT3* binding sites in the promoters of the miRNAs *miR-181b* and *miR-21* [69] (Figures 2 and 10). These tiny regulators in turn were found to block *PTEN* (Figures 2 and 10), stimulating the activity of *NFκB* [69]. The tumor suppressor *PTEN* functions as an antagonist of *PI3K* by dephosphorylating its product *PIP3* [70] (Figure 10).

The *HMGA1* and *HMGA2* genes were reported to be highly expressed during embryogenesis, reexpressed in several cancer types but to be absent or not detectable in most of the adult healthy tissues [57, 71]. The expression of both

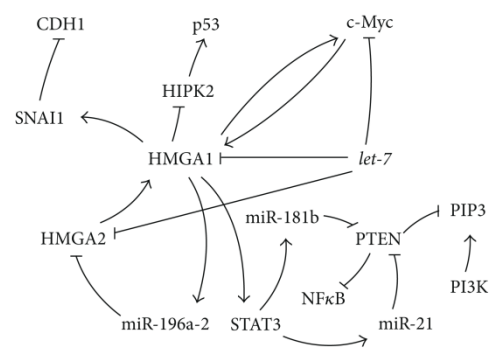


FIGURE 2: Overview of the described interactions between *let-7* and its direct target *HMGA1* with other genes.

HMGA1, *HMGA2*, and of its regulator *let-7* was shown to be negatively correlating in gastroenteropancreatic neuroendocrine tumors [44] and retinoblastomas [72]. In accordance they were found to be directly, negatively regulated by *let-7* [45, 73, 74] (Figures 2 and 10).

4. *HMGA2*

Comparable to the described *HMGA1* knock down, the repression of *HMGA2* in the human PC cell line PC-3 induced an upregulation of *CDH1* indicating an important role in EMT [41]. *SNAIL* and *SNAIL2* are repressors of *CDH1* and were shown to be directly activated by *HMGA2* [45] (Figures 3 and 10).

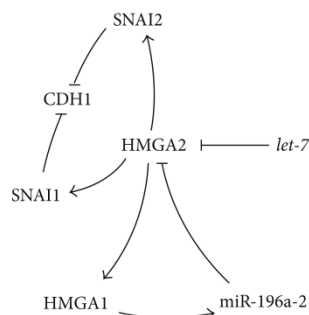


FIGURE 3: Association of the HMGA2/*let-7* axis with the regulation of genes involved in EMT and miRNAs.

Similar to *HMGA1*, an upregulation of *HMGA2* was reported in human lung and breast cancers [75, 76] as well as in a subset of canine PCs [77]. Furthermore, *HMGA2* was recently described to modify gene expression not only as protein but as well as a competing endogenous RNA (ceRNA) by acting as a decoy for mature *let-7* miRNAs [78]. Interestingly, a stimulating *HMGA2* influence on the expression of its sister protein *HMGA1* was found in rat epithelial thyroid cells [79], thus constituting a feedback loop by the stimulation of its suppressor, the *miRNA-196a-2* [66] (Figures 3 and 10). Remarkably *HMGA2* was described to bear seven *let-7*-binding sites in its 3'-untranslated region (3'-UTR) [33]. Aberrations of the chromosomal region 12q14-15 that affect *HMGA2* were frequently found in human cancers [80–82]. Moreover, the disrupted pairing between *let-7* and *HMGA2* by mRNA truncations of the 3'UTR was reported to induce *HMGA2* overexpression leading to tumor formation [33].

5. HMGB1

The high mobility group box 1 (HMGB1) is one of the HMGB superfamily members which was also shown to be implicated in inflammation exercising cytokine like functions [83]. In line with its multiple roles it can be located in the nucleus as well as in the cytoplasm and can even be released passively by necrotic cells or actively secreted in response to inflammatory signals by certain cell types [83, 84].

This proinflammatory cytokine exerts its function by interacting with the toll-like receptors (TLR) 2, and TLR4 and RAGE [85–87] (Figures 4 and 10). Interestingly, the receptor coding gene *TLR4* was found to be a direct *let-7i* target (Figure 4), presenting a mechanism to modify the HMGB1 signaling [88]. The activation of the HMGB1 receptor RAGE results among others in deactivation of MAPK1 and PI3K [89]. PI3K in turn was shown to stimulate NFκB [90]. Furthermore, the TLRs and RAGE were demonstrated to activate NFκB thus, inducing the secretion of angiogenic factors, growth factors, and cytokines [85, 91].

Remarkably, NFκB is able to stimulate RAGE expression by binding to its promoter constituting a positive feedback loop [92] (Figures 4 and 10). Blockade of the RAGE/HMGB1

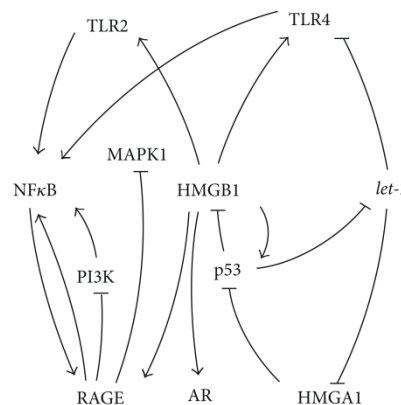


FIGURE 4: Schematic overview over the HMGB1 and *let-7* regulatory pathways affecting each other's activity.

signaling decreased growth and metastasis of implanted and as well of spontaneously developing tumors in susceptible mice [93].

HMGB1 was described to be involved in all proposed hallmarks of cancer and is thus a potential target for therapeutic and diagnostic approaches [94]. Kuniyasu et al. observed the secretion of HMGB1 in primary cultured human prostatic stromal cells after androgen deprivation [95]. *In vitro* suppression of HMGB1 was demonstrated to block the invasion of PC-3 cells which was reversed by culturing the cells in conditioned medium of the above-mentioned stromal cells deprived of androgen [95, 96]. Additionally, HMGB1 was found to stimulate DNA binding of several steroid receptors including the *let-7* downstream target AR (Figure 10) [97]. These facts indicate that *HMGB1* may be a molecular marker for advanced prostate cancer [95, 96].

Although *HMGB1* was not shown to be a direct *let-7* target, its expression is modulated by the direct *let-7* target *HMGA1* [51]. Interestingly HMGB1 was also shown to be involved in the p53 network by facilitating the binding of the tumor suppressor p53 to its cognate DNA [98]. As mentioned before p53 can be inactivated by the HMGB1 sister protein *HMGA1* by translocation of the p53 activator HIPK2 [51] (Figures 4 and 10). The tumor suppressor p53 in turn was found to downregulate the activity of the HMGB1 promoter [99] and to trigger the radiation induced decrease of *let-7a* and *let-7b* expression (Figures 4 and 10) in the human colon cancer cell line HCT116 [100].

6. CCND2

Many tumor cells accumulate mutations resulting in uncontrolled proliferation due to direct or indirect deregulations of the cyclin-dependent kinases (CDKs). Cyclins are known regulating subunits of CDKs being expressed at specific time points during the cell cycle. Consequently cyclin deregulations induce uncontrolled cell proliferation [101].

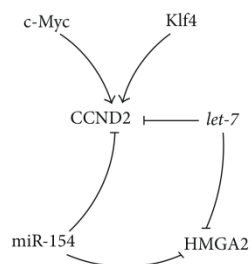


FIGURE 5: *Let-7* and *CCND2* mediated gene regulation.

The cyclin D2 (*CCND2*) is one of the cell cycle regulating factors. This gene, which is highly conserved among mammals, has been associated with human prostate cancer [11], gastric cancer [102], colon cancer [103], and leukemia [104].

Interestingly, *CCND2* was shown to be a direct *let-7* and *miR-154* target like *HMGA2* [11, 41, 45, 105] (Figures 5 and 10). Additionally the *let-7* regulated oncogene *c-Myc* and the stem cell marker *Klf4* were reported to stimulate the *CCND2* transcription [106, 107] (Figures 5 and 10).

Dong et al. described that ectopically overexpressed *let-7a* induced cell cycle arrest at the G1/S phase by suppressing among others the cyclin *CCND2* and additionally inhibited the proliferation of the human prostatic cell lines PC-3 and LnCap [11]. The same group reported that in nude xenograft mice, inoculated with *let-7a* transfected PC-3 cells, the tumor was 80% lighter after 4 weeks of growth compared to controls [11].

7. *c-Myc*

c-Myc is an oncogene frequently activated in human cancers, but is low expressed or absent in quiescent cells [108–110]. In contrast, its overexpression has been connected with PC formation and progression [111, 112]. This gene encodes a transcription factor that has a great impact on the global gene expression pattern and, thus, influences cell-cycle progression, glucose and glutamine metabolism, lipid synthesis, and many other processes, which contribute to tumor progression [109].

Mitogen activated protein kinases (MAPK), glycogen synthase kinase 3 (GSK3), and other CDKs play a key role in the biological function and half-life of *c-Myc* proteins by posttranslational phosphorylation of the Thr58 and Ser62 sites [113] (Figures 6 and 10). Apart from various posttranslational protein modifications and transcriptional regulations of the *c-Myc* gene products, this gene was reported to be directly negatively regulated by members of the *let-7* family [114, 115] (Figures 6 and 10). Additionally, elevated MAPK1 activity, which was associated with advanced, androgen independent human PCs, [116] was demonstrated to influence the *c-Myc* protein, resulting in prolonged function in a human muscle-derived rhabdomyosarcoma cell line [117]. In line with the functions of *c-Myc*, MAPK1 controls diverse cellular processes as growth, differentiation, migration, and apoptosis, its deregulation has often been described to be

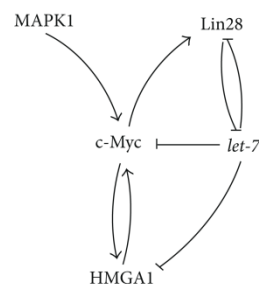


FIGURE 6: Interactions of the oncogene *c-Myc* with *let-7* and MAPK1, Lin28, and HMGA1.

associated with cancer [118]. Furthermore, *c-Myc* was shown to transcriptionally activate *Lin28* [119], which in turn inhibits the biogenesis of its regulator *let-7* constituting a double negative feedback loop [47] (Figures 6 and 10). Interestingly the expression of the direct *let-7* target *HMGA1* is as well induced by *c-Myc* [48], which constitutes a positive feedback loop, stimulating *c-Myc* expression [50] (Figures 6 and 10).

8. IL6

Chronic inflammation of the prostate gained major attention as it is considered to account to the factors contributing to PC [120]. In previous reports a direct causal link between cancer and inflammation has been described with IL6, *let-7*, Lin28, and NFκB being the major players involved in the epigenetic switch from inflammation to cell transformation [31].

Originally identified as an inducer of the terminal differentiation of B-cells into antibody-producing cells [121] interleukin-6 (IL6) appears to be a major regulator of prostate cancer progression [122]. Notably, IL6 is not only released by inflammatory cells but also found to be released by hormone insensitive cell lines DU145 and PC-3 but not by the hormone sensitive LNCaP cells [123]. Furthermore, this pleiotropic cytokine stimulates growth and survival of human PC and promotes its progression [123, 124]. In accordance, increased IL6 levels were found in epithelial cells of PC compared to benign tissues [125]. Moreover, Giri et al. reported a ~18 times higher IL6 expression in malignant prostate tissues compared to “normal” prostate specimens [126]. Michalaki and colleagues described significantly higher IL6 serum levels in patients with metastatic prostatic disease [127].

The biological activities of IL6 are mediated by binding to the α -subunit receptor IL6R and the following association with the ubiquitously expressed signal-transducing β -subunit gp130 [128]. Upon engagement of gp130 various Janus tyrosine kinase (JAK) family members (JAK1, JAK2, JAK3, and Tyk2) [129] are activated by ligand induced receptor oligomerization phosphorylating themselves and the intracellular domains of the receptors [130]. Once gp130 is phosphorylated the second protein family, the signal transducer and activator of transcription (STAT), binds to the intracellular domain of the receptor. This leads to the activation of STATs and the subsequent dissociation, allowing

features for the progression of a growing tumor VEGF is one of the most important inducers of angiogenesis [157]. Niu et al. demonstrated a positive correlation between VEGF and a constitutively active STAT3 [157]. In accordance, it was found that STAT3 binds to the *VEGF* promoter [157] (Figures 8 and 10). Additionally STAT3 was reported to bind the promoter of the *let-7* biogenesis regulating gene *Lin28*, resulting in the concomitant upregulation of the *let-7* targets *RAS*, *c-Myc*, and *HMGA2* [158].

In human tissues the activation of RAS and Rac-MAPK pathways was described to be induced by the extracellular signal transducer FolH1 [159] (Figures 8 and 10). FolH1 is expressed in most of the human prostate cancers and is thus a potential target for diagnostic and therapeutic strategies [160]. The elicited phosphorylation of MAPK1 and MAPK14 induces in turn the activation of the transcription factor NF κ B (Figures 8 and 10) which controls the expression of various genes including the *let-7* biogenesis-controlling *Lin28* [47] and the cytokine *IL6* [31, 161] (Figures 8 and 10). Additionally, NF κ B was also shown to enhance the endogenous transcription of the primary miRNAs *let-7a-3* and *let-7b* through NF κ B responsive binding sites in the promoter regions [141] (Figures 8 and 10).

Remarkably, Johnson et al. reported numerous *let-7* binding sites in the 3'-UTR of the *RAS* genes [42]. In conclusion the expression of the oncogenes *NRAS*, *KRAS*, and *HRAS* was described to be negatively regulated by several members of the *let-7* family [42, 162] (Figures 8 and 10).

10. Androgen Receptor (AR)

The gene of the steroid receptor family member *AR* [163] is located on the human chromosome X and codes for a ligand-dependent transcription factor [164, 165]. Upon ligand binding it translocates into the nucleus and regulates its target genes by binding to the androgen response elements (AREs) [166, 167]. Expressed in nearly all primary human PCs, *AR* plays a pivotal role in carcinogenesis of the prostate. At the initial diagnosis the majority of PCs depends on androgens and progress after hormone therapy to an androgen-independent disease [3, 168].

Continuous androgen expression is required to drive prostate gland formation during embryogenesis and later to maintain the normal function and glandular anatomy in adults [169]. In general the androgen mediated effects in prostate gland development are driven by the interaction with ARs [169]. The bypass mechanisms of *AR* upregulation include among others the HMGB1 enrichment on the *AR* promoter, which enhances the transcription [52] (Figures 9 and 10), an intracrine androgen production [170, 171] additionally ligand independent *AR* activation by cytokines or growth factors were reported as well [172]. Furthermore, altered specificity or sensitivity as for example by alternative splicing is discussed [173].

However, the activated *AR* stimulates the expression of its targets as, for example, the above mentioned *VEGF* [174] and *PSA* [175]. *PSA* is a pivotal downstream target of *AR*, which is used as biomarker for human PC progression [175]. Interestingly, the frequently observed rising of serum *PSA* in

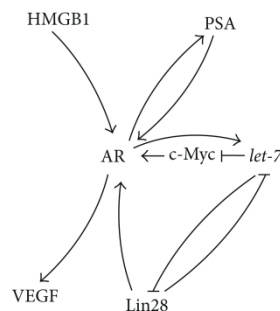


FIGURE 9: Potential AR interaction in prostate cancer development.

castrate-resistant PC patients could in parts be explained by *AR* activity, which is reexpressed/reactivated in advanced PCs [176]. Remarkably, *PSA* constitutes a positive feedback loop stimulating *AR* expression as was demonstrated *in vitro* [175] (Figures 9 and 10).

Furthermore, Tummala et al. highlighted the impact of the *Lin28/let-7/Myc* axis on PC and demonstrated that *Lin28* activates the *AR* (Figures 9 and 10) and promotes growth of PC [177].

Remarkably *AR* was reported to be regulated in a negative way by the miRNA *let-7c* which suppresses its transcriptional activator *c-Myc* [12] (Figures 9 and 10). Additionally Lyu et al. described an *AR* induced upregulation of *let-7a*, *let-7b*, *let-7c*, and *let-7d* (Figures 9 and 10) in the breast cancer cell lines MDA-MB-231 and MDA-MB-453. At least in the case of *let-7a* this upregulation is indicated to be triggered by *AR* binding to AREs located at the *let-7a* promoter [53] (Figures 9 and 10). Furthermore, it was shown that in these cell lines the expression of the direct *let-7a* targets *c-Myc* and *KRAS* was decreased upon treatment with 5 α -dihydrotestosterone and increased after an additional suppression of the miRNA *let-7a* [53].

The spatiotemporal expression of genes and functions depend highly on the cellular and developmental context. Thus, the impact of a single gene can be completely different between diverse tissues and at different time points in development. Nevertheless elucidation of the above described interactions in PC bears great potential due to the ubiquitous existence of the cellular regulatory elements and the potential interactions in each somatic cell of an organism. This idea is supported by the already found implication of each of the described genes in various human cancers. Furthermore several of the reviewed genes are already used as targets for diagnostic, prognostic, and therapeutic approaches. Thus, the master regulator family *let-7* is as well a promising target in cancer of the prostate gland.

For a better overview all described interactions between the master regulator family *let-7* and its major targets are summarized in Figure 10.

11. Conclusion

Although the knowledge of the genetic and epigenetic alterations in prostate cancer has significantly increased in the last

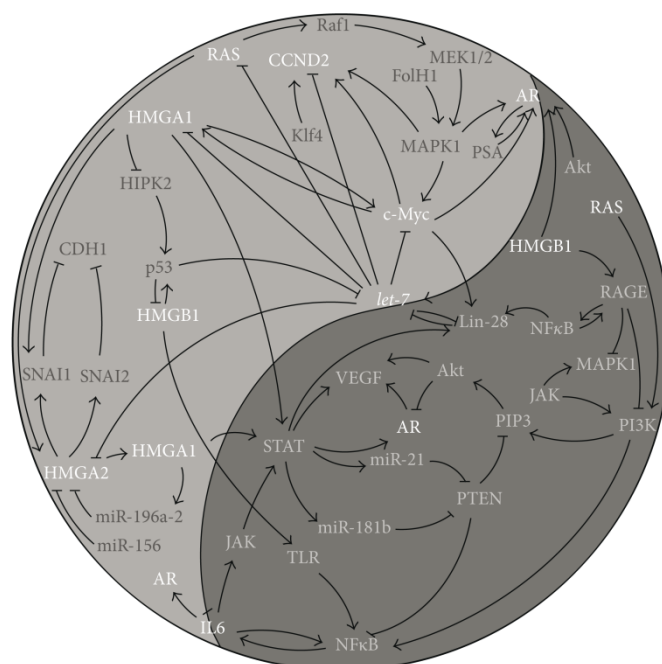


FIGURE 10: This figure represents the described interactions between *let-7* and the reviewed *let-7* associated targets (in white letters) with other genes which are as well commonly deregulated in human cancers (in gray letters). The indicated interactions are on transcriptional, posttranscriptional or posttranslational level.

decades, its diagnosis and therapy still remains a major challenge. The actually described genetic alterations in prostate cancer give more questions than answers. As we could highlight, the genes reviewed in the present paper are not acting in solitude but are closely interwoven with each other (Figure 10). Remarkably, the miRNA *let-7* family members are major players in the regulation of gene expression and appear to contribute greatly to the maintenance of the Ying and Yang in “normal” prostatic cells. However, their impact can be modified greatly by other factors. For that reason the complex intra- and intercellular genetic interactions of *let-7* family members and associated genes must be further investigated and will likely have an impact on diagnostic, prognostic, and treatment modalities in future.

Conflict of Interests

The authors have no conflict of interests.

References

- [1] L. Kopper and J. Tímár, “Genomics of prostate cancer: is there anything to “translate”?” *Pathology & Oncology Research*, vol. 11, no. 4, pp. 197–203, 2005.
- [2] L. Bubendorf, A. Schöpfer, U. Wagner et al., “Metastatic patterns of prostate cancer: an autopsy study of 1,589 patients,” *Human Pathology*, vol. 31, no. 5, pp. 578–583, 2000.
- [3] R. T. Divrik, L. Türkeri, A. F. Şahin et al., “Prediction of response to androgen deprivation therapy and castration resistance in primary metastatic prostate cancer,” *Urologia Internationalis*, vol. 88, no. 1, pp. 25–33, 2012.
- [4] A. Jemal, F. Bray, M. M. Center, J. Ferlay, E. Ward, and D. Forman, “Global cancer statistics,” *CA Cancer Journal for Clinicians*, vol. 61, no. 2, pp. 69–90, 2011.
- [5] R. T. Greenlee, T. Murray, S. Bolden, and P. A. Wingo, “Cancer statistics, 2000,” *CA: A Cancer Journal for Clinicians*, vol. 50, no. 1, pp. 7–33, 2000.
- [6] G. L. Andriole, E. D. Crawford, R. L. Grubb III et al., “Mortality results from a randomized prostate-cancer screening trial,” *New England Journal of Medicine*, vol. 360, no. 13, pp. 1310–1319, 2009.
- [7] F. H. Schröder, J. Hugosson, M. J. Roobol et al., “Screening and prostate-cancer mortality in a randomized european study,” *The New England Journal of Medicine*, vol. 360, no. 13, pp. 1320–1328, 2009.
- [8] E. Basch, T. K. Oliver, A. Vickers et al., “Screening for prostate cancer with prostate-specific antigen testing: american society of clinical oncology provisional clinical opinion,” *Journal of Clinical Oncology*, vol. 30, no. 24, pp. 3020–3025, 2012.
- [9] H. Ramberg, A. Alshbib, V. Berge, A. Svindland, and K. A. Taskén, “Regulation of PBX3 expression by androgen and Let-7d in prostate cancer,” *Molecular Cancer*, vol. 10, article 50, 2011.
- [10] N. Nadiminty, R. Tummala, W. Lou et al., “MicroRNA let-7c is downregulated in prostate cancer and suppresses prostate cancer growth,” *PLoS ONE*, vol. 7, no. 3, Article ID e32832, 2012.
- [11] Q. Dong, P. Meng, T. Wang et al., “MicroRNA let-7a inhibits proliferation of human prostate cancer cells *in vitro* and *in vivo*”

- by targeting E2F2 and CCND2," *PLoS ONE*, vol. 5, no. 4, Article ID e10147, 2010.
- [12] N. Nadiminty, R. Tummala, W. Lou et al., "MicroRNA let-7c suppresses androgen receptor expression and activity via regulation of myc expression in prostate cancer cells," *Journal of Biological Chemistry*, vol. 287, no. 2, pp. 1527–1537, 2012.
- [13] D. P. Bartel, "MicroRNAs: genomics, biogenesis, mechanism, and function," *Cell*, vol. 116, no. 2, pp. 281–297, 2004.
- [14] Y. Lee, C. Ahn, J. Han et al., "The nuclear RNase III Drosha initiates microRNA processing," *Nature*, vol. 425, no. 6956, pp. 415–419, 2003.
- [15] G. Meister, "Argonaute proteins: functional insights and emerging roles," *Nature Reviews Genetics*, vol. 14, no. 7, pp. 447–459, 2013.
- [16] V. Mondol and A. E. Pasquinelli, "Let's make it happen: the role of let-7 microRNA in development," *Current Topics in Developmental Biology*, vol. 99, pp. 1–30, 2012.
- [17] W. Filipowicz, S. N. Bhattacharyya, and N. Sonenberg, "Mechanisms of post-transcriptional regulation by microRNAs: are the answers in sight?" *Nature Reviews Genetics*, vol. 9, no. 2, pp. 102–114, 2008.
- [18] H.-W. Hwang, E. A. Wentzel, and J. T. Mendell, "A hexanucleotide element directs microRNA nuclear import," *Science*, vol. 315, no. 5808, pp. 97–100, 2007.
- [19] R. F. Place, L.-C. Li, D. Pookot, E. J. Noonan, and R. Dahiya, "MicroRNA-373 induces expression of genes with complementary promoter sequences," *Proceedings of the National Academy of Sciences of the United States of America*, vol. 105, no. 5, pp. 1608–1613, 2008.
- [20] B. J. Reinhart, F. J. Slack, M. Basson et al., "The 21-nucleotide let-7 RNA regulates developmental timing in *Caenorhabditis elegans*," *Nature*, vol. 403, no. 6772, pp. 901–906, 2000.
- [21] P.-S. Chen, J.-L. Su, S.-T. Cha et al., "miR-107 promotes tumor progression by targeting the let-7 microRNA in mice and humans," *The Journal of Clinical Investigation*, vol. 121, no. 9, pp. 3442–3455, 2011.
- [22] J. Winter, S. Jung, S. Keller, R. I. Gregory, and S. Diederichs, "Many roads to maturity: microRNA biogenesis pathways and their regulation," *Nature Cell Biology*, vol. 11, no. 3, pp. 228–234, 2009.
- [23] B. N. Davis and A. Hata, "Regulation of MicroRNA Biogenesis: a miRiad of mechanisms," *Cell Communication and Signaling*, vol. 7, article 18, 2009.
- [24] A. E. Pasquinelli, B. J. Reinhart, F. Slack et al., "Conservation of the sequence and temporal expression of let-7 heterochronic regulatory RNA," *Nature*, vol. 408, no. 6808, pp. 86–89, 2000.
- [25] S. Roush and F. J. Slack, "The let-7 family of microRNAs," *Trends in Cell Biology*, vol. 18, no. 10, pp. 505–516, 2008.
- [26] B. Boyerinas, S.-M. Park, A. Hau, A. E. Murmann, and M. E. Peter, "The role of let-7 in cell differentiation and cancer," *Endocrine-Related Cancer*, vol. 17, no. 1, pp. F19–F36, 2010.
- [27] J. M. Thomson, M. Newman, J. S. Parker, E. M. Morin-Kensicki, T. Wright, and S. M. Hammond, "Extensive post-transcriptional regulation of microRNAs and its implications for cancer," *Genes and Development*, vol. 20, no. 16, pp. 2202–2207, 2006.
- [28] M. H. Bao, X. Feng, Y. W. Zhang, X. Y. Lou, Y. Cheng, and H. H. Zhou, "Let-7 in cardiovascular diseases, heart development and cardiovascular differentiation from stem cells," *International Journal of Molecular Sciences*, vol. 14, no. 11, pp. 23086–23102, 2013.
- [29] W. Hou, Q. Tian, N. M. Steuerwald, L. W. Schrum, and H. L. Bonkovsky, "The let-7 microRNA enhances heme oxygenase-1 by suppressing Bach1 and attenuates oxidant injury in human hepatocytes," *Biochimica et Biophysica Acta: Gene Regulatory Mechanisms*, vol. 1819, no. 11–12, pp. 1113–1122, 2012.
- [30] S. Polikepahad, J. M. Knight, A. O. Naghavi et al., "Proinflammatory role for let-7 microRNAs in experimental asthma," *Journal of Biological Chemistry*, vol. 285, no. 39, pp. 30139–30149, 2010.
- [31] D. Iliopoulos, H. A. Hirsch, and K. Struhl, "An epigenetic switch involving NF- κ B, Lin28, Let-7 MicroRNA, and IL6 links inflammation to cell transformation," *Cell*, vol. 139, no. 4, pp. 693–706, 2009.
- [32] C. D. Johnson, A. Esquela-Kerscher, G. Stefani et al., "The let-7 microRNA represses cell proliferation pathways in human cells," *Cancer Research*, vol. 67, no. 16, pp. 7713–7722, 2007.
- [33] C. Mayr, M. T. Hemann, and D. P. Bartel, "Disrupting the pairing between let-7 and Hmga2 enhances oncogenic transformation," *Science*, vol. 315, no. 5818, pp. 1576–1579, 2007.
- [34] F. Meng, R. Henson, H. Wehbe-Janek, H. Smith, Y. Ueno, and T. Patel, "The microRNA let-7a modulates interleukin-6-dependent STAT-3 survival signaling in malignant human cholangiocytes," *The Journal of Biological Chemistry*, vol. 282, no. 11, pp. 8256–8264, 2007.
- [35] G. A. Calin, C. Sevignani, C. D. Dumitru et al., "Human microRNA genes are frequently located at fragile sites and genomic regions involved in cancers," *Proceedings of the National Academy of Sciences of the United States of America*, vol. 101, no. 9, pp. 2999–3004, 2004.
- [36] C. Liu, K. Kelnar, A. V. Vlassov, D. Brown, J. Wang, and D. G. Tang, "Distinct microRNA expression profiles in prostate cancer stem/progenitor cells and tumor-suppressive functions of let-7," *Cancer Research*, vol. 72, no. 13, pp. 3393–3405, 2012.
- [37] T. Reya, S. J. Morrison, M. F. Clarke, and I. L. Weissman, "Stem cells, cancer, and cancer stem cells," *Nature*, vol. 414, no. 6859, pp. 105–111, 2001.
- [38] L. M. Coussens and Z. Werb, "Inflammation and cancer," *Nature*, vol. 420, no. 6917, pp. 860–867, 2002.
- [39] D. Kong, S. Banerjee, A. Ahmad et al., "Epithelial to mesenchymal transition is mechanistically linked with stem cell signatures in prostate cancer cells," *PLoS ONE*, vol. 5, no. 8, Article ID e12445, 2010.
- [40] S. N. Shah, L. Cope, W. Poh et al., "HMGA1: a master regulator of tumor progression in triple-negative breast cancer cells," *PLoS ONE*, vol. 8, no. 5, Article ID e63419, 2013.
- [41] C. Zhu, J. Li, G. Cheng et al., "MiR-154 inhibits EMT by targeting HMGA2 in prostate cancer cells," *Molecular and Cellular Biochemistry*, vol. 379, no. 1–2, pp. 69–75, 2013.
- [42] S. M. Johnson, H. Grosshans, J. Shingara et al., "RAS is regulated by the let-7 microRNA family," *Cell*, vol. 120, no. 5, pp. 635–647, 2005.
- [43] K. Patel, A. Kollory, A. Takashima, S. Sarkar, D. V. Fallar, and S. K. Ghosh, "MicroRNA let-7 downregulates STAT3 phosphorylation in pancreatic cancer cells by increasing SOCS3 expression," *Cancer Letters*, vol. 347, no. 1, pp. 54–64, 2014.
- [44] M. M. Rahman, Z. R. Qian, E. L. Wang et al., "Frequent overexpression of HMGA1 and 2 in gastroenteropancreatic neuroendocrine tumours and its relationship to let-7 downregulation," *British Journal of Cancer*, vol. 100, no. 3, pp. 501–510, 2009.

- [45] S. Watanabe, Y. Ueda, S.-I. Akaboshi, Y. Hino, Y. Sekita, and M. Nakao, "HMGA2 maintains oncogenic RAS-induced epithelial-mesenchymal transition in human pancreatic cancer cells," *The American Journal of Pathology*, vol. 174, no. 3, pp. 854–868, 2009.
- [46] E. Piskounova, C. Polyarchou, J. E. Thornton et al., "Lin28A and Lin28B inhibit let-7 MicroRNA biogenesis by distinct mechanisms," *Cell*, vol. 147, no. 5, pp. 1066–1079, 2011.
- [47] A. Rybak, H. Fuchs, L. Smirnova et al., "A feedback loop comprising lin-28 and let-7 controls pre-let-7 maturation during neural stem-cell commitment," *Nature Cell Biology*, vol. 10, no. 8, pp. 987–993, 2008.
- [48] L. J. Wood, M. Mukherjee, C. E. Dolde et al., "HMG-I/Y, a new c-Myc target gene and potential oncogene," *Molecular and Cellular Biology*, vol. 20, no. 15, pp. 5490–5502, 2000.
- [49] S. Y. Sung, C. H. Liao, H. P. Wu et al., "Loss of let-7 microRNA upregulates IL-6 in bone marrow-derived mesenchymal stem cells triggering a reactive stromal response to prostate cancer," *PLoS ONE*, vol. 8, no. 8, Article ID e71637, 2013.
- [50] S. N. Shah, C. Kerr, L. Cope et al., "HMGA1 reprograms somatic cells into pluripotent stem cells by inducing stem cell transcriptional networks," *PLoS ONE*, vol. 7, no. 11, Article ID e48533, 2012.
- [51] G. M. Pierantoni, C. Rinaldo, M. Mottolise et al., "High-mobility group A1 inhibits p53 by cytoplasmic relocalization of its proapoptotic activator HIPK2," *The Journal of Clinical Investigation*, vol. 117, no. 3, pp. 693–702, 2007.
- [52] T. Ueda and M. Yoshida, "HMGB proteins and transcriptional regulation," *Biochimica et Biophysica Acta—Gene Regulatory Mechanisms*, vol. 1799, no. 1-2, pp. 114–118, 2010.
- [53] S. Lyu, Q. Yu, G. Ying et al., "Androgen receptor decreases CMYC and KRAS expression by upregulating let-7a expression in ER-, PR-, AR+ breast cancer," *International Journal of Oncology*, vol. 44, no. 1, pp. 229–237, 2013.
- [54] M. Bustin, "Revised nomenclature for high mobility group (HMG) chromosomal proteins," *Trends in Biochemical Sciences*, vol. 26, no. 3, pp. 152–153, 2001.
- [55] K. R. Diener, N. Al-Dasooqi, E. L. Lousberg, and J. D. Hayball, "The multifunctional alarmin HMGB1 with roles in the pathophysiology of sepsis and cancer," *Immunology and Cell Biology*, vol. 91, pp. 443–450, 2013.
- [56] R. Reeves, "Nuclear functions of the HMG proteins," *Biochimica et Biophysica Acta—Gene Regulatory Mechanisms*, vol. 1799, no. 1-2, pp. 3–14, 2010.
- [57] M. Fedele and A. Fusco, "HMGA and cancer," *Biochimica et Biophysica Acta: Gene Regulatory Mechanisms*, vol. 1799, no. 1-2, pp. 48–54, 2010.
- [58] Y. Tamimi, H. G. van der Poel, M.-M. Denyn et al., "Increased expression of high mobility group protein I(Y) in high grade prostatic cancer determined by in situ hybridization," *Cancer Research*, vol. 53, no. 22, pp. 5512–5516, 1993.
- [59] J.-J. Wei, X. Wu, Y. Peng et al., "Regulation of HMGA1 expression by MicroRNA-296 affects prostate cancer growth and invasion," *Clinical Cancer Research*, vol. 17, no. 6, pp. 1297–1305, 2011.
- [60] J. Hillion, L. J. Wood, M. Mukherjee et al., "Upregulation of MMP-2 by HMGA1 promotes transformation in undifferentiated, large-cell lung cancer," *Molecular Cancer Research*, vol. 7, no. 11, pp. 1803–1812, 2009.
- [61] R. Reeves, D. D. Edberg, and Y. Li, "Architectural transcription factor HMGI(Y) promotes tumor progression and mesenchymal transition of human epithelial cells," *Molecular and Cellular Biology*, vol. 21, no. 2, pp. 575–594, 2001.
- [62] N. Takaha, A. L. Hawkins, C. A. Griffin, W. B. Isaacs, and D. S. Coffey, "High mobility group protein I(Y): a candidate architectural protein for chromosomal rearrangements in prostate cancer cells," *Cancer Research*, vol. 62, no. 3, pp. 647–651, 2002.
- [63] N. Takaha, L. M. S. Resar, D. Vindivich, and D. S. Coffey, "High mobility group protein HMGI(Y) enhances tumor cell growth, invasion, and matrix metalloproteinase-2 expression in prostate cancer cells," *The Prostate*, vol. 60, no. 2, pp. 160–167, 2004.
- [64] A. Cano, M. A. Pérez-Moreno, I. Rodrigo et al., "The transcription factor Snail controls epithelial-mesenchymal transitions by repressing E-cadherin expression," *Nature Cell Biology*, vol. 2, no. 2, pp. 76–83, 2000.
- [65] J. Pérez-Losada, M. Sánchez-Martin, A. Rodríguez-García et al., "Zinc-finger transcription factor slug contributes to the function of the stem cell factor c-kit signaling pathway," *Blood*, vol. 100, no. 4, pp. 1274–1286, 2002.
- [66] I. De Martino, R. Visone, M. Fedele et al., "Regulation of microRNA expression by HMGA1 proteins," *Oncogene*, vol. 28, no. 11, pp. 1432–1442, 2009.
- [67] J. Hillion, S. Dhara, T. F. Sumter et al., "The high-mobility group A1a/signal transducer and activator of transcription-3 axis: an achilles heel for hematopoietic malignancies?" *Cancer Research*, vol. 68, no. 24, pp. 10121–10127, 2008.
- [68] O. A. Timofeeva, N. I. Tarasova, X. Zhang et al., "STAT3 suppresses transcription of proapoptotic genes in cancer cells with the involvement of its N-terminal domain," *Proceedings of the National Academy of Sciences of the United States of America*, vol. 110, no. 4, pp. 1267–1272, 2013.
- [69] D. Iliopoulos, S. A. Jaeger, H. A. Hirsch, M. L. Bulyk, and K. Struhl, "STAT3 activation of miR-21 and miR-181b-1 via PTEN and CYLD are part of the epigenetic switch linking inflammation to cancer," *Molecular Cell*, vol. 39, no. 4, pp. 493–506, 2010.
- [70] J. Ma, H. Sawai, N. Ochi et al., "PTEN regulate angiogenesis through PI3K/Akt/VEGF signaling pathway in human pancreatic cancer cells," *Molecular and Cellular Biochemistry*, vol. 331, no. 1-2, pp. 161–171, 2009.
- [71] R. Sgarra, S. Zammitti, A. Lo Sardo et al., "HMGA molecular network: from transcriptional regulation to chromatin remodeling," *Biochimica et Biophysica Acta—Gene Regulatory Mechanisms*, vol. 1799, no. 1-2, pp. 37–47, 2010.
- [72] G. Mu, H. Liu, F. Zhou et al., "Correlation of overexpression of HMGA1 and HMGA2 with poor tumor differentiation, invasion, and proliferation associated with let-7 down-regulation in retinoblastomas," *Human Pathology*, vol. 41, no. 4, pp. 493–502, 2010.
- [73] D. Palmieri, D. D'Angelo, T. Valentino et al., "Downregulation of HMGA-targeting microRNAs has a critical role in human pituitary tumorigenesis," *Oncogene*, vol. 31, no. 34, pp. 3857–3865, 2012.
- [74] M. Schubert, M. Spahn, S. Kneitz et al., "Distinct microRNA expression profile in prostate cancer patients with early clinical failure and the impact of let-7 as prognostic marker in high-risk prostate cancer," *PLoS ONE*, vol. 8, no. 6, Article ID e65064, 2013.
- [75] B. Meyer, S. Loeschke, A. Schultze et al., "HMGA2 overexpression in non-small cell lung cancer," *Molecular Carcinogenesis*, vol. 46, no. 7, pp. 503–511, 2007.
- [76] P. Rogalla, K. Drechsler, B. Kazmierczak, V. Rippe, U. Bonk, and J. Bullerdiek, "Expression of HMGI-C, a member of the high mobility group protein family, in a subset of breast cancers:

- relationship to histologic grade," *Molecular Carcinogenesis*, vol. 19, no. 3, pp. 153–156, 1997.
- [77] S. Winkler, H. M. Escobar, B. Meyer et al., "HMGA2 expression in a canine model of prostate cancer," *Cancer Genetics and Cytogenetics*, vol. 177, no. 2, pp. 98–102, 2007.
- [78] M. S. Kumar, E. Armenteros-Monterroso, P. East et al., "HMGA2 functions as a competing endogenous RNA to promote lung cancer progression," *Nature*, vol. 505, no. 7482, pp. 212–217, 2014.
- [79] M. T. Berlingieri, G. Manfioletti, M. Santoro et al., "Inhibition of HMGI-C protein synthesis suppresses retrovirally induced neoplastic transformation of rat thyroid cells," *Molecular and Cellular Biology*, vol. 15, no. 3, pp. 1545–1553, 1995.
- [80] J.-M. Berner, L. A. Meza-Zepeda, P. F. J. Kools et al., "HMGI-C, the gene for an architectural transcription factor, is amplified and rearranged in a subset of human sarcomas," *Oncogene*, vol. 14, no. 24, pp. 2935–2941, 1997.
- [81] F. di Cello, J. Hillion, A. Hristov et al., "HMGA2 participates in transformation in human lung cancer," *Molecular Cancer Research*, vol. 6, no. 5, pp. 743–750, 2008.
- [82] M. Fedele, S. Battista, G. Manfioletti, C. M. Croce, V. Giancotti, and A. Fusco, "Role of the high mobility group A proteins in human lipomas," *Carcinogenesis*, vol. 22, no. 10, pp. 1583–1591, 2001.
- [83] S. Müller, P. Scaffidi, B. Degryse et al., "The double life of HMGB1 chromatin protein: architectural factor and extracellular signal," *The EMBO Journal*, vol. 20, no. 16, pp. 4337–4340, 2001.
- [84] E. Pikarsky, R. M. Porat, I. Stein et al., "NF- κ B functions as a tumour promoter in inflammation-associated cancer," *Nature*, vol. 431, no. 7007, pp. 461–466, 2004.
- [85] J. R. van Beijnum, W. A. Buurman, and A. W. Griffioen, "Convergence and amplification of toll-like receptor (TLR) and receptor for advanced glycation end products (RAGE) signaling pathways via high mobility group B1 (HMGB1)," *Angiogenesis*, vol. 11, no. 1, pp. 91–99, 2008.
- [86] J. S. Park, D. Svetkauskaite, Q. He et al., "Involvement of toll-like receptors 2 and 4 in cellular activation by high mobility group box 1 protein," *The Journal of Biological Chemistry*, vol. 279, no. 9, pp. 7370–7377, 2004.
- [87] O. Hori, J. Brett, T. Slattery et al., "The receptor for advanced glycation end products (RAGE) is a cellular binding site for amphoterin. Mediation of neurite outgrowth and co-expression of RAGE and amphoterin in the developing nervous system," *The Journal of Biological Chemistry*, vol. 270, no. 43, pp. 25752–25761, 1995.
- [88] X. M. Chen, P. L. Splinter, S. P. O'Hara, and N. F. LaRusso, "A cellular micro-RNA, let-7i, regulates Toll-like receptor 4 expression and contributes to cholangiocyte immune responses against *Cryptosporidium parvum* infection," *The Journal of Biological Chemistry*, vol. 282, no. 39, pp. 28929–28938, 2007.
- [89] G. Li, J. Xu, and Z. Li, "Receptor for advanced glycation end products inhibits proliferation in osteoblast through suppression of Wnt, PI3K and ERK signaling," *Biochemical and Biophysical Research Communications*, vol. 423, no. 4, pp. 684–689, 2012.
- [90] J. E. Hutti, A. D. Pfefferle, S. C. Russell, M. Sircar, C. M. Perou, and A. S. Baldwin, "Oncogenic PI3K mutations lead to NF- κ B-dependent cytokine expression following growth factor deprivation," *Cancer Research*, vol. 72, no. 13, pp. 3260–3269, 2012.
- [91] M. Yu, H. Wang, A. Ding et al., "HMGB1 signals through toll-like receptor (TLR) 4 and TLR2," *Shock*, vol. 26, no. 2, pp. 174–179, 2006.
- [92] J. Li and A. M. Schmidt, "Characterization and functional analysis of the promoter of RAGE, the receptor for advanced glycation end products," *The Journal of Biological Chemistry*, vol. 272, no. 26, pp. 16498–16506, 1997.
- [93] A. Taguchi, D. C. Blood, G. Del Toro et al., "Blockade of RAGE-amphoterin signalling suppresses tumour growth and metastases," *Nature*, vol. 405, no. 6784, pp. 354–360, 2000.
- [94] D. Tang, R. Kang, H. J. Zeh III, and M. T. Lotze, "High-mobility group box 1 and cancer," *Biochimica et Biophysica Acta—Gene Regulatory Mechanisms*, vol. 1799, no. 1–2, pp. 131–140, 2010.
- [95] H. Kuniyasu, Y. Chihara, H. Kondo, H. Ohmori, and R. Ukai, "Amphoterin induction in prostatic stromal cells by androgen deprivation is associated with metastatic prostate cancer," *Oncology Reports*, vol. 10, no. 6, pp. 1863–1868, 2003.
- [96] M. Gnanasekar, R. Kalyanasundaram, G. Zheng, A. Chen, M. C. Bosland, and A. Kajdacsy-Balla, "HMGB1: a promising therapeutic target for prostate cancer," *Prostate Cancer*, vol. 2013, Article ID 157103, 8 pages, 2013.
- [97] V. Boonyaratanakornkit, V. Melvin, P. Prendergast et al., "High-mobility group chromatin proteins 1 and 2 functionally interact with steroid hormone receptors to enhance their DNA binding in vitro and transcriptional activity in mammalian cells," *Molecular and Cellular Biology*, vol. 18, no. 8, pp. 4471–4487, 1998.
- [98] J. P. Rowell, K. L. Simpson, K. Stott, M. Watson, and J. O. Thomas, "HMGB1-facilitated p53 DNA binding occurs via HMG-Box/p53 transactivation domain interaction, regulated by the acidic tail," *Structure*, vol. 20, no. 12, pp. 2014–2024, 2012.
- [99] H. Uramoto, H. Izumi, G. Nagatani et al., "Physical interaction of tumour suppressor p53/p73 with CCAAT-binding transcription factor 2 (CTF2) and differential regulation of human high-mobility group 1 (HMGI) gene expression," *The Biochemical Journal*, vol. 371, no. 2, pp. 301–310, 2003.
- [100] A. D. Saleh, J. E. Savage, L. Cao et al., "Cellular stress induced alterations in microRNA let-7a and let-7b expression are dependent on p53," *PLoS ONE*, vol. 6, no. 10, Article ID e24429, 2011.
- [101] M. Malumbres and M. Barbacid, "Cell cycle, CDKs and cancer: a changing paradigm," *Nature Reviews Cancer*, vol. 9, no. 3, pp. 153–166, 2009.
- [102] Y. Takano, Y. Kato, P. J. Van Diest, M. Masuda, H. Mitomi, and I. Okayasu, "Cyclin D2 overexpression and lack of p27 correlate positively and cyclin E inversely with a poor prognosis in gastric cancer cases," *The American Journal of Pathology*, vol. 156, no. 2, pp. 585–594, 2000.
- [103] A. Mermelshtein, A. Gerson, S. Walfisch et al., "Expression of D-type cyclins in colon cancer and in cell lines from colon carcinomas," *British Journal of Cancer*, vol. 93, no. 3, pp. 338–345, 2005.
- [104] T. Igawa, Y. Sato, K. Takata et al., "Cyclin D2 is overexpressed in proliferation centers of chronic lymphocytic leukemia/small lymphocytic lymphoma," *Cancer Science*, vol. 102, no. 11, pp. 2103–2107, 2011.
- [105] C. Zhu, P. Shao, M. Bao et al., "miR-154 inhibits prostate cancer cell proliferation by targeting CCND2," *Urologic Oncology: Seminars and Original Investigations*, vol. 32, no. 1, pp. 31.e9–31.e16, 2014.
- [106] J. Klaewongkram, Y. Yang, S. Golech, J. Katz, K. H. Kaestner, and N.-P. Weng, "Krüppel-like factor 4 regulates B cell number and activation-induced B cell proliferation," *Journal of Immunology*, vol. 179, no. 7, pp. 4679–4684, 2007.

- [107] C. Bouchard, O. Dittrich, A. Kiermaier et al., "Regulation of cyclin D2 gene expression by the Myc/Max/Mad network: Myc-dependent TRRAP recruitment and histone acetylation at the cyclin D2 promoter," *Genes & Development*, vol. 15, no. 16, pp. 2042–2047, 2001.
- [108] C. E. Nesbit, J. M. Tersak, and E. V. Prochownik, "MYC oncogenes and human neoplastic disease," *Oncogene*, vol. 18, no. 19, pp. 3004–3016, 1999.
- [109] C. V. Dang, "MYC, metabolism, cell growth, and tumorigenesis," *Cold Spring Harbor Perspectives in Medicine*, vol. 3, no. 8, 2013.
- [110] B. Nagy, A. Szendroi, and I. Romics, "Overexpression of CD24, c-myc and phospholipase 2A in prostate cancer tissue samples obtained by needle biopsy," *Pathology and Oncology Research*, vol. 15, no. 2, pp. 279–283, 2009.
- [111] R. Buttyan, I. S. Sawczuk, M. C. Benson, J. D. Siegal, and C. Olsson, "Enhanced expression of the c-myc protooncogene in high-grade human prostate cancers," *The Prostate*, vol. 11, no. 4, pp. 327–337, 1987.
- [112] J. Gil, P. Kerai, M. Lleonart et al., "Immortalization of primary human prostate epithelial cells by c-Myc," *Cancer Research*, vol. 65, no. 6, pp. 2179–2185, 2005.
- [113] S. R. Hann, "Role of post-translational modifications in regulating c-Myc proteolysis, transcriptional activity and biological function," *Seminars in Cancer Biology*, vol. 16, no. 4, pp. 288–302, 2006.
- [114] H. K. Hyeon, Y. Kuwano, S. Srikantan, K. L. Eun, J. L. Martindale, and M. Gorospe, "HuR recruits let-7/RISC to repress c-Myc expression," *Genes and Development*, vol. 23, no. 15, pp. 1743–1748, 2009.
- [115] V. B. Sampson, N. H. Rong, J. Han et al., "MicroRNA let-7a down-regulates MYC and reverts MYC-induced growth in Burkitt lymphoma cells," *Cancer Research*, vol. 67, no. 20, pp. 9762–9770, 2007.
- [116] D. Gioeli, J. W. Mandell, G. R. Petroni, H. F. Frierson Jr., and M. J. Weber, "Activation of mitogen-activated protein kinase associated with prostate cancer progression," *Cancer research*, vol. 59, no. 2, pp. 279–284, 1999.
- [117] F. Marampon, C. Ciccarelli, and B. M. Zani, "Down-regulation of c-Myc following MEK/ERK inhibition halts the expression of malignant phenotype in rhabdomyosarcoma and in non muscle-derived human tumors," *Molecular Cancer*, vol. 5, article 31, 2006.
- [118] C. Bradham and D. R. McClay, "p38 MAPK in development and cancer," *Cell Cycle*, vol. 5, no. 8, pp. 824–828, 2006.
- [119] T.-C. Chang, L. R. Zeitels, H.-W. Hwang et al., "Lin-28B transactivation is necessary for Myc-mediated let-7 repression and proliferation," *Proceedings of the National Academy of Sciences of the United States of America*, vol. 106, no. 9, pp. 3384–3389, 2009.
- [120] K. S. Sfanos and A. M. de Marzo, "Prostate cancer and inflammation: the evidence," *Histopathology*, vol. 60, no. 1, pp. 199–215, 2012.
- [121] T. Hirano, K. Yasukawa, H. Harada et al., "Complementary DNA for a novel human interleukin (BSF-2) that induces B lymphocytes to produce immunoglobulin," *Nature*, vol. 324, no. 6092, pp. 73–76, 1986.
- [122] D. P. Nguyen, J. Li, and A. K. Tewari, "Inflammation and prostate cancer: the role of interleukin 6 (IL-6)," *BJU International*, vol. 113, no. 6, pp. 986–992, 2014.
- [123] M. Okamoto, C. Lee, and R. Oyasu, "Interleukin-6 as a paracrine and autocrine growth factor in human prostatic carcinoma cells in vitro," *Cancer Research*, vol. 57, no. 1, pp. 141–146, 1997.
- [124] B. Wegiel, A. Bjartell, Z. Culig, and J. L. Persson, "Interleukin-6 activates PI3K/Akt pathway and regulates cyclin A1 to promote prostate cancer cell survival," *International Journal of Cancer*, vol. 122, no. 7, pp. 1521–1529, 2008.
- [125] P. Sivashanmugam, L. Tang, and Y. Daaka, "Interleukin 6 mediates the lysophosphatidic acid-regulated cross-talk between stromal and epithelial prostate cancer cells," *Journal of Biological Chemistry*, vol. 279, no. 20, pp. 21154–21159, 2004.
- [126] D. Giri, M. Ozen, and M. Ittmann, "Interleukin-6 is an autocrine growth factor in human prostate cancer," *The American Journal of Pathology*, vol. 159, no. 6, pp. 2159–2165, 2001.
- [127] V. Michalaki, K. Syrigos, P. Charles, and J. Waxman, "Serum levels of IL-6 and TNF- α correlate with clinicopathological features and patient survival in patients with prostate cancer," *British Journal of Cancer*, vol. 90, no. 12, pp. 2312–2316, 2004.
- [128] R. J. Simpson, A. Hammacher, D. K. Smith, J. M. Matthews, and L. D. Ward, "Interleukin-6: structure-function relationships," *Protein Science*, vol. 6, no. 5, pp. 929–955, 1997.
- [129] K. Yamaoka, P. Saharinen, M. Pesu, V. E. T. Holt III, O. Silvennoinen, and J. J. O'Shea, "The Janus kinases (Jaks)," *Genome Biology*, vol. 5, no. 12, article 253, 2004.
- [130] X. Wang, P. Lupardus, S. L. LaPorte, and K. C. Garcia, "Structural biology of shared cytokine receptors," *Annual Review of Immunology*, vol. 27, pp. 29–60, 2009.
- [131] J. N. Ihle, "The stat family in cytokine signaling," *Current Opinion in Cell Biology*, vol. 13, no. 2, pp. 211–217, 2001.
- [132] J. Scheller, A. Chalaris, D. Schmidt-Arras, and S. Rose-John, "The pro- and anti-inflammatory properties of the cytokine interleukin-6," *Biochimica et Biophysica Acta: Molecular Cell Research*, vol. 1813, no. 5, pp. 878–888, 2011.
- [133] A. Fahmi, N. Smart, A. Punn, R. Jabr, M. Marber, and R. Heads, "P42/p44-MAPK and PI3K are sufficient for IL-6 family cytokines/gp130 to signal to hypertrophy and survival in cardiomyocytes in the absence of JAK/STAT activation," *Cellular Signalling*, vol. 25, no. 4, pp. 898–909, 2013.
- [134] T. Ueda, N. Bruchovsky, and M. D. Sadar, "Activation of the androgen receptor N-terminal domain by interleukin-6 via MAPK and STAT3 signal transduction pathways," *The Journal of Biological Chemistry*, vol. 277, no. 9, pp. 7076–7085, 2002.
- [135] K. Malinowska, H. Neuwirt, I. T. Cavarretta et al., "Interleukin-6 stimulation of growth of prostate cancer *in vitro* and *in vivo* through activation of the androgen receptor," *Endocrine-Related Cancer*, vol. 16, no. 1, pp. 155–169, 2009.
- [136] L. Yang, L. Wang, H.-K. Lin et al., "Interleukin-6 differentially regulates androgen receptor transactivation via PI3K-Akt, STAT3, and MAPK, three distinct signal pathways in prostate cancer cells," *Biochemical and Biophysical Research Communications*, vol. 305, no. 3, pp. 462–469, 2003.
- [137] Y.-S. Pu, T.-C. Hour, S.-E. Chuang, A.-L. Cheng, M.-K. Lai, and M.-L. Kuo, "Interleukin-6 is responsible for drug resistance and anti-apoptotic effects in prostatic cancer cells," *Prostate*, vol. 60, no. 2, pp. 120–129, 2004.
- [138] Y. Liu, P.-K. Li, C. Li, and J. Lin, "Inhibition of STAT3 signaling blocks the anti-apoptotic activity of IL-6 in human liver cancer cells," *The Journal of Biological Chemistry*, vol. 285, no. 35, pp. 27429–27439, 2010.

- [139] C. Liu, Y. Zhu, W. Lou, Y. Cui, C. P. Evans, and A. C. Gao, "Inhibition of constitutively active Stat3 reverses enzalutamide resistance in LNCaP derivative prostate cancer cells," *The Prostate*, vol. 74, no. 2, pp. 201–209, 2014.
- [140] B. Paule, S. Terry, L. Kheuang, P. Soyeux, F. Vacherot, and A. de Taille, "The NF- κ B/IL-6 pathway in metastatic androgen-independent prostate cancer: new therapeutic approaches?" *World Journal of Urology*, vol. 25, no. 5, pp. 477–489, 2007.
- [141] D. J. Wang, A. Legesse-Miller, E. L. Johnson, and H. A. Collier, "Regulation of the let-7a-3 promoter by NF- κ B," *PLoS ONE*, vol. 7, no. 2, Article ID e31240, 2012.
- [142] S. Rose-John, G. H. Waetzig, J. Cheller, J. Grötzing, and D. Seegert, "The IL-6/sIL-6R complex as a novel target for therapeutic approaches," *Expert Opinion on Therapeutic Targets*, vol. 11, no. 5, pp. 613–624, 2007.
- [143] K. Rajalingam, R. Schreck, U. R. Rapp, and Š. Albert, "Ras oncogenes and their downstream targets," *Biochimica et Biophysica Acta: Molecular Cell Research*, vol. 1773, no. 8, pp. 1177–1195, 2007.
- [144] A. Fernández-Medarde and E. Santos, "Ras in cancer and developmental diseases," *Genes and Cancer*, vol. 2, no. 3, pp. 344–358, 2011.
- [145] P. Gideon, J. John, M. Frech et al., "Mutational and kinetic analyses of the GTPase-activating protein (GAP)-p21 interaction: the C-terminal domain of GAP is not sufficient for full activity," *Molecular and Cellular Biology*, vol. 12, no. 5, pp. 2050–2056, 1992.
- [146] K. Scheffzek, M. R. Ahmadian, W. Kabsch et al., "The Ras-RasGAP complex: structural basis for GTPase activation and its loss in oncogenic ras mutants," *Science*, vol. 277, no. 5324, pp. 333–338, 1997.
- [147] S. Schubert, K. Shannon, and G. Bollag, "Hyperactive Ras in developmental disorders and cancer," *Nature Reviews Cancer*, vol. 7, no. 4, pp. 295–308, 2007.
- [148] N. Gerits, S. Kostenko, A. Shiryaev, M. Johannessen, and U. Moens, "Relations between the mitogen-activated protein kinase and the cAMP-dependent protein kinase pathways: comradeship and hostility," *Cellular Signalling*, vol. 20, no. 9, pp. 1592–1607, 2008.
- [149] A. S. Dhillon, S. Hagan, O. Rath, and W. Kolch, "MAP kinase signalling pathways in cancer," *Oncogene*, vol. 26, no. 22, pp. 3279–3290, 2007.
- [150] G. A. Repasky, E. J. Chenette, and C. J. Der, "Renewing the conspiracy theory debate: does Raf function alone to mediate Ras oncogenesis?" *Trends in Cell Biology*, vol. 14, no. 11, pp. 639–647, 2004.
- [151] E. Castellano and J. Downward, "Ras interaction with PI3K: more than just another effector pathway," *Genes & Cancer*, vol. 2, no. 3, pp. 261–274, 2011.
- [152] J. A. Engelman, J. Luo, and L. C. Cantley, "The evolution of phosphatidylinositol 3-kinases as regulators of growth and metabolism," *Nature Reviews Genetics*, vol. 7, no. 8, pp. 606–619, 2006.
- [153] B. S. Taylor, N. Schultz, H. Hieronymus et al., "Integrative genomic profiling of human prostate cancer," *Cancer Cell*, vol. 18, no. 1, pp. 11–22, 2010.
- [154] J. A. Engelman, "The role of phosphoinositide 3-kinase pathway inhibitors in the treatment of lung cancer," *Clinical Cancer Research*, vol. 13, no. 15, part 2, pp. S4637–S4640, 2007.
- [155] M. A. Davies, "Regulation, role, and targeting of Akt in cancer," *Journal of Clinical Oncology*, vol. 29, no. 35, pp. 4715–4717, 2011.
- [156] V. Poulaki, C. S. Mitsiades, C. McMullan et al., "Regulation of vascular endothelial growth factor expression by insulin-like growth factor I in thyroid carcinomas," *The Journal of Clinical Endocrinology & Metabolism*, vol. 88, no. 11, pp. 5392–5398, 2003.
- [157] G. Niu, K. L. Wright, M. Huang et al., "Constitutive Stat3 activity up-regulates VEGF expression and tumor angiogenesis," *Oncogene*, vol. 21, no. 13, pp. 2000–2008, 2002.
- [158] L. Guo, C. Chen, M. Shi et al., "Stat3-coordinated Lin-28-let-7-HMGA2 and miR-200-ZEB1 circuits initiate and maintain oncostatin M-driven epithelial-mesenchymal transition," *Oncogene*, vol. 32, no. 45, pp. 5272–5282, 2013.
- [159] M. Colombatti, S. Grasso, A. Porzia et al., "The prostate specific membrane antigen regulates the expression of IL-6 and CCL5 in prostate tumour cells by activating the MAPK pathways," *PLoS ONE*, vol. 4, no. 2, Article ID e4608, 2009.
- [160] K. Bouchelouche, P. L. Choyke, and J. Capala, "Prostate specific membrane antigen- a target for imaging and therapy with radionuclides," *Discovery Medicine*, vol. 9, no. 44, pp. 55–61, 2010.
- [161] T. Naka, N. Nishimoto, and T. Kishimoto, "The paradigm of IL-6: from basic science to medicine," *Arthritis Research & Therapy*, vol. 4, supplement 3, pp. S233–S242, 2002.
- [162] F. Yu, H. Yao, P. Zhu et al., "let-7 regulates self renewal and tumorigenicity of breast cancer cells," *Cell*, vol. 131, no. 6, pp. 1109–1123, 2007.
- [163] W. Wahli and E. Martinez, "Superfamily of steroid nuclear receptors: positive and negative regulators of gene expression," *The FASEB Journal*, vol. 5, no. 9, pp. 2243–2249, 1991.
- [164] C. J. Brown, S. J. Goss, D. B. Lubahn et al., "Androgen receptor locus on the human X chromosome: regional localization to Xq11-12 and description of a DNA polymorphism," *The American Journal of Human Genetics*, vol. 44, no. 2, pp. 264–269, 1989.
- [165] E. P. Gelmann, "Molecular biology of the androgen receptor," *Journal of Clinical Oncology*, vol. 20, no. 13, pp. 3001–3015, 2002.
- [166] P. J. Roche, S. A. Hoare, and M. G. Parker, "A consensus DNA-binding site for the androgen receptor," *Molecular Endocrinology*, vol. 6, no. 12, pp. 2229–2235, 1992.
- [167] F. Claessens, G. Verrijdt, E. Schoenmakers et al., "Selective DNA binding by the androgen receptor as a mechanism for hormone-specific gene regulation," *The Journal of Steroid Biochemistry and Molecular Biology*, vol. 76, no. 1–5, pp. 23–30, 2001.
- [168] P. E. Lonergan and D. J. Tindall, "Androgen receptor signaling in prostate cancer development and progression," *Journal of Carcinogenesis*, vol. 10, article 20, 2011.
- [169] A. I. So, A. Hurtado-Coll, and M. E. Gleave, "Androgens and prostate cancer," *World Journal of Urology*, vol. 21, no. 5, pp. 325–337, 2003.
- [170] M. A. Titus, B. Zeithaml, B. Kantor et al., "Dominant-negative androgen receptor inhibition of intracrine androgen-dependent growth of castration-recurrent prostate cancer," *PLoS ONE*, vol. 7, no. 1, Article ID e30192, 2012.
- [171] J. A. Locke, E. S. Guns, A. A. Lubik et al., "Androgen Levels increase by intratumoral de novo steroidogenesis during progression of castration-resistant prostate cancer," *Cancer Research*, vol. 68, no. 15, pp. 6407–6415, 2008.
- [172] M.-L. Zhu and N. Kyprianou, "Androgen receptor and growth factor signaling cross-talk in prostate cancer cells," *Endocrine-Related Cancer*, vol. 15, no. 4, pp. 841–849, 2008.

- [173] Z. Guo and Y. Qiu, "A new trick of an old molecule: androgen receptor splice variants taking the stage?!" *International Journal of Biological Sciences*, vol. 7, no. 6, pp. 815–822, 2011.
- [174] K. Eisermann, C. J. Broderick, A. Bazarov, M. M. Moazam, and G. C. Fraizer, "Androgen up-regulates vascular endothelial growth factor expression in prostate cancer cells via an Sp1 binding site," *Molecular Cancer*, vol. 12, no. 1, article 7, 2013.
- [175] P. Saxena, M. Trerotola, T. Wang et al., "PSA regulates androgen receptor expression in prostate cancer cells," *Prostate*, vol. 72, no. 7, pp. 769–776, 2012.
- [176] G. Attard, C. S. Cooper, and J. S. de Bono, "Steroid hormone receptors in prostate cancer: a hard habit to break?" *Cancer Cell*, vol. 16, no. 6, pp. 458–462, 2009.
- [177] R. Tummala, N. Nadiminty, W. Lou et al., "Lin28 promotes growth of prostate cancer cells and activates the androgen receptor," *The American Journal of Pathology*, vol. 183, no. 1, pp. 288–295, 2013.

IX. Let-7 and associated genes in canine prostate cancer.

Wagner *et al.*, in preparation for submission.

As previously reviewed by us deregulation of the miRNA family *let-7* and associated genes is likely to be an important factor in PC. Thus the expression of *HMGA1*, *HMGA2*, *HMGB1*, *CCND2*, *FoIH1*, *NRAS*, *c-Myc*, *MAPK1*, *PI3KCA*, *PTEN*, *IL6*, *Klf4* and *let-7a* was analyzed in a set of 14 canine prostatic samples. Prior to the screening analyses eight novel real-time PCR assays for the canine *CCND2*, *FoIH1*, *NRAS*, *c-Myc*, *MAPK1*, *PI3KCA*, *PTEN*, and *IL6* genes were evaluated.

The screening of the canine targets revealed elevated *let-7a* levels in the diseased specimen compared to the non-neoplastic tissues. *HMGA2* was highly overexpressed in all adenocarcinoma derived tissues and cell lines, whereas *MAPK1* and *HMGB1* were decreased in the malignant samples.

In summary, four potential molecular marker for canine prostate cancer were identified building the basis for ongoing comparative cancer research.

IX.

Let-7 and associated genes in canine prostate cancer

Siegfried Wagner, Nina Eberle, Anaclet Ngezahayo, Ingo Nolte, Hugo Murua Escobar

In preparation for submission.

Own contribution:

- Partial manuscript drafting
- RNA isolation
- Quantitative real-time PCR assay design and evaluation
- Target quantification by relative real-time PCR
- Statistical analyses of real-time PCR results
- Figure preparation

Micro RNA let-7 and associated genes in canine prostate cancer

- Experimental study -

Siegfried Wagner^{1,2}, Nina Eberle¹, Marion Hewicker-Trautwein³, Anaclet Ngezahayo², Ingo Nolte^{1,§}, Hugo Murua Escobar^{1,4}

¹Small Animal Clinic, University of Veterinary Medicine Hannover, Buenteweg 9, 30559 Hannover, Germany

²Institute of Biophysics, University Hannover, Herrenhaeuserstr. 2, 30419 Hannover, Germany

³Institute of Pathology, University of Veterinary Medicine Hannover, Buenteweg 17, 30559 Hannover, Germany

⁴Division of Medicine, Dept. of Haematology/Oncology, University of Rostock, Ernst-Heydemann-Str. 6, 18057 Rostock, Germany

§Corresponding author

Email addresses:

SW: siegfried.wagner@tiho-hannover.de

NE: nina.eberle@tiho-hannover.de

MH: marion.hewicker-trautwein@tiho-hannover.de

AN: ngezahayo@biophysik.uni-hannover.de

IN: ingo.nolte@tiho-hannover.de

HME: hugo.murua.escobar@med.uni-rostock.de

Keywords: prostate cancer, molecular marker, gene regulation, dog, model organism

Abbreviated running title: Human cancer associated genes in canine prostate cancer

Abstract

Background

Prostate cancer is a polygenic, morphologically heterogeneous disease spontaneously occurring in man and dog. Canine prostate cancer is considered similar to the human an androgen independent malignancy. Herein miRNA *let-7a* and associated genes were analyzed in the context of canine prostate cancer as this miRNA as well as its targets are reported to be commonly deregulated in human cancers.

Material and Methods

Expression of miRNA *let-7a*, six direct as well as six downstream target genes were analyzed by quantitative real-time PCR in 14 canine prostate samples consisting of three non-neoplastic, four hyperplastic and four malignant tissues as well as three canine cell lines.

Results

Eight novel canine real-time PCR assays were successfully established and evaluated. Expression analyses revealed elevated *let-7a* levels in hyperplastic and malignant samples. While HMGA2 was over expressed in adenocarcinoma derived specimens *MAPK1* and *HMGB1* levels were lowest in cancerous tissues.

Conclusion

Also the *let-7a* expression was unexpectedly elevated while *MAPK1* and *HMGB1* levels were decreased in the cancerous tissues partially correlating with malignancy. The over expressed HMGA2 in the malignant samples and these three genes represent potential molecular markers for canine prostate cancer.

Introduction

Prostate cancer (PC) is a multifactorial, heterogeneous malignancy ranging from an asymptomatic to a fatal systemic clinical state (1, 2). The progress of PC is considered to be a multi-step process initiated by genetic and epigenetic alterations (1). These molecular changes favor chronic inflammation, epithelial-to-mesenchymal transition, and acquisition of stem-cell like character and additionally impact cell-cycle progression and deregulation of pathways involved in various cellular processes. Thus the identification of factors connecting these processes with tumor development would be of major value for improvements in PC treatment.

In this regard a promising master switch is potentially represented by the micro RNA *let-7* family. Micro RNAs (miRNAs) fulfill several criteria required for molecular biomarkers as they are considered to regulate more than 60 % of all protein-coding genes (3) thereby being less prone to degradation in biological fluids compared to larger RNAs (4).

The members of the *let-7* family were previously reported to be involved in diverse biological processes (5-9). Further these molecules were also found to be aberrantly expressed in a variety of human malignant neoplasias such as ovarian cancer (10), lung cancer (11), head and neck squamous cell carcinoma (12), and high-risk PC (13). Furthermore, deregulated *let-7* expression in cancer is discussed to be associated with bad patient prognosis and shortened prospective survival (11).

As previously reviewed by us (14) the deregulation of the *let-7* family directly impacts the expression of *CCND2* (8), *c-Myc* (15), *HMGA1* (13, 16), *HMGA2* (17-19), *IL6* (20), and *NRAS* (21). Furthermore, the function of these genes is tightly interwoven with the activity of *FoIH1*, *HMGB1*, *Kif4*, *MAPK1*, *PI3KCA*, and *PTEN*, which are as well commonly deregulated in human cancer (14).

Cancer research relies highly on model organisms, in this regard pet dogs are lately considered to be a valuable large animal model as neoplasias in dogs occur spontaneously under the surveillance of an intact immune system, present a similar biological manifestation and an equivalent response to therapeutic regimens (22, 23). Furthermore, the canine genome shows a higher similarity to the human genome when compared to the genomes of commonly used rodents (24). In particular the coding sequences (CDSs) of the herein investigated genes present identities ranging from 74.2 % to 96.7 % between both species. Remarkably, the mature *let-7* miRNA sequences are even up to 100 % identical (25).

Considering the physiological and molecular similarities in cancers of both species we analyzed herein the expression of the miRNA *let-7* family member *let-7a* and associated genes in the context of canine PC.

Materials and Methods

***In silico* analyses of investigated targets**

To analyse the identity of the human and canine mature *let-7a* miRNA sequences and the CDS of the analyzed protein-coding genes the following human and canine sequences were downloaded from NCBI (<http://www.ncbi.nlm.nih.gov/>) or miRBase (<http://www.mirbase.org>) data base; *CCND2* (Acc. no. NM_001759.3, XM_849493.3), *c-Myc* (Acc. no. NM_002467.4, NM_001003246.2), *FoI1* (Acc. no. NM_001014986.1, NM_001271778.1), *HMGA1* (Acc. no. NM_145899.2, NM_001003387.1), *HMGA2* (Acc. no. NM_003483.4, KC529658.1), *HMGB1* (Acc. no. NM_002128.4, NM_001002937.1), *IL6* (Acc. no., CR450296.1, NM_001003301.1), *Klf4* (Acc. no. NM_004235, XM_005626996), *let-7a* (Acc. no. MIMAT0000062, MIMAT0006594), *MAPK1* (Acc. no. NM_002745.4, NM_001110800.1), *NRAS* (Acc. no. NM_002524.4, NM_001287065.1), *PI3KCA* (Acc. no. NM_006218.2, XM_545208), and *PTEN* (Acc. no. NM_000314, NM_001003192).

All human and canine sequences for the respective target were aligned using the software tool MegAlign (DNASTAR Lasergene Version: 7.1.0 (44), Madison, USA) and compared in a one pair alignment by the Martinez-NW method.

Cell culture and sample information

Three canine prostatic cell lines CT1258 (derived from adenocarcinoma), DT08/40 (derived from a transitional cell carcinoma) and DT08/46 (derived from an adenocarcinoma) were cultured in medium 199 containing 10 % fetal calf serum (Biochrom AG, Berlin, Germany), 2 % penicillin/streptomycin (Biochrom AG, Berlin, Germany) and 29.3 ml (7.5 %) NaHCO₂ (Biochrom AG, Berlin, Germany) in a humidified atmosphere at 37°C, 5 % CO₂.

Immediately after sampling all tissue aliquots were stored at -80°C. Additional information to the donor animal age, breed, castrated status and disease are listed in table I.

Table I Sample details

Sample no.	Additional information	Breed	Age	Neutered
1	Non-neoplastic	Deutsche Dogge	5 Y	-
2	Non-neoplastic	Newfoundland dog	5 Y, 9 M	-
3	Non-neoplastic	Labrador Retriever	8 Y, 1 M	-
4	Hyperplasia	Rottweiler	8 Y, 2 M	-
5	Hyperplasia	Mixed breed	9 Y, 6 M	-
6	Hyperplasia	Yorkshire Terrier	10 Y, 3 M	x
7	Hyperplasia	Australian Shepherd	6 Y, 3 M	-
8	Transitional cell carcinoma	West-Highland Terrier	9 Y, 5 M	-
9	Adenocarcinoma	Dachshund	6 Y, 4 M	-
10	Adenocarcinoma	Mixed breed	7 Y, 10 M	-
11	Adenocarcinoma	Airedale Terrier	10 Y, 11 M	-
12	Adenocarcinoma, cell line CT1258	Briard	9 Y, 8 M	-
13	DT08/40, derive from transitional cell carcinoma	Pitbull Terrier	10 Y, 4 M	x
14	DT08/46, derived from Adenocarcinoma, sample no. 9	Dachshund	6 Y, 4 M	-

Informations about the donor animals age at time point of sampling, castration status and breed as well as the corresponding disease status and sample number.

Y = year, M = month, x = dog was castrated, - = dog was non-castrated

RNA Isolation

Small and large RNAs were purified and eluted in the same fraction from 11 frozen prostate tissue samples (Tab. I), previously homogenized using the iron-beads QIAshredder homogenizer method (Qiagen, Hilden, Germany), and the three cell lines CT1258, DT08/40 and DT08/46 according to the “NucleoSpin miRNA” protocol (Macherey & Nagel, Düren, Germany).

Subsequently RNA samples were quantified with the Synergy 2 reader (BioTek Instruments GmbH, Bad Friedrichshall, Germany) and stored at -80°C.

cDNA synthesis for conventional PCR

For subsequent quantitative real-time PCR assay evaluations 1 µg total RNA from CT1258 cells was reverse transcribed according to the “M-MLV Reverse Transcriptase” protocol (Promega, Mannheim, Germany).

qRT-PCR assay establishment for the canine *CCND2*, *PTEN*, *PIK3CA*, *c-Myc*, *IL6*, *MAPK1*, *FoIH1* and *NRAS* genes

For the evaluation of canine *CCND2* (NCBI Acc. no. XM_849493.3), *PTEN* (NCBI Acc. no. NM_001003192), *PIK3CA* (NCBI Acc. no. XM540208.4), *c-Myc* (NCBI Acc. no. NM_001003246.2), *IL6* (NCBI Acc. no. NM_001003301.1), *MAPK1* (NCBI Acc. no. NM_001110800), *FoIH1* (NCBI Acc. no. NM_001271778.1) and *NRAS* (NCBI Acc. no. NM_001287065.1) quantitative real-time PCR (qRT-PCR) assays exon spanning primers were designed using the software SeqMan Pro (DNASTAR Lasergene Version: 7.1.0 (44), Madison, USA). Sequences of all herein used primers and the sources of assays are listed in table II (supplementary file 2). Each primer pair was tested in an endpoint PCR reaction with CT1258 cDNA as template to evaluate the optimal annealing temperature. Further the reactions were cross evaluated using genomic DNA (gDNA) to exclude unspecific primer binding. The previously described *HMGA1*, *HMGA2*, *HMGB1* and *Kif4* primers (26-28), which were evaluated in combination with FAM-TAMRA probes, were evaluated for a SYBR Green based quantitative one step qRT-PCR.

PCR products were separated in 1.5 % TAE-agarose gels and isolated according to the “GenJET Gel Extraction” kit protocol (Thermoscientific, Schwerte, Germany). Amplicons were ligated into a pGEM-T Easy vector according to the “pGEM-T and pGEM-T Easy vector” protocol (Promega, Mannheim, Germany). Ligation products were cloned into the thermo competent *E. Coli* strain *DH5α* according to the “Subcloning Efficiency DH5α Competent Cells” protocol (Life Technologies, Darmstadt, Germany). Positive clones were amplified and plasmid DNA was isolated with the “GenJET PCR Purification” kit (Thermoscientific, Schwerte, Germany). DNA sequencing confirmed the specificity of each primer pair, samples were sequenced by GATC Biotech AG (Konstanz, Germany) for verification.

Reverse transcription of miRNAs

For qRT-PCR quantification of the mature *let-7a* and *RNU6B* miRNAs 30 ng total RNA were reverse transcribed according to the “TaqMan MicroRNA Reverse Transcription” protocol (Life Technologies GmbH, Darmstedt, Germany).

Relative quantitative real-time PCR

The qRT-PCR analyses were performed using the Mastercycler ep realplex (Eppendorf AG, Hamburg, Germany). Each sample was analyzed in triplicate. In each qRT-PCR run non-template and no-reverse transcriptase controls were included.

mRNA expression of the canine protein-coding genes *CCND2*, *c-Myc*, *FoIH1*, *HMGA1*, *HMGA2*, *HMGB1*, *IL6*, *Klf4*, *MAPK1*, *NRAS*, *PTEN*, and *PIK3CA* was measured relative to the housekeeping gene *ACTB*. Quantification was performed in a SYBR Green one-step qRT-PCR according to the “QuantiFast SYBR Green RT-PCR” kit protocol (Qiagen, Hilden, Germany) using 5 to 25 ng total RNA as template. The primer sequences are listed in the supplementary table II. Finally, melting curve analyses of the products were performed according to the Eppendorf instrument protocol (Eppendorf AG, Hamburg, Germany).

Relative *let-7a* miRNA levels were quantified in comparison to the *RNU6B* expression in a TaqMan based two-step qRT-PCR according to the commercially available “TaqMan miRNA Assay” protocol (Lifetechnologies, Darmstadt, Germany). For the comparison of the gene expression levels based on the $\Delta\Delta CT$ method the gene expression level of the non-neoplastic prostate sample number 1 (when expressed) was used as calibrator (calibrator expression level was set as 1).

Statistical analyses of the qRT-PCR results were done with the relative expression software tool REST 2009 (Version 2.0.13, Qiagen, Hilden, Germany). A p-value of ≤ 0.05 was considered as statistically significant.

Results

***In silico* analyses**

The *in silico* CDS comparison revealed 78.4 % homology for *CCND2*, 89.3 % for *c-Myc*, 86.4 % for *FoIH1*, 95.4 % for *HMGA1*, 96.1 % for *HMGA2*, 95.2 % for *HMGB1*, 74.7 % for *IL6*, 74.2 % for *Klf4*, 100 % for *let-7a*, 94.8 % for *MAPK1*, 95.8 % for *NRAS*, 96.1 % for *PI3KCA*, and 96.7 % for *PTEN*.

let-7a

The results of the present study revealed a more than fourfold higher *let-7a* expression in the three canine cell lines CT1258 (No.12), DT08/40 (No.13) and DT08/46 (No. 14, previously derived from prostatic adenocarcinoma sample (No. 9)) and in the hyperplastic tissue sample no. 7 when compared to the non-neoplastic sample (No. 1, set 1 as calibrator). The significances of the respective expression differences were confirmed by statistical analyses. The non-neoplastic samples no. 1-3 presented lowest *let-7a* levels (Fig. 1).

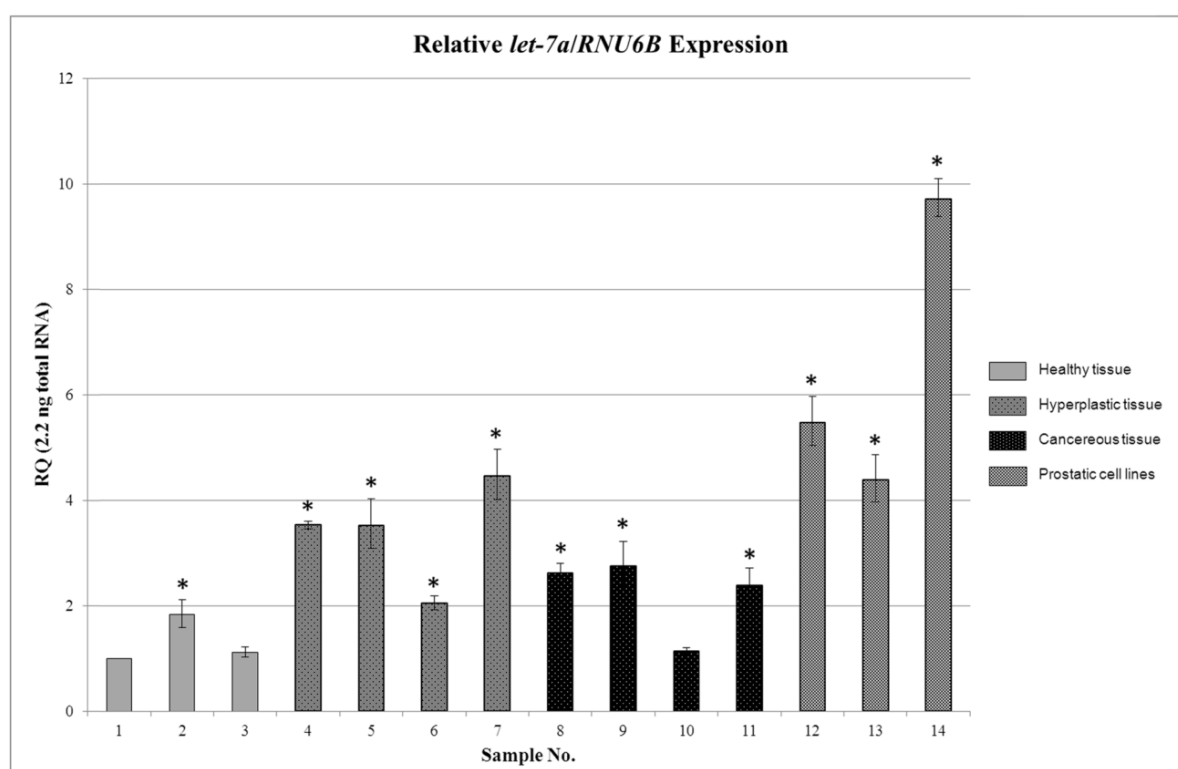


Figure 1 Relative *let-7a* to *RNU6B* expression of the canine prostatic tissue samples and cell lines. Sample no. 1 was set 1 as calibrator.* Indicates statistically significant difference to calibrator.

HMGA1

The miRNA *let-7* target *HMGA1* was 2.7 times higher expressed in CT1258 cells (No. 12). Lowest *HMGA1* levels were found in all adenocarcinoma tissue samples (No. 9-11) as well as in DT08/40 (No. 13). Between the three non-neoplastic samples the *HMGA1* expression differed approximately by factor 2.5 (No. 1 and 2). The target

levels between the adenocarcinoma sample (No. 9) and the derived cell line DT08/46 (No. 14) showed a difference of factor 4.6 (Tab. III).

HMGA2

HMGA2 was over expressed in all prostatic adenocarcinomas (No. 9-11), in the adenocarcinoma derived cell lines CT1258 and DT08/46 (No. 12, 14) and in the hyperplastic sample no. 6. The observed over expression was statistically significant. Lowest statistically relevant *HMGA2* levels were found in the residual hyperplastic specimens (No. 4, 5, 7) and in the malignant transitional cell carcinoma derived samples no. 8 and 13 (Fig. 2).

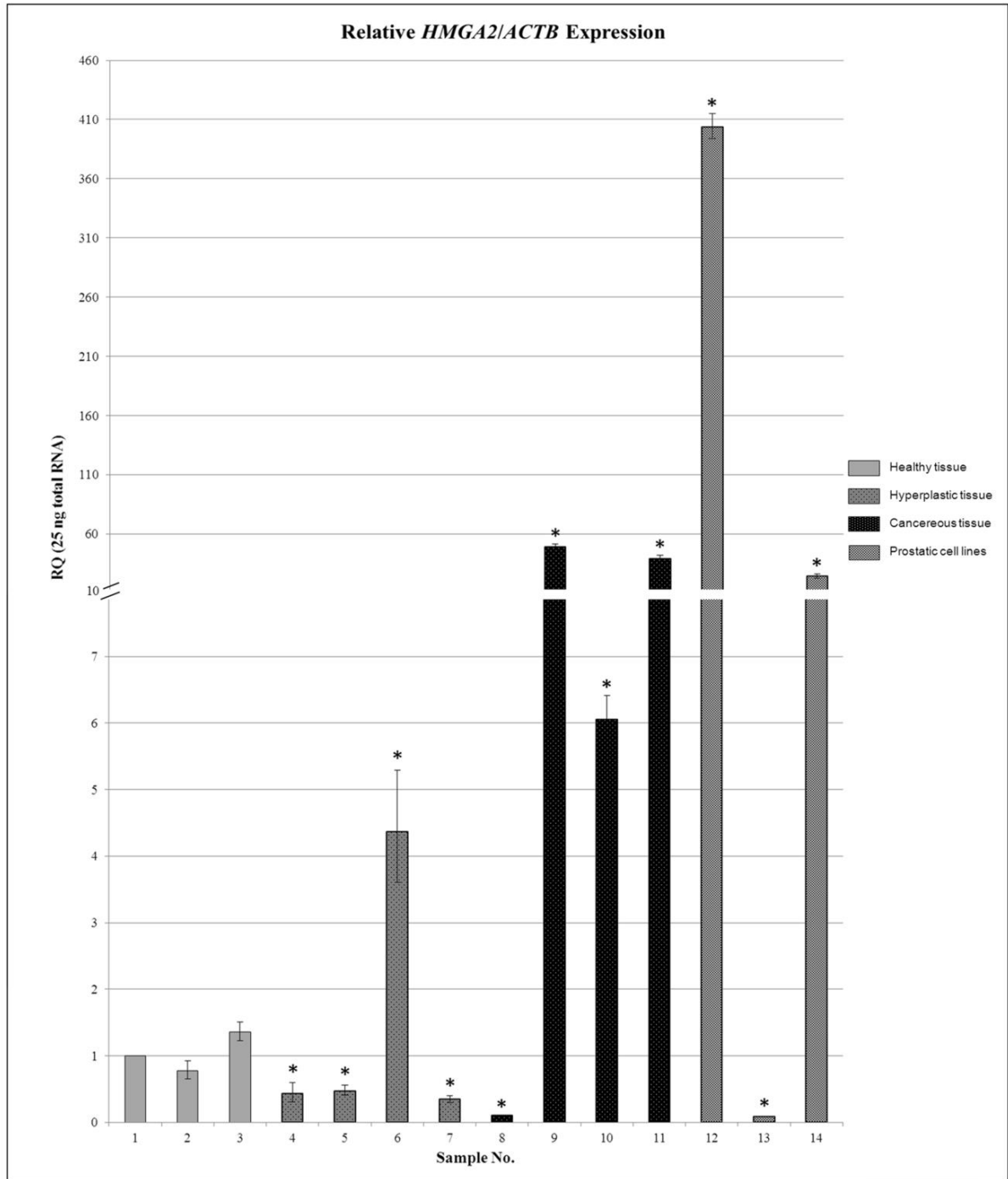


Figure 2 Relative *HMGA2* to *ACTB* expression of the canine prostatic tissue samples and cell lines. Sample no. 1 was set 1 as calibrator. * Indicates statistically significant difference in expression compared to calibrator.

HMGB1

HMGB1 transcript levels were lowest in all malignant tissues and in the adenocarcinoma derived cell lines CT1258 (No. 12) and DT08/46 (No. 14). The expression in the adenocarcinoma derived sample (No. 9) was similar to that in the derived DT08/46 cell line (No. 14). The only specimen which presented statistically significantly elevated target expression was the sample no. 7 (Fig. 3).

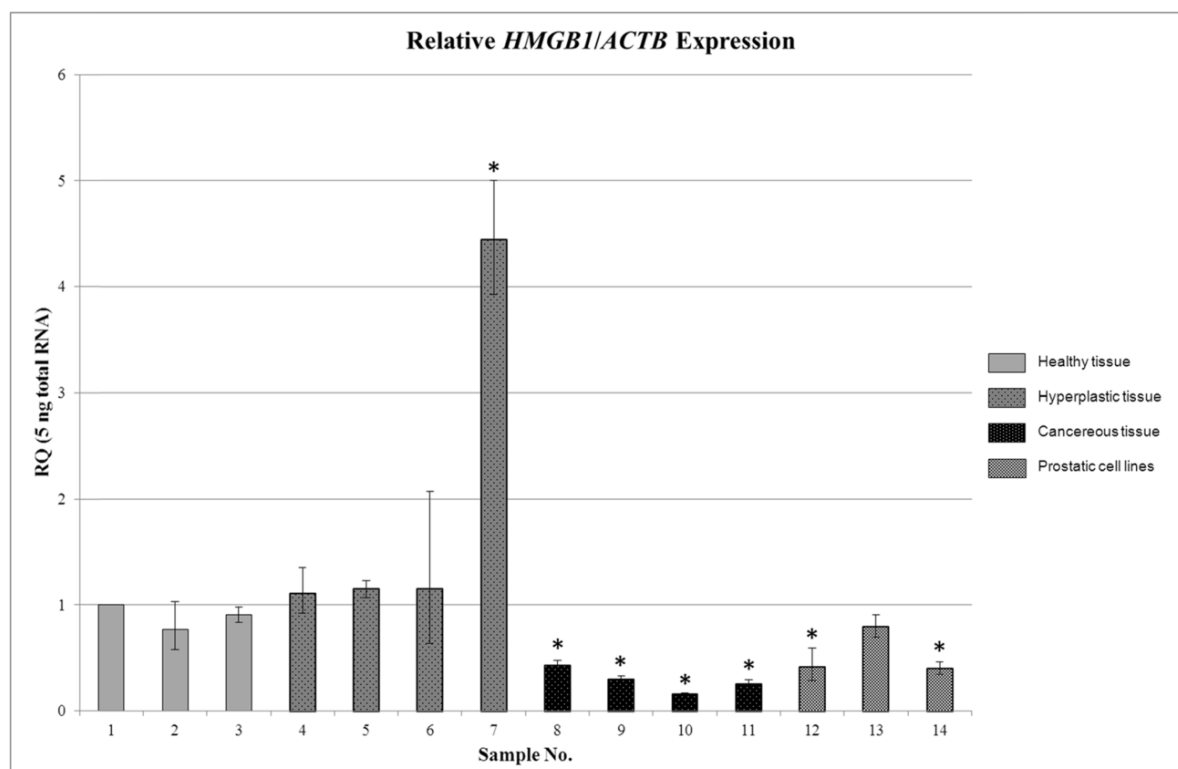


Figure 3 Relative *HMGB1* to *ACTB* expression of the canine prostatic tissue samples and cell lines. Sample no. 1 was set 1 as calibrator. * Indicates statistically significant difference in expression compared to calibrator.

CCND2

CCND2 expression was more than 600 fold higher in the hyperplastic prostate sample no. 6. More than twofold elevated cyclin levels were found in the cancer sample no. 8 and the cell line DT08/40 (No. 13) (Tab. III).

c-Myc

c-Myc levels were at least two times higher in the three cell lines and in one of the malignant prostate samples (No. 8) compared to the calibrator (No. 1). In the

malignant tissue sample no. 10 *c-Myc* levels were lowest. The difference in expression between the adenocarcinoma tissue sample (No. 9) and the corresponding cell line DT08/46 (No. 14) was more than 80 % (Tab. III).

MAPK1

MAPK1 expression was significantly lower in the malignant tumors (No. 8-11) and the cell lines DT08/40 (No.13) and DT08/46 (No.14) compared to the calibrator. The cell line CT1258 (No. 12) and one of the hyperplastic tissues (No. 7) presented elevated *MAPK1* levels. In all samples except sample no. 4 target expression was significantly different compared to the calibrator (Fig. 4).

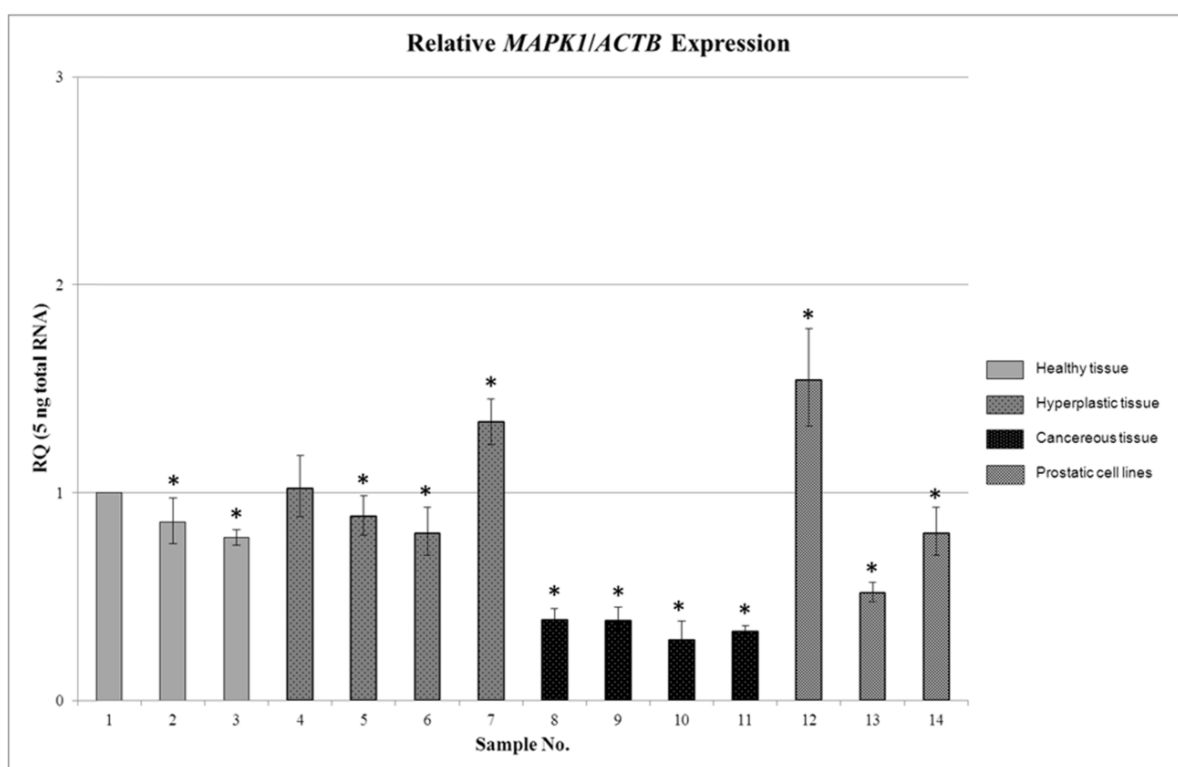


Figure 4 Relative *MAPK1* to *ACTB* expression of the canine prostatic tissue samples and cell lines. Sample no. 1 was set 1 as calibrator. * Indicates statistically significant difference in expression compared to calibrator.

NRAS

The *NRAS* levels were highest in the samples no. 7 and 8. However they differed not more than two fold. The other samples had lower *NRAS* levels than the calibrator but not less than 60 % (Tab. III).

Klf4

Klf4 expression was 1.7 fold higher in the malignant PC sample no. 8 and presented lowest levels in the malignant samples no. 9 and 10. In comparison to the adenocarcinoma tissue sample no. 9 the *Klf4* levels were threefold higher in the derived cell line (No. 14) (Tab. III).

PTEN

PTEN levels were highest in the hyperplastic tissue sample no. 7. The lowest levels were found in the malignant samples no. 8, 10 and additionally in the cell line DT08/46 (No. 14) (Tab. III).

IL6

According to the measured Ct values, *IL6* expression was highest in the malignant tissues (No. 8-11) additionally in the hyperplastic sample no. 5-7 but lowest in all cell lines (No. 12-14), the non-neoplastic samples no. 2-3 and in the hyperplastic tissue sample (No. 4) (Tab. III).

FoIH1

FoIH1 was not detectable in neither of the analyzed samples except at very low levels in the three analyzed cell lines with Ct values higher than 35.

PIK3CA

The relative *PIK3CA* expression was lowest in the non-neoplastic tissue sample no. 3 presenting the highest Ct value (Ct >39) (Tab. III) and the samples no. 2, 6, 8 and 10.

Discussion

The master regulator *let-7* and its direct and downstream targets reveal a very complex regulatory network, presenting positive and negative feedback loops to several cancer associated genes (14).

Notably, in humans abnormal *let-7* expression was associated with tumor malignancy and worse disease outcome after therapy (29-31) indicating a potentially central role in cancer development and progression.

In this regard, gamma-radiation of the human lung cancer cell line H1299 induced suppression of *let-7g* was demonstrated to reduce the sensitivity of cells to radiation

treatment (29). Additionally, an ectopic *let-7c* expression in the docetaxel (DTX) resistant human lung adenocarcinoma cell lines SPC-A1/DTX and H1299/DTX was reported to increase the *in vitro* and *in vivo* chemo- or radiosensitivity (30).

The herein performed analysis of the *let-7* miRNA family member *let-7a* in canine prostatic samples revealed a more than twofold higher expression in the hyperplastic and all malignant samples except sample no. 10. Elevated *let-7a* expression was present in the hyperplastic and malignant samples with highest levels (more than fourfold) in one of the hyperplastic tissue samples as well as in the three analyzed prostatic cell lines. These results are at the first glance unexpected as the *let-7* family was reported to be frequently down regulated in many human malignant neoplasias such as lung cancer (11), gastric tumors (32) and colon cancer (33). Matching these results the *let-7* family discussed to be acting as an oncogene suppressor (34, 35). A possible explanation for the herein observed increased *let-7a* levels in the hyperplastic and malignant samples might be that the canine cells respond to the elevated expression of oncogenes by up regulating its suppressor as indicated in Willenbrock *et al.* (36).

However, deregulated *let-7* levels appear to be associated with human PC and as shown herein with elevated expression in canine prostatic tissues and cell lines. Whether the observed elevation is an early event in transformation remains unclear, as only the miRNA and respective direct and indirect targets were analyzed. However, as an elevation is also seen in the analyzed hyperplasias an early deregulation appears likely.

The analyses of one of the most popular *let-7* targets the *HMGA1*, which is implicated in epithelial-to-mesenchymal transition (37) and stemness (38), was only higher expressed in the cell line CT1258 (No. 12) compared to the reference sample. The other samples presented lower *HMGA1* levels with lowest expression in the malignant tissues (No. 9-11). *HMGA1* levels were described to be low in human, murine and canine healthy tissues (28, 39). It is of interest that herein the *HMGA1* levels are very low in the malignant samples except in the cell line CT1258 (No. 12) and even varied remarkably between the presented non-neoplastic tissues. Thus at first glance the *HMGA1* appears likely to play a subordinate role in advanced canine PC. However the much lower levels in the malignant samples compared to the non-neoplastic and hyperplastic tissues are remarkable.

As mentioned before the analysis of *HMGA2* revealed significant up regulation in all adenocarcinoma derived samples, matching our previously reports describing overexpression in canine prostatic adenocarcinomas (40). Interestingly, *HMGA2* was low in the transitional cell carcinoma derived tissue no. 9 as well as the cell line DT08/40 (No. 13). However, as the number of samples is small, this has to be proven in following studies. Interestingly, the cell line DT08/46 (No. 14), which was derived from the adenocarcinoma sample (No. 9), showed similar *HMGA2* levels as the original tissue.

The *HMGA1/2* sister gene *HMGB1* was only over expressed in one of the analyzed hyperplastic samples (No. 7). In contrast a the significantly lower *HMGB1* expression in the malignant samples (No. 8-12 and 14) appears interesting as *HMGB1* was reported to be deregulated in various human cancers and might be a canine PC associated deregulation but must be further investigated.

The cyclin *CCND2* was, similarly to *HMGA2*, over expressed in one of the hyperplastic samples (No. 6) and presented more than 2 fold higher expression levels in the malignant samples no. 8 and 13. The expression of the oncogene *c-Myc* is at least two fold higher in the malignant samples no. 8, 12, 13, and 14 when compared to the reference sample (No. 1). The remarkable difference between *c-Myc* levels in the tissue sample (No. 8) and the derived cell line DT08/46 (No. 14) shows that gene expression can differ greatly, among others due to chromosomal aberrations and mutations, between original tissues and derived cell lines. Interestingly, the *c-Myc* levels were highest in the three cell lines. However, a correlation between *c-Myc* and canine PC was not found in the used set of prostatic samples.

In accordance to a previous report, where human PC-3 cells were reported to exhibit a defective *MAPK* pathway (41), *MAPK1* expression was lowest in all malignant canine tissues. Reconstitution of this pathway by expression of a constitutively active, recombinant *MAPK1* was shown to reverse the neoplastic phenotype effectively and prevented aberrant cell proliferation (41). On the other hand up regulated *MAPK1* was monitored to be associated with survival of castrate-resistant human PCs (42).

IL6 expression is highest in the cancerous tissue no. 11. Interestingly *IL6* levels were lowest in the three non-neoplastic tissues as well as in the cell lines, which might be the result of the *in vitro* cultivation over a long period. However, the potential of *IL6* as diagnostic marker for canine PC appears to be low.

NRAS, *PIK3CA*, *PTEN*, and *Klf4* seemed as well not to correlate with canine PC.

The canine *FoIH1* mRNA was, in accordance with Aggarwal *et al.*, not detectable in neither of the analyzed prostatic tissues except at very low levels in the human cell lines (43). However, Lai *et al.* reported a *FoIH1* over expression in canine PC. As the herein used qRT-PCR assay was not amplifying the same transcript region the *FoIH1* the difference might be explained by the detection of different splice variants.

All of the herein analyzed genes were previously shown to be implicated in a variety of human malignant neoplasias. In accordance, the results of the present study showed as well an aberrant expression of four of these, the *let-7a*, *HMGA2*, *MAPK1* and *HMGB1* in the canine prostate cancer samples.

The average donor animal age of the malignant samples was approximately 9 years confirming the observation that older individuals are more often affected by this malignancy (44). Additionally, in accordance with previous reports the risk to develop prostate cancer appears to be increased in non-castrated dogs (45, 46) as all donor animals except one (sample no. 13) of the malignant samples were non-castrated (Tab. I).

However, this study has some limitations such as the low sample number (n=14) due to the low incidence of canine PC, which is ranging between 0.2 and 0.6 % (47) and the resulting limited availability of fresh prostatic tissue.

Additionally, qPCR assays in general should be evaluated carefully as the most are not adequate to discriminate between transcripts with mutations, which could have additional to the simple deregulation also a major impact on the functionality of the target gene. Furthermore, it is of interest that canine PCs present, similarly to other types of cancer, an accumulation of heterogeneous cells. Thus the up or down regulation of the gene of interest in a specific cell population might be titrated away as several thousands of cells were used for the RNA isolation.

As the expression and function of genes are context dependent the herein observed discrepancies in target gene expression levels between the previously described human and the analyzed canine prostatic tissues are not consequently revealing a contradictory as they do not necessary reflect the gene product activity in a cell.

Thus for future studies it could be advantageous to separate the cells in subpopulations due to different physical/molecular parameters and afterwards to analyze target expression and activity in each of these.

Conclusion

Herein we present four potential biomarkers for canine PC and additionally eight novel potent qRT-PCR assays for comparative studies in the dog. Although identification of good molecular PC markers is challenging it is still necessary and will deliver benefits for both species in future

Acknowledgments

We thank DVM Heike Thiemeyer who provided the data on canine patients and samples history of the samples/donors and made an important finding underlining the outcome of the present study.

References

- 1 Kopper L and Timar J: Genomics of prostate cancer: is there anything to "translate"? *Pathol Oncol Res* 11: 197-203, 2005.
- 2 Prajapati A, Gupta S, Mistry B, and Gupta S: Prostate stem cells in the development of benign prostate hyperplasia and prostate cancer: emerging role and concepts. *BioMed research international* 2013: 107954, 2013.
- 3 Davis BN and Hata A: Regulation of MicroRNA Biogenesis: A miRiad of mechanisms. *Cell Commun Signal* 7: 18, 2009.
- 4 Chen X, Ba Y, Ma L, Cai X, Yin Y, Wang K, Guo J, Zhang Y, Chen J, Guo X, Li Q, Li X, Wang W, Zhang Y, Wang J, Jiang X, Xiang Y, Xu C, Zheng P, Zhang J, Li R, Zhang H, Shang X, Gong T, Ning G, Wang J, Zen K, Zhang J, and Zhang CY: Characterization of microRNAs in serum: a novel class of biomarkers for diagnosis of cancer and other diseases. *Cell research* 18: 997-1006, 2008.
- 5 Iliopoulos D, Hirsch HA, and Struhl K: An epigenetic switch involving NF-kappaB, Lin28, Let-7 MicroRNA, and IL6 links inflammation to cell transformation. *Cell* 139: 693-706, 2009.
- 6 Chang CJ, Hsu CC, Chang CH, Tsai LL, Chang YC, Lu SW, Yu CH, Huang HS, Wang JJ, Tsai CH, Chou MY, Yu CC, and Hu FW: Let-7d functions as novel regulator of epithelial-mesenchymal transition and chemoresistant property in oral cancer. *Oncology reports* 26: 1003-1010, 2011.
- 7 Legesse-Miller A, Elemento O, Pfau SJ, Forman JJ, Tavazoie S, and Collier HA: let-7 Overexpression leads to an increased fraction of cells in G2/M, direct down-regulation of Cdc34, and stabilization of Wee1 kinase in primary fibroblasts. *The Journal of biological chemistry* 284: 6605-6609, 2009.
- 8 Dong Q, Meng P, Wang T, Qin W, Qin W, Wang F, Yuan J, Chen Z, Yang A, and Wang H: MicroRNA let-7a inhibits proliferation of human prostate cancer cells in vitro and in vivo by targeting E2F2 and CCND2. *PloS one* 5: e10147, 2010.
- 9 Schultz J, Lorenz P, Gross G, Ibrahim S, and Kunz M: MicroRNA let-7b targets important cell cycle molecules in malignant melanoma cells and interferes with anchorage-independent growth. *Cell research* 18: 549-557, 2008.
- 10 Shell S, Park SM, Radjabi AR, Schickel R, Kistner EO, Jewell DA, Feig C, Lengyel E, and Peter ME: Let-7 expression defines two differentiation stages of cancer. *Proceedings of the National Academy of Sciences of the United States of America* 104: 11400-11405, 2007.
- 11 Takamizawa J, Konishi H, Yanagisawa K, Tomida S, Osada H, Endoh H, Harano T, Yatabe Y, Nagino M, Nimura Y, Mitsudomi T, and Takahashi T: Reduced expression of the let-7 microRNAs in human lung cancers in association with shortened postoperative survival. *Cancer research* 64: 3753-3756, 2004.
- 12 Childs G, Fazzari M, Kung G, Kawachi N, Brandwein-Gensler M, McLemore M, Chen Q, Burk RD, Smith RV, Prystowsky MB, Belbin TJ, and Schlecht NF: Low-level expression of microRNAs let-7d and miR-205 are prognostic markers of head and neck squamous cell carcinoma. *The American journal of pathology* 174: 736-745, 2009.
- 13 Schubert M, Spahn M, Kneitz S, Scholz CJ, Joniau S, Stroebel P, Riedmiller H, and Kneitz B: Distinct microRNA expression profile in prostate cancer patients with early clinical failure and the impact of let-7 as prognostic marker in high-risk prostate cancer. *PloS one* 8: e65064, 2013.
- 14 Wagner S, Ngezhayo A, Murua Escobar H, and Nolte I: Role of miRNA and Its Major Targets in Prostate Cancer. *BioMed research international* 2014: 376326, 2014.

- 15 Sampson VB, Rong NH, Han J, Yang Q, Aris V, Soteropoulos P, Petrelli NJ, Dunn SP, and Krueger LJ: MicroRNA let-7a down-regulates MYC and reverts MYC-induced growth in Burkitt lymphoma cells. *Cancer research* 67: 9762-9770, 2007.
- 16 Rahman MM, Qian ZR, Wang EL, Sultana R, Kudo E, Nakasono M, Hayashi T, Kakiuchi S, and Sano T: Frequent overexpression of HMGA1 and 2 in gastroenteropancreatic neuroendocrine tumours and its relationship to let-7 downregulation. *British journal of cancer* 100: 501-510, 2009.
- 17 Mayr C, Hemann MT, and Bartel DP: Disrupting the pairing between let-7 and Hmga2 enhances oncogenic transformation. *Science (New York, NY)* 315: 1576-1579, 2007.
- 18 Kumar MS, Armenteros-Monterroso E, East P, Chakravorty P, Matthews N, Winslow MM, and Downward J: HMGA2 functions as a competing endogenous RNA to promote lung cancer progression. *Nature* 505: 212-217, 2014.
- 19 Park SM, Shell S, Radjabi AR, Schickel R, Feig C, Boyerinas B, Dinulescu DM, Lengyel E, and Peter ME: Let-7 prevents early cancer progression by suppressing expression of the embryonic gene HMGA2. *Cell cycle (Georgetown, Tex)* 6: 2585-2590, 2007.
- 20 Sung SY, Liao CH, Wu HP, Hsiao WC, Wu IH, Jinpu, Yu, Lin SH, and Hsieh CL: Loss of let-7 microRNA upregulates IL-6 in bone marrow-derived mesenchymal stem cells triggering a reactive stromal response to prostate cancer. *PLoS one* 8: e71637, 2013.
- 21 Johnson SM, Grosshans H, Shingara J, Byrom M, Jarvis R, Cheng A, Labourier E, Reinert KL, Brown D, and Slack FJ: RAS is regulated by the let-7 microRNA family. *Cell* 120: 635-647, 2005.
- 22 Waters DJ, Hayden DW, Bell FW, Klausner JS, Qian J, and Bostwick DG: Prostatic intraepithelial neoplasia in dogs with spontaneous prostate cancer. *The Prostate* 30: 92-97, 1997.
- 23 Leroy BE and Northrup N: Prostate cancer in dogs: comparative and clinical aspects. *Vet J* 180: 149-162, 2009.
- 24 Lindblad-Toh K, Wade CM, Mikkelsen TS, Karlsson EK, Jaffe DB, Kamal M, Clamp M, Chang JL, Kulbokas EJ, 3rd, Zody MC, Mauceli E, Xie X, Breen M, Wayne RK, Ostrander EA, Ponting CP, Galibert F, Smith DR, DeJong PJ, Kirkness E, Alvarez P, Biagi T, Brockman W, Butler J, Chin CW, Cook A, Cuff J, Daly MJ, DeCaprio D, Gnerre S, Grabherr M, Kellis M, Kleber M, Bardeleben C, Goodstadt L, Heger A, Hitte C, Kim L, Koepfli KP, Parker HG, Pollinger JP, Searle SM, Sutter NB, Thomas R, Webber C, Baldwin J, Abebe A, Abouelleil A, Aftuck L, Ait-Zahra M, Aldredge T, Allen N, An P, Anderson S, Antoine C, Arachchi H, Aslam A, Ayotte L, Bachantsang P, Barry A, Bayul T, Benamara M, Berlin A, Bessette D, Blitshteyn B, Bloom T, Blye J, Boguslavskiy L, Bonnet C, Boukhgalter B, Brown A, Cahill P, Calixte N, Camarata J, Cheshatsang Y, Chu J, Citroen M, Collymore A, Cooke P, Dawoe T, Daza R, Decktor K, DeGray S, Dhargay N, Dooley K, Dooley K, Dorje P, Dorjee K, Dorris L, Duffey N, Dupes A, Egbiremolen O, Elong R, Falk J, Farina A, Faro S, Ferguson D, Ferreira P, Fisher S, FitzGerald M, Foley K, Foley C, Franke A, Friedrich D, Gage D, Garber M, Gearin G, Giannoukos G, Goode T, Goyette A, Graham J, Grandbois E, Gyaltsen K, Hafez N, Hagopian D, Hagos B, Hall J, Healy C, Hegarty R, Honan T, Horn A, Houde N, Hughes L, Hunnicutt L, Husby M, Jester B, Jones C, Kamat A, Kanga B, Kells C, Khazanovich D, Kieu AC, Kisner P, Kumar M, Lance K, Landers T, Lara M, Lee W, Leger JP, Lennon N, Leuper L, LeVine S, Liu J, Liu X, Lokyitsang Y, Lokyitsang T, Lui A, Macdonald J, Major J, Marabella R, Maru K, Matthews C, McDonough S, Mehta T, Meldrim J, Melnikov A, Meneus L, Mihalev A, Mihova T, Miller K, Mittelman R, Mlenga V, Mulrain L, Munson G, Navidi A, Naylor J, Nguyen T, Nguyen N, Nguyen C, Nguyen T, Nicol R, Norbu N, Norbu C, Novod N, Nyima T, Olandt P, O'Neill B, O'Neill K, Osman S, Oyono L, Patti C, Perrin D, Phunkhang P, Pierre F, Priest M, Rachupka A, Raghuraman S, Rameau R, Ray V, Raymond C, Rege F, Rise C, Rogers J, Rogov P, Sahalie J, Settipalli S, Sharpe T, Shea

- T, Sheehan M, Sherpa N, Shi J, Shih D, Sloan J, Smith C, Sparrow T, Stalker J, Stange-Thomann N, Stavropoulos S, Stone C, Stone S, Sykes S, Tchuinga P, Tenzing P, Tesfaye S, Thoulutsang D, Thoulutsang Y, Topham K, Topping I, Tsamla T, Vassiliev H, Venkataraman V, Vo A, Wangchuk T, Wangdi T, Weiland M, Wilkinson J, Wilson A, Yadav S, Yang S, Yang X, Young G, Yu Q, Zainoun J, Zembek L, Zimmer A and Lander ES: Genome sequence, comparative analysis and haplotype structure of the domestic dog. *Nature* 438: 803-819, 2005.
- 25 Wagner S, Willenbrock S, Nolte I, and Murua Escobar H: Comparison of non-coding RNAs in human and canine cancer. *Frontiers in genetics* 4: 46, 2013.
- 26 Sterenczak KA, Kleinschmidt S, Wefstaedt P, Eberle N, Hewicker-Trautwein M, Bullerdiek J, Nolte I, and Murua Escobar H: Quantitative PCR and immunohistochemical analyses of HMGB1 and RAGE expression in canine disseminated histiocytic sarcoma (malignant histiocytosis). *Anticancer research* 31: 1541-1548, 2011.
- 27 Ismail AA, Wagner S, Murua Escobar H, Willenbrock S, Sterenczak KA, Samy MT, Abd El-Aal AM, Nolte I, and Wefstaedt P: Effects of high-mobility group a protein application on canine adipose-derived mesenchymal stem cells in vitro. *Veterinary medicine international* 2012: 752083, 2012.
- 28 Joetzke AE, Sterenczak KA, Eberle N, Wagner S, Soller JT, Nolte I, Bullerdiek J, Murua Escobar H, and Simon D: Expression of the high mobility group A1 (HMGA1) and A2 (HMGA2) genes in canine lymphoma: analysis of 23 cases and comparison to control cases. *Veterinary and comparative oncology* 8: 87-95, 2010.
- 29 Arora H, Qureshi R, Jin S, Park AK, and Park WY: miR-9 and let-7g enhance the sensitivity to ionizing radiation by suppression of NFKappaB1. *Experimental & molecular medicine* 43: 298-304, 2011.
- 30 Cui SY, Huang JY, Chen YT, Song HZ, Feng B, Huang GC, Wang R, Chen LB, and De W: Let-7c governs the acquisition of chemo- or radioresistance and epithelial-to-mesenchymal transition phenotypes in docetaxel-resistant lung adenocarcinoma. *Mol Cancer Res* 11: 699-713, 2013.
- 31 Sugimura K, Miyata H, Tanaka K, Hamano R, Takahashi T, Kurokawa Y, Yamasaki M, Nakajima K, Takiguchi S, Mori M, and Doki Y: Let-7 expression is a significant determinant of response to chemotherapy through the regulation of IL-6/STAT3 pathway in esophageal squamous cell carcinoma. *Clin Cancer Res* 18: 5144-5153, 2012.
- 32 Zhang HH, Wang XJ, Li GX, Yang E, and Yang NM: Detection of let-7a microRNA by real-time PCR in gastric carcinoma. *World J Gastroenterol* 13: 2883-2888, 2007.
- 33 Akao Y, Nakagawa Y, and Naoe T: let-7 microRNA functions as a potential growth suppressor in human colon cancer cells. *Biological & pharmaceutical bulletin* 29: 903-906, 2006.
- 34 Buechner J, Tomte E, Haug BH, Henriksen JR, Lokke C, Flaegstad T, and Einvik C: Tumour-suppressor microRNAs let-7 and mir-101 target the proto-oncogene MYCN and inhibit cell proliferation in MYCN-amplified neuroblastoma. *British journal of cancer* 105: 296-303, 2011.
- 35 Lee YS and Dutta A: The tumor suppressor microRNA let-7 represses the HMGA2 oncogene. *Genes & development* 21: 1025-1030, 2007.
- 36 Willenbrock S, Wagner S, Reimann-Berg N, Moulay M, Hewicker-Trautwein M, Nolte I, and Murua Escobar H: Generation and Characterisation of a Canine EGFP-HMGA2 Prostate Cancer In Vitro Model. *PloS one* 9: e98788, 2014.
- 37 Pegoraro S, Ros G, Piazza S, Sommaggio R, Ciani Y, Rosato A, Sgarra R, Del Sal G, and Manfioletti G: HMGA1 promotes metastatic processes in basal-like breast cancer regulating EMT and stemness. *Oncotarget* 4: 1293-1308, 2013.

- 38 Shah SN, Kerr C, Cope L, Zambidis E, Liu C, Hillion J, Belton A, Huso DL, and Resar LM: HMGA1 reprograms somatic cells into pluripotent stem cells by inducing stem cell transcriptional networks. *PloS one* 7: e48533, 2012.
- 39 Chiappetta G, Avantiaggiato V, Visconti R, Fedele M, Battista S, Trapasso F, Merciai BM, Fidanza V, Giancotti V, Santoro M, Simeone A, and Fusco A: High level expression of the HMGI (Y) gene during embryonic development. *Oncogene* 13: 2439-2446, 1996.
- 40 Winkler S, Murua Escobar H, Meyer B, Simon D, Eberle N, Baumgartner W, Loeschke S, Nolte I, and Bullerdiek J: HMGA2 expression in a canine model of prostate cancer. *Cancer genetics and cytogenetics* 177: 98-102, 2007.
- 41 Moro L, Arbini AA, Marra E, and Greco M: Constitutive activation of MAPK/ERK inhibits prostate cancer cell proliferation through upregulation of BRCA2. *International journal of oncology* 30: 217-224, 2007.
- 42 Mukherjee R, McGuinness DH, McCall P, Underwood MA, Seywright M, Orange C, and Edwards J: Upregulation of MAPK pathway is associated with survival in castrate-resistant prostate cancer. *British journal of cancer* 104: 1920-1928, 2011.
- 43 Aggarwal S, Ricklis RM, Williams SA, and Denmeade SR: Comparative study of PSMA expression in the prostate of mouse, dog, monkey, and human. *The Prostate* 66: 903-910, 2006.
- 44 Waters DJ, Patronek GJ, Bostwick DG, and Glickman LT: Comparing the age at prostate cancer diagnosis in humans and dogs. *Journal of the National Cancer Institute* 88: 1686-1687, 1996.
- 45 Sorenmo KU, Goldschmidt M, Shofer F, Goldkamp C, and Ferracone J: Immunohistochemical characterization of canine prostatic carcinoma and correlation with castration status and castration time. *Veterinary and comparative oncology* 1: 48-56, 2003.
- 46 Teske E, Naan EC, van Dijk EM, Van Garderen E, and Schalken JA: Canine prostate carcinoma: epidemiological evidence of an increased risk in castrated dogs. *Molecular and cellular endocrinology* 197: 251-255, 2002.
- 47 Withrow JS and Vail DM: Withrow and MacEwen's Small Animal Clinical Oncology. Saunders Company, St Louis Missouri 63146 Fifth edition 2012.
- 48 Sterenczak KA, Joetzke AE, Willenbrock S, Eberle N, Lange S, Junghanss C, Nolte I, Bullerdiek J, Simon D, and Murua Escobar H: High-mobility group B1 (HMGB1) and receptor for advanced glycation end-products (RAGE) expression in canine lymphoma. *Anticancer research* 30: 5043-5048, 2010.

Supplementary File

Table II Quantitative real-time PCR assay information

Primer/assay name	Primer sequence	Previously described
hsa-let-7a	Information not provided by manufacturer	Life Technologies GmbH, Darmstadt, Germany
RNU6B	Information not provided by manufacturer	Life Technologies GmbH, Darmstadt, Germany
cfa_ACTB_up cfa_ACTB_lo	TCGCTGACAGGATGCAGAAG GTGGACAGTGAGGCCAGGAT	Dr. Sabine Essler, Institute of Immunology, University of Veterinary Medicine Vienna, Austria.
cfa_HMGA1_up cfa_HMGA1_lo	ACCCAGTGAAGTGCCAACACCTAA CCTCCTTCTCCAGTTTTTTGGGTCT	[28]
cfa_HMGA2_up cfa_HMGA2_lo	AGTCCCTCCAAAGCAGCTCAAAG GCCATTTCTAGGTCTGCCTC	[28]
cfa_HMGB1_up cfa_HMGB1_lo	AAGTGAGAGCCAGACGGG TCCTTTGCCCATGTTTAATTATTTTC	[48]
cfa_Klf4_up cfa_Klf4_lo	CCACATTAATGAGGCCAGCCA CTCCCGCCAGCGGTTATT	
cfa_Myc_up cfa_Myc_lo	TCGACTCTCTGCTCTCCTC TTCTTCTCCGAGTCGCT	-
cfa_FolH1_up cfa_FolH1_lo	CATGCCCAGAATTAGTAAGTT CAATGGATAACTCCTGAATTTG	-
cfa_IL6_up cfa_IL6_lo	AATCTGGGTTCAATCAGGAGA GATCTTGTACTIONCATGTGCA	-
cfa_MAPK1_up cfa_MAPK1_lo	CTCAAGATCTGTGACTTTGGCTT ACTTGGTATAGCCCTTGAATT	-
cfa_NRas_up cfa_NRas_lo	CTTCCTCTGTGTATTTGCCAT CCTTGTTGGCAAATCACACTT	-
cfa_CCND2_up cfa_CCND2_lo	ATCGAGGAGCGCTACCTT CTCACAGACCTCCAGCAT	-
cfa_PIK3CA_up cfa_PIK3CA_lo	TTCTAATCCCAGGTGGAATGA CAATGGACAGTGTTCTCTTT	-
cfa_PTEN_up cfa_PTEN_lo	GAACAATATTGATGATGTAGTAAGGTT ATACTGTGCAACTCTGCAGTT	-

- Not described previously

Table III qRT-PCR results

Sample no.	Ct Mean	RQ	SD+	SD-
Relative HMGA1/ACTB expression				
1	22.84	1.00	-	-
2	22.48	0.39	0.06	0.05
3	22.42	0.76	0.08	0.07
4	22.11	0.51	0.04	0.04
5	22.10	0.50	0.05	0.05
6	23.46	0.47	0.32	0.19
7	22.15	0.61	0.07	0.06

Results

8	19.44	0.76	0.09	0.08
9	17.32	0.19	0.01	0.01
10	21.99	0.09	0.02	0.02
11	21.52	0.25	0.04	0.04
12	17.32	2.74	0.27	0.24
13	21.24	0.16	0.01	0.01
14	18.54	0.87	0.05	0.05
Relative CCND2/ACTB expression				
1	25.32	1.00	-	-
2	22.96	1.58	0.21	0.19
3	24.00	1.27	0.18	0.16
4	24.34	0.56	0.12	0.10
5	24.51	0.57	0.05	0.05
6	14.91	664.00	42.00	39.00
7	23.47	1.62	0.11	0.11
8	20.40	2.11	0.23	0.21
9	22.41	0.61	0.05	0.04
10	24.86	0.06	0.01	0.01
11	21.75	1.19	0.08	0.09
12	21.74	0.73	0.06	0.06
13	20.48	2.73	0.20	0.19
14	20.85	1.93	0.48	0.39
Relative Myc/ACTB expression				
1	24.56	1.00	-	-
2	22.84	1.05	0.14	0.12
3	23.08	1.41	0.23	0.21
4	22.35	1.51	0.17	0.15
5	23.06	0.84	0.06	0.06
6	23.03	1.48	0.23	0.20
7	22.68	1.63	0.07	0.08
8	19.69	1.97	0.13	0.12
9	21.07	0.82	0.05	0.05
10	22.68	0.37	0.04	0.04
11	20.65	1.48	0.15	0.13
12	18.66	2.88	0.77	0.61
13	19.33	2.62	0.27	0.24
14	18.09	5.68	1.63	1.26
Relative NRAS/ACTB expression				
1	25.61	1.00	-	-
2	24.57	0.63	0.12	0.10
3	25.23	0.67	0.07	0.06
4	24.42	0.67	0.20	0.15
5	24.46	0.66	0.11	0.09
6	25.41	0.60	0.07	0.06
7	23.92	1.39	0.43	0.32
8	21.42	1.26	0.13	0.11

Results

9	22.47	0.69	0.13	0.11
10	22.31	0.44	0.12	0.10
11	23.23	0.46	0.07	0.06
12	21.47	0.96	0.12	0.10
13	21.71	1.05	0.07	0.07
14	21.50	1.15	0.30	0.23
Relative Klf4/ACTB expression				
1	27.90	1.00	-	-
2	26.86	0.67	0.11	0.10
3	27.87	0.61	0.04	0.03
4	27.24	0.58	0.09	0.08
5	26.88	0.68	0.04	0.04
6	27.40	0.86	0.05	0.05
7	27.40	1.19	0.07	0.07
8	23.75	1.71	0.05	0.04
9	26.63	0.23	0.02	0.02
10	24.77	0.46	0.01	0.01
11	25.37	0.65	0.03	0.03
12	24.11	0.78	0.08	0.07
13	25.29	0.55	0.02	0.02
14	24.47	0.75	0.14	0.12
Relative PTEN/ACTB expression				
1	29.46	1.00	-	-
2	28.49	0.50	0.11	0.09
3	30.41	0.38	0.04	0.03
4	28.20	0.81	0.33	0.24
5	28.58	0.71	0.31	0.22
6	29.32	0.53	0.21	0.15
7	27.76	1.27	0.43	0.32
8	28.38	0.18	0.05	0.04
9	27.11	0.39	0.04	0.03
10	27.76	0.19	0.10	0.07
11	28.15	0.35	0.12	0.09
12	27.11	0.32	0.02	0.02
13	27.42	0.35	0.04	0.04
14	27.79	0.19	0.04	0.03
Relative IL6/ACTB expression				
1	37.48	1.00	-	-
2	38.14	0.21	0.11	0.07
3	37.51	0.83	0.41	0.27
4	36.78	0.64	1.47	0.97
5	34.82	2.83	0.72	0.49
6	36.00	1.51	2.86	2.12
7	33.48	7.94	0.98	0.73
8	33.35	1.82	1.32	0.88
9	33.95	2.75	0.48	0.28
10	32.09	2.58	0.34	0.29

Results

11	29.55	80.60	14.90	12.50
12	36.72	0.31	0.25	0.14
13	38.72	0.10	0.11	0.05
14	36.25	0.42	0.15	0.11
Relative PIK3CA/ACTB expression				
1	39.43	1.00	-	-
2	37.14	0.62	0.49	0.27
3	39.76	-	-	-
4	36.50	2.02	0.27	0.24
5	36.77	1.27	0.43	0.33
6	37.99	0.63	0.74	0.34
7	35.57	3.78	0.24	0.24
8	36.39	0.32	0.06	0.05
9	36.45	0.75	0.12	0.10
10	36.14	0.42	0.02	0.02
11	35.41	1.46	0.26	0.22
12	36.45	1.45	0.38	0.31
13	35.88	0.69	0.12	0.10
14	33.24	2.11	0.53	0.43

qRT-PCR results of the *HMGA1*, *CCND2*, *Myc*, *NRAS*, *Kif4*, *PTEN*, *IL6*, and *PI3KCA* analyses. Analyzed samples are indicated in first column. Measured mean threshold values (Ct) are listed in the second column. The corresponding target expression relative to the housekeeping gene *ACTB* (RQ) is listed in the third column. The RQ is always shown in relation to the calibrator (No. 1), which was set as 1. Additionally, the calculated standard deviations (SD+ and SD-) are shown in the right column.

- = Not calculated.

4.1.2. Lymphoma

Non-Hodgkin lymphoma treatment strategies depend on the specific type of lymphoma, in this regard the value of the canine model depends on the possibility to discriminate between the lymphoma subgroups (Ponce *et al.*, 2010).

This section deals with expression analyses of the *let-7* regulated *HMGA1* and *HMGA2* genes in canine B- and T-cell lymphomas. The following research study provides information concerning the potency of these two genes as marker for canine lymphoma. This knowledge is precondition for the following development/application of miRNA *let-7* based therapeutic approaches.

V. **Expression of the high mobility group A1 (HMGA1) and A2 (HMGA2) genes in canine lymphoma: analysis of 23 cases and comparison to control cases.**

Joetzke *et al.*, Veterinary and Comparative Oncology, 2010

Aberrant *HMGA1* and *HMGA2* expression was found in many human malignancies but their precise role in canine hematopoietic cancer was not addressed so far.

By that reason the potential of the *HMGA* genes as diagnostic and therapeutic targets in lymphomas was evaluated in the following study analyzing the expression pattern of *HMGA1* and *HMGA2* in canine samples.

HMGA expression in lymph node specimens of 23 dogs with lymphoma was compared to three samples from dogs euthanized by the reason of other diseases. It could be shown by quantitative real-time PCR that the median *HMGA1* expression was significantly higher in lymph nodes of lymphoma patients compared to the control specimens. In contrary to *HMGA1*, *HMGA2* did not show significant differences in expression levels between the lymphoma-affected and non-affected groups. However, *HMGA2* levels were found to be increased in the T-cell lymphomas subpopulation.

In conclusion the observed *HMGA* deregulation in the analyzed set of canine lymphomas indicates an important role of the *HMGA* genes as differentiation markers in canine lymphomas. The herein presented study provides the basis for

Results

future comparative research dealing with prognostic, diagnostic and therapeutic approaches.

V.

Expression of the high mobility group A1 (HMGA1) and A2 (HMGA2) genes in canine lymphoma: analysis of 23 cases and comparison to control cases

Joetzke AE, Sterenczak KA, Eberle N, Wagner S, Soller JT, Nolte I, Bullerdiek J, Murua Escobar H, Simon D.

Vet Comp Oncol. 2010 Jun;8(2):87-95.

Own contribution:

- Canine *HMGA1* real-time PCR assay design and evaluation

Expression of the high mobility group A1 (*HMGA1*) and A2 (*HMGA2*) genes in canine lymphoma: analysis of 23 cases and comparison to control cases

A. E. Joetzke¹, K. A. Sterenczak^{1,2}, N. Eberle¹, S. Wagner^{1,2}, J. T. Soller^{1,2}, I. Nolte¹, J. Bullerdiek^{1,2}, H. Murua Escobar^{1,2} and D. Simon¹

¹Small Animal Clinic and Research Cluster of Excellence 'REBIRTH', University of Veterinary Medicine Hannover, Hannover, Germany

²Centre for Human Genetics, University of Bremen, Bremen, Germany

Abstract

Overexpression of high mobility group A (*HMGA*) genes was described as a prognostic marker in different human malignancies, but its role in canine haematopoietic malignancies was unknown so far. The objective of this study was to analyse *HMGA1* and *HMGA2* gene expression in lymph nodes of canine lymphoma patients. The expression of *HMGA1* and *HMGA2* was analysed in lymph node samples of 23 dogs with lymphoma and three control dogs using relative quantitative real-time RT-PCR. Relative quantity of *HMGA1* was significantly higher in dogs with lymphoma compared with reference samples. *HMGA2* expression did not differ between lymphoma and control dogs. With the exception of immunophenotype, comparison of disease parameters did not display any differences in *HMGA1* and *HMGA2* expression. The present findings indicate a role of *HMGA* genes in canine lymphoma. This study represents the basis for future veterinary and comparative studies dealing with their diagnostic, prognostic and therapeutic values.

Keywords

dogs, gene expression, *HMGA*, lymphoma, relative quantitative real-time RT-PCR

Introduction

The high mobility group A (*HMGA*) protein family consists of three members: *HMGA1a*, *HMGA1b* and *HMGA2*. These highly conserved,¹ small, chromatin associated non-histone proteins are encoded for by two different genes (*HMGA1* and *HMGA2*) and regulate gene expression by inducing genomic DNA conformation changes. These changes indirectly take effect on transcription regulation by influencing the binding of various transcription factors.² Although *HMGA* genes are abundantly expressed in embryonic cells, their expression in most human adult healthy tissues is low or even absent.³

The *HMGA* proteins are known to play a significant role in the pathogenesis of various diseases

including cancer. Re-expression of *HMGA1* was detected in various human malignancies including thyroid, lung, prostatic and colorectal carcinoma, as well as leukaemia and lymphoma,^{4–11} whereas *HMGA2* re-expression was described, for example, in leukaemia, mammary, non-small cell lung, oral squamous cell and thyroid carcinoma.^{12–16} In several of these malignancies *HMGA* overexpression has been reported to be associated with aggressive biologic behaviour.^{4,7,9–11,13,15} Furthermore, *HMGA1* and *HMGA2* have attracted interest as potential therapeutic targets and future influencers on the choice of therapy.¹⁷ Demonstration of *HMGA2* expression in canine prostate carcinoma tissue provided evidence that *HMGA* expression may also play a role in malignant tumours of dogs.¹⁸

Correspondence address:
Alexa E. Joetzke
Small Animal Clinic and
Research Cluster of
Excellence 'REBIRTH'
University of Veterinary
Medicine Hannover
Bischofsholer Damm 15
30173 Hannover, Germany
e-mail: alexa.joetzke@
tiho-hannover.de

The various similarities in biologic behaviour of many canine and human neoplastic diseases suggest similar mechanisms to be involved in the respective pathogenic events. Numerous canine malignancies are considered to be appropriate models for human oncology: among these, osteosarcoma, mammary carcinoma, oral melanoma, pulmonary carcinoma and non-Hodgkin's lymphoma.¹⁹

Lymphoma is one of the most common neoplastic diseases in the dog with an estimated annual incidence of 24–114 per 100 000 dogs.^{20,21} Furthermore, it belongs to the most chemoresponsive malignancies in dogs.¹⁹ Therefore, factors involved in the pathogenesis of canine lymphoma are of great interest for veterinarians as well as for comparative oncology. A wide variety of factors, for example, has been investigated for prognostic relevance,^{22–27} but there are still strong variations in outcome of canine lymphoma that cannot be completely predicted. Molecular markers may provide new insight into the pathogenesis of canine lymphoma and therefore might help in predicting outcome.

As a result of the reported role of *HMGA* re-expression in malignant tumours and its association with tumour aggressiveness in humans, the expression of the corresponding proteins is presumed to represent a powerful diagnostic and prognostic molecular marker. Therefore, it was the aim of the present study to analyse the *HMGA1* and *HMGA2* gene expression in canine lymphomas and to compare it with findings in a group of control cases.

Materials and methods

Patients

Dogs with cytologically or histologically confirmed lymphoma were included in the analysis. Dogs that had received chemotherapy prior to sampling were excluded, whereas those pretreated only with glucocorticoids were included. Control lymph node samples were acquired from dogs with clinically unaltered peripheral lymph nodes diagnosed with diseases other than haematopoietic neoplasia. Signed owner consent was obtained for every patient and the study design was reviewed and approved by the governmental animal care committee.

Staging and immunophenotyping

Clinical staging in dogs with lymphoma was performed according to the WHO clinical staging system²⁸ based on physical examination, complete blood count, serum biochemistry, thoracic and abdominal radiographs and bone marrow aspiration cytology. Flow cytometry was used to determine the immunophenotype of multicentric lymphoma cases as previously described.²⁹

Samples

Enlarged peripheral (multicentric lymphoma) or abdominal (intestinal lymphoma) lymph nodes were sampled via fine needle aspiration. Control samples were obtained from excised peripheral popliteal or superficial cervical lymph nodes within 20 min following euthanasia. All samples were immediately frozen in liquid nitrogen and stored at -80°C until RNA isolation.

RNA isolation and complementary DNA synthesis for transcript characterization

The samples were homogenized using the iron-beads QIAshredder homogenizer method (Qiagen, Hilden, Germany). Following, total RNA was isolated using the RNeasy Mini Kit according to the manufacturer's instructions (Qiagen, Hilden, Germany). In order to avoid genomic DNA contaminations, on-column DNase digestion with the RNase-Free DNase set (Qiagen, Hilden, Germany) was performed.

The respective complementary DNA (cDNA) syntheses were performed using 250 ng total RNA of each sample, the adaptor primer AP2: AAG GAT CCG TCG ACA TC(17)T and Quantiscript Reverse Transcriptase following the manufacturer's protocol (Qiagen, Hilden, Germany) with an integrated removal of genomic DNA contamination.

Quantitative real-time RT-PCR

For relative quantification of the *HMGA1* and *HMGA2* transcript levels, reverse transcription PCR (RT-PCR) amplifications were carried out using the Applied Biosystems 7300 real-time PCR System (Applied Biosystems, Darmstadt, Germany). Two

Table 1. Sequences of the primers and fluorogenic probes used in the RT-PCR procedures

Gene	Forward primer 5' → 3'	Reverse primer 5' → 3'	Fluorogenic probe 5' → 3'
HMGA1	ACCCAGTGAAGTGCCAACA CCTAA	CCTCCTTCTCCAGTTT TTTGGGTCT	6-FAM-AGGGTGCTGCCAA GACCCGGAAAACCTACC A-TAMRA
HMGA2	AGTCCCTCAAAGC AGCTCA AAAG	GCCATTCTAGGTCT GCCTC	6-FAM-AGAAGCCACTGGAGAAAAACG GCCA-TAMRA
GUSB	TGGTGCTGAGGATTGGCA	CTGCCACATGGACCC ATTC	6-FAM-CGCCCACTACTATGCCATCGT GTG-TAMRA

GUSB, glucuronidase beta.

microlitres of each cDNA corresponding to 25 ng of total RNA was amplified in a total volume of 25 µL using universal PCR Mastermix (Applied Biosystems, Darmstadt, Germany) with 600 nM each of the respective forward and reverse primer (Table 1) and 200 nM of the respective fluorogenic probe (Table 1). PCR conditions were as follows: 2 min at 50 °C and 10 min at 95 °C, followed by 45 cycles with 15 s at 95 °C and 1 min at 60 °C.

For relative quantification based on the comparison of the *HMGA* expression with the expression of a housekeeping gene the canine glucuronidase beta transcript was chosen as endogenous control.³⁰ Two microlitres of each cDNA corresponding to 25 ng of total RNA was amplified with 600 nM of each primer (Table 1) and 200 nM fluorogenic probe (Table 1). The PCR was performed under the same conditions as the PCR reactions of the target genes.

All samples were measured in triplicate and for each run, non-template controls and no reverse transcriptase control reactions were included. Before performing the relative real-time quantifications, an absolute real-time PCR reaction was performed with all assays (results not shown), in order to ensure the comparability between the endogenous control and the respective target PCR reactions. All PCR reactions showed similar amplification efficiencies. To compare the gene expression levels based on the delta-delta-CT method, the expression in the control lymph node sample with the lowest variations between the three measurements of both *HMGA1* and *HMGA2* was used as a calibrator (expression level = 1).³¹

Statistical analysis

Expression levels of *HMGA1* and *HMGA2* were evaluated for statistically significant differences

between anatomic type (multicentric versus intestinal lymphoma, Mann–Whitney test), immunophenotype (B-cell versus T-cell, Mann–Whitney test), WHO-substage (substage a versus substage b, Mann–Whitney test) and WHO-stage (clinical stage 3 versus 4 versus 5, Kruskal–Wallis test and clinical stage 3 and 4 versus 5, Mann–Whitney test). A Mann–Whitney test was also used to compare expression levels in lymphomas with those in control dogs.

A *P*-value of <0.05 was considered to be statistically significant. Statistical analysis was performed using SPSS 15.0 statistics software (SPSS, Chicago, IL, USA).

Results

Patient population

Twenty-three dogs with lymphoma were included in the study. Control lymph node samples were obtained from three dogs that were euthanized because of a sarcoma of the liver, pneumonia and a mediastinal sarcoma, respectively. Patient characteristics are summarized in Table 2.

HMGA1 and *HMGA2* expression analyses

Lymph node expression of *HMGA1* was measured in all 23 dogs with lymphoma, whereas *HMGA2* expression was determined in 22 of the 23 lymphoma patients. Expression of both genes was analysed in three control lymph node samples.

HMGA expression in lymphoma samples and comparison to control

The median expression level of *HMGA1* in lymphoma samples (*n* = 23) was 6.88 (range

Table 2. Patient characteristics of the lymphoma-affected and the control dogs

	Lymphoma Patients (n = 23)	Control Dogs (n = 3)
Breeds		
Mixed-breed	n = 6	n = 1
Rottweiler	n = 3	
Beagle	n = 2	
Small Munsterlander	n = 2	
Jagdterrier	n = 2	
Pitbull Terrier	n = 2	
Dachshund	n = 1	
German Shepherd	n = 1	n = 1
White Shepherd	n = 1	
Hovawart	n = 1	
Golden Retriever	n = 1	
Dogo Argentino	n = 1	
Jack Russel Terrier		n = 1
Age (years)		
Median	9	
Range	4–13	7–12
Body weight (kg)		
Median	26.5	
Range	8.8–52	6–40
Gender		
Female (spayed)	n = 9 (n = 4)	n = 2 (n = 2)
Male (castrated)	n = 14 (n = 7)	n = 1 (n = 0)
Anatomic form		
Multicentric	n = 19 (83%)	
Intestinal	n = 4 (17%)	
WHO-stage		
3	n = 3 (13%)	
4	n = 5 (22%)	
5	n = 15 (65%)	
WHO-substage		
a	n = 7 (30%)	
b	n = 16 (70%)	
Immunophenotype		
B	n = 15	
T	n = 3	
Not determined	n = 5	

1.09–12.14), which was significantly higher than the expression measured in control samples (median 0.95, range 0.94–1.00, $P = 0.006$). *HMGA2* expression showed no significant difference between lymphoma-affected ($n = 22$; median 0.32, range 0.03–317.66) and control lymph nodes (median 0.52, range 0.33–1.00, $P = 0.738$).

HMGA expression in multicentric lymphoma

In a separate evaluation including only the dogs with multicentric lymphoma ($n = 19$), *HMGA1* was detected with a median relative quantity

of 7.20 (range 1.09–12.14). The median relative quantity of *HMGA2* in these dogs ($n = 18$) was 0.28 (range 0.03–317.66). The expression levels of *HMGA1* in the multicentric lymphoma cases were higher than in the control samples (median 0.95, range 0.94–1.00, $P = 0.001$, Fig. 1A). Expression of *HMGA2* did not differ significantly between multicentric lymphoma and control samples (median 0.52, range 0.33–1.00, $P = 0.534$, Fig. 1B).

HMGA1 and *HMGA2* expression levels in the dogs with multicentric lymphoma did not differ from those in dogs with intestinal lymphoma ($n = 4$ *HMGA1*: median 4.59, range 1.63–10.04, $P = 0.505$; *HMGA2*: median 7.02, range 0.14–138.69, $P = 0.118$).

In the dogs with multicentric lymphoma, clinical stage and clinical substage were not significantly associated with different *HMGA1* ($P = 0.340$ and $P = 0.482$, respectively) and *HMGA2* ($P = 0.964$ and $P = 0.126$, respectively) expression values. Comparison of a combined group of dogs in stages 3 and 4 with dogs in stage 5 also did not display any differences in *HMGA1* and *HMGA2* expression ($P = 0.940$ and $P = 0.965$, respectively).

Median relative *HMGA1* expression level in the multicentric lymphoma dogs with B-cell subtype ($n = 15$) was 7.42 (range 4.79–12.14). This was significantly higher than the respective relative quantity in the T-cell lymphoma cases ($n = 3$; 1.09, 1.50 and 1.53, respectively, $P = 0.002$, Fig. 2A). The relative quantity of *HMGA2* expression was on the other hand significantly higher in the T-cell subtype ($n = 3$; 21.98, 93.48 and 317.66, respectively) than in the B-cell lymphoma dogs ($n = 14$; median 0.17, range 0.03–5.33, $P = 0.003$, Fig. 2B).

Discussion

The present study aimed at the quantification of *HMGA1* and *HMGA2* expression in canine lymphoma and a comparison to control cases. It is the first report of *HMGA* expression analysis in canine haematopoietic malignancy. In the present population of dogs with lymphoma, *HMGA1* was overexpressed when compared with control dogs. In certain subtypes of human non-Hodgkin's lymphoma an alternative methodical approach using microarray technology indicated differences in

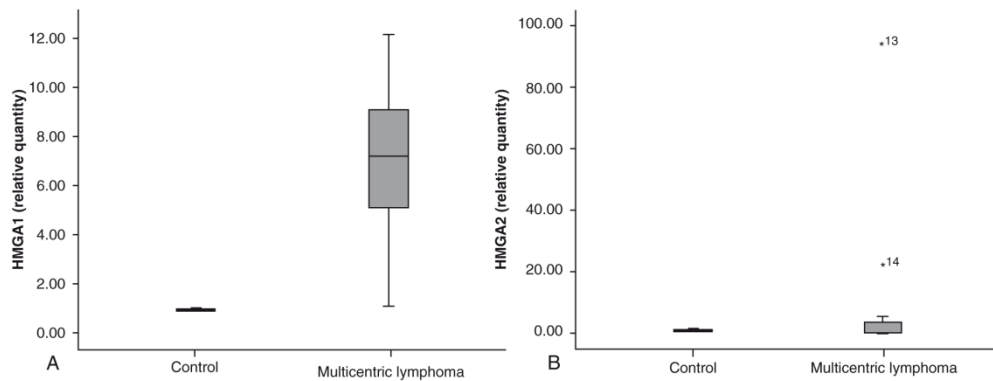


Figure 1. Relative quantity of *HMGA1* (A) and *HMGA2* (B) in dogs with multicentric lymphoma and control dogs. Boxplots graphs comparing multicentric lymphoma to control lymph nodes. (A) Median relative *HMGA1* quantity in multicentric lymphoma ($n = 19$): 7.20 (range 1.09–12.14), control samples ($n = 3$): 0.95 (range 0.94–1.00; $P = 0.001$); (B) median relative *HMGA2* quantity in multicentric lymphoma ($n = 18$): 0.28 (range 0.03–317.66), control samples ($n = 3$): 0.52 (range 0.33–1.00; $P = 0.534$).

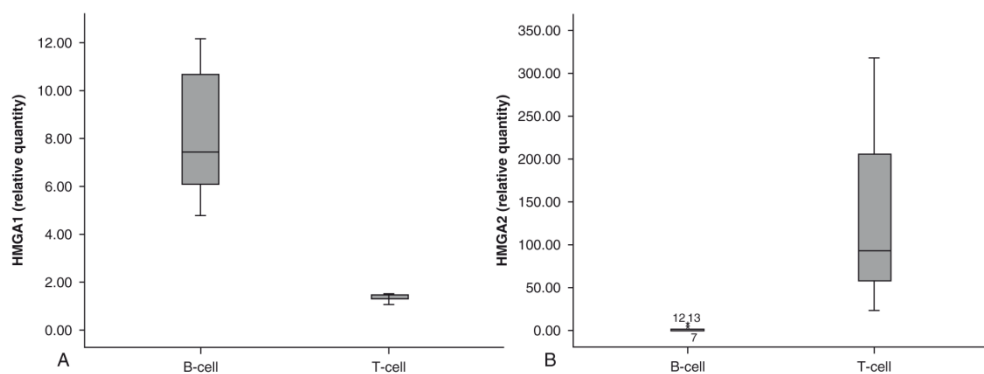


Figure 2. Relative quantity of *HMGA1* (A) and *HMGA2* (B) in multicentric lymphoma with different immunophenotype. Boxplots graphs comparing B-cell and T-cell lymphoma. (A) Median relative *HMGA1* quantity in B-cell lymphoma ($n = 15$): 7.42 (range 4.79–12.14), in T-cell lymphoma ($n = 3$): 1.50 (range 1.09–1.53; $P = 0.002$); (B) median relative *HMGA2* quantity in B-cell lymphoma ($n = 14$): 0.17 (range 0.03–5.33), in T-cell lymphoma ($n = 3$): 93.48 (range 21.98–317.66; $P = 0.003$).

HMGA1 expression levels as well. The expression was found to be significantly upregulated in the aggressive phase of follicular lymphoma compared with the indolent phase.¹⁰ Human mantle cell lymphomas with a high proliferative index as determined immunohistochemically via Ki-67 expression showed a 3.3-fold higher *HMGA1* expression than those with a low proliferative index.¹¹ Increased levels of *HMGA1* proteins were also described in Burkitt's lymphoma cell lines with increased c-Myc protein.³² Furthermore, *HMGA1* overexpression has been shown in human leukaemias both of lymphoid and myeloid origin.^{6,8}

In addition, findings in mice emphasize the importance of *HMGA1* in haematopoietic malignancies. Induction of *HMGA1* overexpression in transgenic mice was found to be associated with the development of NK-cell lymphomas.³³ Interestingly, the loss of function of the *HMGA1* gene shows significant pathogenic effects, as well. Heterozygous and homozygous *HMGA1* knock-out mice develop cardiac hypertrophy combined with haematopoietic malignancies, for example, B-cell lymphoma and myeloid granulocytic leukaemia.³⁴

No significant difference in *HMGA2* expression levels between canine lymphoma and control lymph

node samples was detected in the study population. In human haematopoietic malignancies, both of lymphoid and myeloid origin, aberrant expression and/or chromosomal rearrangements affecting *HMGA2* have been described.^{35–38} Transgenic mice carrying a truncated *HMGA2* gene develop NK-cell lymphomas with a high frequency and thus show an association of *HMGA2* expression with haematopoietic neoplasia, as well.³⁹ Although increased *HMGA2* expression levels seem to play a role in several human myeloid neoplasias,^{14,38,40} findings in lymphoid malignancies are more heterogeneous. Significantly lower expression levels of *HMGA2* were found in the bone marrow of human acute lymphoblastic leukaemia (ALL) patients when compared with healthy bone marrow.³⁵ In contrast, there is a report of *HMGA2* locus rearrangement with overexpression of a *HMGA2* mRNA lacking a carboxy-terminal tail in a case of ALL.³⁷ Another paper showed *HMGA2* protein expression in bone marrow blasts associated with chromosomal translocation involving *HMGA2* in Richter transformation of a chronic lymphocytic leukaemia.³⁶

Despite the lack of significant differences in *HMGA2* expression between canine lymphoma and control lymph nodes in the present study, the *HMGA2* expression in canine lymphomas varied widely. This indicates that aberrant *HMGA2* expression may play a role in canine lymphoma but that its overexpression is not a consistent finding. The role of these expression differences in the respective pathogenesis remains to be investigated in future studies incorporating a larger study population. Interestingly, *HMGA2* expression levels were found to be significantly higher in T-cell than in B-cell lymphomas. The T-cell immunophenotype is observed less frequently in canine lymphoma, comprising approximately 19–33% of lymphoma cases.^{22,24,29} Consistent with these findings, T-cell lymphomas accounted for 17% of phenotyped lymphoma cases in the present study. A higher proportion of T-cell lymphomas may have resulted in a significant difference in *HMGA2* expression between multicentric lymphomas and control samples. Expression of *HMGA1* as well was significantly different between T-cell and B-cell lymphomas. In contrast to *HMGA2*, *HMGA1* was expressed

significantly higher in B-cell lymphomas. The known association of immunophenotype with prognosis of canine lymphoma^{22,24,25} in addition to the proven prognostic significance of *HMGA* expression in several human malignancies^{4,7,9,13,15} gives rise to the assumption that *HMGA* expression levels and especially the different expression of *HMGA1* and *HMGA2* may be associated with prognosis in canine lymphoma, as well. Further studies are needed to verify the present findings and to prove an association with prognosis. It is interesting, that there seems to be a low expression of *HMGA1* especially in the subgroup (T-cell lymphomas) with a significantly higher expression of *HMGA2*. When reviewing other studies about *HMGA* expression in different human tumours concurrent overexpression of *HMGA1* and *HMGA2* is found in some tumour types⁷ and overexpression of either *HMGA1* or *HMGA2* in others.^{41,42} In some human tumour entities, the expression profile of *HMGA* seems to be useful as a diagnostic tool to differentiate between histologically similar tumours.^{41,42} It is possible, that differential expression of *HMGA1* and *HMGA2* may be attributed to different roles they play in tissue differentiation and tumour pathogenesis. Whether it possesses diagnostic or prognostic importance in canine tumours and especially in canine lymphomas may become subject of future studies.

The present study has some limitations that need to be considered. Some subgroups within the study population were relatively small, which decreases the statistical significance of the results but reflects the epidemiological situation in the canine lymphoma population. The low number of control cases must be regarded as a limitation, as well. This group consisted of euthanized dogs with clinically unaltered peripheral lymph nodes and without haematopoietic neoplasia. Other neoplastic or non-neoplastic diseases were not excluded. It cannot be ruled out that the *HMGA* gene expression levels measured in the apparently unaltered peripheral lymph nodes of these dogs has been influenced by their respective disease or the postmortem sampling.

In the present study, overexpression of *HMGA* genes was demonstrated in dogs with lymphoma. The findings indicate that *HMGA* gene expression

may possess a role in the pathogenesis of canine lymphoma. Hence, the results of the present study may provide the basis for future veterinary and comparative studies on the diagnostic, prognostic and therapeutic use of *HMGA1* and *HMGA2*.

Acknowledgments

This study was supported in part by the German Excellence Cluster 'REBIRTH' (From Regenerative Biology to Reconstructive Therapy, Hannover) within the Excellence Initiative of the German Federal Ministry of Education and Research and the German Research Foundation. Additionally, this study was supported in part by the SFB Transregio 37 (Micro- and Nanosystems in Medicine). A. E. J. was sponsored by the German National Academic Foundation.

References

- Murua Escobar H, Soller JT, Richter A, Meyer B, Winkler S, Bullerdiek J and Nolte I. 'Best friends' sharing the *HMGA1* gene: comparison of the human and canine *HMGA1* to orthologous other species. *Journal of Heredity* 2005; **96**: 777–781.
- Bustin M and Reeves R. High-mobility-group chromosomal proteins: architectural components that facilitate chromatin function. *Progress in Nucleic Acid Research and Molecular Biology* 1996; **54**: 35–100.
- Rogalla P, Drechsler K, Frey G, Hennig Y, Helmke B, Bonk U and Bullerdiek J. HMGI-C expression patterns in human tissues. Implications for the genesis of frequent mesenchymal tumors. *American Journal of Pathology* 1996; **149**: 775–779.
- Bussemakers MJ, van de Ven WJ, Debruyne FM and Schalken JA. Identification of high mobility group protein I(Y) as potential progression marker for prostate cancer by differential hybridization analysis. *Cancer Research* 1991; **51**: 606–611.
- Chiappetta G, Tallini G, De Biasio MC, Manfioletti G, Martinez-Tello FJ, Pentimalli F, de Nigris F, Mastro A, Botti G, Fedele M, Berger N, Santoro M, Giancotti V and Fusco A. Detection of high mobility group I HMGI(Y) protein in the diagnosis of thyroid tumors: HMGI(Y) expression represents a potential diagnostic indicator of carcinoma. *Cancer Research* 1998; **58**: 4193–4198.
- Xu Y, Sumter TF, Bhattacharya R, Tesfaye A, Fuchs EJ, Wood LJ, Huso DL and Resar LM. The *HMG-I* oncogene causes highly penetrant, aggressive lymphoid malignancy in transgenic mice and is overexpressed in human leukemia. *Cancer Research* 2004; **64**: 3371–3375.
- Sarhadi VK, Wikman H, Salmenkivi K, Kuosma E, Sioris T, Salo J, Karjalainen A, Knuutila S and Anttila S. Increased expression of high mobility group A proteins in lung cancer. *Journal of Pathology* 2006; **209**: 206–212.
- Pierantoni GM, Agosti V, Fedele M, Bond H, Caliendo I, Chiappetta G, Lo Coco F, Pane F, Turco MC, Morrone G, Venuta S and Fusco A. High-mobility group A1 proteins are overexpressed in human leukaemias. *Biochemical Journal* 2003; **372**: 145–150.
- Abe N, Watanabe T, Sugiyama M, Uchimura H, Chiappetta G, Fusco A and Atomi Y. Determination of high mobility group I(Y) expression level in colorectal neoplasias: a potential diagnostic marker. *Cancer Research* 1999; **59**: 1169–1174.
- Glas AM, Kersten MJ, Delahaye LJ, Witteveen AT, Kibbelaar RE, Velds A, Wessels LF, Joosten P, Kerkhoven RM, Bernards R, van Krieken JH, Kluin PM, van't Veer LJ and de Jong D. Gene expression profiling in follicular lymphoma to assess clinical aggressiveness and to guide the choice of treatment. *Blood* 2005; **105**: 301–307.
- Ek S, Bjorck E, Porwit-MacDonald A, Nordenskjold M and Borrebaeck CA. Increased expression of Ki-67 in mantle cell lymphoma is associated with de-regulation of several cell cycle regulatory components, as identified by global gene expression analysis. *Haematologica* 2004; **89**: 686–695.
- Meyer B, Loeschke S, Schultze A, Weigel T, Sandkamp M, Goldmann T, Vollmer E and Bullerdiek J. *HMGA2* overexpression in non-small cell lung cancer. *Molecular Carcinogenesis* 2007; **46**: 503–511.
- Rogalla P, Drechsler K, Kazmierczak B, Rippe V, Bonk U and Bullerdiek J. Expression of HMGI-C, a member of the high mobility group protein family, in a subset of breast cancers: relationship to histologic grade. *Molecular Carcinogenesis* 1997; **19**: 153–156.
- Rommel B, Rogalla P, Jox A, Kalle CV, Kazmierczak B, Wolf J and Bullerdiek J. HMGI-C, a member of the high mobility group family of proteins, is expressed in hematopoietic stem cells and in leukemic cells. *Leukemia and Lymphoma* 1997; **26**: 603–607.
- Miyazawa J, Mitoro A, Kawashiri S, Chada KK and Imai K. Expression of mesenchyme-specific gene

- HMGA2 in squamous cell carcinomas of the oral cavity. *Cancer Research* 2004; **64**: 2024–2029.
16. Belge G, Meyer A, Klemke M, Burchardt K, Stern C, Wosniok W, Loeschke S and Bullerdiek J. Upregulation of HMGA2 in thyroid carcinomas: a novel molecular marker to distinguish between benign and malignant follicular neoplasias. *Genes, Chromosomes and Cancer* 2008; **47**: 56–63.
 17. Fusco A and Fedele M. Roles of HMGA proteins in cancer. *Nature Reviews Cancer* 2007; **7**: 899–910.
 18. Winkler S, Escobar HM, Meyer B, Simon D, Eberle N, Baumgartner W, Loeschke S, Nolte I and Bullerdiek J. HMGA2 expression in a canine model of prostate cancer. *Cancer Genetics and Cytogenetics* 2007; **177**: 98–102.
 19. MacEwen EG. Spontaneous tumors in dogs and cats: models for the study of cancer biology and treatment. *Cancer and Metastasis Reviews* 1990; **9**: 125–136.
 20. Dorn CR, Taylor DO and Schneider R. The epidemiology of canine leukemia and lymphoma. *Bibliotheca haematologica* 1970; **36**: 403–415.
 21. Dobson JM, Samuel S, Milstein H, Rogers K and Wood JL. Canine neoplasia in the UK: estimates of incidence rates from a population of insured dogs. *Journal of Small Animal Practice* 2002; **43**: 240–246.
 22. Greenlee PG, Filippa DA, Quimby FW, Patnaik AK, Calvano SE, Matus RE, Kimmel M, Hurvitz AI and Lieberman PH. Lymphomas in dogs. A morphologic, immunologic, and clinical study. *Cancer* 1990; **66**: 480–490.
 23. Simon D, Nolte I, Eberle N, Abbrederis N, Killich M and Hirschberger J. Treatment of dogs with lymphoma using a 12-week, maintenance-free combination chemotherapy protocol. *Journal of Veterinary Internal Medicine* 2006; **20**: 948–954.
 24. Teske E, van Heerde P, Rutteman GR, Kurzman ID, Moore PF and MacEwen EG. Prognostic factors for treatment of malignant lymphoma in dogs. *Journal of the American Veterinary Medical Association* 1994; **205**: 1722–1728.
 25. Vail DM, Kisseberth WC, Obradovich JE, Moore FM, London CA, MacEwen EG and Ritter MA. Assessment of potential doubling time (Tpot), argyrophilic nucleolar organizer regions (AgNOR), and proliferating cell nuclear antigen (PCNA) as predictors of therapy response in canine non-Hodgkin's lymphoma. *Experimental Hematology* 1996; **24**: 807–815.
 26. Bergman PJ, Ogilvie GK and Powers BE. Monoclonal antibody C219 immunohistochemistry against P-glycoprotein: sequential analysis and predictive ability in dogs with lymphoma. *Journal of Veterinary Internal Medicine* 1996; **10**: 354–359.
 27. Gentilini F, Calzolari C, Turba ME, Agnoli C, Fava D, Forni M and Bergamini PF. Prognostic value of serum vascular endothelial growth factor (VEGF) and plasma activity of matrix metalloproteinase (MMP) 2 and 9 in lymphoma-affected dogs. *Leukemia Research* 2005; **29**: 1263–1269.
 28. Owen LN. TNM Classification of tumours in domestic animals. *World Health Organization, Geneva* 1980: 46–47.
 29. Culmsee K, Simon D, Mischke R and Nolte I. Possibilities of flow cytometric analysis for immunophenotypic characterization of canine lymphoma. *Journal of Veterinary Medicine, Series A: Physiology, Pathology, Clinical Medicine* 2001; **48**: 199–206.
 30. Brinkhof B, Spee B, Rothuizen J and Penning LC. Development and evaluation of canine reference genes for accurate quantification of gene expression. *Analytical Biochemistry* 2006; **356**: 36–43.
 31. Schmittgen TD and Livak KJ. Analyzing real-time PCR data by the comparative C(T) method. *Nature Protocols* 2008; **3**: 1101–1108.
 32. Wood LJ, Mukherjee M, Dolde CE, Xu Y, Maher JF, Bunton TE, Williams JB and Resar LM. HMG-I/Y, a new c-Myc target gene and potential oncogene. *Molecular and Cellular Biology* 2000; **20**: 5490–5502.
 33. Fedele M, Pentimalli F, Baldassarre G, Battista S, Klein-Szanto AJ, Kenyon L, Visone R, De Martino I, Ciarmiello A, Arra C, Viglietto G, Croce CM and Fusco A. Transgenic mice overexpressing the wild-type form of the HMGA1 gene develop mixed growth hormone/prolactin cell pituitary adenomas and natural killer cell lymphomas. *Oncogene* 2005; **24**: 3427–3435.
 34. Fedele M, Fidanza V, Battista S, Pentimalli F, Klein-Szanto AJ, Visone R, De Martino I, Curcio A, Morisco C, Del Vecchio L, Baldassarre G, Arra C, Viglietto G, Indolfi C, Croce CM and Fusco A. Haploinsufficiency of the Hmga1 gene causes cardiac hypertrophy and myeloid lymphoproliferative disorders in mice. *Cancer Research* 2006; **66**: 2536–2543.
 35. Patel HS, Kantarjian HM, Bueso-Ramos CE, Medeiros LJ and Haidar MA. Frequent deletions at 12q14.3 chromosomal locus in adult acute lymphoblastic leukemia. *Genes, Chromosomes and Cancer* 2005; **42**: 87–94.
 36. Santulli B, Kazmierczak B, Napolitano R, Caliendo I, Chiappetta G, Rippe V, Bullerdiek J and Fusco A. A 12q13 translocation involving the HMGI-C gene in Richter transformation of a chronic lymphocytic leukemia. *Cancer Genetics and Cytogenetics* 2000; **119**: 70–73.

37. Pierantoni GM, Santulli B, Caliendo I, Pentimalli F, Chiappetta G, Zanesi N, Santoro M, Bulrich F and Fusco A. HMGA2 locus rearrangement in a case of acute lymphoblastic leukemia. *International Journal of Oncology* 2003; **23**: 363–367.
38. Odero MD, Grand FH, Iqbal S, Ross F, Roman JP, Vizmanos JL, Andrieux J, Lai JL, Calasanz MJ and Cross NC. Disruption and aberrant expression of HMGA2 as a consequence of diverse chromosomal translocations in myeloid malignancies. *Leukemia* 2005; **19**: 245–252.
39. Baldassarre G, Fedele M, Battista S, Vecchione A, Klein-Szanto AJ, Santoro M, Waldmann TA, Azimi N, Croce CM and Fusco A. Onset of natural killer cell lymphomas in transgenic mice carrying a truncated HMGI-C gene by the chronic stimulation of the IL-2 and IL-15 pathway. *Proceedings of the National Academy of Sciences of the United States of America* 2001; **98**: 7970–7675.
40. Meyer B, Krisponeit D, Junghanss C, Escobar HM and Bullerdiek J. Quantitative expression analysis in peripheral blood of patients with chronic myeloid leukaemia: Correlation between HMGA2 expression and white blood cell count. *Leukemia and Lymphoma* 2007; **48**: 2008–2013.
41. Franco R, Esposito F, Fedele M, Liguori G, Pierantoni GM, Botti G, Tramontano D, Fusco A and Chieffi P. Detection of high-mobility group proteins A1 and A2 represents a valid diagnostic marker in post-pubertal testicular germ cell tumours. *The Journal of Pathology* 2008; **214**: 58–64.
42. Hui P, Li N, Johnson C, De Wever I, Sciort R, Manfioletti G and Tallini G. HMGA proteins in malignant peripheral nerve sheath tumor and synovial sarcoma: preferential expression of HMGA2 in malignant peripheral nerve sheath tumor. *Modern Pathology* 2005; **18**: 1519–1526.

4.1.3. Comparison of non-coding RNAs in human and canine cancer

The microRNA (miRNA) family *let-7* appears to play a major role in human and canine cancer. Thus deciphering the mode of action and regulation of *let-7* but also of other miRNAs will greatly contribute to the development of novel cancer treatment strategies.

The post-transcriptional gene silencing (PTGS) is a conserved phenomenon triggered among others by miRNAs. These are highly conserved among eukaryotes and influence diverse biological processes by regulating genes on post-transcriptional and evidently on transcriptional level. Owing to their high stability in body fluids (Brase *et al.*, 2010) and involvement in various diseases miRNAs bear great potential for the development of novel prognostic, diagnostic and treatment modalities.

III. Comparison of non-coding RNAs in human and canine cancer.

Wagner *et al.*, Frontiers in Genetics, 2013.

Herein the previously described miRNA expression patterns in non-neoplastic diseases and malignant neoplasias of the human and the domesticated dog were reviewed and compared.

Additionally, all known human and canine mature miRNA sequences listed in the miRBase data base (Sanger Institute, version 16.0) were aligned with each other.

The *in silico* analyses revealed that more than 2/3 of the listed canine miRNAs present absolute sequence complementarity to the human homologs, indicating a similar function in human and dog as evidenced by similar expression pattern in the analyzed malignancies.

Finally the potential and advantages of the canine model for tumor research were highlighted.

III.

Comparison of non-coding RNAs in human and canine cancer

Siegfried Wagner, Saskia Willenbrock, Ingo Nolte and Hugo Murua Escobar

Front Genet. 2013;4:46.

Own contribution:

- Literature search and data analyses
- Partial manuscript drafting



Comparison of non-coding RNAs in human and canine cancer

Siegfried Wagner, Saskia Willenbrock, Ingo Nolte and Hugo Murua Escobar*

Small Animal Clinic, University of Veterinary Medicine Hannover, Hannover, Germany

Edited by:

Peng Jin, Emory University School of Medicine, USA

Reviewed by:

Chris Sullivan, University of Texas at Austin, USA

Alan G. Ramsay, Queen Mary University of London, UK

Yujing Li, Emory University, USA

*Correspondence:

Hugo Murua Escobar, Small Animal Clinic, University of Veterinary Medicine Hannover, Buenteweg 9, 30559 Hannover, Germany.
e-mail: hescobar@tih-hannover.de

The discovery of the post-transcriptional gene silencing (PTGS) by small non-protein-coding RNAs is considered as a major breakthrough in biology. In the last decade we just started to realize the biologic function and complexity of gene regulation by small non-coding RNAs. PTGS is a conserved phenomenon which was observed in various species such as fungi, worms, plants, and mammals. Micro RNAs (miRNA) and small interfering RNAs (siRNAs) are two gene silencing mediators constituting an evolutionary conserved class of non-coding RNAs regulating many biological processes in eukaryotes. As these small RNAs appear to regulate gene expression at translational and transcriptional level it is not surprising that during the last decade many human diseases among them Alzheimer's disease, cardiovascular diseases, and various cancer types were associated with deregulated miRNA expression. Consequently small RNAs are considered to hold big promises as therapeutic agents. However, despite of the enormous therapeutic potential many questions remain unanswered. A major critical point, when evaluating novel therapeutic approaches, is the transfer of *in vitro* settings to an *in vivo* model. Classical animal models rely on the laboratory kept animals under artificial conditions and often missing an intact immune system. Model organisms with spontaneously occurring tumors as e.g., dogs provide the possibility to evaluate therapeutic agents under the surveillance of an intact immune system and thereby providing an authentic tumor reacting scenario. Considering the genomic similarity between canines and humans and the advantages of the dog as cancer model system for human neoplasias the analyses of the complex role of small RNAs in canine tumor development could be of major value for both species. Herein we discuss comparatively the role of miRNAs in human and canine cancer development and highlight the potential and advantages of the model organism dog for tumor research.

Keywords: RNAi, PTGS, model organism, cancer research, dog, miRNA, siRNA

BIOGENESIS AND FUNCTION OF SMALL RNAs IN MAMMALS

In 2006, Andrew Fire and Craig C. Mello were awarded with the Nobel Prize in medicine for their work on RNA interference (RNAi). Since the discovery of post-transcriptional gene silencing (PTGS) mechanism in various species, the interest in using small RNA molecules and its endogenous mechanisms as a new pharmacological approach to human diseases is constantly rising (Fire et al., 1998; Elbashir et al., 2001). Micro RNAs (miRNA) and small interfering RNAs (siRNA) are two small non-protein-coding RNA molecule types which play a leading role in PTGS. Thereby, contrary to siRNAs, miRNAs appear to act as "fine tuner" of gene regulation (Sevignani et al., 2006).

miRNAs are endogenously expressed as primary miRNA (pri-miRNA) transcripts composed of up to several thousand nucleotides (Mondol and Pasquinelli, 2012) which are processed by the nuclear enzyme Drosha to precursor miRNAs (pre-miRNA) (Zeng and Cullen, 2006). Following the enzymatic processing, the cytoplasmic enzyme Dicer cleaves the pre-miRNAs generating the mature double-stranded miRNAs (Bohnsack et al.,

2004; Lund et al., 2004). Dicer not only processes pre-miRNAs, it also cleaves long double stranded RNA molecules and generates the second class of small RNAs, named siRNAs, which show a miRNA-similar size of ~20 base pairs (Tomari and Zamore, 2005).

Mature miRNAs and siRNAs are chemically and physiologically indistinguishable, apparently only differing in their respective origins (Ambros et al., 2003). Further comparison of these molecules shows that the "guide strand" of miRNAs seen in mammals, is in most cases significantly but not obligatorily completely complementary to the 3'-untranslated region of the respective target mRNA. In the case of siRNAs the "guide strand" shares absolute complementarity to a small region in the target structure. After "guide strand" incorporation into the RNA-induced silencing complex (RISC), the respective target mRNA stability and/or translation are modulated (Tomari and Zamore, 2005). Interestingly many miRNAs, their biogenesis and functions are conserved among several organisms of higher and lower complexity as fungi, worms, *Drosophila*, and mammals confirming the general importance of the PTGS mechanism

(Filippov et al., 2000; Pasquinelli et al., 2000; Wu et al., 2000; Fortin et al., 2002; Yan et al., 2003; Han et al., 2004; Ibanez-Ventoso et al., 2008).

miRNA genes itself show to be very versatile, they were described to be polycistronic or monocistronic and occasionally located in intron- as well as exon-regions of protein-coding genes. Some miRNAs are co-expressed with their target-mRNAs as one transcript (Bartel, 2004; Kim et al., 2009). Different miRNAs target a single mRNA, and a single miRNA can also be regulating the expression of many different targets. Additionally, miRNAs were also reported to be able to regulate other miRNAs by direct interactions (Winter et al., 2009; Chen et al., 2011) and in some cases miRNAs were described to be regulated by proteins translated from their respective target mRNA, constituting a regulatory negative feedback loop (Bracken et al., 2008; Rybak et al., 2008).

In general, long double stranded RNA molecules are not common in mammals, suggesting that the RNAi mechanism mediated by siRNAs evolved for defense of viral infections and transposable elements (Obbard et al., 2009).

Despite their different origin these small non-coding RNA molecules have many things in common including the small size, specificity of inhibition, and potency and considering therapeutic applications a diminished risk to induce unspecific effects as immune responses. Due to these properties, these molecule types are considered to be potential key players in the development of next generation therapeutics for treatment of a variety of major diseases including cancer (Barh et al., 2010).

miRNA transcription and maturation is not the only process regulating functional miRNA levels. Stability of functional miRNAs is a further key factor in miRNA regulation. Molecule stability was reported to be dependent on several cis- and trans-acting factors varying considerably between miRNAs and their spatiotemporal expression (Kai and Pasquinelli, 2010). Exosomal release of miRNAs into the extracellular environment (Ohshima et al., 2010) and long non-coding RNAs (lncRNA) mimicking target mRNA sites and thereby acting as decoys, were also shown to decrease functional miRNA levels in cells (Cesana et al., 2011). Interestingly, numerous lncRNAs were reported to be deregulated in human cancer (Shore et al., 2012).

Typically one strand of the mature miRNA hybrid, the “guide strand” is maintained during interaction with RISC proteins while the “passenger strand” is degraded. This dichotomy is generally known to be caused by the stabilization of the “guide strand” by RISC loading, while the “passenger strand” stays unprotected (Kai and Pasquinelli, 2010). miRNA methylation, uridylation, and adenylation are some of the modifications having an influence on small RNAs half-life as well (Burroughs et al., 2010; Kai and Pasquinelli, 2010). However, miRNA stability-enhancing proteins were also described to be actively involved in miRNA half-life, suggesting that the miRNA-mediated gene regulation processes are more complex and as variable as these genes are itself (Kai and Pasquinelli, 2010).

THE DOG AS MODEL ORGANISM

In recent years, the role of the domestic dog as model organism for various human diseases constantly gained increasing importance. Many canine inherited diseases were described, including

Alzheimer’s disease (Rofina et al., 2003), narcolepsy (Lin et al., 1999), diabetes (Ionut et al., 2008), epilepsy (Lohi et al., 2005), atrial fibrillation (Shan et al., 2009), Duchenne muscular dystrophy (Mizuno et al., 2011), heart diseases (Eaton et al., 1995), and cancer (Mueller et al., 2007; Boggs et al., 2008; Noguchi et al., 2011; Uhl et al., 2011). All these disorders occur in dogs, just as in humans, spontaneously during their lifetime and many of them show similar clinical manifestations (Ostrander et al., 2000; Sutter and Ostrander, 2004).

Cancer is a complex, polygenic disease spontaneously occurring in man and dog (~1 million diagnosed pet dog cancer cases per year in the United States), whereas tumors in most laboratory animals must be artificially induced (Mueller et al., 2007; Karlsson and Lindblad-Toh, 2008; Paoloni and Khanna, 2008). Indeed, man’s best friend shares many features, including tumor genetics, molecular targets, histological appearance, and response to conventional therapies (Paoloni and Khanna, 2008). Additionally dogs often cohabitate with their owners, are exposed to similar environmental stresses, which may have a big impact on cancer development, and enjoy the best medical care among pets (Sutter and Ostrander, 2004; Rowell et al., 2011). Furthermore, dogs show a higher genetic variability than inbred laboratory mice and enable an easier and faster surgical intervention and imaging due to body size (Mueller et al., 2007). The five- to eight-fold faster aging of dogs in comparison to humans facilitates long-term studies of cancer treatments (Rowell et al., 2011). In 2005, the sequenced canine genome was published (Lindblad-Toh et al., 2005). Having a less different genome from humans than rodents and sharing a similar metabolism, according to their body size, the dog classifies as a very good model organism for molecular studies on human diseases (Sutter and Ostrander, 2004; Karlsson and Lindblad-Toh, 2008; Pinho et al., 2012).

In contrast to investigations on human miRNAs in cancer, the research on canine miRNAs is often limited by the lack of specific canine assays. Up to now only a limited number of studies were done on canine non-neoplastic and tumor tissues. In 2008, Zhou et al. identified 357 canine miRNA-genes by computational analysis, 300 of these were homologs of known human miRNAs (Zhou et al., 2008). Currently 1527 human and 323 canine miRNA matches of hairpin precursors are registered in the web-database, miRBase (Sanger Institute, version 16.0) (Kozomara and Griffiths-Jones, 2011).

Due to high homology of mature miRNAs between human and dog (Table 1), many of the human miRNA assays can be used for analyses of canine miRNA expression. In Table 1 canine miRNAs are listed, which share absolute homology to the human counterparts. Homologous canine miRNAs with overhangs or major sequential differences are not listed.

COMPARATIVE miRNA EXPRESSION IN HUMAN AND CANINE DISEASES

Humans share many diseases with their canine companions including atrial fibrillation, Duchenne muscular dystrophy, and cancer, but the number of comparative studies, focussing on the role of miRNAs in canine diseases, is still relatively low (Karlsson and Lindblad-Toh, 2008; Shan et al., 2009; Mizuno et al., 2011). However, the published data is constantly growing

Table 1 | Comparison of canine and human mature miRNAs.

Canine mature miRNA	Human mature miRNA
cfa-miR-1	hsa-miR-1
cfa-let-7a	hsa-let-7a
cfa-let-7b	hsa-let-7b
cfa-let-7c	hsa-let-7c
cfa-let-7e	hsa-let-7e
cfa-let-7f	hsa-let-7f-5p
cfa-let-7g	hsa-let-7g-5p
cfa-miR-7	hsa-miR-7-5p
cfa-miR-9	hsa-miR-9-5p
cfa-miR-10	hsa-miR-10a-5p
cfa-miR-15a	hsa-miR-15a-5p
cfa-miR-15b	hsa-miR-15b-5p
cfa-miR-16	hsa-miR-16-5p
cfa-miR-17	hsa-miR-17-3p
cfa-miR-18a	hsa-miR-18a-5p
cfa-miR-18b	hsa-miR-18b-5p
cfa-miR-19a	hsa-miR-19a-3p
cfa-miR-19b	hsa-miR-19b-3p
cfa-miR-20a	hsa-miR-20a-5p
cfa-miR-20b	hsa-miR-17-5p
cfa-miR-21	hsa-miR-21-5p
cfa-miR-22	hsa-miR-22-3p
cfa-miR-23a	hsa-miR-23a-3p
cfa-miR-23b	hsa-miR-23b-3p
cfa-miR-25	hsa-miR-25-3p
cfa-miR-26a	hsa-miR-26a-5p
cfa-miR-27a	hsa-miR-27a-3p
cfa-miR-27b	hsa-miR-27b-3p
cfa-miR-28	hsa-miR-28-3p
cfa-miR-29a	hsa-miR-29a-3p
cfa-miR-29b	hsa-miR-29b-3p
cfa-miR-29c	hsa-miR-29c-3p
cfa-miR-30b	hsa-miR-30b-5p
cfa-miR-30e	hsa-miR-30e-3p
cfa-miR-33	hsa-miR-33a-5p
cfa-miR-34a	hsa-miR-34a-5p
cfa-miR-34c	hsa-miR-34c-5p
cfa-miR-92a	hsa-miR-92a-3p
cfa-miR-92b	hsa-miR-92b-3p
cfa-miR-93	hsa-miR-93-5p
cfa-miR-95	hsa-miR-95
cfa-miR-96	hsa-miR-96-5p
cfa-miR-98	hsa-miR-98
cfa-miR-99a	hsa-miR-99a-5p
cfa-miR-99b	hsa-miR-99b-5p
cfa-miR-101	hsa-miR-101-3p
cfa-miR-103	hsa-miR-103a-3p
cfa-miR-105a	hsa-miR-105-5p
cfa-miR-106a	hsa-miR-17-5p
cfa-miR-106a	hsa-miR-106a-5p
cfa-miR-106b	hsa-miR-106b-5p

(Continued)

Table 1 | Continued

Canine mature miRNA	Human mature miRNA
cfa-miR-107	hsa-miR-107
cfa-miR-122	hsa-miR-122-5p
cfa-miR-125a	hsa-miR-125a-5p
cfa-miR-125b	hsa-miR-125b-5p
cfa-miR-126	hsa-miR-126-5p
cfa-miR-127	hsa-miR-127-3p
cfa-miR-128	hsa-miR-128
cfa-miR-129	hsa-miR-129-5p
cfa-miR-130a	hsa-miR-130a-3p
cfa-miR-130b	hsa-miR-130b-3p
cfa-miR-133b	hsa-miR-133b
cfa-miR-133c	hsa-miR-133a
cfa-miR-134	hsa-miR-134
cfa-miR-135a-5p	hsa-miR-135a-5p
cfa-miR-135b	hsa-miR-135b-5p
cfa-miR-136	hsa-miR-136-5p
cfa-miR-137	hsa-miR-137
cfa-miR-138a	hsa-miR-138-5p
cfa-miR-143	hsa-miR-143-3p
cfa-miR-145	hsa-miR-145-5p
cfa-miR-146a	hsa-miR-146a-5p
cfa-miR-146b	hsa-miR-146b-5p
cfa-miR-147	hsa-miR-147b
cfa-miR-148a	hsa-miR-148a-3p
cfa-miR-148b	hsa-miR-148b-3p
cfa-miR-149	hsa-miR-149-5p
cfa-miR-150	hsa-miR-150-5p
cfa-miR-151	hsa-miR-151a-5p
cfa-miR-152	hsa-miR-152
cfa-miR-153	hsa-miR-153
cfa-miR-155	hsa-miR-155-5p
cfa-miR-181a	hsa-miR-181a-5p
cfa-miR-181b	hsa-miR-181b-5p
cfa-miR-181d	hsa-miR-181d
cfa-miR-182	hsa-miR-182-5p
cfa-miR-183	hsa-miR-183-5p
cfa-miR-184	hsa-miR-184
cfa-miR-185	hsa-miR-185-5p
cfa-miR-186	hsa-miR-186-5p
cfa-miR-187	hsa-miR-187-3p
cfa-miR-190a	hsa-miR-190a
cfa-miR-190b	hsa-miR-190b
cfa-miR-191	hsa-miR-191-5p
cfa-miR-192	hsa-miR-192-5p
cfa-miR-193a	hsa-miR-193a-5p
cfa-miR-193b	hsa-miR-193b-5p
cfa-miR-194	hsa-miR-194-5p
cfa-miR-196a	hsa-miR-196a-5p
cfa-miR-197	hsa-miR-197-3p
cfa-miR-199	hsa-miR-199a-3p
cfa-miR-200a	hsa-miR-200a-5p

(Continued)

Table 1 | Continued

Canine mature miRNA	Human mature miRNA
cfa-miR-200b	hsa-miR-200b-5p
cfa-miR-200c	hsa-miR-200c-3p
cfa-miR-202	hsa-miR-202-5p
cfa-miR-203	hsa-miR-203a
cfa-miR-204	hsa-miR-204-5p
cfa-miR-205	hsa-miR-205-5p
cfa-miR-206	hsa-miR-206
cfa-miR-208a	hsa-miR-208a
cfa-miR-208b	hsa-miR-208b
cfa-miR-212	hsa-miR-212-5p
cfa-miR-214	hsa-miR-214-3p
cfa-miR-216a	hsa-miR-216a-5p
cfa-miR-216b	hsa-miR-216b
cfa-miR-218	hsa-miR-218-5p
cfa-miR-219	hsa-miR-219-5p
cfa-miR-219*	hsa-miR-219-2-3p
cfa-miR-221	hsa-miR-221-3p
cfa-miR-222	hsa-miR-222-3p
cfa-miR-223	hsa-miR-223-3p
cfa-miR-299	hsa-miR-299
cfa-miR-301a	hsa-miR-301a-3p
cfa-miR-301b	hsa-miR-301b
cfa-miR-302a	hsa-miR-302a-5p
cfa-miR-302c	hsa-miR-302c-5p
cfa-miR-302d	hsa-miR-302d-5p
cfa-miR-320	hsa-miR-320a
cfa-miR-323	hsa-miR-323a-3p
cfa-miR-324	hsa-miR-324-5p
cfa-miR-326	hsa-miR-326
cfa-miR-328	hsa-miR-328
cfa-miR-329b	hsa-miR-329
cfa-miR-330	hsa-miR-330-5p
cfa-miR-331	hsa-miR-331-3p
cfa-miR-335	hsa-miR-335-5p
cfa-miR-338	hsa-miR-3065-5p
cfa-miR-33b	hsa-miR-33b-5p
cfa-miR-340	hsa-miR-340-5p
cfa-miR-342	hsa-miR-342-3p
cfa-miR-346	hsa-miR-346
cfa-miR-361	hsa-miR-361-5p
cfa-miR-362	hsa-miR-362-5p
cfa-miR-365	hsa-miR-365a-3p
cfa-miR-367	hsa-miR-367-5p
cfa-miR-370	hsa-miR-370
cfa-miR-374a	hsa-miR-374a-5p
cfa-miR-374b	hsa-miR-374b-5p
cfa-miR-375	hsa-miR-375
cfa-miR-376a	hsa-miR-376a-3p
cfa-miR-376b	hsa-miR-376b-3p
cfa-miR-377	hsa-miR-377-5p
cfa-miR-379	hsa-miR-379-5p

(Continued)

Table 1 | Continued

Canine mature miRNA	Human mature miRNA
cfa-miR-381	hsa-miR-381-3p
cfa-miR-383	hsa-miR-383
cfa-miR-410	hsa-miR-410
cfa-miR-421	hsa-miR-421
cfa-miR-423a	hsa-miR-423-5p
cfa-miR-424	hsa-miR-424-3p
cfa-miR-425	hsa-miR-425-5p
cfa-miR-432	hsa-miR-432-5p
cfa-miR-433	hsa-miR-433
cfa-miR-448	hsa-miR-448
cfa-miR-449	hsa-miR-449a
cfa-miR-450b	hsa-miR-450b-5p
cfa-miR-451	hsa-miR-451a
cfa-miR-452	hsa-miR-452-5p
cfa-miR-454	hsa-miR-454-3p
cfa-miR-455	hsa-miR-455-5p
cfa-miR-487a	hsa-miR-487a
cfa-miR-487b	hsa-miR-487b
cfa-miR-488	hsa-miR-488-5p
cfa-miR-489	hsa-miR-489
cfa-miR-490	hsa-miR-490-3p
cfa-miR-491	hsa-miR-491-3p
cfa-miR-493	hsa-miR-493-3p
cfa-miR-494	hsa-miR-494
cfa-miR-495	hsa-miR-495-3p
cfa-miR-496	hsa-miR-496
cfa-miR-497	hsa-miR-497-5p
cfa-miR-499	hsa-miR-499a-5p
cfa-miR-500	hsa-miR-500a-3p
cfa-miR-504	hsa-miR-504
cfa-miR-505	hsa-miR-505-5p
cfa-miR-532	hsa-miR-532-5p
cfa-miR-539	hsa-miR-539-5p
cfa-miR-542	hsa-miR-542-3p
cfa-miR-543	hsa-miR-543
cfa-miR-544	hsa-miR-544a
cfa-miR-551a	hsa-miR-551a
cfa-miR-551b	hsa-miR-551b-3p
cfa-miR-568	hsa-miR-568
cfa-miR-574	hsa-miR-574-3p
cfa-miR-590	hsa-miR-590-3p
cfa-miR-599	hsa-miR-599
cfa-miR-628	hsa-miR-628-5p
cfa-miR-652	hsa-miR-652-3p
cfa-miR-660	hsa-miR-660-5p
cfa-miR-671	hsa-miR-671-3p
cfa-miR-708	hsa-miR-708-5p
cfa-miR-758	hsa-miR-758-3p
cfa-miR-761	hsa-miR-761
cfa-miR-802	hsa-miR-802
cfa-miR-874	hsa-miR-874

(Continued)

Table 1 | Continued

Canine mature miRNA	Human mature miRNA
cfa-miR-875	hsa-miR-875-5p
cfa-miR-876	hsa-miR-876-5p
cfa-miR-885	hsa-miR-885-5p
cfa-miR-1306	hsa-miR-1306-5p
cfa-miR-1307	hsa-miR-1307-3p

207 of the canine mature miRNAs listed in miRBase (Sanger Institute, version 16.0) show absolute sequence complementarity to the human counterparts. The sequence identity of the canine mature miRNA sequences with the corresponding human homologs was confirmed by miRBase, single sequence search (<http://www.mirbase.org/search.shtml>).

and thus it is likely that in future miRNA studies on the canine model, like in the following examples, will gain more importance.

miRNAs in non-neoplastic diseases

Recent studies showed that nicotine can induce atrial structural remodeling and increase atrial fibrosis vulnerability in dogs. Shan et al. reported a decreased *miR-133* and *miR-590* expression in smoking individuals with atrial fibrosis and showed that an ectopic over-expression of *miR-133* and *miR-590* resulted in a post-transcriptional suppression of TGF- β 1 and TGF- β R2 in cultured canine atrial fibroblasts (Shan et al., 2009).

Another disease affecting man as well as dogs is Duchenne muscular dystrophy. It is a lethal X-chromosome linked disorder caused by mutations in the *dystrophin* gene, which encodes a cytoskeletal protein. Mizuno et al. studied serum miRNA expression in the X-linked muscular dystrophy in Japan dog model (CXMD₁) and found, as in humans, increased *miR-1*, *miR-133a*, and *miR-206* levels (Cacchiarelli et al., 2010, 2011; Mizuno et al., 2011). The study indicates that serum miRNAs might be a reliable biomarker for muscular dystrophy (Mizuno et al., 2011).

miRNAs in cancer

Focusing cancer in more detail, deregulated miRNA expression was associated with many human and canine neoplasias (Mueller et al., 2007; Barh et al., 2010; Noguchi et al., 2011; Uhl et al., 2011). As miRNAs are involved in a variety of biological processes as regulation of apoptosis, angiogenesis, cell cycle control, and cell migration it is not surprising that these molecules show an enormous influence on cancer etiology (Bueno and Malumbres, 2011; Donnem et al., 2012; Landskroner-Eiger et al., 2012). For example the human *miR-17-92* cluster coded miRNAs were reported to act tumorigenic, while others such as the *let-7* family members, were reported to be like a coin with two sides, acting in some cases as tumor suppressors or promoting tumor development (Blenkiron and Miska, 2007; Boyerinas et al., 2010; Olive et al., 2010; Ryland et al., 2012).

In cancer, miRNA target sites and miRNA genes itself were found to be directly mutated or their expression deregulated by other factors (Ikeda et al., 2011; Ryland et al., 2012). Due to the complex acting and regulation mechanisms it is very likely

that many miRNA deregulations associated with their respective disease are not even identified.

However, despite of the fact that the detailed mechanisms of miRNA action are still under debate, many diagnostic and therapeutic miRNA-based approaches show promising results (Li et al., 2009; Krell et al., 2012).

As in humans, in dogs, many miRNAs are conserved emphasizing the role of the domestic dog as model organism for miRNA in cancer research. It is very likely that these molecules also follow comparable expression patterns and similar function in canine neoplasias. The analysis of miRNA biogenesis and expression pattern could decipher the role of human and canine miRNAs in cancer and enable the design of new therapies based on small RNA delivery.

miRNAs in mammary tumors

Mammary tumors are among the most common neoplasias of female dogs, with an estimated lifetime risk for malignant tumors varying from 2 to more than 20%. The risk for malignant mammary tumors in dogs spayed before and after their first estrus, is in comparison to intact dogs 0.05 and 8%. In dogs spayed after their second estrus, the risk rises up to 26% (Withrow and Vail, 2007). Data from a Swedish study, based on 80,000 insured female, mostly sexually intact dogs, reported a rate of 111 mammary tumors (benign and malignant) per 10,000 dog-years risk (Egenvall et al., 2005). The age-standardized incidence rate for human breast cancer estimates 66.4 per 100,000 in more developed areas and is thus the most common cancer (Jemal et al., 2011).

According to a recent study, nine miRNAs, *let-7f*, *miR-15a*, *miR-16*, *miR-17-5p*, *miR-21*, *miR-29b*, *miR-125b*, *miR-155*, and *miR-181b* involved in human mammary cancer, appear to follow the same expression pattern in the canine counterpart. In this study, only the investigated *miR-145* was not shown to be differently expressed comparing non-neoplastic and neoplastic canine tissues (Boggs et al., 2008).

miRNAs linked to lymphomas

Besides mammary cancer, canine lymphomas show the highest estimated annual incidence with 13 to 24 cases per 100,000 accounting for up to 24% of all canine neoplasias (Withrow and Vail, 2012). In human, chronic lymphocytic leukemia (CLL) is the most common leukemia in the Western world with an annual incidence of approximately 10,000 new cases in the United States (Calin and Croce, 2009).

In a recent study, the relative expression pattern of 12 canine miRNAs (*cfa-let-7a*, *cfa-miR-15a*, *cfa-miR-16*, *cfa-miR-17-5p*, *cfa-miR-21*, *cfa-miR-26b*, *cfa-miR-29b*, *cfa-miR-125b*, *cfa-miR-150*, *cfa-miR-155*, *cfa-miR-181a*, and *cfa-miR-223*) in CLL was analyzed. Due to stable expression between the investigated samples four of the 12 miRNAs (*cfa-let-7a*, *cfa-miR-17-5p*, *cfa-miR-26b* and *cfa-miR-223*) were used as endogenous controls. *miR-15a*, *miR-16*, and *miR-181a* were reported to be downregulated in canine and human CLL (Calin et al., 2002; Gioia et al., 2011; Zhu et al., 2012). Four of the investigated miRNAs (*cfa-miR-21*, *cfa-miR-125b*, *cfa-miR-150*, *cfa-miR-155*) were described to be upregulated in human and canine B-CLL as well (Pekarsky et al.,

2006; Fulci et al., 2007; Wang et al., 2008; Bousquet et al., 2010; Palamarchuk et al., 2010; Rossi et al., 2010). Only *miR-29b*, which was shown to be downregulated in human B-CLL, was upregulated in canine CLL (Pekarsky et al., 2006; Fulci et al., 2007; Wang et al., 2008; Bousquet et al., 2010; Palamarchuk et al., 2010; Rossi et al., 2010).

It was also observed by Gioia et al. that in comparison to canine B-CLL the *miR-125* expression was significantly downregulated in canine T-CLL. On the basis of the mature miRNA expression ratio between *miR-150/miR-125b*, and *miR-150/miR-155*, it was reported that it is also possible to distinguish among normal blood, B-CLL and T-CLL samples (Gioia et al., 2011). This illustrates the potential of miRNA expression analyses not solely as tumor marker but as an instrument to distinguish between different but similar cell or cancer types.

miRNAs associated with melanomas

Melanomas are very aggressive malignant skin cancers in man and dog (Noguchi et al., 2011). Accounting for 5–7% of canine skin tumors. Tumors of the melanocytes and melanoblasts are relatively common in dogs (Withrow and Vail, 2007; Uhl et al., 2011). In human melanoma cell lines A2058, Mewo, and canine melanoma LMeC cells as well as malignant melanoma tissues the *miR-145*, *miR-203*, and *miR-205* expression was reported to be downregulated. An ectopic expression of each of these miRNAs-induced *in vitro* growth inhibition in A2058, Mewo, and LMeC cells (Noguchi et al., 2011, 2012a,b), indicating their potential for treatment of human and canine malignant melanoma.

miRNAs involved in epithelial to mesenchymal transition

Furthermore, aberrant activation of the epithelial to mesenchymal transition (EMT) has been observed to promote invasion and metastasis in several human cancers. The EMT inducers ZEB1 and ZEB2 have been shown to be direct targets of the *miR-200* family (*miR-200a*, *miR-200b*, *miR-200c*, *miR-141*, and *miR-429*) in the human breast cancer cell line MDA-MB-231 and in Madin Darby canine kidney epithelial cells (MDCK). Lost expression of these miRNAs was detected in human metastatic breast cancer specimens, indicating that downregulation of *miR-200* family members may be an important step in tumor progression (Bracken et al., 2008; Gregory et al., 2008; Adam et al., 2009).

miRNAs with prognostic significance in osteosarcoma

Representing 1% of diagnosed cancer cases in the United States, osteosarcoma is one of the most common primary malignancies of human bone in children and adolescents (Mirabello et al., 2009). Estimated at >10,000 cases per year, canine osteosarcoma is relatively common in contrast to humans. Like in man, the canine counterpart also arises spontaneously in dogs and shows similar anatomical and functional biology (Khanna et al., 2006; Sarver et al., 2013). Recently Sarver et al. demonstrated an inverse correlation between human 14q32 cluster miRNA expression and aggressive tumor behavior in human and canine osteosarcoma. The group mapped the 14q32 cluster to the canine genome. The *miR-134* and *miR-544* of the

14q32 cluster, showing 100% homology between both species, were used to examine the expression in canine samples. They showed a lower *miR-134* and *miR-544* expression in canine and human bone tumors in comparison to healthy tissues (Sarver et al., 2013). The expression levels of these two miRNAs could provide prognostic utility in osteosarcoma, a disease that shows conserved features between human and dog (Sarver et al., 2013).

For a better overview the previously described miRNA expression patterns in the different canine and human neoplasias were summarized in the **Table 2**. The described results should be considered with care as major differences could be present in the comparison depending on species, organism the system of tumor

Table 2 | Overview of the above described miRNAs involved in canine and human cancer.

MAMMARY TUMORS			
cfa-let-7f	↑	hsa-let-7f-5p	↑
cfa-miR-15a	↓	hsa-miR-15a-5p	↓
cfa-miR-16	↓	hsa-miR-16-5p	↓
cfa-miR-17-5p	↓	hsa-miR-17-5p	↓
cfa-miR-21	↑	hsa-miR-21-5p	↑
cfa-miR-29b	↑	hsa-miR-29b-3p	↑
cfa-miR-125b	↓	hsa-miR-125b-5p	↓
cfa-miR-145	=	hsa-miR-145-5p	↓
cfa-miR-155	↓	hsa-miR-155-5p	↓
cfa-miR-181b	↑	hsa-miR-181b-5p	↑
EMT			
cfa-miR-141	↓	hsa-miR-141-3p	↓
cfa-miR-200a	↓	hsa-miR-200a-5p	↓
cfa-miR-200b	↓	hsa-miR-200b-5p	↓
cfa-miR-200c	↓	hsa-miR-200c-5p	↓
cfa-miR-429	↓	hsa-miR-429	↓
B-CLL/T-CLL			
cfa-miR-15a	↓/↓	hsa-miR-15a-5p	↓/-
cfa-miR-16	↓/↓	hsa-miR-16-5p	↓/-
cfa-miR-21	↑/↑	hsa-miR-21-5p	↑/-
cfa-miR-29b	↑/↑	hsa-miR-29b	↓/-
cfa-miR-125b	↑/↓	hsa-miR-125b	↑/-
cfa-miR-150	↑/↑	hsa-miR-150-5p	↑/-
cfa-miR-155	↑/↑	hsa-miR-155-5p	↑/-
cfa-miR-181a	↓/↓	hsa-miR-181a-5p	↓/-
MELANOMA			
cfa-miR-145	↓	hsa-miR-145-5p	↓
cfa-miR-203	↓	hsa-miR-203a	↓
cfa-miR-205	↓	hsa-miR-205-5p	↓
OSTEOSARCOMA			
cfa-miR-134	↓	hsa-miR-134	↓
cfa-miR-544	↓	hsa-miR-544a	↓

In the 1st column are the canine and in the 3rd the human miRNAs listed. In the 2nd and 4th column the relative expression or tendencies in comparison to non-neoplastic samples are presented. “-” indicates that no reports were found for involvement in CLL. “=” means that no differences in expression between tumor and healthy cells were described. “↑” signifies upregulation or “↓” downregulation in comparison to non-neoplastic samples.

classification, type of miRNA preparation and quantification and the used type of normalization.

FUTURE PROSPECTS

As the majority of miRNAs involved in human and canine diseases are evolutionary conserved, it is likely that the expression patterns are also similar. Nevertheless homologous miRNAs, showing similar pattern of expression in different species, should be considered with care as it is possible that the functions still deviate. Even individual miRNAs in the same species can show oncogene suppressive functions or act oncogenic (Boggs et al., 2008).

However, some miRNAs were shown to be a potential non-invasive biomarker for different clinically relevant subtypes of human breast cancer (Cortez et al., 2012; Shore et al., 2012). As aberrant miRNA expression is partially postulated to be an early event in human tumorigenesis (Cortez et al., 2012) it is tempting to speculate that specific miRNAs could also be used as prognostic tools (Li et al., 2009; Krell et al., 2012) for canine neoplasias and thus should be further evaluated as novel agents in the future.

Further knowledge of spatiotemporal miRNA expression and their respective targets will allow more specific modulation of target or effector molecule expression by delivery of miRNAs, siRNAs, or similar modified oligonucleotides.

A directed ectopic expression of naturally occurring miRNAs could have the capability to act therapeutically in an organism by replenishing the missing tumor suppressor miRNA and interfering with oncogenic properties of cancer cells. In perspective oncomiRs (cancer-promoting miRNAs) could be suppressed by antagomiRs (chemically engineered oligonucleotides that act as miRNA inhibitors) or functionally inhibited by titering them away with lncRNAs (Cesana et al., 2011). Due to the fact that a

single miRNA can act on several targets, a miRNA-based therapy could have significant advantages but also bears the risk to induce unintended side effects. Thus, modifications of gene expression by more stringent artificial miRNAs or siRNAs sharing 100% homology to a single target of interest could lower the risk for off target effects, improve treatment, and reduce unwanted side effects.

However, two major obstacles still remain: intracellular delivery and expression level. The ectopic expressed miRNAs must show a certain expression level to reconstitute the “normal” state of genes and the applied small RNAs must be taken up by cancer cells and be further correctly incorporated into RISC. Until now, multiple delivery strategies such as nanoparticles, liposomes, peptide nucleic acids, and viral vectors have been described to achieve this goal but none of these can be used ubiquitously for different types of neoplasias in different locations (Petrocca and Lieberman, 2010; Pan et al., 2011).

Showing many advantages concerning specificity, potency, number of accessible targets, species cross-reactivity, fast development and the scalability, small RNAs may have an enormous diagnostic and therapeutic potential in cancer treatment (Li et al., 2009; Krell et al., 2012) as single agents or e.g., substituting antibody-based cancer therapies.

Homology between human and canine miRNAs could not only enable to use the dog as model organism, but also the transfer of therapeutic and diagnostic approaches established for humans to canines and vice versa. Further elucidation of miRNA functions and biogenesis will facilitate and improve the design and entry of small RNA therapeutic programs into clinical practice. Until now only a few studies describe miRNA expression in canines. Thus, a systematic profiling of miRNA expression would be of great value.

REFERENCES

- Adam, L., Zhong, M., Choi, W., Qi, W., Nicoloso, M., Arora, A., et al. (2009). miR-200 expression regulates epithelial-to-mesenchymal transition in bladder cancer cells and reverses resistance to epidermal growth factor receptor therapy. *Clin. Cancer Res.* 15, 5060–5072.
- Ambros, V., Bartel, B., Bartel, D. P., Burge, C. B., Carrington, J. C., Chen, X., et al. (2003). A uniform system for microRNA annotation. *RNA* 9, 277–279.
- Barh, D., Malhotra, R., Ravi, B., and Sindhurani, P. (2010). MicroRNA let-7: an emerging next-generation cancer therapeutic. *Curr. Oncol.* 17, 70–80.
- Bartel, D. P. (2004). MicroRNAs: genomics, biogenesis, mechanism, and function. *Cell* 116, 281–297.
- Blenkiron, C., and Miska, E. A. (2007). miRNAs in cancer: approaches, aetiology, diagnostics and therapy. *Hum. Mol. Genet.* 16, R106–R113.
- Boggs, R. M., Wright, Z. M., Stickney, M. J., Porter, W. W., and Murphy, K. E. (2008). MicroRNA expression in canine mammary cancer. *Mamm. Genome* 19, 561–569.
- Bohnsack, M. T., Czaplinski, K., and Gorlich, D. (2004). Exportin 5 is a RanGTP-dependent dsRNA-binding protein that mediates nuclear export of pre-miRNAs. *RNA* 10, 185–191.
- Bousquet, M., Harris, M. H., Zhou, B., and Lodish, H. F. (2010). MicroRNA miR-125b causes leukemia. *Proc. Natl. Acad. Sci. U.S.A.* 107, 21558–21563.
- Boyerinas, B., Park, S. M., Hau, A., Murmann, A. E., and Peter, M. E. (2010). The role of let-7 in cell differentiation and cancer. *Endocr. Relat. Cancer* 17, F19–F36.
- Bracken, C. P., Gregory, P. A., Kolesnikoff, N., Bert, A. G., Wang, J., Shannon, M. F., et al. (2008). A double-negative feedback loop between ZEB1-SIP1 and the microRNA-200 family regulates epithelial-mesenchymal transition. *Cancer Res.* 68, 7846–7854.
- Bueno, M. J., and Malumbres, M. (2011). MicroRNAs and the cell cycle. *Biochim. Biophys. Acta* 1812, 592–601.
- Burroughs, A. M., Ando, Y., De Hoon, M. J., Tomaru, Y., Nishibu, T., Ukekawa, R., et al. (2010). A comprehensive survey of 3' animal miRNA modification events and a possible role for 3' adenylation in modulating miRNA targeting effectiveness. *Genome Res.* 20, 1398–1410.
- Cacchiarelli, D., Legnini, I., Martone, J., Cazzella, V., D'Amico, A., Bertini, E., et al. (2011). miRNAs as serum biomarkers for Duchenne muscular dystrophy. *EMBO Mol. Med.* 3, 258–265.
- Cacchiarelli, D., Martone, J., Girardi, E., Cesana, M., Incitti, T., Morlando, M., et al. (2010). MicroRNAs involved in molecular circuitries relevant for the Duchenne muscular dystrophy pathogenesis are controlled by the dystrophin/nNOS pathway. *Cell Metab.* 12, 341–351.
- Calin, G. A., and Croce, C. M. (2009). Chronic lymphocytic leukemia: interplay between noncoding RNAs and protein-coding genes. *Blood* 114, 4761–4770.
- Calin, G. A., Dumitru, C. D., Shimizu, M., Bichi, R., Zupo, S., Noch, E., et al. (2002). Frequent deletions and down-regulation of micro-RNA genes miR15 and miR16 at 13q14 in chronic lymphocytic leukemia. *Proc. Natl. Acad. Sci. U.S.A.* 99, 15524–15529.
- Cesana, M., Cacchiarelli, D., Legnini, I., Santini, T., Sthandier, O., Chinappi, M., et al. (2011). A long noncoding RNA controls muscle differentiation by functioning as a competing endogenous RNA. *Cell* 147, 358–369.
- Chen, P. S., Su, J. L., Cha, S. T., Tarn, W. Y., Wang, M. Y., Hsu, H. C., et al. (2011). miR-107 promotes tumor progression by targeting the let-7 microRNA in mice and humans. *J. Clin. Invest.* 121, 3442–3455.
- Cortez, M. A., Welsh, J. W., and Calin, G. A. (2012). Circulating

- microRNAs as noninvasive biomarkers in breast cancer. *Recent Results Cancer Res.* 195, 151–161.
- Donnem, T., Fenton, C. G., Lonvik, K., Berg, T., Eklo, K., Andersen, S., et al. (2012). MicroRNA signatures in tumor tissue related to angiogenesis in non-small cell lung cancer. *PLoS ONE* 7:e29671. doi: 10.1371/journal.pone.0029671
- Eaton, G. M., Cody, R. J., Nunziata, E., and Binkley, P. F. (1995). Early left ventricular dysfunction elicits activation of sympathetic drive and attenuation of parasympathetic tone in the paced canine model of congestive heart failure. *Circulation* 92, 555–561.
- Egenvall, A., Bonnett, B. N., Ohagen, P., Olson, P., Hedhammar, A., and Von Euler, H. (2005). Incidence of and survival after mammary tumors in a population of over 80,000 insured female dogs in Sweden from 1995 to 2002. *Prev. Vet. Med.* 69, 109–127.
- Elbashir, S. M., Harborth, J., Lendeckel, W., Yalcin, A., Weber, K., and Tuschl, T. (2001). Duplexes of 21-nucleotide RNAs mediate RNA interference in cultured mammalian cells. *Nature* 411, 494–498.
- Filippov, V., Solovyev, V., Filippova, M., and Gill, S. S. (2000). A novel type of RNase III family proteins in eukaryotes. *Gene* 245, 213–221.
- Fire, A., Xu, S., Montgomery, M. K., Kostas, S. A., Driver, S. E., and Mello, C. C. (1998). Potent and specific genetic interference by double-stranded RNA in *Caenorhabditis elegans*. *Nature* 391, 806–811.
- Fortin, K. R., Nicholson, R. H., and Nicholson, A. W. (2002). Mouse ribonuclease III. cDNA structure, expression analysis, and chromosomal location. *BMC Genomics* 3:26. doi: 10.1186/1471-2164-3-26
- Fulci, V., Chiaretti, S., Goldoni, M., Azzalin, G., Carucci, N., Tavoraro, S., et al. (2007). Quantitative technologies establish a novel microRNA profile of chronic lymphocytic leukemia. *Blood* 109, 4944–4951.
- Gioia, G., Mortarino, M., Gelain, M. E., Albonico, E., Ciusani, E., Forno, L., et al. (2011). Immunophenotype-related microRNA expression in canine chronic lymphocytic leukemia. *Vet. Immunol. Immunopathol.* 142, 228–235.
- Gregory, P. A., Bert, A. G., Paterson, E. L., Barry, S. C., Tszyk, A., Farshid, G., et al. (2008). The miR-200 family and miR-205 regulate epithelial to mesenchymal transition by targeting ZEB1 and SIP1. *Nat. Cell Biol.* 10, 593–601.
- Han, J., Lee, Y., Yeom, K. H., Kim, Y. K., Jin, H., and Kim, V. N. (2004). The Drosha-DGCR8 complex in primary microRNA processing. *Genes Dev.* 18, 3016–3027.
- Ibanez-Ventoso, C., Vora, M., and Driscoll, M. (2008). Sequence relationships among *C. elegans*, *D. melanogaster* and human microRNAs highlight the extensive conservation of microRNAs in biology. *PLoS ONE* 3:e2818. doi: 10.1371/journal.pone.0002818
- Ikeda, K., Mason, P. J., and Bessler, M. (2011). 3'UTR-truncated Hmg2 cDNA causes MPN-like hematopoiesis by conferring a clonal growth advantage at the level of HSC in mice. *Blood* 117, 5860–5869.
- Ionut, V., Liu, H., Mooradian, V., Castro, A. V., Kabir, M., Stefanovski, D., et al. (2008). Novel canine models of obese prediabetes and mild type 2 diabetes. *Am. J. Physiol. Endocrinol. Metab.* 298, E38–E48.
- Jemal, A., Bray, F., Center, M. M., Ferlay, J., Ward, E., and Forman, D. (2011). Global cancer statistics. *CA Cancer J. Clin.* 61, 69–90.
- Kai, Z. S., and Pasquinelli, A. E. (2010). MicroRNA assassins: factors that regulate the disappearance of miRNAs. *Nat. Struct. Mol. Biol.* 17, 5–10.
- Karlsson, E. K., and Lindblad-Toh, K. (2008). Leader of the pack: gene mapping in dogs and other model organisms. *Nat. Rev. Genet.* 9, 713–725.
- Khanna, C., Lindblad-Toh, K., Vail, D., London, C., Bergman, P., Barber, L., et al. (2006). The dog as a cancer model. *Nat. Biotechnol.* 24, 1065–1066.
- Kim, V. N., Han, J., and Siomi, M. C. (2009). Biogenesis of small RNAs in animals. *Nat. Rev. Mol. Cell Biol.* 10, 126–139.
- Kozomara, A., and Griffiths-Jones, S. (2011). miRBase: integrating microRNA annotation and deep-sequencing data. *Nucleic Acids Res.* 39, D152–D157.
- Krell, J., Frampton, A. E., Jacob, J., Castellano, L., and Stebbing, J. (2012). miRNAs in breast cancer: ready for real time? *Pharmacogenomics* 13, 709–719.
- Landskroner-Eiger, S., Moneke, I., and Sessa, W. C. (2012). miRNAs as modulators of angiogenesis. *Cold Spring Harb. Perspect. Med.* 3:a006643. doi: 10.1101/cshperspect.a006643
- Li, W., Duan, R., Kooy, F., Sherman, S. L., Zhou, W., and Jin, P. (2009). Germline mutation of microRNA-125a is associated with breast cancer. *J. Med. Genet.* 46, 358–360.
- Lin, L., Faraco, J., Li, R., Kadotani, H., Rogers, W., Lin, X., et al. (1999). The sleep disorder canine narcolepsy is caused by a mutation in the hypocretin (orexin) receptor 2 gene. *Cell* 98, 365–376.
- Lindblad-Toh, K., Wade, C. M., Mikkelsen, T. S., Karlsson, E. K., Jaffe, D. B., Kamal, M., et al. (2005). Genome sequence, comparative analysis and haplotype structure of the domestic dog. *Nature* 438, 803–819.
- Lohi, H., Young, E. J., Fitzmaurice, S. N., Rusbridge, C., Chan, E. M., Vervoort, M., et al. (2005). Expanded repeat in canine epilepsy. *Science* 307, 81.
- Lund, E., Guttinger, S., Calado, A., Dahlberg, J. E., and Kutay, U. (2004). Nuclear export of microRNA precursors. *Science* 303, 95–98.
- Mirabello, L., Troisi, R. J., and Savage, S. A. (2009). Osteosarcoma incidence and survival rates from 1973 to 2004: data from the Surveillance, Epidemiology, and End Results Program. *Cancer* 115, 1531–1543.
- Mizuno, H., Nakamura, A., Aoki, Y., Ito, N., Kishi, S., Yamamoto, K., et al. (2011). Identification of muscle-specific microRNAs in serum of muscular dystrophy animal models: promising novel blood-based markers for muscular dystrophy. *PLoS ONE* 6:e18388. doi: 10.1371/journal.pone.0018388
- Mondol, V., and Pasquinelli, A. E. (2012). Let's make it happen: the role of let-7 microRNA in development. *Curr. Top. Dev. Biol.* 99, 1–30.
- Mueller, F., Fuchs, B., and Kaser-Hotz, B. (2007). Comparative biology of human and canine osteosarcoma. *Anticancer Res.* 27, 155–164.
- Noguchi, S., Mori, T., Hoshino, Y., Yamada, N., Maruo, K., and Akao, Y. (2011). MicroRNAs as tumour suppressors in canine and human melanoma cells and as a prognostic factor in canine melanomas. *Vet. Comp. Oncol.* 9, 1476–5829.
- Noguchi, S., Mori, T., Hoshino, Y., Yamada, N., Nakagawa, T., Sasaki, N., et al. (2012a). Comparative study of anti-oncogenic microRNA-145 in canine and human malignant melanoma. *J. Vet. Med. Sci.* 74, 1–8.
- Noguchi, S., Mori, T., Otsuka, Y., Yamada, N., Yasui, Y., Iwasaki, J., et al. (2012b). Anti-oncogenic microRNA-203 induces senescence by targeting E2F3 protein in human melanoma cells. *J. Biol. Chem.* 287, 11769–11777.
- Obbard, D. J., Gordon, K. H., Buck, A. H., and Jiggins, F. M. (2009). The evolution of RNAi as a defence against viruses and transposable elements. *Philos. Trans. R Soc. Lond. B Biol. Sci.* 364, 99–115.
- Oshima, K., Inoue, K., Fujiwara, A., Hatakeyama, K., Kanto, K., Watanabe, Y., et al. (2010). Let-7 microRNA family is selectively secreted into the extracellular environment via exosomes in a metastatic gastric cancer cell line. *PLoS ONE* 5:e13247. doi: 10.1371/journal.pone.0013247
- Olive, V., Jiang, I., and He, L. (2010). mir-17-92, a cluster of miRNAs in the midst of the cancer network. *Int. J. Biochem. Cell Biol.* 42, 1348–1354.
- Ostrander, E. A., Galibert, F., and Patterson, D. F. (2000). Canine genetics comes of age. *Trends Genet.* 16, 117–124.
- Palamarchuk, A., Efanov, A., Nazaryan, N., Santanam, U., Alder, H., Rassenti, L., et al. (2010). 13q14 deletions in CLL involve cooperating tumor suppressors. *Blood* 115, 3916–3922.
- Pan, X., Thompson, R., Meng, X., Wu, D., and Xu, L. (2011). Tumor-targeted RNA-interference: functional non-viral nanovectors. *Am. J. Cancer Res.* 1, 25–42.
- Paoloni, M., and Khanna, C. (2008). Translation of new cancer treatments from pet dogs to humans. *Nat. Rev. Cancer* 8, 147–156.
- Pasquinelli, A. E., Reinhart, B. J., Slack, F., Martindale, M. Q., Kuroda, M. I., Maller, B., et al. (2000). Conservation of the sequence and temporal expression of let-7 heterochronic regulatory RNA. *Nature* 408, 86–89.
- Pekarsky, Y., Santanam, U., Cimmino, A., Palamarchuk, A., Efanov, A., Maximov, V., et al. (2006). Tc11 expression in chronic lymphocytic leukemia is regulated by miR-29 and miR-181. *Cancer Res.* 66, 11590–11593.
- Petrocca, F., and Lieberman, J. (2010). Promise and challenge of RNA interference-based therapy for cancer. *J. Clin. Oncol.* 29, 747–754.
- Pinho, S. S., Carvalho, S., Cabral, J., Reis, C. A., and Gartner, F. (2012). Canine tumors: a spontaneous animal model of human carcinogenesis. *Transl. Res.* 159, 165–172.
- Rofina, J., Van Andel, I., Van Ederen, A. M., Papaioannou, N., Yamaguchi, H., and Gruys, E. (2003). Canine counterpart of senile dementia of the Alzheimer type: amyloid plaques near capillaries but lack of spatial relationship with activated microglia and macrophages. *Amyloid* 10, 86–96.

- Rossi, S., Shimizu, M., Barbarotto, E., Nicoloso, M. S., Dimitri, F., Sampath, D., et al. (2010). microRNA fingerprinting of CLL patients with chromosome 17p deletion identify a miR-21 score that stratifies early survival. *Blood* 116, 945–952.
- Rowell, J. L., McCarthy, D. O., and Alvarez, C. E. (2011). Dog models of naturally occurring cancer. *Trends Mol. Med.* 17, 380–388.
- Rybak, A., Fuchs, H., Smirnova, L., Brandt, C., Pohl, E. E., Nitsch, R., et al. (2008). A feedback loop comprising lin-28 and let-7 controls pre-let-7 maturation during neural stem-cell commitment. *Nat. Cell Biol.* 10, 987–993.
- Ryland, G. L., Bearfoot, J. L., Doyle, M. A., Boyle, S. E., Choong, D. Y., Rowley, S. M., et al. (2012). MicroRNA genes and their target 3'-untranslated regions are infrequently somatically mutated in ovarian cancers. *PLoS ONE* 7:e35805. doi: 10.1371/journal.pone.0035805
- Sarver, A. L., Thayanythy, V., Scott, M. C., Cleton-Jansen, A. M., Hogendoorn, P. C., Modiano, J. F., et al. (2013). MicroRNAs at the human 14q32 locus have prognostic significance in osteosarcoma. *Orphanet J. Rare Dis.* 8:7. doi: 10.1186/1750-1172-8-7
- Sevignani, C., Calin, G. A., Siracusa, L. D., and Croce, C. M. (2006). Mammalian microRNAs: a small world for fine-tuning gene expression. *Mamm. Genome* 17, 189–202.
- Shan, H., Zhang, Y., Lu, Y., Zhang, Y., Pan, Z., Cai, B., et al. (2009). Downregulation of miR-133 and miR-590 contributes to nicotine-induced atrial remodeling in canines. *Cardiovasc. Res.* 83, 465–472.
- Shore, A. N., Herschkowitz, J. I., and Rosen, J. M. (2012). Noncoding RNAs involved in mammary gland development and tumorigenesis: there's a long way to go. *J. Mammary Gland Biol. Neoplasia* 17, 43–58.
- Sutter, N. B., and Ostrander, E. A. (2004). Dog star rising: the canine genetic system. *Nat. Rev. Genet.* 5, 900–910.
- Tomari, Y., and Zamore, P. D. (2005). Perspective: machines for RNAi. *Genes Dev.* 19, 517–529.
- Uhl, E., Krimer, P., Schliekelman, P., Tompkins, S. M., and Suter, S. (2011). Identification of altered MicroRNA expression in canine lymphoid cell lines and cases of B- and T-Cell lymphomas. *Genes Chromosomes Cancer* 50, 950–967.
- Wang, M., Tan, L. P., Dijkstra, M. K., Van Lom, K., Robertus, J. L., Harms, G., et al. (2008). miRNA analysis in B-cell chronic lymphocytic leukaemia: proliferation centres characterized by low miR-150 and high BIC/miR-155 expression. *J. Pathol.* 215, 13–20.
- Winter, J., Jung, S., Keller, S., Gregory, R. I., and Diederichs, S. (2009). Many roads to maturity: microRNA biogenesis pathways and their regulation. *Nat. Cell Biol.* 11, 228–234.
- Withrow, J. S., and Vail, D. M. (2007). *Withrow and MacEwen's Small Animal Clinical Oncology, 4th Edn.* St. Louis MO: Saunders Company.
- Withrow, J. S., and Vail, D. M. (2012). *Withrow and MacEwen's Small Animal Clinical Oncology, 5th Edn.* St. Louis MO: Saunders Company.
- Wu, H., Xu, H., Miraglia, L. J., and Crooke, S. T. (2000). Human RNase III is a 160-kDa protein involved in preribosomal RNA processing. *J. Biol. Chem.* 275, 36957–36965.
- Yan, K. S., Yan, S., Farooq, A., Han, A., Zeng, L., and Zhou, M. M. (2003). Structure and conserved RNA binding of the PAZ domain. *Nature* 426, 468–474.
- Zeng, Y., and Cullen, B. R. (2006). Recognition and cleavage of primary microRNA transcripts. *Methods Mol. Biol.* 342, 49–56.
- Zhou, D., Li, S., Wen, J., Gong, X., Xu, L., and Luo, Y. (2008). Genome-wide computational analyses of microRNAs and their targets from *Canis familiaris*. *Comput. Biol. Chem.* 32, 60–65.
- Zhu, D. X., Zhu, W., Fang, C., Fan, L., Zou, Z. J., Wang, Y. H., et al. (2012). miR-181a/b significantly enhances drug sensitivity in chronic lymphocytic leukemia cells via targeting multiple anti-apoptosis genes. *Carcinogenesis* 33, 1294–1301.

Conflict of Interest Statement: The authors declare that the research was conducted in the absence of any commercial or financial relationships that could be construed as a potential conflict of interest.

Received: 22 August 2012; paper pending published: 04 November 2012; accepted: 13 March 2013; published online: 08 April 2013.

Citation: Wagner S, Willenbrock S, Nolte I and Escobar HM (2013) Comparison of non-coding RNAs in human and canine cancer. *Front. Genet.* 4:46. doi: 10.3389/fgene.2013.00046

This article was submitted to *Frontiers in Non-Coding RNA*, a specialty of *Frontiers in Genetics*.

Copyright © 2013 Wagner, Willenbrock, Nolte and Escobar. This is an open-access article distributed under the terms of the Creative Commons Attribution License, which permits use, distribution and reproduction in other forums, provided the original authors and source are credited and subject to any copyright notices concerning any third-party graphics etc.

4.2. Structural and functional *HMGA* analyses

As it was shown in the previous sections and previously described by other groups the miRNA *let-7* family appears to be one of the key players in gene regulation. Thus *let-7* based therapeutic approaches might be an option to treat cancer in future. However, before treating a defined cancer entity with *let-7* based/modifying therapeutics it is precondition to know why *let-7* regulated genes are aberrantly expressed and what is their function in a cell.

Thus the gene structure of the canine *HMGA1* gene was analyzed in this part of the thesis. Additionally the influence of *HMGA2* on the *HMGA2/let-7* axis in a canine prostatic cell line was investigated. And finally the potency of the HMGA1 and HMGA2 proteins on maintenance of the stem-cell character was evaluated.

VI. Genomic characterisation, chromosomal assignment and in vivo localisation of the canine high mobility group A1 (HMGA1) gene the Canine High Mobility Group A1 (HMGA1) Gene.

Beuing *et al.*, BMC Genetics, 2008

Herein the canine *HMGA1* gene was characterized revealing a structure consisting of seven exons and six introns lacking the equivalent to the human exon 4. Additionally, the canine *HMGA1* gene which spans in total 9524 nt was assigned to the chromosome 12 (CFA 12q11). Furthermore the canine HMGA1 protein was localized in the nucleus of canine cells.

Finally, 55 Dachshunds were screened for a previously described exon 6 mutation of the *HMGA1* gene. The results indicate that the previously found mutation of this locus seems not to be a frequent, breed specific event in the Dachshund population. The obtained results will enable comparative analysis of the human and canine *HMGA1* products, thereby providing the basis for ongoing investigations of *HMGA1* related diseases.

VI.

Genomic Characterisation, Chromosomal Assignment and in Vivo Localisation of the Canine High Mobility Group A1 (HMGA1) Gene

Claudia Beuing, Jan T Soller, Michaela Muth, Siegfried Wagner, Gaudenz Dolf, Claude Schelling, Andreas Richter, Saskia Willenbrock, Nicola Reimann-Berg, Susanne Winkler, Ingo Nolte, Jorn Bullerdiek, Hugo Murua Escobar

BMC Genet. 2008; 9: 49.

Own contribution:

- *HMGA1* gene amplification, cloning and characterization
- Transfection experiments
- Localization and documentation of the recombinant EGFP-HMGA1 fusion protein by fluorescence microscopy
- Partial figure preparation (Fig. 2)

Research article

Open Access

Genomic characterisation, chromosomal assignment and *in vivo* localisation of the canine High Mobility Group A1 (HMGA1) geneClaudia Beuing^{†1}, Jan T Soller^{†1,2}, Michaela Muth², Sigfried Wagner², Gaudenz Dolf³, Claude Schelling⁴, Andreas Richter², Saskia Willenbrock^{1,2}, Nicola Reimann-Berg^{1,2}, Susanne Winkler², Ingo Nolte¹, Jorn Bullerdiek^{1,2} and Hugo Murua Escobar*^{1,2}

Address: ¹Clinic for Small Animals and Research Cluster of Excellence "REBIRTH", University of Veterinary Medicine Hanover, Bischofsholer Damm 15, 30173 Hanover, Germany, ²Centre for Human Genetics, University of Bremen, Leobener Str ZHG, 28359 Bremen, Germany, ³Institute of Animal Genetics, Nutrition and Housing, University of Berne, Berne, Switzerland and ⁴Department of Animal Sciences, Swiss Federal Institute of Technology Zurich and Vetsuisse Faculty Zurich, University of Zurich, Zurich, Switzerland

Email: Claudia Beuing - claudia.beuing@tiho-hannover.de; Jan T Soller - soller@uni-bremen.de; Michaela Muth - mmuth@uni-bremen.de; Sigfried Wagner - siegfried.wagner@mail.uni-oldenburg.de; Gaudenz Dolf - dolf.gaudenz@itz.unibe.ch; Claude Schelling - claude.schelling@inw.agrl.ethz.ch; Andreas Richter - arichter@uni-bremen.de; Saskia Willenbrock - swillenbrock@uni-bremen.de; Nicola Reimann-Berg - nicola.reimann-berg@uni-bremen.de; Susanne Winkler - susewinkler@web.de; Ingo Nolte - inolte@klt.tiho-hannover.de; Jorn Bullerdiek - bullerd@uni-bremen.de; Hugo Murua Escobar* - escobar@uni-bremen.de

* Corresponding author †Equal contributors

Published: 23 July 2008

Received: 1 April 2008

BMC Genetics 2008, 9:49 doi:10.1186/1471-2156-9-49

Accepted: 23 July 2008

This article is available from: <http://www.biomedcentral.com/1471-2156/9/49>

© 2008 Beuing et al; licensee BioMed Central Ltd.

This is an Open Access article distributed under the terms of the Creative Commons Attribution License (<http://creativecommons.org/licenses/by/2.0>), which permits unrestricted use, distribution, and reproduction in any medium, provided the original work is properly cited.

Abstract

Background: The high mobility group A1 proteins (HMGA1a/HMGA1b) are highly conserved between mammalian species and widely described as participating in various cellular processes. By inducing DNA conformation changes the HMGA1 proteins indirectly influence the binding of various transcription factors and therefore effect the transcription regulation. In humans chromosomal aberrations affecting the *HMGA1* gene locus on HSA 6p21 were described to be the cause for various benign mesenchymal tumours while high titres of HMGA1 proteins were shown to be associated with the neoplastic potential of various types of cancer. Interestingly, the absence of HMGA1 proteins was shown to cause insulin resistance and diabetes in humans and mice.

Due to the various similarities in biology and presentation of human and canine cancers the dog has joined the common rodent animal model for therapeutic and preclinical studies. Accordingly, the canine genome was sequenced completely twice but unfortunately this could not solve the structure of canine *HMGA1* gene.

Results: Herein we report the characterisation of the genomic structure of the canine *HMGA1* gene consisting of 7 exons and 6 introns spanning in total 9524 bp, the *in vivo* localisation of the HMGA1 protein to the nucleus, and a chromosomal assignment of the gene by FISH to CFA12q11. Additionally, we evaluated a described canine *HMGA1* exon 6 SNP in 55 Dachshunds.

Conclusion: The performed characterisations will make comparative analyses of aberrations affecting the human and canine gene and proteins possible, thereby providing a basis for revealing mechanisms involved in HMGA1 related pathogenesis in both species.

Background

The high mobility group A (HMGA) proteins are small chromatin associated non-histone proteins named according to their characteristic motility in acid-urea polyacrylamide gel electrophoresis. The protein family consists of the three proteins HMGA1a, HMGA1b and HMGA2 which are encoded for by two different genes (HMGA1 and HMGA2). The functional motifs of these proteins, named AT-hooks, bind to the minor groove of DNA causing conformational changes of the DNA molecule. On genomic level these structural changes influence the binding of various transcription factors and thus indirectly influence the transcription regulation, which classifies the HMGA proteins as so called architectural transcription factors (for detail see [1]).

In previous studies we characterised the canine HMGA1 cDNAs and proteins and in comparative analyses of these molecules showed that they are highly conserved between different mammalian species. The observed number of amino acid changes seen across mammalian species (cattle, dog, hamster, horse, mouse, pig, and rat) vary between 0 to 3 when compared to the human molecules [2-10]. Interestingly, only the canine HMGA1 proteins are 100% identical to their respective human counterparts [11].

The HMGA1 proteins are well known to play a significant role in the pathogenesis of various diseases including cancer. In humans, chromosomal aberrations affecting the HMGA1 gene locus on 12p21 were described for various benign mesenchymal tumours, e.g. endometrial polyps, lipomas, pulmonary chondroid hamartomas, and uterine leiomyomas [12-14]. The observed aberrations are supposed to lead to an up-regulation of the HMGA1 gene in the affected tumours, as opposed to adult healthy tissues where HMGA gene expression is low or hardly measurable [9,15,16]. In malignant neoplasias HMGA1 expression is reported to be associated with an aggressive behaviour of tumours. Accordingly, HMGA1 overexpression was detected in various malignancies including thyroid, lung, prostatic, pancreatic, uterine cervical, and colorectal carcinoma [17-22]. Thus HMGA expression is supposed to present a powerful diagnostic and prognostic molecular marker due to the described correlation between HMGA expression and tumour aggressiveness.

Whilst overexpression of HMGA1 is clearly associated with cancerogenesis the disruption of the HMGA1 gene and thus induced loss of HMGA1 expression shows significant pathogenic effects. Heterozygous and homozygous Hmga1 knock-out mice develop cardiac hypertrophy combined with hematologic malignancies e.g. B cell lymphoma and myeloid granulocytic leukemia [23]. Additional research with Hmga1 knock-out mice targeting diabetes presented by Foti et al. (2005) showed that loss

of Hmga1 expression is clearly associated with significantly decreased insulin receptor expression and thus causes a characteristic diabetes type 2 phenotype in mice [24].

The various similarities in presentation and biology of numerous canine and human diseases including cancer suggest similar mechanisms to be involved in the respective pathogenic events. Accordingly, at least a dozen distinct canine cancers are hypothesized to be appropriate models for their human counterparts, among those osteosarcoma, breast carcinoma, oral melanomas, lung carcinomas and malignant non-Hodgkin's lymphomas [25].

The characterization of disease related genes and their protein biology will allow for comparative studies to reveal the molecular mechanisms involved therein and serve as a basis for future clinical studies.

Results and discussion

The HMGA1 gene and its proteins HMGA1a and HMGA1b are described as regulating multiple cellular processes and are widely reported to be associated with various diseases including diabetes and cancer. In previous studies we characterised the canine HMGA1 cDNAs and proteins completely and did comparative analyses of these molecules to the respective counterparts of different species and showed high evolutionary conservation. The fact that several canine and human cancer types show striking similarities in presentation and biological behaviour, e.g. spontaneous occurrence and metastasis patterns, strongly suggests similar mechanisms to be involved in the respective pathogenic events of both species. Thus, various canine tumours are currently used as models for several human cancer types. Accordingly, comprehension of the canine gene and its gene products is precondition for comparative analyses, allowing the revelation of molecular effects involved in these pathogenic presentations. Understanding and comparison of the respective genes will thus benefit both species. The exact mechanism for the emergence of the pathogenic effects caused by chromosomal aberrations affecting the human HMGA1 gene in benign mesenchymal tumours, e.g. endometrial polyps, lipomas, pulmonary chondroid hamartomas, and uterine leiomyomas [12-14] are not completely understood. However, it is currently supposed that the aberration causes up-regulation of the HMGA1 gene in the affected neoplasias. The principal aim of the study was to characterize the genomic structure of the canine HMGA1 gene allowing the comparison of its genomic structure to the counterparts of other mammals and thus allowing a further evaluation of evolutionary conservation of the gene and a comparative analysis of chromosomal aberrations in both species. Additional aims were the *in vivo* localization of the canine HMGA1 protein and the evalu-

ation of a previously described point mutation which causes a disrupted protein.

Genomic structure, BAC Screening and FISH

A canine *HMGA1* genomic PCR reaction was established and used for screening of a canine BAC for identification of the canine *HMGA1* gene locus by FISH. The verified BAC 572 P20 K12 RC was used for FISH experiments. Ten well spread metaphases were analysed and showed signals on both chromatids of both chromosomes CFA 12q11 (Figure 1). The chromosomal localisation was done following the nomenclature established by Reimann et al. [26]. Existing painting probe based synteny studies and RH analyses [27] indicated that the canine CFA 12 shares homology with the human chromosome 6 on which the *HMGA1* gene is located at HSA 6p21. Chromosomal aberrations affecting CFA 12 are not or barely reported to be significantly associated with canine neoplasias [28,29]. While previous studies reported the localization of a *HMGA1* gene positive BAC to CFA 23 [30], the performed *in silico* analyses and the recently published canine genome assembly [31] support the herein described assignment of the canine *HMGA1* gene to CFA 12q11 by FISH described in this study. Comparative chromosomal *in silico* analyses using the "Evolutionary Highway" <http://evolutionhighway.ncsa.uiuc.edu/results.html> showed similar results.

The genomic structure of the canine *HMGA1* gene consists in total of the 7 exons and 6 introns. Overall the canine *HMGA1* gene spans 9524 bp. The exon/intron structure, size and the homologies to their human counterparts were analysed and defined (Figure 2, Table 1). The total identity to the corresponding human region is 62.8%. In detail, the identities of the exons vary between 74.6% and 97.8% to their human counterpart, while the introns show identities between 58.9% and 92.4% (for details see Table 1). The newly characterized sequences combined with the analyses performed *in silico* revealed that the exon 4, which exists in humans, is missing on genomic level in the canine genome. This exon 4 deletion also exists in the mouse genome and affects the respective mRNAs of both species in their 5' UTR. As the genomic characterization of the canine *HMGA1* gene was not available when the exons were named previously, the numbering at that time was based on the respective human exon numbers as defined by Friedmann et al. [32]. Consequently, as it is now known that the canine genomic sequence is lacking an equivalent to human exon 4, the previously used canine exon numbering should be revised with the then named canine exon 5 now being canine exon 4 and so on (Figure 2, Table 1). However, a part of intron 2 remains unsequenced due to an extensive CG repeat which also exists in the human counterpart (90%CG), and only the number of nucleotides (311 bp) could be identified. The genomic sequences were submit-

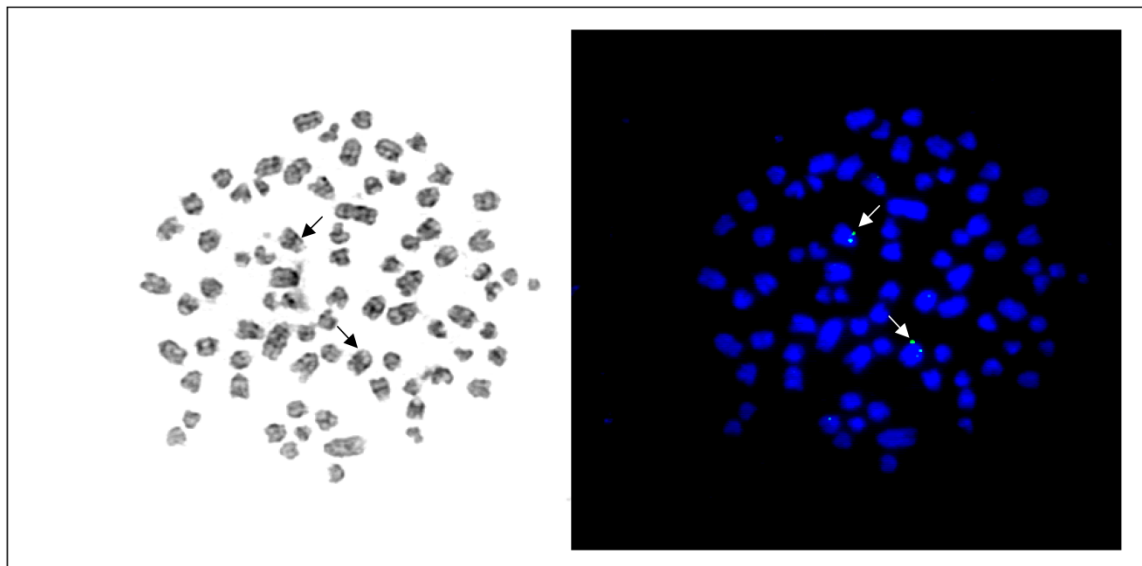
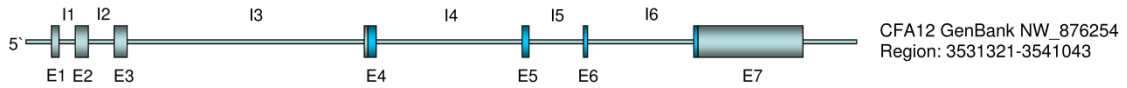


Figure 1
FISH-Mapping of the canine *HMGA1*. Canine metaphase spread after GTG-banding (left) and the same metaphase after fluorescence *in situ* hybridisation with BAC MGA 572 P20 K12 RC showing signals on both chromosomes 12 (right).

Canine *HMGA1*



Human *HMGA1*

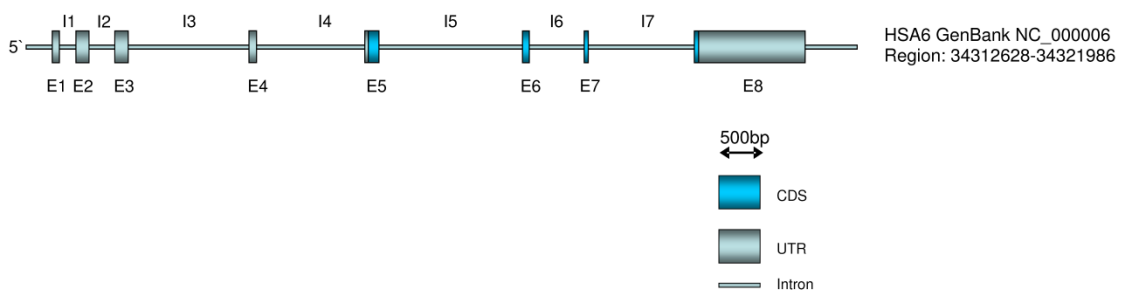


Figure 2
Genomic structure of the canine *HMGA1* gene. Detailed structure of the genomic organisation of the canine *HMGA1* gene.

ted to the NCBI database (bankit1078465, bankit1078536, bankit1078968).

Exon 6 SNP evaluation

While characterising the canine *HMGA1* gene we screened twelve different canine breeds for point mutations affect-

Table 1: Detailed analysis of the canine *HMGA1* gene genomic elements

Element of canine <i>HMGA1</i> gene	Size in bp	Identity to human counterpart in % (GenBank NC_000006)
Total gene	9524	62.8
Detail exons/introns (revised numbering)*		
Exon 1	94	97.8
Intron 1	196	92.4
Exon 2	164	95.8
Intron 2	311	-
Exon 3	162	74.6
Intron 3	3096	58.9
Exon 4 (5)	179	93.9
Intron 4 (5)	1761	51.1
Exon 5 (6)	84	96.4
Intron 5 (6)	584	57.5
Exon 6 (7)	51	94.1
Intron 6 (7)	1459	58.1
Exon 7 (8)	1386	75.4

Identity comparison of the genomic elements of the canine *HMGA1* gene with its respective human counterparts.

ing the protein coding region. A Dachshund sample showed a transition from A to G in exon 6 (according to revised exon numeration) leading to an amino acid exchange from threonine to alanine causing a mutated HMGA1 protein [9]. To elucidate if the observed exchange is frequently existent in the Dachshund population we screened 55 Dachshunds for the respective mutation (Figure 3). The results obtained by sequencing and restriction fragment analysis clearly showed that the previously found mutation is a rare event, as none of the screened 55 Dachshunds showed the mutation. Thus our findings suggest that the previously found aberrant *HMGA1* allele leading to a mutated protein form is unlikely to play a major role in *HMGA1* pathogenesis in Dachshunds.

In general, different species show significant differences considering the number and probability of described SNPs. This fact surely is directly dependent on total numbers of studies and sequencing reactions performed for the different species. While in 2001 Sachidanandam et al. [33] detected 1.42 million SNPs in the human genome with one SNP per 1.9 kb the currently estimated total number reported SNPs in the public databases is approx. 9 million for the human genome [34]. For the dog Lind-

blad-Toh et al. reported 2.5 million SNPs, whereas the probability differs depending on the breed between one SNP per 1500 bp and 900 bp [31]. Comparable to the human genome the total numbers of reported SNPs in the other different species is expected to increase significantly according to the performed research efforts, leading to increased knowledge of effects caused by SNPs in general.

HMGA1 in vivo localization

The *in vivo* localization of the canine *HMGA1* proteins via expression of a canine *HMGA1a*-GFP fusion protein showed that equivalently to its human counterpart the protein is located in the nucleus (Figure 4). Proteins of the *HMG*A family are described to be architectural transcription factors, and thus a localisation in the nucleus seems obvious. However, further localisation and function of these proteins seem to be very likely, due to the fact that application of recombinant *HMGA1* proteins to porcine cartilage cells *in vitro* showed significant increase of cell proliferation (Richter et al. accepted for publication). For a further member of the *HMG* proteins called *HMGB1* the existence of an extracellular function was recognised only a long time after its initial characterisation as an architectural transcription factor, revealing a direct influence of

Part of the canine *HMGA1a* gene

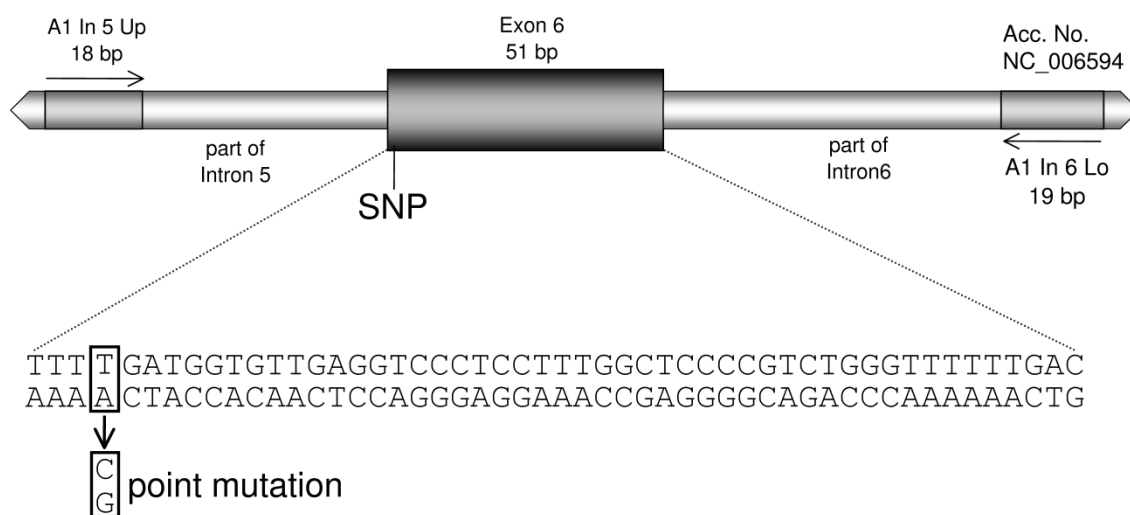
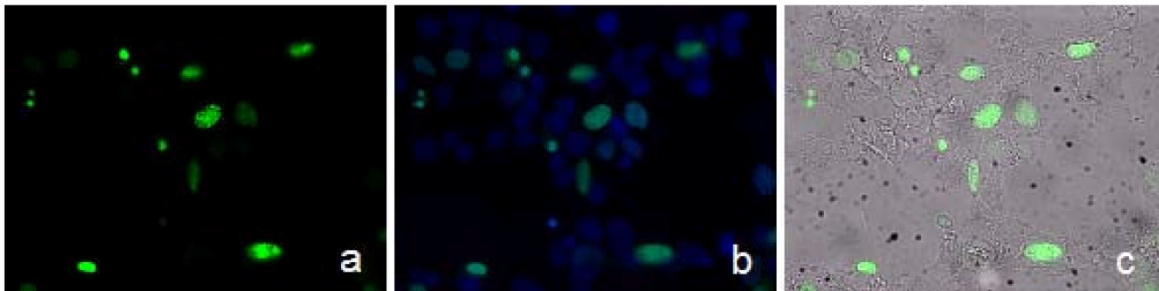


Figure 3
Position of the evaluated Dachshund point mutation. Strategic position of the evaluated point mutation screened in 55 Dachshunds.

**Figure 4**

In vivo localisation of the canine HMGA1 protein. *In vivo* localization of a canine HMGA1a-GFP fusion protein in culture canine MTH53A cells, 24 h posttranslational. a) GFP expression in canine mammary cell line MTH53A, b) DAPI fluorescent staining of cell nuclei, merged GFP and DAPI image, c) merged GFP and transmitted light image (magnification $\times 400$).

extracellular HMGB1 on metastatic events [35-37]. Thus, we suppose that a similar mechanism could also exist for HMGA proteins and are currently working towards its identification.

Conclusion

Knowledge about the structure of genes and proteins is precondition to use them as potential therapeutic targets, markers or for revealing mechanisms involved in relevant pathogenic events. The canine and human HMGA genes and proteins have widely been shown to be involved in various diseases especially in cancer. Due to the numerous reasons for using the dog as a model system for human cancer research the characterisation of canine genes and proteins is of special interest. The performed characterisations of the canine HMGA1 gene and proteins will allow performing comparative analyses of aberrations affecting the human and canine genes and proteins as basis for revealing mechanisms involved in HMGA1 related pathogenesis in both species.

Methods

BAC library screening

A PCR reaction for the use in PCR-based screening of the *Canis familiaris* DogBAC library (Schelling et al., 2002) (Institute of Animal Genetics, Nutrition and Housing, University of Berne, Berne, Switzerland) for a BAC clone containing *HMGA1* was established using canine genomic DNA derived from blood. The primers A1In5up (5' GGCATCCGGTGAGCAGTG 3') and A1In6lo (5' CAG-GCAGAGCACGCAGGAC 3') were designed using GeneBank sequences [AY366395](#) & [NW_876254](#). PCR parameters were: 95°C for 5 min, followed by 30 cycles of 95°C 30 sec, 59.3°C 30 sec, 72°C 30 sec, and a final elongation of 72°C for 10 min. The corresponding 201 bp PCR product was cloned into the pGEM-T Easy vector system (Promega, Mannheim, Germany) and verified by sequencing. The DNA contigs and alignments were done

with Lasergene software (DNASTar, Madison, USA) and various sequences from the NCBI database ([AY366395](#), [NW_876254](#)). The verified BAC clone MGA 572 P20 K12 RC was used as probe for the following FISH experiments.

Slide Preparation

1 ml of canine whole blood was incubated for 72 h in Chromosome Medium B (Biochrom, Berlin, Germany). Subsequently, colcemide (0.1 $\mu\text{g/ml}$) (Biochrom, Berlin, Germany) was added for 2 hours. The cells were centrifuged at 135 \times g for 10 min and incubated for 20 min in 0.05 M KCl. Finally the cells were fixed with methanol/glacial acetic acid. This suspension was dropped on ice-cold slides and dried for at least 7 days at 37°C. The chromosomes were stained by GTG banding for karyotype description. Prior to use in FISH investigations, the slides were destained with 70% ethanol.

Fluorescence in situ Hybridization

MGA 572 P20 K12 RC BAC-DNA was digoxigenin labelled (Dig-Nick-Translation-Kit, Roche, Mannheim, Germany). The hybridization mixture contained 200 ng probe, 40 ng ssDNA, 600 ng sonicated dog DNA, 2 \times SSC, 2 \times SSPE, 50% formamide and 10% dextran sulfate. 50 μl of this mixture were applied to each slide and the cover slips were sealed with rubber cement. Probe and chromosomes were denatured at 75°C on an Eppendorf Thermocycler gradient, using the *in situ* adapter. Afterwards, the slides were incubated in a moist chamber at 37°C overnight. Cover slips were carefully removed and the slides were incubated in 0.1 \times SSC at 61°C and 1 \times PBS at RT. Slides were then covered with 100 μl non fat dry milk (NFD) for 20 min. at 37°C in a moist chamber. For signal detection 100 μl NFD containing 3 μg of Anti-Digoxigenin-Rhodamine, Fab fragments (Roche, Mannheim, Germany), were added to each slide and again incubated for 20 min at 37°C in a moist chamber, followed by washes with 1 \times PBS, 3 \times 3 min. at RT. Slides were air dried

before chromosomes staining was performed with 25 μ l of Vectashield Mounting Medium with DAPI (Vector Laboratories, Burlingame, CA, USA)

Ten well spread metaphases were examined indicating a signal on CFA 12q11 on both chromatids of both chromosomes CFA 12q11 (Fig. 1). The determination of chromosomes follows the nomenclature of the canine karyotype as described previously [26].

Genomic characterisation

For genomic characterisation of the canine *HMGA1* gene the missing parts were amplified by PCR on the screened BAC clone MGA 572 P20 K12 RC. For the missing part 1 a 858 bp fragment (bankit 1078968) was generated with primer pair A1_6640-6997_upa (5'-GGCCGGCTCCAA-GAA-3'), A1_6_lo_2 (5'-CCAACAGAGCCCTGCAA-3'), a 1879 bp fragment (bankit 1078465 for the missing part 2 was generated by the primer pair A1_8864-10549_upa (5'-GTCTCACCGTCTGGAGAAT-3'), A1_8864-10549_loa (5'-TCACCGGAGGCTGCTT-3') and for the third missing part a 979 bp fragment (bankit 1078536) was generated with primer pair A1_11223-11834_upa (5'-CTGAGCCCATGCCAGATAA-3'), A1_11223-11834_loa (5'-AGAGATCCCTGCCGTAGT-3'). The obtained PCR products were separated on a 1.5% agarose gel, recovered with QIAquick Gel Extraction Kit (QIAGEN, Germany), cloned in pGEM-T Easy vector system (Promega, Mannheim, Germany) and sequenced for verification. The final genomic canine *HMGA1* contig and the identity alignments were created with Lasergene software (DNASTar, Madison, USA) with the generated sequences from the cloned cDNAs described previously and various sequences from the NCBI database derived from the canine genome sequencing ([AY366394](#), [AY366395](#), [AY366396](#), [NM_001003387](#), [NW_876254](#)).

SNP screening

Genomic DNA was isolated from the collected 55 Dachshunds samples using the QiaAmp kit (QIAGEN, Hilden, Germany). A specific genomic PCR using the primer pair A1In5up (5' GGCATCCGGTGAGCAGTG 3') and A1In6lo (5' CAGGCAGAGCACGCAGGAC 3') was established allowing the amplification of the complete exon 6 and flanking regions of intron 5 and 6, respectively (Figure 3). In detail the PCRs were performed in a 25 μ l volume containing 0.5 μ M of both primers (MWG Biotech, Martinsried, Germany), 0.1 mM of each dNTP (Invitrogen, Karlsruhe, Germany) 0.6 units Taq-DNA polymerase (Promega, Mannheim, Germany), 1.5 mM MgCl₂ (Promega, Mannheim, Germany), PCR buffer (Promega, Mannheim, Germany) and 2.5 μ l template DNA, containing averaged 26.5 ng/ μ l.

After an initial denaturation step of 5 min at 95°C, the amplification followed in 30 cycles (30 sec. at 95°C, 30 sec at 59.3°C and 30 sec at 72°C). To complete, a final elongation step for 10 min. at 72°C completed the process. The obtained PCR products were purified using the QIAquick PCR Purification Kit (Qiagen, Hilden, Germany), directly sequenced by MWG Biotech (Martinsried, Germany), and additionally digested enzymatically with AluI (Fermentas, St. Leon-Rot, Germany). The occurrence of the described SNP creates a new restriction site for the enzyme AluI (5' AG ∇ CT 3'). Thus, a digestion with AluI cuts the 201 bp PCR product in two fragments of 69 bp and 132 bp, respectively allowing a verification of the sequencing results.

HMGA1 in vivo localisation

For the *HMGA1 in vivo* localisation the protein coding sequence of the canine *HMGA1a* was amplified by PCR using primer pair EcoR1_IY-upATG (5'-CGGAATTCAC-CATGAGCCGAGTCGAGCTCGA-3'), BamH1_IY-loSTOP (5'-CGGGATCCTCACTGCTCCTCTTCGGAGGACT-3'). The obtained PCR products were separated on a 1.5% agarose gel, recovered with QIAquick Gel Extraction Kit (QIAGEN, Hilden, Germany), ligated into the pEGFP-C1 vector plasmid (BD Bioscience Clontech) and sequenced for verification.

Cells from canine mammary tumour cell line M1H53a were cultivated using medium 199 (Invitrogen, Karlsruhe, Germany) supplemented with 20% FCS, penicillin, and streptomycin. The transfection was performed according to the manufacturer's instructions using 3 μ l EugeneHD reagent (Roche, Mannheim, Germany) in 100 μ l PBS (without Mg²⁺) containing 2 μ g of recombinant pEGFP-C1-*HMGA1a*. After treatment, the cells were incubated for 48 hours in the culture media. The uptake and expression of DNA was verified by fluorescence microscopy.

Authors' contributions

CB: collected the Dachshund samples and performed the point mutation screening, JB: head of the centre for human genetics, took part in the conception design of the study, GD: constructed the screened BAC library, JTS: *in silico* analyses and construction of the *HMGA1* gene structure, MM: construction of expression vectors for the *in vivo* localisation, HME: principal study design, IN: head of the small animal clinic, took part in the conception design of the study, NR-B: karyotyping, AR: transfection of cells for *in vivo* localisation, CS: screening of the canine BAC library, SiW: molecular cloning of the newly characterised *HMGA1* fragments, SaW: supervision point mutation screening, SuW: performed the FISH experiments.

Acknowledgements

We would like to thank Melissa Domel and Merle Skischus for technical assistance.

This work was supported in part by the German Excellence Cluster "REBIRTH" (From Regenerative Biology to Reconstructive Therapy, Hannover) within the Excellence Initiative of the German Federal Ministry of Education and Research and the German Research Foundation.

References

- Bustin M, Reeves R: **High-mobility-group chromosomal proteins: architectural components that facilitate chromatin function.** *Prog Nucleic Acid Res Mol Biol* 1996, **54**:35-100.
- Fujisaki S, Eguchi T, Watanabe Y, Honma D, Saitou T, and Yasue H: **Construction of a full-length library of swine olfactory bulb and its preliminary characterization.** *Unpublished manuscript* 2003.
- Johnson KR, Lehn DA, Elton TS, Barr PJ, Reeves R: **Complete murine cDNA sequence, genomic structure, and tissue expression of the high mobility group protein HMG-I(Y).** *The Journal of biological chemistry* 1988, **263**(34):18338-18342.
- Aldrich TL, RR Lee CC, Thomas JN, and Morris AE: **HMG-I(Y) proteins implicated in amplification of CHO cell DNA.** *Unpublished manuscript* 1999.
- Strausberg RL, Feingold EA, Grouse LH, Derge JG, Klausner RD, Collins FS, Wagner L, Shenmen CM, Schuler GD, Altschul SF, Zeeberg B, Buetow KH, Schaefer CF, Bhat NK, Hopkins RF, Jordan H, Moore T, Max SI, Wang J, Hsieh F, Diatchenko L, Marusina K, Farmer AA, Rubin GM, Hong L, Stapleton M, Soares MB, Bonaldo MF, Casavant TL, Scheetz TE, Brownstein MJ, Ustin TB, Toshiyuki S, Carninci P, Prange C, Raha SS, Loquellano NA, Peters GJ, Abramson RD, Mullahy SJ, Bosak SA, McEwan PJ, McKernan KJ, Malek JA, Gunaratne PH, Richards S, Worley KC, Hale S, Garcia AM, Gay LJ, Hulyk SW, Villalon DK, Muzny DM, Sodergren EJ, Lu X, Gibbs RA, Fahey J, Helton E, Kesteman M, Madan A, Rodrigues S, Sanchez A, Whiting M, Madan A, Young AC, Shevchenko Y, Bouffard GG, Blakesley RW, Touchman JW, Green ED, Dickson MC, Rodriguez AC, Grimwood J, Schmutz J, Myers RM, Butterfield YS, Krzywinski MI, Skalska U, Smailus DE, Scherch A, Schein JE, Jones SJ, Marra MA: **Generation and initial analysis of more than 15,000 full-length human and mouse cDNA sequences.** *Proceedings of the National Academy of Sciences of the United States of America* 2002, **99**(26):16899-16903.
- Sgarra R, Diana F, Bellarosa C, Dekleva V, Rustighi A, Toller M, Manfioletti G, Giaccotti V: **During apoptosis of tumor cells HMGAIa protein undergoes methylation: identification of the modification site by mass spectrometry.** *Biochemistry* 2003, **42**(12):3575-3585.
- Sgarra R, DF Bellarosa C, Rustighi A, Toller M, Manfioletti G, and Giaccotti V: **Increase of HMGAIa protein methylation is a distinctive characteristic of tumor cells induced to apoptosis.** *Unpublished manuscript* 2002.
- Vandenplas M, CPM Suzuki Y, Sugano S, Moore JN, Liang C, Sun F, Sullivan R, Shah M, and Pratt LH: **An EST database from equine (*Equus caballus*) unstimulated peripheral blood leukocytes.** *Unpublished manuscript* 2003.
- Murua Escobar H, Soller JT, Richter A, Meyer B, Winkler S, Flohr AM, Nolte I, Bullerdiek J: **The canine HMGAI.** *Gene* 2004, **330**:93-99.
- Sonstegard TS, VTCP Matukumalli LK, Harhay GP, Bosak S, Rubenfield M, and Gasbarre LC: **Production of EST from cDNA libraries derived from immunologically activated bovine gut.** *Unpublished manuscript* 2004.
- Murua Escobar H, Soller JT, Richter A, Meyer B, Winkler S, Bullerdiek J, Nolte I: **"Best friends" sharing the HMGAI gene: comparison of the human and canine HMGAI to orthologous other species.** *The Journal of heredity* 2005, **96**(7):777-781.
- Kazmierczak B, Dal Cin P, Wanschura S, Borrmann L, Fusco A, Van den Berghe H, Bullerdiek J: **HMGII is the target of 6p21.3 rearrangements in various benign mesenchymal tumors.** *Genes Chromosomes Cancer* 1998, **23**(4):279-285.
- Tallini G, Vanni R, Manfioletti G, Kazmierczak B, Faa G, Pauwels P, Bullerdiek J, Giaccotti V, Van Den Berghe H, Dal Cin P: **HMGII-C and HMGII(Y) immunoreactivity correlates with cytogenetic abnormalities in lipomas, pulmonary chondroid hamartomas, endometrial polyps, and uterine leiomyomas and is compatible with rearrangement of the HMGII-C and HMGII(Y) genes.** *Lab Invest* 2000, **80**(3):359-369.
- Williams AJ, Powell WL, Collins T, Morton CC: **HMGII(Y) expression in human uterine leiomyomata. Involvement of another high-mobility group architectural factor in a benign neoplasm.** *Am J Pathol* 1997, **150**(3):911-918.
- Chiappetta G, Avantaggiato V, Visconti R, Fedele M, Battista S, Trappasso F, Merciai BM, Fidanza V, Giaccotti V, Santoro M, Simeone A, Fusco A: **High level expression of the HMGII (Y) gene during embryonic development.** *Oncogene* 1996, **13**(11):2439-2446.
- Rogalla P, Drechsler K, Frey G, Hennig Y, Helmke B, Bonk U, Bullerdiek J: **HMGII-C expression patterns in human tissues. Implications for the genesis of frequent mesenchymal tumors.** *The American journal of pathology* 1996, **149**(3):775-779.
- Fedele M, Bandiera A, Chiappetta G, Battista S, Viglietto G, Manfioletti G, Casamassimi A, Santoro M, Giaccotti V, Fusco A: **Human colorectal carcinomas express high levels of high mobility group HMGII(Y) proteins.** *Cancer research* 1996, **56**(8):1896-1901.
- Bandiera A, Bonifacio D, Manfioletti G, Mantovani F, Rustighi A, Zanconati F, Fusco A, Di Bonito L, Giaccotti V: **Expression of HMGII(Y) proteins in squamous intraepithelial and invasive lesions of the uterine cervix.** *Cancer research* 1998, **58**(3):426-431.
- Abe N, Watanabe T, Masaki T, Mori T, Sugiyama M, Uchimura H, Fujioka Y, Chiappetta G, Fusco A, Atomi Y: **Pancreatic duct cell carcinomas express high levels of high mobility group I(Y) proteins.** *Cancer research* 2000, **60**(12):3117-3122.
- Diana F, Di Bernardo J, Sgarra R, Tessari MA, Rustighi A, Fusco A, Giaccotti V, Manfioletti G: **Differential HMGII expression and post-translational modifications in prostatic tumor cells.** *International journal of oncology* 2005, **26**(2):515-520.
- Frasca F, Rustighi A, Malaguarnera R, Altamura S, Vigneri P, Del Sal G, Giaccotti V, Pezzino V, Vigneri R, Manfioletti G: **HMGII inhibits the function of p53 family members in thyroid cancer cells.** *Cancer research* 2006, **66**(6):2980-2989.
- Sarhadi VK, Wikman H, Salmenkivi K, Kuosma E, Sioris T, Salo J, Karjalainen A, Knuutila S, Anttila S: **Increased expression of high mobility group A proteins in lung cancer.** *The Journal of pathology* 2006, **209**(2):206-212.
- Fedele M, Fidanza V, Battista S, Pentimalli F, Klein-Szanto AJ, Visone R, De Martino I, Curcio A, Morisco C, Del Vecchio L, Baldassarre G, Arra C, Viglietto G, Indolfi C, Croce CM, Fusco A: **Haploinsufficiency of the HmgII gene causes cardiac hypertrophy and myelo-lymphoproliferative disorders in mice.** *Cancer research* 2006, **66**(5):2536-2543.
- Foti D, Chiefari E, Fedele M, Iuliano R, Brunetti L, Paonessa F, Manfioletti G, Barbetti F, Brunetti A, Croce CM, Fusco A, Brunetti A: **Lack of the architectural factor HMGII causes insulin resistance and diabetes in humans and mice.** *Nature medicine* 2005, **11**(7):765-773.
- MacEwen EG: **Spontaneous tumors in dogs and cats: models for the study of cancer biology and treatment.** *Cancer metastasis reviews* 1990, **9**(2):125-136.
- Reimann N, Bartnitzke S, Bullerdiek J, Schmitz U, Rogalla P, Nolte I, Ronne M: **An extended nomenclature of the canine karyotype.** *Cytogenetics and cell genetics* 1996, **73**(1-2):140-144.
- Breen M, Bullerdiek J, Langford CF: **The DAPI banded karyotype of the domestic dog (*Canis familiaris*) generated using chromosome-specific paint probes.** *Chromosome Res* 1999, **7**(5):401-406.
- Reimann N, Bartnitzke S, Nolte I, Bullerdiek J: **Working with canine chromosomes: current recommendations for karyotype description.** *The Journal of heredity* 1999, **90**(1):31-34.
- Reimann N, Nolte I, Bartnitzke S, Bullerdiek J: **Re: Sit, DNA, sit: cancer genetics going to the dogs.** *Journal of the National Cancer Institute* 1999, **91**(19):1688-1689.
- Becker K, Murua Escobar H, Richter A, Meyer B, Nolte I, Bullerdiek J: **The canine HMGII gene maps to CFA 23.** *Animal genetics* 2003, **34**(1):68-69.
- Lindblad-Toh K, Wade CM, Mikkelsen TS, Karlsson EK, Jaffe DB, Kamal M, Clamp M, Chang JL, Kulbokas EJ 3rd, Zody MC, Mauceli E, Xie X, Breen M, Wayne RK, Ostrander EA, Ponting CP, Galibert F, Smith DR, DeJong PJ, Kirkness E, Alvarez P, Biagi T, Brockman W, Butler J, Chin CW, Cook A, Cuff J, Daly MJ, Decaprio D, Gnerre S, Grabherr M, Kellis M, Kleber M, Bardeleben C, Goodstadt L, Heger A, Hitte C, Kim L, Koepfli KP, Parker HG, Pollinger JP, Searle SM, Suter NB, Thomas R, Webber C, Baldwin J, Abebe A, Abouelleil A, Aftuck L, Ait-Zahra M, Aldredge T, Allen N, An P, Anderson S, Antoinette C, Arachchi H, Aslam A, Ayotte L, Bachantsang P, Barry A, Bayul T, Benamara M, Berlin A, Bessette D, Blitshteyn B, Bloom T, Blye J,

- Boguslavskiy L, Bonnet C, Boukhgalter B, Brown A, Cahill P, Calixte N, Camarata J, Cheshatsang Y, Chu J, Citroen M, Collymore A, Cooke P, Dawoe T, Daza R, Decktor K, DeGray S, Dhargay N, Dooley K, Dooley K, Dorje P, Dorjee K, Dorris L, Duffey N, Dupes A, Egbiremolan O, Elong R, Falk J, Farina A, Faro S, Ferguson D, Ferreira P, Fisher S, FitzGerald M, Foley K, Foley C, Franke A, Friedrich D, Gage D, Garber M, Gearin G, Giannoukos G, Goode T, Goyette A, Graham J, Grandbois E, Gyaltsen K, Hafez N, Hagopian D, Hagos B, Hall J, Healy C, Hegarty R, Honan T, Horn A, Houde N, Hughes L, Hunnicutt L, Husby M, Jester B, Jones C, Kamat A, Kanga B, Kells C, Khazanovich D, Kieu AC, Kisner P, Kumar M, Lance K, Landers T, Lara M, Lee W, Leger JP, Lennon N, Leuper L, LeVine S, Liu J, Liu X, Lokysang Y, Lokysang T, Lui A, Macdonald J, Major J, Marabella R, Maru K, Matthews C, McDonough S, Mehta T, Meldrim J, Melnikov A, Meneus L, Mihalev A, Mihova T, Miller K, Mittelman R, Mlenga V, Mulrain L, Munson G, Navidi A, Naylor J, Nguyen T, Nguyen N, Nguyen C, Nguyen T, Nicol R, Norbu N, Norbu C, Novod N, Nyima T, Olandt P, O'Neill B, O'Neill K, Osman S, Oyono L, Patti C, Perrin D, Phunkhang P, Pierre F, Priest M, Rachupka A, Raghuraman S, Rameau R, Ray V, Raymond C, Rege F, Rise C, Rogers J, Rogov P, Sahalie J, Settipalli S, Sharpe T, Shea T, Sheehan M, Sherpa N, Shi J, Shih D, Sloan J, Smith C, Sparrow T, Stalker J, Stange-Thomann N, Stavropoulos S, Stone C, Stone S, Sykes S, Tchuinga P, Tenzing P, Tesfaye S, Thoulut-sang D, Thoulut-sang Y, Topham K, Topping I, Tsamla T, Vassiliev H, Venkataraman V, Vo A, Wangchuk T, Wangdi T, Weiland M, Wilkinson J, Wilson A, Yadav S, Yang S, Yang X, Young G, Yu Q, Zainoun J, Zembek L, Zimmer A, Lander ES: **Genome sequence, comparative analysis and haplotype structure of the domestic dog.** *Nature* 2005, **438(7069)**:803-819.
32. Friedmann M, Holth LT, Zoghbi HY, Reeves R: **Organization, inducible-expression and chromosome localization of the human HMG-I(Y) nonhistone protein gene.** *Nucleic acids research* 1993, **21(18)**:4259-4267.
33. Sachidanandam R, Weissman D, Schmidt SC, Kakol JM, Stein LD, Marth G, Sherry S, Mullikin JC, Mortimore BJ, Willey DL, Hunt SE, Cole CG, Coggill PC, Rice CM, Ning Z, Rogers J, Bentley DR, Kwok PY, Mardis ER, Yeh RT, Schultz B, Cook L, Davenport R, Dante M, Fulton L, Hillier L, Waterston RH, McPherson JD, Gilman B, Schaffner S, Van Etten WJ, Reich D, Higgins J, Daly MJ, Blumenstiel B, Baldwin J, Stange-Thomann N, Zody MC, Linton L, Lander ES, Altshuler D: **A map of human genome sequence variation containing 1.42 million single nucleotide polymorphisms.** *Nature* 2001, **409(6822)**:928-933.
34. Kim S, Misra A: **SNP genotyping: technologies and biomedical applications.** *Annual review of biomedical engineering* 2007, **9**:289-320.
35. Muller S, Scaffidi P, Degryse B, Bonaldi T, Ronfani L, Agresti A, Beltrame M, Bianchi ME: **New EMBO members' review: the double life of HMGB1 chromatin protein: architectural factor and extracellular signal.** *The EMBO journal* 2001, **20(16)**:4337-4340.
36. Huttunen HJ, Fages C, Kuja-Panula J, Ridley AJ, Rauvala H: **Receptor for advanced glycation end products-binding COOH-terminal motif of amphoterin inhibits invasive migration and metastasis.** *Cancer research* 2002, **62(16)**:4805-4811.
37. Taguchi A, Blood DC, del Toro G, Canet A, Lee DC, Qu W, Tanji N, Lu Y, Lalla E, Fu C, Hofmann MA, Kislinger T, Ingram M, Lu A, Tanaka H, Hori O, Ogawa S, Stern DM, Schmidt AM: **Blockade of RAGE-amphoterin signalling suppresses tumour growth and metastases.** *Nature* 2000, **405(6784)**:354-360.

Publish with **BioMed Central** and every scientist can read your work free of charge

"BioMed Central will be the most significant development for disseminating the results of biomedical research in our lifetime."

Sir Paul Nurse, Cancer Research UK

Your research papers will be:

- available free of charge to the entire biomedical community
- peer reviewed and published immediately upon acceptance
- cited in PubMed and archived on PubMed Central
- yours — you keep the copyright

Submit your manuscript here:
http://www.biomedcentral.com/info/publishing_adv.asp



II. Generation and Characterisation of a Canine EGFP-HMGA2 Prostate Cancer In Vitro Model.

Willenbrock *et al.*, PLoS One, 2014

HMGA2 re-expression was found in several cancer entities including canine prostate cancer. Additionally the balance between *HMGA2* and its regulator the micro RNA *let-7* is discussed to play a major role in tumor etiology. Thus the canine prostatic cell line CT1258-EGFP-*HMGA2* stably overexpressing *HMGA2*, which was fused to *EGFP* and additionally the reference cell line CT1258-EGFP, which expresses solely the green fluorescent protein EGFP, were established and characterized by flow cytometry, fluorescence microscopy, immunocytochemistry, quantitative real-time PCR, karyotype analyses and proliferation assays.

Both cell lines presented hyperdiploid karyotypes as described for the native prostate cell line CT1258. *HMGA2* transcript over expression in CT1258-EGFP-*HMGA2* was confirmed by quantitative real-time PCR, nuclear *HMGA2* protein accumulation was verified by fluorescence microscopy and immunocytochemistry. Proliferation tests revealed a positive *HMGA2* impact on cell growth. Analyses by qRT-PCR showed a statistically significant positive effect on the miRNA *let-7a* and *HMGA1* levels but not on the other analyzed *HMGA2* associated genes.

II.

Generation and Characterisation of a Canine EGFP-HMGA2 Prostate Cancer In Vitro Model.

Saskia Willenbrock, Siegfried Wagner, Nicola Reimann-Berg, Mohammed Moulay, Marion Hewicker-Trautwein, Ingo Nolte, Hugo Murua Escobar

PLoS One. 2014 Jun 10;9(6):e98788.

Own contribution:

- RNA isolation and cDNA synthesis
- Quantitative real-time PCR
- Statistical analyses of real-time PCR results
- Figure preparation (real-time PCR results)
- Partial manuscript drafting



Generation and Characterisation of a Canine EGFP-HMGA2 Prostate Cancer *In Vitro* Model

Saskia Willenbrock¹, Siegfried Wagner^{1,2}, Nicola Reimann-Berg¹, Mohammed Moulay¹, Marion Hewicker-Trautwein³, Ingo Nolte¹, Hugo Murua Escobar^{1,4*}

1 Small Animal Clinic, University of Veterinary Medicine Hannover, Hannover, Germany, **2** Institute of Biophysics, Leibniz University Hannover, Hannover, Germany, **3** Department of Pathology, University of Veterinary Medicine Hannover, Hannover, Germany, **4** Division of Medicine, Haematology, Oncology and Palliative Medicine, University of Rostock, Rostock, Germany

Abstract

The architectural transcription factor HMGA2 is abundantly expressed during embryonic development. In several malignant neoplasias including prostate cancer, high re-expression of *HMGA2* is correlated with malignancy and poor prognosis. The *let-7* miRNA family is described to regulate *HMGA2* negatively. The balance of *let-7* and *HMGA2* is discussed to play a major role in tumour aetiology. To further analyse the role of HMGA2 in prostate cancer a stable and highly reproducible *in vitro* model system is precondition. Herein we established a canine CT1258-EGFP-HMGA2 prostate cancer cell line stably overexpressing HMGA2 linked to EGFP and in addition the reference cell line CT1258-EGFP expressing solely EGFP to exclude EGFP-induced effects. Both recombinant cell lines were characterised by fluorescence microscopy, flow cytometry and immunocytochemistry. The proliferative effect of ectopically overexpressed HMGA2 was determined via BrdU assays. Comparative karyotyping of the derived and the initial CT1258 cell lines was performed to analyse chromosome consistency. The impact of the ectopic *HMGA2* expression on its regulator *let-7a* was analysed by quantitative real-time PCR. Fluorescence microscopy and immunocytochemistry detected successful expression of the EGFP-HMGA2 fusion protein exclusively accumulating in the nucleus. Gene expression analyses confirmed *HMGA2* overexpression in CT1258-EGFP-HMGA2 in comparison to CT1258-EGFP and native cells. Significantly higher *let-7a* expression levels were found in CT1258-EGFP-HMGA2 and CT1258-EGFP. The BrdU assays detected an increased proliferation of CT1258-HMGA2-EGFP cells compared to CT1258-EGFP and native CT1258. The cytogenetic analyses of CT1258-EGFP and CT1258-EGFP-HMGA2 resulted in a comparable hyperdiploid karyotype as described for native CT1258 cells. To further investigate the impact of recombinant overexpressed HMGA2 on CT1258 cells, other selected targets described to underlie HMGA2 regulation were screened in addition. The new fluorescent CT1258-EGFP-HMGA2 cell line is a stable tool enabling *in vitro* and *in vivo* analyses of the HMGA2-mediated effects on cells and the development and pathogenesis of prostate cancer.

Citation: Willenbrock S, Wagner S, Reimann-Berg N, Moulay M, Hewicker-Trautwein M, et al. (2014) Generation and Characterisation of a Canine EGFP-HMGA2 Prostate Cancer *In Vitro* Model. PLoS ONE 9(6): e98788. doi:10.1371/journal.pone.0098788

Editor: Zoran Culig, Innsbruck Medical University, Austria

Received: February 17, 2014; **Accepted:** May 7, 2014; **Published:** June 10, 2014

Copyright: © 2014 Willenbrock et al. This is an open-access article distributed under the terms of the Creative Commons Attribution License, which permits unrestricted use, distribution, and reproduction in any medium, provided the original author and source are credited.

Funding: No third party funds supported this study. The study was financed with the internal budget of the Small Animal Clinic, University of Veterinary Medicine, Hannover. The funders had no role in study design, data collection and analysis, decision to publish, or preparation of the manuscript.

Competing Interests: Herewith the authors confirm that Jörn Bullerdiek, a co-author within former collaborative publications, is a PLOS ONE Editorial Board member. This does not alter the authors' adherence to PLOS ONE Editorial policies.

* E-mail: Hugo.Murua.Escobar@med.uni-rostock.de

Introduction

According to recent global cancer statistics, prostate cancer is the second most frequent diagnosed cancer and sixth leading cause of death among males in economically developed countries [1]. Besides man, the dog is the only known domesticated mammalian species developing spontaneous prostate cancer with considerable interest [2].

Unlike the situation in men, the incidence of canine prostate carcinomas is low accounting for 0.2 to 0.6% of canine neoplasias [3]. However, the disease is locally invasive in both species with a comparable progression, metastatic pattern and histopathology [2,4].

The mean age at diagnosis in dogs is ten years and thus, predominantly affecting elder individuals as it is also reported in men [5–7]. Considering the physiologic age at prostate cancer diagnosis, the respective life span is similar between the two species showing increased incidence with age [6].

In humans, prostate cancer is usually a rather slow-progressing cancer whereas canine prostate cancer is growing rapidly, highly aggressive and less differentiated presenting a poor prognosis [3,8]. Cancer of the canine prostate gland is unresponsive to androgen withdrawal therapy resembling mostly human poorly differentiated, androgen refractory prostate cancer [4,9]. Due to the similarities concerning the presentation of human and canine prostate cancer, the dog has lately been focused as useful natural complementary animal model for evaluating novel prostate cancer therapies [10].

Early detection of prostate cancer in men is currently being done using established biochemical molecular markers such as prostate specific antigen (PSA) and prostate specific membrane antigen (PSMA) with considerable success.

In comparison to the situation in humans, in dogs prostate cancer is diagnosed at a very late disease stage due to the absence of reliable prostate-specific biochemical prognostic marker tools and the treatment remains palliative since still no standard

therapeutic approach for treatment of canine prostate cancer is available [11,12]. Although several studies report immunoreactivity for human PSA in canine non-neoplastic prostate tissue and prostate cancer, up to now PSA could not be found in the plasma of prostate cancer bearing dogs [9,12–16].

Consequently, the identification of reliable molecular biomarkers, such as PSA and PSMA in men, allowing an early detection and reliable prognosis of canine prostatic cancer would be of significant value for future development and evaluation of therapeutic strategies as well as the assessment of treatment response [2].

In this context the High-Mobility-Group Protein A2 (HMGA2) was recently found to serve potentially as a prognostic marker for canine prostatic neoplasias [17]. Herein, the analysis of a subset of different canine prostate tissue samples clearly showed that expression of *HMGA2* increases significantly in correlation to the malign grade of the tissue samples [17]. Furthermore, *HMGA2* was found to serve as a potential differentiation marker of canine malignant T- and B-cell lymphoma [18] and to be strongly upregulated in canine oral squamous cell carcinoma (unpublished data).

In humans, a re-expression of *HMGA2* was also found in various malignant tumours such as leukaemia [19,20], lymphoma [18], mammary [21], pancreas [22], non-small cell lung [23], oral squamous cell [24], and thyroid carcinoma [25] being an indicator of poor prognosis. In a recent study, the HMGA2 protein expression was demonstrated to be significantly higher in tumour tissues compared with adjacent normal tissues [26]. In addition, an *HMGA2* involvement in the induction of epithelial-to-mesenchymal transition (EMT) in the human prostate cancer cell line PC-3 was found [26].

These findings suggest that HMGA2 plays a central role in different tumour entities including prostate cancer within both species strongly supporting *HMGA2* re-expression as a prognostic tumour marker.

In general, the highly conserved HMGA2 protein is abundantly expressed during embryonic development acting as an architectural transcription factor in the nucleus [27,28]. Within this role, HMGA2 is widely reported to be involved in a variety of cellular processes such as gene expression, induction of neoplastic transformation, and promotion of metastasis [29,30].

The expression of *HMGA2* is regulated via micro RNAs (miRNA) of the *let-7* family by binding to sequences located in the 3' untranslated region (UTR) of the transcript [31–35], all of which are conserved in rodents, dog, and chicken [36–38]. Binding of *let-7* miRNAs to complementary sequences regulates post-transcriptionally the expression of *HMGA2* in a negative way [31,35,39,40]. Recently a deregulated *let-7* expression was associated with lung [41,42], breast [43] and prostate cancer [44].

The canine prostate adenocarcinoma derived cell line CT1258 [45–47] used within the present study was also analysed for *HMGA2* marker expression by us revealing a strong overexpression (unpublished data). This result allows to hypothesise that an overexpression of this target gene is likely to play an important role in canine prostate cancer, promoting the proliferation of tumour cells.

To verify this hypothesis, the availability of stable tools allowing evaluating the described *HMGA2-let-7* axis in prostate cancer *in vitro* and *in vivo* is precondition. Therefore we established stably transfected cell lines of CT1258 providing a reliable *in vitro* system to analyse the key aspects of our hypothesis.

We analysed the proliferative effects of abundantly expressed recombinant *HMGA2* on CT1258 cells. Therefore, a stable CT1258 cell line expressing recombinant EGFP-tagged HMGA2

(CT1258-EGFP-HMGA2) was generated using an expression vector construct containing the coding sequence (CDS) of the canine *HMGA2* gene lacking the 5'UTR and 3'UTR and therefore not underlying the direct negative regulation mechanisms by *let-7* [31].

To assess the functionality of the recombinant HMGA2 expression vector and to monitor the biological activity of the recombinant expressed HMGA2, a GFP-tag was added to the *HMGA2* CDS generating a HMGA2-GFP fusion protein. To exclude that the GFP protein has an effect on cell proliferation, a further stable CT1258 cell line (CT1258-EGFP) expressing solely GFP was generated. The *HMGA2* and *let-7a* expression was determined via quantitative real-time PCR in CT1258-EGFP-HMGA2 and CT1258-EGFP in comparison to native CT1258 cells.

Additionally, the expression of selected direct and indirect HMGA2-targets such as *HMGA1* [48], *SNAIL1* [49], *SNAIL2* and *CDH1* [49] was analysed.

To characterise the proliferation of the described three cell lines, BrdU incorporation assays were performed. Comparative karyotype analyses of the newly generated and the initial CT1258 cell lines were additionally carried out to identify cytogenetic changes possibly occurring during plasmid integration into the genome of CT1258 during the establishment of the stable recombinant cell lines.

In summary the new fluorescent canine CT1258-EGFP-HMGA2 cell line provides a valuable tool for further investigations on HMGA2-mediated proliferative effects and HMGA2 regulation mechanisms elucidating the development and pathogenesis of canine prostate cancer. As the dog represents a unique natural model for human prostate cancer, the insights concerning the involvement of HMGA2 in canine prostate cancer will provide benefit for both, humans and dogs, concerning the development of therapeutic strategies and the assessment of the treatment success.

Methods

CT1258 Cell Line

The cell culture conditions, as well as the characteristics of the canine prostate carcinoma cell line CT1258 have been described previously by us [45,46].

pEGFP-C1-*HMGA2* Expression Plasmid

The protein coding sequence of the canine *HMGA2* was amplified by PCR using primer pair EcoRI_sA2_lo (5'-CGGAATTCTTAGTCTCTTCGGCAGACT-3'), BamHI_sA2_Up (5'-CGGGATCCCACCATGAGCGCACGCGGT-3'). The obtained PCR products were separated on a 1.5% agarose gel, recovered with QIAquick Gel Extraction Kit (QIAGEN, Hilden, Germany), ligated in the pEGFP-C1 vector plasmid (BD Bioscience Clontech, Palo Alto, CA, USA) and sequenced for verification. Transfection with the pEGFP-C1-*HMGA2* construct leads to the expression of a recombinant EGFP-HMGA2 fusion protein which is expected to be localised in the nucleus.

Generation of Fluorescent CT1258 Cell Lines

Transfection of CT1258 cells. 300,000 native CT1258 cells were seeded in 6-well plates 24 hours prior transfection and cultivated at standard conditions using medium 199 (Life Technologies GmbH, Darmstadt, Germany) supplemented with 10% FCS (PAA Laboratories GmbH, Coelbe, Germany), and 2% penicillin/streptomycin (Biochrom AG, Berlin, Germany).

The transfection was performed according to the manufacturer's instructions using 7.5 µl Mirus TransIT-2020 reagent

(Mirusbio LLC, Madison, WI, USA) in 250 μ l serum-reduced Opti-MEM I medium (Life Technologies, Darmstadt, Germany) containing 2.5 μ g of pEGFP-C1 (BD Bioscience Clontech, Palo Alto, CA, USA) or recombinant pEGFP-C1-HMGA2 plasmid. After treatment, the cells were incubated for 24 hours in the culture media. The uptake and expression of DNA was verified by fluorescence microscopy using a Leica DMI 6000B fluorescence microscope (Leica Microsystems GmbH, Wetzlar, Germany).

G418 selective antibiotic kill curve assay. Prior generation of the fluorescent CT1258 cell lines, the titration of the proper amount of the selective antibiotic G418 (syn. Geneticin; Life Technologies, Darmstadt, Germany) required for selection of CT1258 cells was carried out with a kill curve assay. Different G418 concentrations were applied (0, 100, 200, 400, 600, 800, 1000 μ g/ml) on 100,000 native CT1258 cells seeded in the wells of a 12-well plate. For selection of positive cells after transfection the concentration was used in which no cell survived the upper conditions after seven days.

Selection of positively transfected CT1258 cells. Fluorescent variants of the cell line CT1258 were established to constitutively express the enhanced green fluorescent protein (EGFP) encoded by the empty pEGFP-C1 plasmid and an EGFP-HMGA2 fusion protein by expression of the recombinant pEGFP-C1-HMGA2 plasmid. To establish the stable CT1258 cell lines, the transfected cells were selected with the antibiotic G418 (Life Technologies, Darmstadt, Germany).

Initially a concentration of 400 μ g/ml G418 in the medium was used when selecting for stable cells. One day after transfection, the cultivation medium 199 was replaced with medium 199 containing G418. Subsequently the selection medium was changed each 24 to 48 hours for the first two weeks which leads to the selection of cells that have stably incorporated the GFP plasmid with the encoded antibiotic resistance gene neomycin for selection in mammalian cells into their genomic DNA. Cells not expressing the construct will be killed by G418. The concentration of G418 was lowered to 300 μ g/ml after three months of consistent selection for maintenance of the generated fluorescent cell lines.

Fluorescence Microscopy and Flow Cytometry (FCM)

GFP expression of the fluorescent cell lines CT1258-EGFP and CT258-EGFP-HMGA2 was analysed after G418-selection by fluorescence microscopy and quantified in a FACSCalibur flow cytometer (Becton, Dickinson and Company, Heidelberg, Germany) with the FL-1 channel to determine the percentage of GFP-positive cells. Cells were trypsinised for 3–5 min, resuspended in BD FACSFlores Sheath Fluid (Becton, Dickinson and Company, Franklin Lakes, NJ, USA) containing 1 μ M TO-PRO-3 (Life Technologies GmbH, Darmstadt, Germany), and at a total number of 1×10^4 events was measured for each sample by flow cytometry. TO-PRO-3 is a far-red cell impermeant nucleic acid stain measured in the FL-4 channel allowing ultrasensitive detection of double-stranded DNA of dead cells. The analysis of the flow cytometry data was done using with Cell Quest software (Becton, Dickinson and Company, Franklin Lakes, NJ, USA).

Immunocytochemistry

Embedding of the cell lines. Cell suspensions of cultured cell lines were fixed in 4% formalin. Cell pellets obtained by centrifugation were embedded in paraffin and cut in 3–4 μ m slices for immunocytochemical staining.

Immunocytochemical staining. For antigen retrieval, microwave heating of paraffin sections in 0.01 M citric acid buffer (pH 6.0 for 20 min) (Quartett, Berlin, Germany) was performed. The inhibition of endogenous peroxidase activity was achieved by

immersion in 0.5% H_2O_2 (v/v) in methanol (20 min). After draining the blocking serum the sections were incubated with a polyclonal goat anti-human HMGA2 antibody (R & D Systems, Minneapolis, MN, USA) diluted 1:400 in phosphate-buffered saline (PBS, pH 7.2, 0.15 M) approximately 16–18 h at 4°C. After washing in PBS, the sections were incubated with a biotin-conjugated antibody to goat IgG (Vector Laboratories, Burlingame, CA, USA). The avidin-biotin-peroxidase reagent (Vector Laboratories) was applied according to the manufacturer's instructions. The chromogen used was 3',3'-diaminobenzidine-tetrahydrochloride (Sigma Aldrich, München, Germany) 0.05% (w/v) with 0.03% H_2O_2 (v/v) as substrate in 0.1 M Tris-buffered saline (Tris-hydroxymethyl-aminomethane; Merck, Darmstadt, Germany). The sections were counterstained with Mayers haematoxylin and mounted. Negative controls were performed by replacing the primary antibodies by normal goat serum. For establishing the immunocytochemical staining reactions, paraffin sections from a canine oral squamous cell carcinoma were used.

RNA Isolation and cDNA Synthesis

Total RNA of the EGFP and EGFP-HMGA2 expressing as well as native CT1258 cells were isolated using the NucleoSpin miRNA (Macherey-Nagel, Düren, Germany) kit according to the manufacturer's instructions including an on column DNase digest to remove potential genomic DNA contaminations.

The respective cDNA syntheses with mRNAs as template were performed using 250 ng total RNA of each sample and the QuantiTect Reverse Transcription Kit following the manufacturer's protocol (Qiagen, Hilden, Germany).

For the reverse transcription of the miRNAs 30 ng total RNA of each sample, the TaqMan MicroRNA Reverse Transcription Kit and the reverse transcription primer provided with the TaqMan MicroRNA Assays were used. All steps were carried out following the manufacturer's protocol (Applied Biosystems, Darmstadt, Germany).

HMGA1, HMGA2, SNAI1, SNAI2 and CDH1 Real-time PCR

For relative quantification of the *HMGA2*, *HMGA1*, *SNAI1*, *SNAI2* and *CDH1* transcript levels in relation to the endogenous gene controls *GUSB* and *HPRT1* PCR amplifications were carried out using the Eppendorf Mastercycler ep realplex real-time PCR System (Eppendorf AG, Hamburg, Germany).

2 μ l of each cDNA corresponding to 25 ng of total RNA were amplified in a total volume of 20 μ l using the TaqMan Universal PCR Master Mix (Applied Biosystems, Darmstadt, Germany) with 600 nM of each primer and 200 nM fluorogenic probe for canine *HMGA1*, *HMGA2* gene expression analysis (previously published by us in Joetzke et al. [18]). Commercially available TaqMan gene expression assays were used for the analysis of the canine targets *SNAI1* (Cf02705362_s1), *SNAI2* (Cf02701218_u1) and *CDH1* (Cf02697525_m1) as well as for the endogenous controls, canine *GUSB* (Cf02622808_m1) and canine *HPRT1* (Cf02626258_m1) (Applied Biosystems, Darmstadt, Germany).

PCR conditions were as follows: 2 min at 50°C and 10 min at 95°C, followed by 40 cycles with 15 s at 95°C and 1 min at 60°C.

All samples were measured in triplicate and for each run non-template controls and non-reverse transcriptase control reactions were included. A precedent efficiency analysis of all PCR assays used in this study was performed by applying the same template in different dilution steps covering a magnitude of five (cDNA corresponding to 100–0.001 ng RNA). The PCR reactions of all analysed target genes showed comparable efficiencies ensuring an appropriate relative real-time PCR analysis. For the analysis based on $\Delta\Delta CT$ method native CT1258 cells were defined as calibrator.

Let-7a, *RNU6B* Real-time PCR

Relative quantification of the canine *let-7a* and *RNU6B* miRNA transcript levels were carried out using the Eppendorf Mastercycler ep realplex real-time PCR System (Eppendorf AG, Hamburg, Germany). 1.33 μ l of each cDNA were amplified in a total volume of 20 μ l using TaqMan Universal PCR Master Mix (Applied Biosystems, Darmstadt, Germany), No AmpErase UNG and TaqMan MicroRNA assays for *let-7a* (Assay ID: 000377) and *RNU6B* (Assay ID: 001093) (Applied Biosystems, Darmstadt, Germany).

PCR conditions were as follows: 10 min at 95°C, followed by 40 cycles with 15 s at 95°C and 1 min at 60°C.

All samples were measured in quadruplicate and for each run non-template controls and non-reverse transcriptase control reactions were included.

A precedent efficiency analysis of the miRNA PCR assays which were used in this study was performed by applying the same template in different dilution steps, showing comparable efficiencies. For the analysis based on $\Delta\Delta$ CT method the control group was defined as calibrator performing relative real-time PCR with *let-7a* as target gene.

Real-time PCR Statistical Analysis

Statistical analysis of the relative real-time PCR results was performed applying the hypothesis test with the software tool REST 2009, version 2.0.13 (Qiagen, Hilden, Germany) [50]. REST determines whether there is a significant difference between samples and controls taking into account reaction efficiencies and using randomisation techniques. A p-value of ≤ 0.05 was considered to be statistically significant.

Cell Proliferation Assay

The proliferation of native CT1258 cells in comparison to the established fluorescent CT1258-EGFP and CT1258-EGFP-HMGA2 cell lines was evaluated using a colorimetric BrdU cell proliferation ELISA (Roche Applied Science, Mannheim, Germany). This assay measures the incorporation of the thymidine analogue 5-bromo-2-deoxyuridine (BrdU) into newly synthesised DNA of replicating cells by ELISA using an anti-BrdU monoclonal antibody.

A total number of 15,000 cells/well from each CT1258 cell line was seeded in eight different wells and cultivated at the previously described conditions. BrdU was added after 24 h and incubated for two hours. The proliferation assay was carried out according to manufacturer's protocol (Cell proliferation ELISA, colorimetric, Roche Applied Science, Mannheim, Germany). The reaction products were quantified by measuring the absorbance at 370 nm (reference wavelength 492 nm) with a maximum of 27 single reads over a time period of 30 min using a scanning multi-well spectrophotometer equipped with the analysis software Gen 5 (Synergy HT multi-mode microplate reader, BioTek Instruments Inc., Bad Friedrichshall Germany). The absorbance results directly correlate to the amount of DNA synthesis and hereby to the number of proliferating cells.

Results are stated as mean absorbance values expressed as Max V [Δ 370–492] and presented as mean \pm standard deviation. All statistical analyses were performed using OriginPro 8 software (OriginLab Corporation, Northampton, USA). The Shapiro-Wilk test was applied to test if the data are normally distributed. Based on the outcome of the Shapiro-Wilk test, a paired sample t-test was performed to assess the significance of proliferative differences between CT1258-EGFP, CT1258-EGFP-HMGA2 and native CT1258 cells. Differences were considered statistically significant for * $p \leq 0.05$, ** $p \leq 0.001$ to 0.01 and *** $p < 0.001$.

Chromosome Preparation

For chromosome preparation of CT1258-EGFP and CT1258-EGFP-HMGA2 cells colcemid (Biochrom AG, Berlin, Germany) was added at a final concentration of 0.1 μ g/ml for 90 min before harvesting. Subsequently, the cells were incubated for 20 min in hypotonic medium (1: 6; medium 199: H₂O; (medium 199: Life Technologies GmbH, Darmstadt, Germany)) and finally fixed with methanol/glacial acetic acid (3:1) following routine methods [51]. The suspension was dropped on ice-cold slides and dried for 5 days at 37°C followed by GTG-banding which was performed as previously described by [52]. Results were processed and recorded with BandView, 6.0, MultiSpecies, Applied Spectral Imaging, Israel. Karyotype description followed the nomenclature proposed by Reimann et al. [53].

Results

Fluorescence Microscopy and FCM

Fluorescence microscopy. CT258 cells transfected with the non-recombinant pEGFP-C1 expression vector showed green fluorescence all over the cytoplasm due to EGFP expression (Fig. 1B) whereas unmodified native CT1258 cells showed no EGFP fluorescence (Fig. 1A).

Transfection of CT1258 with pEGFPC1-HMGA2 resulted in the expression of a recombinant canine EGFP-HMGA2 fusion protein which could solely be detected in the nucleus of the transfected cells (Fig. 1C).

FCM. For determination of EGFP positive cells by FCM, both fluorescent cell lines were compared to native non-transfected CT1258 cells (Fig. 1D). Dead, TO-PRO-3 positive cells were eliminated by gating prior to the EGFP positivity analysis. The cells were measured for CT1258 in the 319th passage, for CT1258-EGFP in the 27th passage, and for CT1258-EGFP-HMGA2 in the 113th passage.

The vitality of the cell lines ranged from 85% to 93% (data not shown). A mean percentage of 84.1% EGFP positive cells from the total cell population of the G418 selected CT1258-EGFP cell line (Fig. 1E) and 97.0% EGFP positive cells for the CT1258-EGFP-HMGA2 cell line (Fig. 1F) was determined.

Immunocytochemistry

Approximately 50% of the CT1258-EGFP cell line had nuclear labelling for HMGA2 (Fig. 2B). In approximately 70–80% of CT1258-EGFP-HMGA2 cells strong labelling for HMGA2 was detected, which was exclusively present in the nucleus (Fig. 2C).

Relative HMGA2 Real-time PCR Expression Analysis

All real-time PCR results were analysed based on $\Delta\Delta$ CT method. The expression ratio of *HMGA2* mRNA in CT1258-EGFP cells was found to be 0.88/0.92 relative to *HPRT1/GUSB* expression when compared to the level seen in native CT1258 cells (Fig. 3). In contrast, the *HMGA2* expression in CT1258-EGFP-HMGA2 cells was 7.0/8.0 fold increased (relative to *HPRT1/GUSB*) when compared to the respective expression in native CT1258 cells (Fig. 3).

Relative *Let-7a* Real-time PCR Expression Analysis

The *let-7a* expression level in CT1258-EGFP and CT1258-EGFP-HMGA2 cells was 2.0 and 3.1 fold higher (relative to *RNU6B*) when compared to the detected expression in native CT1258 cells (Fig. 4).

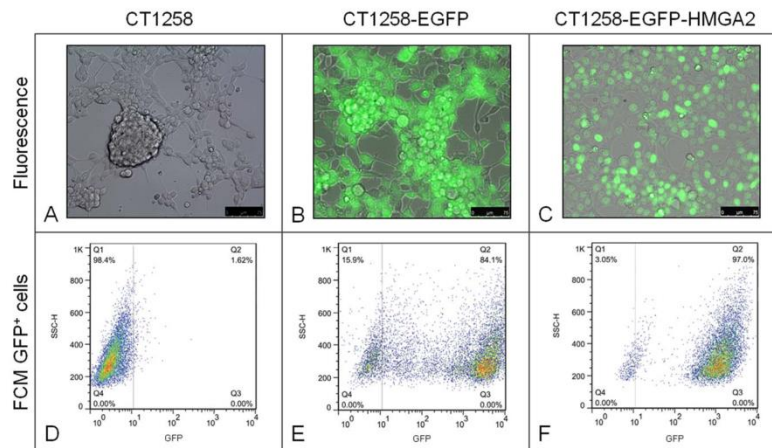


Figure 1. Fluorescence microscopy and flow cytometry analyses. A: Transmitted light image of the characteristic growth pattern of native CT1258 cells. B: Merged image of EGFP expressing CT1258-EGFP cells; EGFP is localised in the cytoplasm. C: Merged image of CT1258-EGFP-HMGA2 cells expressing the nuclear localised EGFP-HMGA2 fusion protein. D–F: Flow cytometric analyses of EGFP expression in the three CT1258 cell lines depicted in dot-plots showing side scatter (SSC) vs. EGFP fluorescence. No GFP fluorescence is detectable in native CT1258 cells (D), 84.1% of EGFP-positive cells are present in the CT1258-EGFP cell line and (F) 97.0% EGFP-positive cells in CT1258-EGFP-HMGA2. Per sample 1×10^4 events were analysed.

doi:10.1371/journal.pone.0098788.g001

Relative *HMGA1* Real-time PCR Expression Analysis

The *HMGA1* level was 1.5 and 1.7 fold increased (relative to *HPRT1* and *GUSB*) in CT1258-EGFP-HMGA2. In CT1258-EGFP cells a comparable increased expression could not be detected (1.0/1.0 relative to *HPRT1* and *GUSB*) when compared to the native cells (Fig. 5).

Relative *SNAI1*, *SNAI2* and *CDH1* Real-time PCR Expression Analysis

Relative *SNAI1* expression to the housekeeping genes *HPRT1*/*GUSB* was found to be 0.8/0.8 respectively in CT1258-EGFP and 1/1.2 in the CT1258-EGFP-HMGA2 when compared to native cells CT1258 (figure S1).

Relative *SNAI2* expression (relative to *HPRT1*/*GUSB*) was found 1.5/1.6 in CT1258-EGFP cells and 1.4/1.6 in CT1258-EGFP-HMGA2 cells when compared to CT1258 (figure S2).

CDH1 was barely expressed in all cell lines with Ct values higher than 36, thus an analysis by the $\Delta\Delta Ct$ method was not possible.

Real-time PCR Statistical Analysis

The hypothesis test of the relative real-time PCR results was performed using REST software tool 2009, version 2.0.13

(Qiagen, Hilden, Germany) [50]. The statistical analyses were carried out separately for the CT1258-EGFP and CT1258-EGFP-HMGA2 cells in comparison to native CT1258. A p-value of ≤ 0.05 was considered as statistically significant.

The statistical analysis showed no significant differences of the relative *HMGA2* expression in the CT1258-EGFP cells in comparison to native CT1258 cells ($p = 0.075$) (Fig. 3). The CT1258-EGFP-HMGA2 cell line showed a significant *HMGA2* over-expression in comparison to native CT1258 cells ($p = 0.009$) and CT1258-EGFP cells ($p = 0.000$) (Fig. 3).

The relative *let-7a* expression differed significantly in CT1258-EGFP ($p = 0.003$) and CT1258-EGFP-HMGA2 ($p = 0.012$) compared to the native CT1258 cells (Fig. 4). The additional statistical analysis of the *let-7a* expression between the CT1258-EGFP and CT1258-EGFP-HMGA2 cells showed also statistical significance ($p = 0.021$).

The *HMGA1* showed no statistical difference in CT1258-EGFP ($p = 0.087$) but a significantly higher expression level in CT1258-EGFP-HMGA2 in comparison to the native cell line CT1258 ($p = 0.000$) and the CT1258-EGFP cells ($p = 0.000$) (Fig. 5).

SNAI1 expression was statistically significantly different in CT1258-EGFP in comparison to the *SNAI1* levels in the native

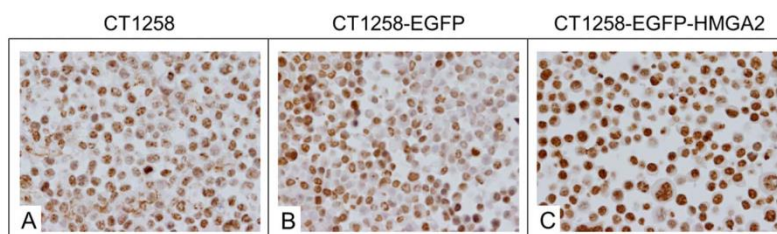


Figure 2. Immunocytochemical staining. A: Native CT1258 cells, B: CT1258-EGFP cells, C: CT1258-EGFP-HMGA2 cells. Approximately 50% of the native CT1258 cell line and of CT1258-EGFP cells showed a HMGA2-positive nuclear labelling. In approximately 70–80% of CT1258-EGFP-HMGA2 cells, a strong and exclusively nuclear labelling for HMGA2 was detectable.

doi:10.1371/journal.pone.0098788.g002

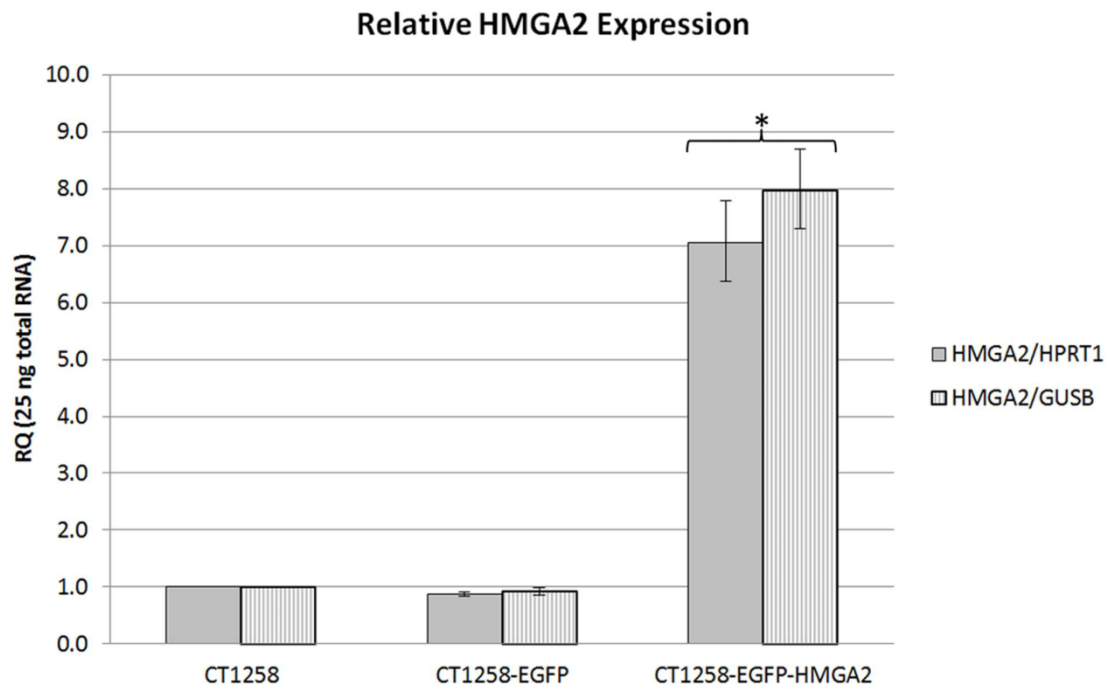


Figure 3. *HMGA2* real-time PCR analyses. Relative *HMGA2/HPRT1* and *HMGA2/GUSB* expression in native CT1258, CT1258-EGFP and CT1258-HMGA2-EGFP cells. Error bars are standard deviations. * $p \leq 0.05$ indicates a statistical significant expression deregulation of *HMGA2* in CT1258-HMGA2-EGFP cells when compared to native CT1258. doi:10.1371/journal.pone.0098788.g003

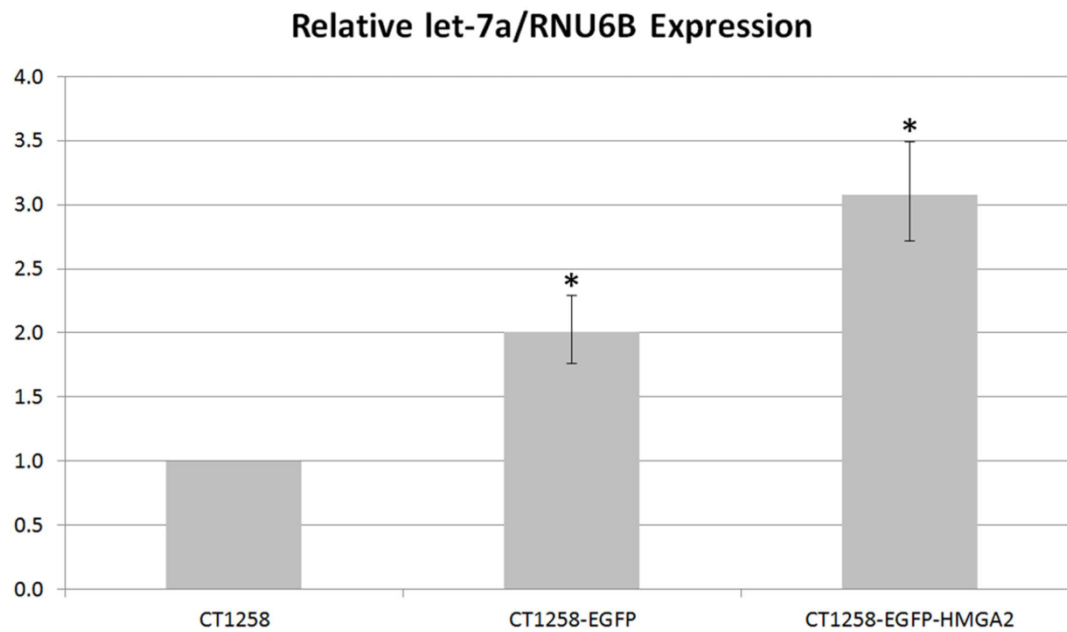


Figure 4. *let-7a* real-time PCR analyses. Relative *let-7a/RNU6B* expression in native CT1258, CT1258-EGFP and CT1258-HMGA2-EGFP cells. Error bars are standard deviations. No statistical significant expression deregulation of *let-7a* in CT1258-EGFP and CT1258-HMGA2-EGFP was detected when compared to native CT1258 cells. Statistical significant p value was defined as ≤ 0.05 . doi:10.1371/journal.pone.0098788.g004

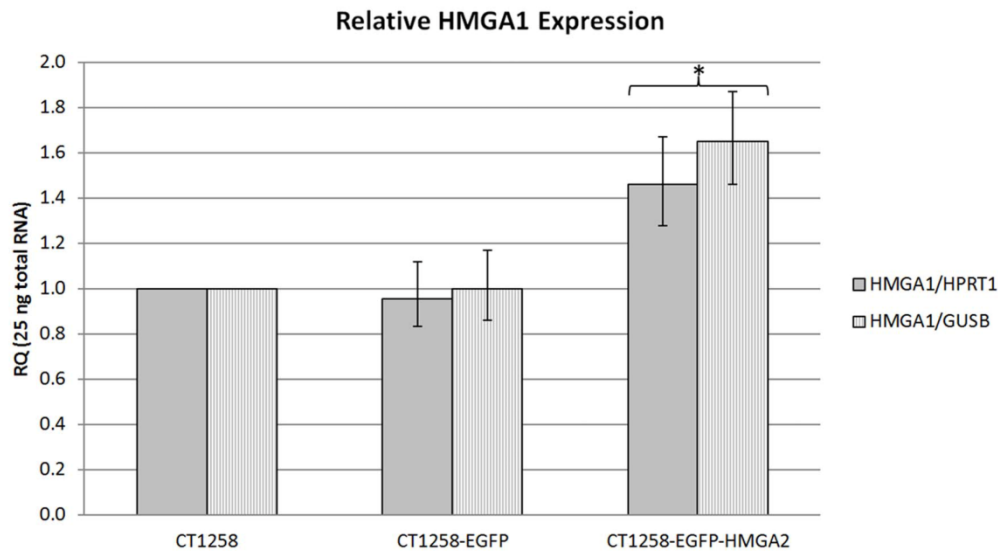


Figure 5. HMGA1 real-time PCR analyses. Relative *HMGA1/HPRT1* and *HMGA1/GUSB* expression in native CT1258, CT1258-EGFP and CT1258-HMGA2-EGFP cells. Error bars are standard deviations. * $p \leq 0.05$ indicates a statistical significant increased expression of *HMGA1* in CT1258-HMGA2-EGFP cells when compared to native CT1258 and CT1258-EGFP. doi:10.1371/journal.pone.0098788.g005

cell line ($p = 0.016$). In CT1258-EGFP-HMGA2 the *SNAI1* expression was comparable to native CT1258 cells ($p = 0.462$) (figure S1).

SNAI2 expression of CT1258-EGFP ($p = 0.100$) and CT1258-EGFP-HMGA2 ($p = 0.066$) were both not significantly different in comparison to the native cell line (figure S2). For *CDH1* expression no statistical analyses was performed due to barely detectable or absent gene expression.

Cell Proliferation Assay

The proliferation of the two established fluorescent CT1258 cell lines and native CT1258 cells was measured using a BrdU proliferation test to analyse the effect of EGFP-HMGA2 expressed in CT1258-EGFP-HMGA2 cells.

The proliferation of each cell line was compared with the two other cell lines (Fig. 6). A significantly increased cell proliferation activity with a p -value of < 0.05 was ascertained for CT1258-EGFP-HMGA2 cells in comparison to native CT1258 cells. Comparing CT1258-EGFP-HMGA2 cells vs. CT1258-EGFP cells resulted also in significantly increased cell proliferation for CT1258 expressing EGFP-HMGA2, but with a p -value of < 0.01 . The analysis of native CT1258 vs. CT1258-EGFP cells resulted in no significant proliferative differences ($p > 0.05$) between both cell lines.

Cytogenetic Analyses

The analysis of native CT1258 cells revealed the presence of a hyperdiploid karyotype (Fig. 7A). Centromeric fusions between the canine chromosomes 1 (CFA1) and 5 (CFA 5), in the following named as der(1;5), were present (Fig. 8). Additionally, one large bi-armed marker (mar) consisting of material from chromosomes 1 and 2 was found (Fig. 8). The gained results are comparable to our previous cytogenetic analysis of primary CT1258 cells carried out by Winkler *et al.* in 2005 [45] concerning the present der(1;5) and the bi-armed marker chromosome (mar). In contrast, native CT1258 cells showed no longer the centric fusions of chromo-

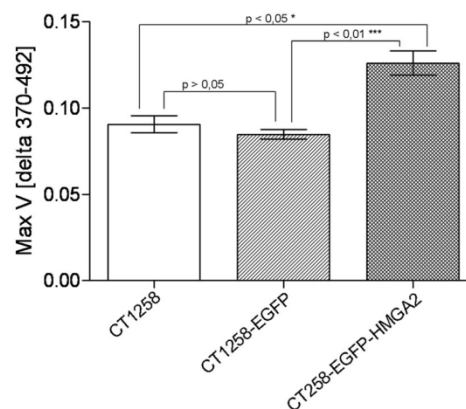


Figure 6. BrdU cell proliferation assay. Measured proliferation of native CT1258, CT1258-EGFP and CT1258-HMGA2-EGFP cells. A statistical significant increased proliferation was detected for CT1258 cells expressing the EGFP-HMGA2 fusion protein in comparison to native CT1258 and EGFP expressing CT1258 cells. Each bar represents a mean \pm SD, * $p \leq 0.05$, *** $p \leq 0.001$. doi:10.1371/journal.pone.0098788.g006

somes 4 (CFA4) and 5 (CFA5) (named der(4;5)) as described in 50% of the initially analysed metaphases of primary CT1258 cells [45].

The chromosome analyses of CT1258-EGFP and CT1258-EGFP-HMGA2 revealed a comparable hyperdiploid karyotype as described for native CT1258 cells (Fig. 7B, 7C). The same large bi-armed marker chromosome (mar) and the two der(1;5) chromosomes as described for native CT1258 cells were also present (Fig. 7B, 7C and Fig. 8).

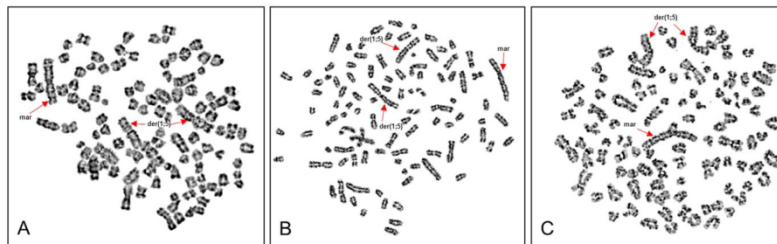


Figure 7. Cytogenetic analyses. Metaphase spreads derived from CT1258 (A), CT1258-EGFP (B) and CT1258-EGFP-HMGA2 (C) cells after GTG-banding. The arrows indicate the centromeric fusions between the canine chromosomes 1 and 5 (der(1;5)) and a large bi-armed marker (mar) consisting of material from chromosomes 1 and 2 being characteristic for the CT1258 cell line. doi:10.1371/journal.pone.0098788.g007

Discussion

Re-expression of *HMGA2* is reported to be associated with the formation of malignant and benign tumours [17–25,54–57], but the exact mechanism of *HMGA2* acting in tumour formation and progression is still unclear. In general, miRNA *let-7* family members are regulating *HMGA2* time-dependently in a negative way by binding to multiple target sites in the 3'UTR of *HMGA2* mRNA [31–34,39]. In different tumours, the *HMGA2* 3'UTR was described to be affected by deletions or rearrangements [58] leading to a loss of *let-7* complementary target sequences [39,59]. A truncated *HMGA2* mRNA without *let-7* binding sites escapes the *let-7* regulation resulting in increased expression of *HMGA2* protein [31,32,39]. Generally, a delicate balance of *let-7* and *HMGA2* is discussed to be necessary for cells to switch between undifferentiated and differentiated state and also plays a central role in cancer development and progression [33,60–63]. How *HMGA2* exerts these changes is not completely understood.

Within this study, we analysed the described *let-7-HMGA2* regulation mechanism in canine prostate cancer using the naturally *HMGA2*-overexpressing canine adenocarcinoma derived cell line CT1258 as an *in vitro* model.

The CT1258 cell line was as previously described to be derived from an aggressive canine prostate carcinoma [45]. In previous studies we characterised the *in vivo* behaviour and tumour formation capacity of CT1258 in NOD/SCID [47,48]. Herein, it could be shown that a very low number of 1×10^3 subcutaneously injected CT1258 cells [47] and an intraperitoneal inoculation of 1×10^3 cells was sufficient to induce stable tumour growth [46]. The induced tumours showed highly aggressive growth

mimicking the character of the original neoplasia [46,47]. Comparative analyses of the primary neoplasia, the initial established CT1258 cell line and the CT1258 generated tumours showed that the cell line and the induced tumours kept their characteristics including cytogenetics, marker expression and in case of the induced tumours the histopathological presentation [45–47].

Thus, the native CT1258 cell line provides a well-characterised basis to identify and characterise molecular mechanisms playing a key role in prostate cancer.

With the recombinant CT1258-EGFP-HMGA2 cell line, expressing an EGFP-HMGA2 transcript lacking the 3'UTR, we investigated if the proliferative effect of *HMGA2* can even be further enhanced although the endogenous *HMGA2* mRNA level in native CT1258 cells is already highly elevated compared to non-neoplastic prostate tissue (unpublished data). Moreover, we analysed the potential impact of the ectopic *HMGA2* expression on the miRNA *let-7a* as one of its regulators within the CT1258-EGFP-HMGA2 cell line in comparison to native CT1258 cells and the control cell line CT1258-EGFP.

In addition the gene expression of the direct *HMGA2* target genes *HMGA1*, *SNAIL1*, *SNAIL2* and the downstream target *CDH1* were examined [48,49].

Verification using fluorescence microscopy detected high numbers of EGFP-positive cells expressing either the cytoplasmic EGFP protein localised throughout the cell or the EGFP-HMGA2 fusion protein. The EGFP-HMGA2 protein was shown to be accumulating exclusively into the nucleus as known for the native protein.

The nuclear accumulation of the recombinant EGFP-HMGA2 fusion protein represents *HMGA2*-typical characteristics such as a functional nuclear localisation signal and chromatin-binding properties enabling proper EGFP-HMGA2 protein function. Further, an irregular distribution of EGFP-HMGA2 amongst the chromatin could be observed matching previous reports characterising native *HMGA2* by other groups [49,60,64,65]. This irregular nuclear distribution of *HMGA2* could also be shown by our immunocytochemistry analyses. The results of the *HMGA2* immunocytochemistry revealed a distinct nuclear labelling in approx. 50% of native and CT1258-EGFP cells, while 70–80% of the CT1258-EGFP-HMGA2 cells showed a strong nuclear labelling. Due to the strong nuclear signal in the CT1258-HMGA2-EGFP cells showing the same irregular labelling as seen by fluorescence microscopy, the presence and the functionality of the ectopically expressed *HMGA2*-GFP fusion protein could be detected via both methodologies.

The flow cytometry analyses confirmed the observed high numbers of fluorescent cells resulting in 84.1% CT1258-EGFP

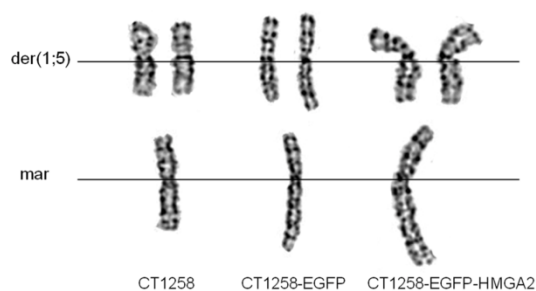


Figure 8. Details of CT1258 chromosomal aberrations. Detailed presentation of chromosomal aberrations found in metaphases of CT1258, CT1258-EGFP and CT1258-EGFP-HMGA2. Two derivative chromosomes (der(1;5)) and the large bi-armed marker chromosome (mar) were found in each cell line. doi:10.1371/journal.pone.0098788.g008

and 97.1% CT1258-EGFP-HMGA2 positive cells expressing EGFP. Thus, the antibiotic selection with G418 showed as very effective to generate nearly pure recombinant derivatives of the CT1258 cell line which can be used as a tool for subsequent *in vivo* experiments.

Real-time PCR analyses of *HMGA2* expression revealed comparable *HMGA2* levels in native CT1258 and CT1258-EGFP cells while a statistically significant *HMGA2* overexpression could be detected in the CT1258-EGFP-HMGA2 cell line. This leads to the assumption that by transfection of CT1258 cells with the pEGFP-C1-*HMGA2* expression vector construct and selection with G418 an ectopic EGFP-HMGA2 expression could be successfully implemented.

Furthermore, *let-7a* real-time PCR expression analyses were performed to investigate potential connections on the *HMGA2-let-7*-axis in canine prostate cancer. The results showed significantly increased *let-7a* expression levels in CT1258-EGFP and CT1258-EGFP-HMGA2 in comparison to the native cell line, whereupon the highest *let-7a* level was detected in CT1258-EGFP-HMGA2. The CT1258-EGFP cell line was intended to serve as a control cell line to exclude EGFP-induced effects. Thus, a comparable *let-7a* expression was expected in native CT1258 cells and the CT1258-EGFP cell line. Interestingly, significantly higher *let-7a* levels were found in CT1258-EGFP. This might be explained by off-target effects induced by the treatment with G418 or the unidentified integration loci of the expression vector into the genome potentially affecting *let-7a* regulatory sites. An effect of EGFP overexpression on the *let-7a* expression is unlikely as EGFP was used as a reporter protein within previously published *let-7* studies showing no EGFP-induced side-effects on *let-7* expression [66,67].

As described previously, the recombinant inserted canine *HMGA2* CDS in the CT1258-HMGA2-EGFP cell line is lacking the 3'UTR which was expected to result in an escape of the recombinant transcript from the *let-7a* miRNA suppression [31]. Owing to the fact that several protein products encoded by the *let-7a*-regulated mRNAs as e.g. *Lin-28*, *Dicer*, *Myc* and *Argonaute* [68–71] were reported to constitute a feedback loop with its regulator, we hypothesized if a *HMGA2* protein overexpression might influence the *let-7a* level as well. However, a significantly higher expression of *let-7a* was detected not only in CT1258-EGFP-HMGA2 but as well in the CT1258-EGFP control cell line. Further statistical analysis revealed that the expression of *let-7a* in CT1258-EGFP-HMGA2 was not only significantly higher in comparison to native cells but also in comparison to the CT1258-EGFP control cell line. It seems that the cells responded to the elevated levels of the recombinant *HMGA2* with increased *let-7a* expression. However, the elevated *let-7a* levels can not solely be attributed to a direct feedback loop as the one previously described for the above mentioned *let-7* targets [68,70,71]. An alternative, indirect response of the cells which are “sensing” the *HMGA2* overproduction or unspecific plasmid DNA integration into the genome might be possible as well. Although the stimulated *let-7a* expression by the ectopic *HMGA2* overexpression was not entirely proofed within this study the newly generated CT1258-EGFP-HMGA2 cell line is nevertheless a suitable tool to further investigate the impact of *HMGA2* expression on other *HMGA2* regulating and regulated genes in canine prostate cancer.

To further examine the role of ectopically overexpressed *HMGA2*, the expression of the *HMGA2*-regulated targets *HMGA1*, *SNAIL*, *SNAIL2* and the downstream target *CDH1* was analysed. These targets are of considerable interest as they were described to be involved in the EMT and thus are able to promote the invasion, migration and subsequent metastasis of prostate cancer cells [72,73]. The analyses of the *HMGA2*-related family

member *HMGA1* revealed a potential positive regulation by the overexpression of the *HMGA2*-EGFP fusion protein. We could show that *HMGA1* was significantly higher expressed in CT1258-EGFP-HMGA2 cells compared to native CT1258 and the CT1258-EGFP control cell line. Interestingly, the *HMGA1* transcript is also described to be negatively regulated by the same *let-7* mechanism as previously described for *HMGA2* [35,74]. In accordance with our results, Berlingieri *et al.* described in a previous study a positive, *HMGA2*-dependent regulation of *HMGA1* in rat thyroid cells [48].

The analysis of the other *HMGA2* targets *SNAIL*, *SNAIL2* and its negatively regulated downstream target *CDH1* [49] showed no differences in expression except *SNAIL*. *SNAIL* was significantly lower expressed in the CT1258-EGFP but not significantly different in CT1258-EGFP-HMGA2 compared to native CT1258 cells.

The cell proliferation analyses by BrdU incorporation assay showed that the ectopic overexpression of recombinant *HMGA2*-EGFP in the CT1258-HMGA2-EGFP cell line resulted in a significantly increased cell proliferation in comparison to native CT1258 and CT1258-EGFP cells. The results revealed that native CT1258 and CT1258-EGFP cells presented nearly the same proliferative rate and thereby excluding that a cell proliferative effect might be mediated by EGFP expression. Consequently the seen effect can be attributed to the ectopic overexpression of *HMGA2* within the CT1258-HMGA2-EGFP cell line.

The present results are in accordance with other studies where ectopic overexpression of recombinant *HMGA2* was also shown to have a positive effect on cell proliferation in e.g. rat fibroblasts [75], or murine myeloblasts [76] *in vitro* and on hematopoietic tissue derived from transgenic *HMGA2*-overexpressing mice [59]. The comparability of these previous results and the proliferative characteristics of CT1258-HMGA2-EGFP underline the functionality of the introduced recombinant protein.

The cytogenetic analyses of the recombinant fluorescent cell lines CT1258-EGFP and CT1258-HMGA2-EGFP revealed stable chromosome copy numbers resembling the hyperdiploid karyotype with der(1;5) chromosomal fusions and the characteristic large bi-armed marker chromosome mainly consisting of material from CFA1 and CFA2 found in native CT1258 cells. The karyotype of CT1258 native cells and their fluorescent derivatives has changed slightly compared to cells of CT1258, which were analysed in a very early passage by Winkler *et al.* in 2005 [45]. In addition to the marker chromosome and the der(1;5) chromosome, the centric fusion of CFA4 and CFA5 (der(4;5)) found in 50% of the analysed metaphases of primary CT1258 cells [45] was no longer present in the native CT1258 cells used in the present study. This loss of der(4;5) can probably be explained due to selection in direction to der(1;5) during the cultivation of the cells over time as the der(4;5) was only found in 50% of the primary analysed CT1258 cells. With the comparative cytogenetic we could assure that no macroscopic chromosomal aberrations such as fusions or breakpoints were induced by the transfection and subsequent integration of the expression vectors pEGFP-C1 and pEGFP-C1-*HMGA2* into the genome under G418 antibiotic selection pressure.

Cell lines represent a key tool in cancer research allowing investigating complex interrelations of certain target genes in tumour development *in vitro* in basic research experiments. With the newly established canine CT1258-EGFP-HMGA2 cell line we could demonstrate *in vitro* an increased cell-proliferative effect of ectopic overexpressed EGFP-HMGA2. Moreover, the generated data adds functional data helping to understand the complex

regulation mechanisms between *HMGA2*, *let-7a* and further selected targets in the progression of prostate cancer.

This CT1258-EGFP-HMGA2 cell line provides a valuable tool to further decipher the HMGA2-mediated molecular mechanisms of prostate cancer and to identify potential targets for development of novel therapies.

Additionally, the ability of the CT1258-EGFP-HMGA2 cell line to express an enhanced EGFP tagged HMGA2 fusion protein can be utilised to monitor the *in vivo* behaviour of the cell line using fluorescence imaging subcutaneously.

To further extend the presented *in vitro* findings, *in vivo* studies need to be carried out. In perspective, this could allow to characterise if abundantly expressed recombinant HMGA2 can increase the highly tumorigenic potential of CT1258 which was previously demonstrated in a murine NOD/SCID *in vivo* model [46,47]. The first characterisation of this hypothesis needs to be carried out carefully in an intermediary *in vivo* mouse model. Such an HMGA2-overexpressing *in vivo* mouse model will help to elucidate, if the previously described correlation between HMGA2 and the malignant and metastatic potential of prostate cancer [17] can be reflected and to characterise the underlying molecular mechanisms. Based on this, novel therapeutic options can be established within an *in vivo* mouse model and subsequently applied to treat dogs being affected by prostate cancer.

Xenograft mouse models with implanted human prostate cancer cell lines such as LNCaP [77], PC-3 [78] or DU145 [79] are extremely useful to study the biology of prostate cancer and are used routinely in human research to evaluate prostate cancer therapies. However, xenografts mouse models miss some important characteristics of naturally occurring tumours which experimentally induced tumours or tumours transplanted into immunocompromised animals cannot provide and bear limitations concerning metabolism, body size and age [80,81]. Thus, long term disease studies are difficult to accomplish within mouse models due to a short life span in comparison to humans [82]. Since prostate cancer develops in dogs spontaneously under the surveillance of an intact immune system in a syngeneic host and tumour microenvironment [83], the dog as a companion animal model provides an important translational bridge between the mouse xenografts and human clinical trials [10,84]. In fact, dogs were suggested by the National Cancer Institute as a potential population to incorporate into studies of new therapeutics [84,85].

Consequently, the dog's contribution to translational research provides reciprocal benefit for both species with the potential to significantly enhance the understanding of prostate cancer development and progression.

Conclusions

In conclusion, with the herein generated new fluorescent canine CT1258-EGFP-HMGA2 cell line a stable highly reproducible tool

for further investigation of HMGA2-mediated cell proliferative effects *in vitro* and *in vivo* in prostate cancer is provided. Screenings as done herein exemplarily for the *HMGA2* regulator *let-7a* and the HMGA2 targets *HMGA1*, *SNAI1*, *SNAI2* and *CDH1* will help to reveal the tumour acting mechanisms. The gained insights of HMGA2-involvement in canine prostate cancer contribute to the identification and evaluation of novel therapeutic options. As the dog displays a unique animal model for prostate cancer, the development of therapeutic strategies provides an important contribution to translational research directed to treat humans, thus providing benefit for both species.

Supporting Information

Figure S1 *SNAI1* real-time PCR analyses. Relative *SNAI1/HPRT1* and *SNAI1/GUSB* expression in native CT1258, CT1258-EGFP and CT1258-HMGA2-EGFP cells. Error bars are standard deviations. * $p \leq 0.05$ indicates a statistical significant deregulation of *SNAI1* expression in CT1258-EGFP when compared to native CT1258 cells. The CT1258-EGFP-HMGA2 cell line showed no statistical significant different *SNAI1* expression in comparison to native CT1258 cells.

(TIF)

Figure S2 *SNAI2* real-time PCR analyses. Relative *SNAI2/HPRT1* and *SNAI2/GUSB* expression in native CT1258, CT1258-EGFP and CT1258-HMGA2-EGFP cells. Error bars are standard deviations. No statistical significant deregulation of *SNAI2* expression was detected in CT1258-EGFP and CT1258-HMGA2-EGFP when compared to native CT1258 cells. Statistical significant p value was defined as ≤ 0.05 .

(TIF)

Acknowledgments

We would like to acknowledge the assistance of the Cell Sorting Lab, Dr. Matthias Krienke, Stiftung Tierärztliche Hochschule Hannover, Klinik für Rinder, Bischofsholer Damm 15, 30173 Hannover.

Author Contributions

Conceived and designed the experiments: IN HME. Performed the experiments: S. Willenbrock S. Wagner NRB MM MHT. Analyzed the data: S. Willenbrock S. Wagner NRB MHT. Contributed reagents/materials/analysis tools: MHT NRB IN HME. Wrote the paper: S. Willenbrock IN HME. Cell culture, generation of the novel cell lines, cell proliferation analyses, chromosome preparation, partial manuscript drafting: S. Willenbrock. qRT-PCR analyses, partial manuscript drafting: S. Wagner. Cytogenetic data analyses: NRB. Flow cytometry: MM. Immunocytochemical analyses and interpretation: MHT. Head of the research group, partial study design, approved the final manuscript: IN. Principal study design, coordination and supervision of all work packages, partial manuscript drafting and finalization: HME.

References

- Jemal A, Bray F, Center MM, Ferlay J, Ward E, et al. (2011) Global cancer statistics. *CA Cancer J Clin* 61: 69–90.
- Waters DJ, Sakr WA, Hayden DW, Lang CM, McKinney L, et al. (1998) Workgroup 4: spontaneous prostate carcinoma in dogs and nonhuman primates. *Prostate* 36: 64–67.
- Fan TM, de Lorimier LP (2007) Tumors of the male reproductive System. In: *Withrow & MacEwen's Small Animal Clinical Oncology*, 4th edition.; Withrow SJ, Vail DM, editors. St. Louis: Saunders Elsevier. 864 p.
- MacEwen EG (1990) Spontaneous tumors in dogs and cats: models for the study of cancer biology and treatment. *Cancer Metastasis Rev* 9: 125–136.
- Bell FW, Klausner JS, Hayden DW, Feeney DA, Johnston SD (1991) Clinical and pathologic features of prostatic adenocarcinoma in sexually intact and castrated dogs: 31 cases (1970–1987). *J Am Vet Med Assoc* 199: 1623–1630.
- Waters DJ, Patronek GJ, Bostwick DG, Glickman LT (1996) Comparing the age at prostate cancer diagnosis in humans and dogs. *J Natl Cancer Inst* 88: 1686–1687.
- Cornell KK, Bostwick DG, Cooley DM, Hall G, Harvey HJ, et al. (2000) Clinical and pathologic aspects of spontaneous canine prostate carcinoma: a retrospective analysis of 76 cases. *Prostate* 45: 173–183.
- Leroy BE, Northrup N (2009) Prostate cancer in dogs: comparative and clinical aspects. *Vet J* 180: 149–162.
- Lai CL, van den Ham R, van Leenders G, van der Lugt J, Mol JA, et al. (2008) Histopathological and immunohistochemical characterization of canine prostate cancer. *Prostate* 68: 477–488.
- Khanna C, Lindblad-Toh K, Vail D, London C, Bergman P, et al. (2006) The dog as a cancer model. *Nat Biotechnol* 24: 1065–1066.

11. Aggarwal S, Ricklis RM, Williams SA, Denmeade SR (2006) Comparative study of PSMA expression in the prostate of mouse, dog, monkey, and human. *Prostate* 66: 903–910.
12. Bell FW, Klausner JS, Hayden DW, Lund EM, Liebenstein BB, et al. (1995) Evaluation of serum and seminal plasma markers in the diagnosis of canine prostatic disorders. *J Vet Intern Med* 9: 149–153.
13. Sorenmo KU, Goldschmidt M, Shofer F, Goldkamp C, Ferracane J (2003) Immunohistochemical characterization of canine prostatic carcinoma and correlation with castration status and castration time. *Vet Comp Oncol* 1: 48–56.
14. McEntee M, Isaacs W, Smith C (1987) Adenocarcinoma of the canine prostate: immunohistochemical examination for secretory antigens. *Prostate* 11: 163–170.
15. Aumuller G, Seitz J, Lijla H, Abrahamsson PA, von der Kammer H, et al. (1990) Species- and organ-specificity of secretory proteins derived from human prostate and seminal vesicles. *Prostate* 17: 31–40.
16. Anidjar M, Villette JM, Devauchelle P, Delisle F, Cotard JP, et al. (2001) In vivo model mimicking natural history of dog prostate cancer using DPC-1, a new canine prostate carcinoma cell line. *Prostate* 46: 2–10.
17. Winkler S, Murua Escobar H, Meyer B, Simon D, Eberle N, et al. (2007) HMGA2 expression in a canine model of prostate cancer. *Cancer Genet Cytogenet* 177: 98–102.
18. Joetke AE, Sterenczak KA, Eberle N, Wagner S, Soller JT, et al. (2010) Expression of the high mobility group A1 (HMGA1) and A2 (HMGA2) genes in canine lymphoma: analysis of 23 cases and comparison to control cases. *Vet Comp Oncol* 8: 87–95.
19. Rommel B, Rogalla P, Jox A, Kalle CV, Kazmierczak B, et al. (1997) HMGI-C, a member of the high mobility group family of proteins, is expressed in hematopoietic stem cells and in leukemic cells. *Leuk Lymphoma* 26: 603–607.
20. Meyer B, Krispeneit D, Junghans C, Murua Escobar H, Bullerdiek J (2007) Quantitative expression analysis in peripheral blood of patients with chronic myeloid leukaemia: correlation between HMGA2 expression and white blood cell count. *Leuk Lymphoma* 48: 2008–2013.
21. Rogalla P, Drechsler K, Kazmierczak B, Rippe V, Bonk U, et al. (1997) Expression of HMGI-C, a member of the high mobility group protein family, in a subset of breast cancers: relationship to histologic grade. *Mol Carcinog* 19: 153–156.
22. Abe N, Watanabe T, Suzuki Y, Matsumoto N, Masaki T, et al. (2003) An increased high-mobility group A2 expression level is associated with malignant phenotype in pancreatic exocrine tissue. *Br J Cancer* 89: 2104–2109.
23. Meyer B, Loeschke S, Schultze A, Weigel T, Sandkamp M, et al. (2007) HMGA2 overexpression in non-small cell lung cancer. *Mol Carcinog* 46: 503–511.
24. Miyazawa J, Mitoro A, Kawashiri S, Chada KK, Imai K (2004) Expression of mesenchyme-specific gene HMGA2 in squamous cell carcinomas of the oral cavity. *Cancer Res* 64: 2024–2029.
25. Belge G, Meyer A, Klemke M, Burchardt K, Stern C, et al. (2008) Upregulation of HMGA2 in thyroid carcinomas: a novel molecular marker to distinguish between benign and malignant follicular neoplasias. *Genes Chromosomes Cancer* 47: 56–63.
26. Zhu C, Li J, Cheng G, Zhou H, Tao L, et al. (2013) miR-154 inhibits EMT by targeting HMGA2 in prostate cancer cells. *Mol Cell Biochem* 379: 69–75.
27. Bustin M (1999) Regulation of DNA-dependent activities by the functional motifs of the high-mobility-group chromosomal proteins. *Mol Cell Biol* 19: 5237–5246.
28. Bustin M, Reeves R (1996) High-mobility-group chromosomal proteins: architectural components that facilitate chromatin function. *Prog Nucleic Acid Res Mol Biol* 54: 35–100.
29. Sgarra R, Rustighi A, Tessari MA, Di Bernardo J, Altamura S, et al. (2004) Nuclear phosphoproteins HMGA and their relationship with chromatin structure and cancer. *FEBS Lett* 574: 1–8.
30. Wolffe AP (1994) Architectural transcription factors. *Science* 264: 1100–1101.
31. Mayr C, Hemann MT, Bartel DP (2007) Disrupting the pairing between let-7 and Hmga2 enhances oncogenic transformation. *Science* 315: 1576–1579.
32. Lee YS, Dutta A (2007) The tumor suppressor microRNA let-7 represses the HMGA2 oncogene. *Genes Dev* 21: 1025–1030.
33. Shell S, Park SM, Radjabi AR, Schickel R, Kistner EO, et al. (2007) Let-7 expression defines two differentiation stages of cancer. *Proc Natl Acad Sci U S A* 104: 11400–11405.
34. Peng Y, Laser J, Shi G, Mittal K, Melamed J, et al. (2008) Antiproliferative effects by Let-7 repression of high-mobility group A2 in uterine leiomyoma. *Mol Cancer Res* 6: 663–673.
35. Rahman MM, Qian ZR, Wang EL, Sultana R, Kudo E, et al. (2009) Frequent overexpression of HMGA1 and 2 in gastroenteropancreatic neuroendocrine tumours and its relationship to let-7 downregulation. *Br J Cancer* 100: 501–510.
36. Roush SF, Slack FJ (2009) Transcription of the *C. elegans* let-7 microRNA is temporally regulated by one of its targets, hbl-1. *Dev Biol* 334: 523–534.
37. Pasquinelli AE, Reinhart BJ, Slack F, Martindale MQ, Kuroda MI, et al. (2000) Conservation of the sequence and temporal expression of let-7 heterochronic regulatory RNA. *Nature* 408: 86–89.
38. Gioia G, Mortarino M, Gelain ME, Albonico F, Ciusani E, et al. (2011) Immunophenotype-related microRNA expression in canine chronic lymphocytic leukemia. *Vet Immunol Immunopathol* 142: 228–235.
39. Young AR, Narita M (2007) Oncogenic HMGA2: short or small? *Genes Dev* 21: 1005–1009.
40. Qian ZR, Asa SL, Siomi H, Siomi MC, Yoshimoto K, et al. (2009) Overexpression of HMGA2 relates to reduction of the let-7 and its relationship to clinicopathological features in pituitary adenomas. *Mod Pathol* 22: 431–441.
41. Takamizawa J, Konishi H, Yanagisawa K, Tomida S, Osada H, et al. (2004) Reduced expression of the let-7 microRNAs in human lung cancers in association with shortened postoperative survival. *Cancer Res* 64: 3753–3756.
42. Kumar MS, Erkeland SJ, Pester RE, Chen CY, Ebert MS, et al. (2008) Suppression of non-small cell lung tumor development by the let-7 microRNA family. *Proc Natl Acad Sci U S A* 105: 3903–3908.
43. Iorio MV, Ferracin M, Liu CG, Veronese A, Spizzo R, et al. (2005) MicroRNA gene expression deregulation in human breast cancer. *Cancer Res* 65: 7065–7070.
44. Dong Q, Meng P, Wang T, Qin W, Qin W, et al. (2010) MicroRNA let-7a inhibits proliferation of human prostate cancer cells in vitro and in vivo by targeting E2F2 and CCND2. *PLoS One* 5: e10147.
45. Winkler S, Murua Escobar H, Eberle N, Reimann-Berg N, Nolte I, et al. (2005) Establishment of a cell line derived from a canine prostate carcinoma with a highly rearranged karyotype. *J Hered* 96: 782–785.
46. Fork MA, Murua Escobar H, Soller JT, Sterenczak KA, Willenbrock S, et al. (2008) Establishing an in vivo model of canine prostate carcinoma using the new cell line CT1258. *BMC Cancer* 8: 240.
47. Sterenczak KA, Meier M, Glage S, Meyer M, Willenbrock S, et al. (2012) Longitudinal MRI contrast enhanced monitoring of early tumour development with manganese chloride (MnCl₂) and superparamagnetic iron oxide nanoparticles (SPIOs) in a CT1258 based in vivo model of prostate cancer. *BMC Cancer* 12: 284.
48. Berlingieri MT, Manfoletti G, Santoro M, Bandiera A, Visconti R, et al. (1995) Inhibition of HMGI-C protein synthesis suppresses retrovirally induced neoplastic transformation of rat thyroid cells. *Mol Cell Biol* 15: 1545–1553.
49. Watanabe S, Ueda Y, Akaboshi S, Hino Y, Sekita Y, et al. (2009) HMGA2 maintains oncogenic RAS-induced epithelial-mesenchymal transition in human pancreatic cancer cells. *Am J Pathol* 174: 854–868.
50. Pfaffl MW, Horgan GW, Dempfle L (2002) Relative expression software tool (REST) for group-wise comparison and statistical analysis of relative expression results in real-time PCR. *Nucleic Acids Res* 30: e36.
51. Bullerdiek J, Boschen C, Bartnitzke S (1987) Aberrations of chromosome 8 in mixed salivary gland tumors—cytogenetic findings on seven cases. *Cancer Genet Cytogenet* 24: 205–212.
52. Reimann-Berg N, Willenbrock S, Murua Escobar H, Eberle N, Gerhauer I, et al. (2010) Two new cases of polysomy 13 in canine prostate cancer. *Cytogenet Genome Res* 132: 16–21.
53. Reimann N, Bartnitzke S, Bullerdiek J, Schmitz U, Rogalla P, et al. (1996) An extended nomenclature of the canine karyotype. *Cytogenet Cell Genet* 73: 140–144.
54. Hess JL (1998) Chromosomal translocations in benign tumors: the HMGI proteins. *Am J Clin Pathol* 109: 251–261.
55. Tallini G, Dal Cin P (1999) HMGI(Y) and HMGI-C dysregulation: a common occurrence in human tumors. *Adv Anat Pathol* 6: 237–246.
56. Wisniewski JR, Schwanbeck R (2000) High mobility group I/Y: multifunctional chromosomal proteins causally involved in tumor progression and malignant transformation (review). *Int J Mol Med* 6: 409–419.
57. Cleynen I, Van de Ven WJ (2008) The HMGA proteins: a myriad of functions (Review). *Int J Oncol* 32: 289–305.
58. Battista S, Fidanza V, Fedele M, Klein-Szanto AJ, Outwater E, et al. (1999) The expression of a truncated HMGI-C gene induces gigantism associated with lipomatosis. *Cancer Res* 59: 4793–4797.
59. Ikeda K, Mason PJ, Bessler M (2011) 3'UTR-truncated Hmga2 cDNA causes MPN-like hematopoiesis by conferring a clonal growth advantage at the level of HSC in mice. *Blood* 117: 5860–5869.
60. Henriksen J, Stabell M, Meza-Zepeda LA, Lauvrak SA, Kassem M, et al. (2010) Identification of target genes for wild type and truncated HMGA2 in mesenchymal stem-like cells. *BMC Cancer* 10: 329.
61. Langelotz C, Schmid P, Jakob C, Heider U, Wernecke KD, et al. (2003) Expression of high-mobility-group-protein HMGI-C mRNA in the peripheral blood is an independent poor prognostic indicator for survival in metastatic breast cancer. *Br J Cancer* 88: 1406–1410.
62. Motoyama K, Inoue H, Nakamura Y, Uetake H, Sugihara K, et al. (2008) Clinical significance of high mobility group A2 in human gastric cancer and its relationship to let-7 microRNA family. *Clin Cancer Res* 14: 2334–2340.
63. Yu F, Yao H, Zhu P, Zhang X, Pan Q, et al. (2007) let-7 regulates self renewal and tumorigenicity of breast cancer cells. *Cell* 131: 1109–1123.
64. Narita M, Krizhanovsky V, Nunez S, Chicas A, Hearn SA, et al. (2006) A novel role for high-mobility group A proteins in cellular senescence and heterochromatin formation. *Cell* 126: 503–514.
65. Cattaruzzi G, Altamura S, Tessari MA, Rustighi A, Giaccotti V, et al. (2007) The second AT-hook of the architectural transcription factor HMGA2 is determinant for nuclear localization and function. *Nucleic Acids Res* 35: 1751–1760.
66. Trujillo RD, Yue SB, Tang Y, O'Gorman WE, Chen CZ (2010) The potential functions of primary microRNAs in target recognition and repression. *Embo J* 29: 3272–3285.
67. Johnson SM, Lin SY, Slack FJ (2003) The time of appearance of the *C. elegans* let-7 microRNA is transcriptionally controlled utilizing a temporal regulatory element in its promoter. *Dev Biol* 259: 364–379.

68. Rybak A, Fuchs H, Smirnova L, Brandt C, Pohl EE, et al. (2008) A feedback loop comprising lin-28 and let-7 controls pre-let-7 maturation during neural stem-cell commitment. *Nat Cell Biol* 10: 987–993.
69. Sampson VB, Rong NH, Han J, Yang Q, Aris V, et al. (2007) MicroRNA let-7a down-regulates MYC and reverts MYC-induced growth in Burkitt lymphoma cells. *Cancer Res* 67: 9762–9770.
70. Tokumaru S, Suzuki M, Yamada H, Nagino M, Takahashi T (2008) let-7 regulates Dicer expression and constitutes a negative feedback loop. *Carcinogenesis* 29: 2073–2077.
71. Zisoulis DG, Kai ZS, Chang RK, Pasquinelli AE (2012) Autoregulation of microRNA biogenesis by let-7 and Argonaute. *Nature* 486: 541–544.
72. Pegoraro S, Ros G, Piazza S, Sommaggio R, Ciani Y, et al. (2013) HMGA1 promotes metastatic processes in basal-like breast cancer regulating EMT and stemness. *Oncotarget* 4: 1293–1308.
73. Smith BN, Odero-Marrah VA (2012) The role of Snail in prostate cancer. *Cell Adh Migr* 6: 433–441.
74. Schubert M, Spahn M, Kneitz S, Scholz CJ, Joniau S, et al. (2013) Distinct microRNA expression profile in prostate cancer patients with early clinical failure and the impact of let-7 as prognostic marker in high-risk prostate cancer. *PLoS One* 8: e65064.
75. Wood IJ, Maher JF, Bunton TE, Resar LM (2000) The oncogenic properties of the HMG-I gene family. *Cancer Res* 60: 4256–4261.
76. Li Z, Gilbert JA, Zhang Y, Zhang M, Qiu Q, et al. An HMGA2-IGF2BP2 axis regulates myoblast proliferation and myogenesis. *Dev Cell* 23: 1176–1188.
77. Veldscholte J, Voorhorst-Ogink MM, Bolt-de Vries J, van Rooij HC, Trapman J, et al. (1990) Unusual specificity of the androgen receptor in the human prostate tumor cell line LNCaP: high affinity for progestagenic and estrogenic steroids. *Biochim Biophys Acta* 1052: 187–194.
78. Kaighn ME, Narayan KS, Ohnuki Y, Lechner JF, Jones LW (1979) Establishment and characterization of a human prostatic carcinoma cell line (PC-3). *Invest Urol* 17: 16–23.
79. Stone KR, Mickey DD, Wunderli H, Mickey GH, Paulson DF (1978) Isolation of a human prostate carcinoma cell line (DU 145). *Int J Cancer* 21: 274–281.
80. Sutter NB, Ostrander EA (2004) Dog star rising: the canine genetic system. *Nat Rev Genet* 5: 900–910.
81. Mueller F, Fuchs B, Kaser-Hotz B (2007) Comparative biology of human and canine osteosarcoma. *Anticancer Res* 27: 155–164.
82. Rowell JL, McCarthy DO, Alvarez CE (2011) Dog models of naturally occurring cancer. *Trends Mol Med* 17: 380–388.
83. Pinho SS, Carvalho S, Cabral J, Reis CA, Gartner F (2012) Canine tumors: a spontaneous animal model of human carcinogenesis. *Transl Res* 159: 165–172.
84. Ittmann M, Huang J, Radaelli E, Martin P, Signoretti S, et al. (2013) Animal models of human prostate cancer: the consensus report of the New York meeting of the Mouse Models of Human Cancers Consortium Prostate Pathology Committee. *Cancer Res* 73: 2718–2736.
85. Khanna C, London C, Vail D, Mazcko C, Hirschfeld S (2009) Guiding the optimal translation of new cancer treatments from canine to human cancer patients. *Clin Cancer Res* 15: 5671–5677.

4.2.1. HMGA protein impact analyses on stem cells

Well defined and reproducible cell culture conditions that allow large-scale production of stem cells whilst maintaining their characteristic features are of great interest in the field of tissue engineering.

In addition, as cancer stem cells (CSC) are hypothesized to contribute to cancer aggressiveness (Adams and Strasser, 2008) and are difficult to enrich, basic cancer research relies as well on alternative stem cell sources.

Multipotency and self-renewal are believed to be the most important features of stem cells enabling persistence in adult tissues throughout life. Therefore the proliferation impacting role of the *let-7* regulated transcription factors HMGA1 and HMGA2 on adipose-tissue-derived mesenchymal stem cells (ADMSCs), were analyzed in the following study.

IV. Effects of High-Mobility Group A Protein Application on Canine Adipose-Derived Mesenchymal Stem Cells In Vitro.

Ismail *et al.*, Veterinary Medicine International, 2010

The multilineage differentiation potential of the used canine ADMSCs was demonstrated by induced differentiation into osteogenic, chondrogenic and adipogenic cell lineages.

The effect of the ectopic HMGA1 and HMGA2 proteins on the proliferation rate of the treated canine ADMSCs was investigated *in vitro* with a colorimetric BrdU cell proliferation ELISA. Growth analysis revealed a negative HMGA1 effect on the ADMSCs at all tested concentrations (10 – 200 ng/ml). The combined cell treatment with HMGA1 and HMGA2 (100, 200 ng/ml) presented as well as in HMGA1 stimulated cells an anti-proliferative effect. The application of HMGA2 alone in the same concentrations as HMGA1 had no measurable impact on canine ADMSC proliferation.

The *in vitro* HMGA2 impact on the expression of the multi-potency factors *Klf4*, *SOX2*, *c-Myc*, *OCT4*, and additionally endogenic *HMGA2* was analyzed by a quantitative two-step real-time PCR. Treatment with ectopic HMGA2 was

Results

demonstrated to have no measurable influence on the expression these genes in canine ADMSCs.

IV.

Effects of High-Mobility Group A Protein Application on Canine Adipose-Derived Mesenchymal Stem Cells In Vitro

A. A. Ismail*, S. Wagner*, H. Murua Escobar, S. Willenbrock, K. A. Sterenczak, M. T. Samy, A. M. Abd El-Aal, I. Nolte, P. Wefstaedt

* Authors contributed equally to the study

Vet Med Int. 2012; 2012: 752083.

Own contribution:

- Design of the Klf4 real-time PCR assay
- Total RNA isolation
- Quantitative real-time PCRs
- Figure preparation (real-time PCR results)
- Proliferation tests and data analysis
- Partial manuscript drafting

Research Article

Effects of High-Mobility Group A Protein Application on Canine Adipose-Derived Mesenchymal Stem Cells *In Vitro*

A. A. Ismail,^{1,2} S. Wagner,^{1,3} H. Murua Escobar,¹ S. Willenbrock,^{1,3} K. A. Sterenczak,^{1,3} M. T. Samy,² A. M. Abd El-Aal,² I. Nolte,¹ and P. Wefstaedt¹

¹Small Animal Hospital, University of Veterinary Medicine Foundation, 30559 Hannover, Germany

²Department of Surgery, Anesthesiology and Radiology, Faculty of Veterinary Medicine, Zagazig University, El-Sharkia, Egypt

³Centre for Human Genetics, University of Bremen, 28359 Bremen, Germany

Correspondence should be addressed to P. Wefstaedt, patrick.wefstaedt@tiho-hannover.de

Received 12 July 2011; Revised 21 September 2011; Accepted 25 October 2011

Academic Editor: Philip H. Kass

Copyright © 2012 A. A. Ismail et al. This is an open access article distributed under the Creative Commons Attribution License, which permits unrestricted use, distribution, and reproduction in any medium, provided the original work is properly cited.

Multipotency and self-renewal are considered as most important features of stem cells to persist throughout life in tissues. In this context, the role of HMGA proteins to influence proliferation of adipose-derived mesenchymal stem cell (ASCs) while maintaining their multipotent and self-renewal capacities has not yet been investigated. Therefore, extracellular HMGA1 and HMGA2 application alone (10–200 ng/mL) and in combination with each other (100, 200 ng/mL each) was investigated with regard to proliferative effects on canine ASCs (cASCs) after 48 hours of cultivation. Furthermore, mRNA expression of multipotency marker genes in unstimulated and HMGA2-stimulated cASCs (50, 100 ng/mL) was analyzed by RT-qPCR. HMGA1 significantly reduced cASCs proliferation in concentrations of 10–200 ng/mL culture medium. A combination of HMGA1 and HMGA2 protein (100 and 200 ng/mL each) caused the same effects, whereas no significant effect on cASCs proliferation was shown after HMGA2 protein application alone. RT-qPCR results showed that expression levels of marker genes including KLF4, SOX2, OCT4, HMGA2, and cMYC mRNAs were on the same level in both HMGA2-protein-stimulated and -unstimulated cASCs. Extracellular HMGA protein application might be valuable to control proliferation of cASCs in context with their employment in regenerative approaches without affecting their self-renewal and multipotency abilities.

1. Introduction

Mesenchymal stem cells (MSCs) are considered as one source of progenitor cells for therapeutic approaches in regenerative medicine. Although MSCs are commonly derived from bone marrow (BMSCs) [1], adipose-tissue-derived MSCs (ASCs) might be used as an alternative multipotent cell source [2–4]. Similar to BMSCs, ASCs have been also evaluated for multilineage differentiation capacities including differentiation into a chondrogenic [5, 6], osteogenic [5–7], adipogenic [5–7], neurogenic [8, 9], myogenic [6, 8, 10], angiogenic [11], and cardiomyogenic [10] lineage. In contrast to bone marrow, a large amount of adipose tissue can easily be obtained via less invasive and harmful methods making the use of ASCs as a source of stem cells very attractive [12]. Furthermore, it has recently been reported that ASCs have stronger capabilities than BMSCs

to maintain their phenotype and multipotency potential even after 25 passages of *in vitro* cultivation [10]. The self-renewal and multipotency characteristics through regular and organized cell division are the most important features of stem cells to persist throughout life in tissues. These features are regulated by stem-cell-specific transcription factors, so-called multipotency genes, including SOX2 [13], cMYC [14], KLF4 [15], OCT4 [13, 16], NANOG [16], UTF1 [17], and LIN28 [18]. For maintaining the self-renewal ability of MSCs, the balance of growth factors and signaling molecules is strongly required. Therefore, the recognition of the key environmental cues that regulate the phenomena of steady proliferation and self-renewal of adult stem cells is crucial for both *in vitro* and *in vivo* applications. On this occasion, recent studies have shown that HMGA proteins have the potential to maintain and influence efficiently these features [19–21]. The high-mobility group A (HMGA) proteins

(formerly known as HMGI/Y) are a class of large and specialized nuclear nonhistone chromosomal architectural proteins [22, 23]. The common functional and structural motifs in this unique group are three DNA-binding domains, so-called AT hooks, which bind preferentially to short AT-rich DNA sequences and an acidic C-terminus [24]. HMGA proteins are encoded by two distinct genes, HMGA1 and HMGA2 [25]. High expression of both HMGA proteins in undifferentiated and proliferating mesenchymal cells of early embryos indicate an important role of HMGA proteins in the regulation of stem cell proliferation and differentiation [26]. HMGA1 is mainly expressed during cell differentiation, whereas HMGA2 expression is mainly present during cell growth and proliferation [27].

HMGA2 expression is present in human and mouse ES cells in the inner cell mass of blastocysts indicating a key role of these proteins during prenatal development and growth [26, 28]. Furthermore, it has been found that HMGA2 expression in pluripotent human ES is closely correlated to the expression of pluripotency specific genes UTF1, SOX2, and OCT4 [29]. Additionally, Eda et al. [30] have investigated that HMGA2 and LIN28 were down-regulated upon upregulation of let-7, miR-9, and miR-125b microRNAs after neuronal induction of mouse P19 embryonic carcinoma cells. In contrast Nishino et al. [19] have found that self-renewal of mouse neural stem cells was maintained by downregulation of P16 (INK4a), P19 (Arf), and let-7b microRNA upon HMGA2-mediated expression. With regard to the effects of HMGA1 expression on cell proliferation, one previous *in vitro* study has demonstrated that downregulation of cMYC transcripts in gastric cancer cell lines led to an inhibition of HMGA1 expression upon the wnt3a/beta-catenin pathway finally resulting in reduced cell growth and proliferation [31]. The role of truncated HMGA1 protein has been evaluated for an increased adipocytic cell growth as well as development of human lipomas through its rearrangements [32]. Only few *in vitro* studies have been carried out to evaluate the role of HMGA proteins on proliferation of both undifferentiated embryonic stem cells as well as already differentiated cells. Caron et al. [33] have suggested that the HMGA2 transcription factor has a function in skeletal myogenesis of mouse embryonic cells. Li et al. [29] have demonstrated regulatory influences of HMGA2 protein expression on genes linked to human ES cell growth, mesenchymal stem cell differentiation, and adipogenic differentiation. Richter et al. [34] have found that HMGA1a, HMGA1b, and HMGA2 protein application *in vitro* results in a strong positive effect on proliferation of chondrocytes derived from porcine hyalin cartilage. In conclusion HMGA proteins are considered to play a crucial role in regulating the expression of many different genes important for cell growth and proliferation, especially of stem cells. On the basis of the introduced literature, one hypothesis of this study is that the proliferation rate of cultivated stem cells, for example, ASCs, can be enhanced or decreased by either HMGA2 or HMGA1 protein application without having an effect on the multipotent status of the cells. For a possible future *in vivo* usage of stem cells in context with regenerative or tumour therapies in dogs as

well as in humans it is highly desirable to control their proliferation, for example, by local application of proteins at the target site. The dog represents a valuable biomedical model for evaluation of novel therapeutic approaches in human medicine and for the dog itself. Additionally, the dog genome is highly similar to the human genome, making it an ideal model organism for the development of human cell and gene therapeutic approaches [35]. Therefore, our study was conducted to evaluate the effect of HMGA Proteins on canine ASCs. However, the influence of ectopic HMGA1 and HMGA2 protein application on cultivated ASCs is so far unknown. Thus, the aim of the present study was to evaluate the *in vitro* influence of HMGA proteins on canine ASCs proliferation and self-renewal. Moreover, it intended to investigate expression levels of multipotency specific marker genes in HMGA2 stimulated and unstimulated cASCs.

2. Materials and Methods

2.1. Isolation and Cultivation of cASCs. All experiments were carried out in accordance with the German law guidelines for governing the care and use of animals [TSchG, §4(3)]. The methods used for isolation of canine adipose-derived mesenchymal stem cells (cASCs) were adapted from previously published protocols as described by Zuk et al. [6]. Briefly, adipose tissue samples were obtained from subcutaneous fat depots of healthy dogs, weighed and then minced into small pieces. In total 20 subcutaneous fat samples of 20 dogs of different breeds were harvested. These dogs underwent orthopaedic surgeries or ovariohysterectomies and had no any other evident disease. The tissue pieces were enzymatically dissociated at 37°C for 30 min with 0.026% collagenase I (Sigma, St. Louis, MO, USA). Enzyme activity was neutralized with Dulbecco's modified Eagle's medium (DMEM, Biochrom AG, Berlin) containing 10% fetal calf serum (FCS, PAA Laboratories GmbH, Austria). Afterwards, the digested fat samples were filtered using a 100 µm cell strainer (BD Bioscience, Bedford, USA) to remove debris. The cell pellets obtained after centrifugation were resuspended in DMEM with 10% FCS and plated in 25 cm² flasks (TPP AG, Switzerland). The cultured cells were then maintained in an incubator supplied with humidified atmosphere of 5% CO₂ and 95% air at 37°C. Next day, the medium was exchanged in order to remove cell debris and red blood cells. Medium change was performed every second day. When the monolayer of adherent cells reached approximately 70–80% confluence; trypsinization for cell splitting was performed using trypsin-EDTA solution (0.05%/0.02%, Biochrom AG, Berlin, Germany). After centrifugation, the cell pellets were subcultured at a concentration of 3×10^5 cells/mL medium on 25 cm² tissue culture flasks containing DMEM/10% FCS. Cell counting was carried out by an automatic cell counter (Cellometer Nexcelom Bioscience, Lawrence, USA).

2.2. Multilineage Differentiation Capacity of cASCs. cASCs at passage 3 were verified for their developmental capacity to differentiate into cells of the osteogenic, adipogenic, and chondrogenic lineage. For each differentiation experiment three 25 cm² tissue culture flasks were used. In addition,

each differentiation experiment was repeated more than one time.

2.3. Osteogenic Differentiation of cASCs. For osteogenic differentiation, cASCs at passage 3 were cultured in 25 cm² flasks at a concentration of 6×10^5 in presence of osteogenic induction medium for 5 weeks. Osteogenic induction medium was prepared as previously described by Pittenger et al. [36]. DMEM containing 10% FCS was supplemented with dexamethasone (Dexa, # D8893, Sigma-Aldrich Chemie GmbH, Steinheim, Germany) at a concentration of 0.1 μ M, 2-phospho-L-ascorbic acid trisodium salts (Asc 2P; # 49752, Sigma-Aldrich Chemie) at a concentration of 50 μ M, and β -glycerophosphate disodium at a concentration of 10 mM (# 50020, Sigma-Aldrich Chemie). Osteogenic induction medium was changed every third day. Negative controls consisted of cASCs cells maintained in DMEM with 10% FCS. Before staining, the cells were washed with PBS (2 times) and fixed in 4% paraformaldehyde solution (PFA) for 10 min at room temperature, followed again by rinsing 3 times with PBS. To verify osteogenic differentiation, von Kossa staining was carried out to detect calcified extracellular matrix deposits (ECM).

2.4. Chondrogenic Differentiation of cASCs. For chondrogenic induction, the micromass culture technique was used [37]. cASCs at passage 2 were seeded out in 25 cm² flasks (with flat cultivation surface) using chondrogenic induction medium at a concentration of 2×10^6 /flask. Chondrogenic induction medium consisted of DMEM, 10% FCS, 0.1 μ M Dexa, 50 μ M Asc-2p, 0.35 g/100mL D(+)-glucose (# G-7021, Sigma-Aldrich Chemie), 50 mg/mL (1x) ITS + 1 liquid media supplement (10 μ g/mL insulin, 5.5 μ g/mL transferrin, 5 ng/mL selenium, 0.5 mg/mL bovine albumin, 4.7 μ g/mL linoleic acid) (# I-2521, Sigma-Aldrich Chemie), and 10 ng/mL transforming growth factor (rhTGF- β 1; #100-21, PeproTech GmbH, Hamburg, Germany). After seeding, cells were allowed to adhere for 4 hours (37°C, humidified atmosphere, 5% CO₂). Afterwards, the cells were maintained in induction medium for 21 days. The culture medium was changed every third day. Negative controls consisted of cASCs maintained in noninductive basal medium. Fixation of the cells was carried out as described above. Chondrogenic induction was confirmed by Alcian blue staining for chondrocyte-specific proteoglycans.

2.5. Adipogenic Differentiation of cASCs. For adipogenic induction, cASCs were seeded in 25 cm² flasks at a concentration of 2×10^6 cells/flask using DMEM medium containing 10% FCS. After a cultivation period of 3 h the medium was discarded, followed by a cultivation period of 72 h in adipogenic induction medium. Adipogenic induction medium consisted of DMEM supplemented with 10% FCS, 1 μ M dexa, 10 μ g/mL insulin (# I-6634, Sigma-Aldrich Chemie), 100 μ M indomethacin (#I-7378, Sigma-Aldrich Chemie), and 500 μ M isobutylmethylxanthine (#I-5879, Sigma-Aldrich Chemie GmbH, Steinheim, Germany). After removal of adipogenic induction medium the cells were cultivated for 24 h in adipogenic maintenance medium

consisting of DMEM basal medium, 10% FCS, and 10 μ g/mL insulin. Cells were then cultivated again in adipogenic induction medium for 72 h, followed by another 24 h in adipogenic maintenance medium. This cycle was repeated four times in total (16 d), followed by one week of cultivation in adipogenic maintenance medium. Negative controls consisted of cASCs maintained in noninductive basal medium for 23 days. Fixation of the cells was carried out as described above. Adipogenic differentiation was confirmed by intracellular lipid droplets accumulation after Oil Red O staining.

2.6. In Vitro cASCs Proliferation Assay. cASCs were harvested by trypsinization and resuspended in fresh tissue culture medium as described above. The viable cell percentage from the harvested cells was calculated after trypan blue staining by an automatic cell counter (Cellometer Nexcelom Bioscience, Lawrence, USA). The cell concentration used for the proliferation assay was adjusted to 7×10^3 cells/100 μ L medium. Liquid HMGA protein solution of HMGA1 (#:TP301458, AMS Biotechnology, Ltd, Germany) and HMGA2 (#H00008091-Q01, Abnova, Germany) were added to the DMEM culture medium with 10% FCS at concentrations of 10, 50, 100, and 200 ng/mL. Furthermore a combination of HMGA1 and HMGA2 (100 and 200 ng/mL each) was used for cASC stimulation. The negative control condition consisted of unstimulated cASCs. To achieve the correct protein concentrations in the culture medium, directly before usage, stock solutions with protein concentrations of 1 μ g/mL DMEM culture medium (with 10% FCS) were prepared. The desired concentration of HMGA proteins was achieved by further dilution of the stock solution with DMEM (with 10% FCS). Proliferation of stimulated and unstimulated cASCs was evaluated using a bromodeoxyuridine (BrdU) cell proliferation enzyme-linked immunosorbent assay (ELISA kit; #11647229001, Roche Diagnostics GmbH, Mannheim, Germany) according to the manufacturer's instructions. For each of the analyzed protein concentrations cASCs were seeded out in eight separate wells of a 96-well cell culture microtiter plate (#353075, Microtest-Falcon, Becton Dickinson Biosciences, USA) at a concentration of 7×10^3 cells per well (100 μ L of cell suspension). Cells were incubated for 3 hours (95% humidified air, 37°C, 5% CO₂) for cell adhesion, followed by the addition of the corresponding amounts of each protein. After a coculturing period of 24 hours (95% humidified air, 37°C, 5% CO₂), 10 μ L/well of BrdU labeling solution (final concentration; 10 μ M/well BrdU) was added, followed by reincubation at 37°C and 5% CO₂ for another 24 h. During this labeling period, the pyrimidine analogue BrdU was incorporated into the DNA of the proliferating cASCs. After 48 hours as a total treatment period of HMGA protein, the culture medium was carefully removed. Afterwards, the cells were fixed and the DNA was denatured in one step by adding FixDenat solution (200 μ L/well). The cells were then incubated for half an hour at room temperature. The denaturation of the DNA was necessary to improve the accessibility of the incorporated BrdU for detection by the antibody. FixDenat solution was removed thoroughly via careful pipetting. Anti-BrdU-conjugate-peroxidase (Anti-BrdU-POD) working solution

was then added in an amount of 100 μL /well. The anti-BrdU-POD binds to the BrdU incorporated in newly synthesized, cellular DNA. After 90 minutes incubation at RT, the antibody conjugate was removed. Afterwards, the cells were rinsed three times with washing solution (PBS; 300 μL /well). The immune complexes were detected by the subsequent substrate reaction. Finally the substrate solution (TMB; tetramethyl-benzidine) was added to the cells (100 μL /well), and the cells were incubated at RT for another 25 minutes. The photometric absorbance values of the reaction products were measured using a scanning multiwell spectrophotometer (Synergy 2 Multi-Mode Microplate Reader, Biotek Instruments GmbH, Germany) at 370 nm and a reference wavelength of 492 nm at 10 time points between 0 and 30 minutes. The blanked 370 nm data minor 497 nm were plotted against the timescale. The maximal slope of the absorbance curve was calculated and used for statistical comparisons. The absorbance values directly correlate to the amount of synthesized DNA and the corresponding number of proliferating cells in the respective microcultures. Absorbance values for the negative control condition were normalized to 100%. Values of all other conditions were converted, respectively.

2.7. Stimulation of cASCs with HMGA2 Protein for Subsequent RT-qPCR. According to the above-mentioned protocols cASCs were seeded in six-well tissue culture plates at a concentration of 2×10^4 cells/well in DMEM (volume/well:1000 μL) supplemented with 10% FCS. Cells were allowed to adhere for 4 hours. Afterwards cASCs were stimulated in triplicates with HMGA2 supplemented medium at a concentration of 50 and 100 ng HMGA2/mL culture medium (volume/well:1000 μL). Unstimulated cASCs served as control. After incubation for 48 hours (humidified atmosphere, 5% CO_2 , 37°C) the cells were harvested by trypsinization, followed by centrifugation at $800 \times g$ for 10 minutes. The cell pellet was used for subsequent RT-qPCR.

2.8. Relative Quantitative Real-Time Polymerase Chain Reaction (RT-qPCR)

2.8.1. RNA Isolation and cDNA Synthesis for Transcript Characterization. Total RNA was isolated from unstimulated as well as HMGA2 stimulated cASCs (100, 200 ng) using NucleoSpin miRNA (#740971.250; Macherey & Nagel GmbH, Düren, Germany) isolation kit according to the manufacturer's instructions. The concentration and purity of the isolated RNA was verified by the OD260/280 nm absorption ratio using the Multi-Mode Microplate Reader SynergyTM2 and Gene5TM microplate software (Biotek Instruments, inc, USA). cDNA was synthesised using Quantitect Reverse Transcription Kit (#205313; Qiagen, Hilden, Germany) following the manufacturer's protocol. For the reverse transcription, 250 ng of total RNA were used for the relative characterization of mRNA transcript levels of Klf4, HMGA2, SOX2, cMYC, NANOG, and Pou5F/OCT4.

2.8.2. RT-qPCR. RT-qPCR was carried out using the Master Cycler Gradient Cycler (Eppendorf, Germany). The canine

Hypoxanthine Phosphoribosyl Transferase-1 (HPRT1) [38] and Glucuronidase Beta transcript (GUSB) [39] were used as endogenous reference genes. The amplification was carried out in a total reaction volume of 20 μL using the TaqMan Universal PCR Master Mix (# 4304437; Applied Biosystems, Darmstadt, Germany). For establishing the canine HMGA2- and Klf4-Assays, the primers and probes were designed by the software SeqMan Pro and Editseq 7.1.0 DNASTAR, Inc. (Lasergene MADISON, USA) using the murine KLF4 mRNA NM_010637, human KLF4 mRNA NM_004235 (<http://www.ncbi.nlm.nih.gov/>), and canine KLF4 cDNA ENSCAFT00000004467 (<http://www.ensembl.org/>). The designed primers and probes related to KLF4 and HMGA2 mRNA were supplied by Biomers (Ulm, Germany). The Primer and probe sequences of all other examined transcripts were synthesized by Applied Biosystems (Darmstadt, Germany). For amplification of gene transcripts, 500 nM of each primer and 200 nM of the corresponding fluorogenic probe were used. From each sample 2 μL cDNA were used as template. All reactions were carried out on the same RT-qPCR plate. PCR cycles were carried out starting with 2 min for activation at 50°C and 10 min at 95°C for template denaturation, followed by 40 cycles with 15 s at 95°C and 1 min at 60°C. All samples were measured in triplicate and for each run nontemplate controls and nonreverse transcriptase control reactions were included. The quotient of the threshold cycles for the analysed multipotency marker genes was set in relation to the expression level of the housekeeping genes HPRT1 and GUSB using the $\Delta\Delta$ cycle threshold ($\Delta\Delta\text{CT}$) method. Gene expression levels of the marker genes in HMGA2 stimulated cASCs were normalised to the expression level in unstimulated cASCs.

2.8.3. Statistics. The statistical analyses were performed using GraphPad Prism 4 software (GraphPad Software, La Jolla, CA). The obtained data were expressed as means \pm SD. Differences between groups were analyzed using a one-way ANOVA and a Tukey test for post hoc comparisons. The significance levels were set at $P < 0.05$, $P < 0.01$ and $P < 0.001$.

3. Results

3.1. Morphology of Canine ASCs. After 24 hours of cultivation, most of the seeded cells were remaining nonadherent in suspension. After washing to remove these cells, few adhered single cells or cell aggregates were observed. Initially adherent cells grew into spindle or fibroblast-like cells, which then developed into visible colonies after 3–5 days in culture. Furthermore, formation of cell-cell contacts and proliferation could be observed. After a cultivation period of two weeks adherent cells had proliferated to near confluence in 25 cm^2 flasks. After the first passage, the fibroblast-like shape became more regular and could be maintained throughout further subcultivation (Figure 1(a)).

3.2. Demonstration of Multilineage Potential of cASCs. cASCs isolated from subcutaneous fat were evaluated for their ability to differentiate into cells with an osteogenic (Figure 1(b)),

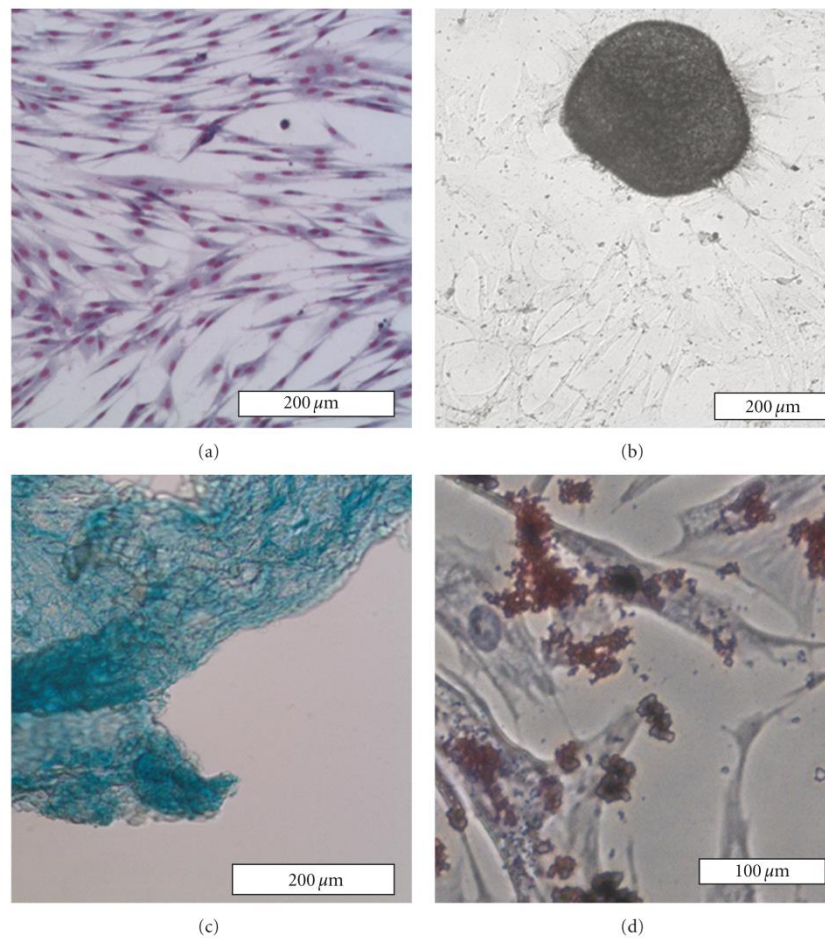


FIGURE 1: Example of Diff-Quik stained undifferentiated cASCs with flattened fibroblast-like morphology (a). After 5 weeks of osteogenic induction, von Kossa staining was positive, showing large black calcifying nodules (b). Chondrogenic differentiated cASCs show polygonal morphology after 21 days of induction in addition to positive Alcian blue staining of the chondrocyte-specific glycosaminoglycans (c). In (c) an adherent double cell layer is to be seen. Adipogenic induction could be shown 23 days after induction by positive red lipid droplets after Oil Red O staining (d). Scale bar: 200 μm (a–c) and 100 μm (d).

chondrogenic (Figure 1(c)), and adipogenic (Figure 1(d)) phenotype after cultivation in a respectively supplemented medium (see below).

3.3. Osteogenic Differentiation. After two weeks of cultivation in presence of osteogenic induction medium, cells changed from a fibroblastic phenotype to a more polygonal appearance. Furthermore, a small amount of the calcium deposition, normally indicative for osteogenesis, could be detected. Additionally, osteogenic differentiation was confirmed by positive von Kossa staining. Within a cultivation period of 5 weeks after induction of the cells continued to proliferate actively and formed cell aggregates with an increased amount of calcified extracellular matrix and mineralized nodules (Figure 1(b)). These findings were absent in cultures of unstimulated cASCs which maintained their fibroblast-like appearance and did not form cell aggregates (Figure 1(a)).

Furthermore, no calcified ECM deposition could be observed in undifferentiated cells.

3.4. Chondrogenic Differentiation. Chondrogenic differentiation of cASCs was achieved after 3 weeks of micromass culture in chondrogenic induction medium. At this time-point chondrocyte-differentiated cASCs showed a polygonal morphology. Furthermore, chondrogenic induction was confirmed by positive Alcian blue staining which is indicative for the presence of chondrocyte-specific proteoglycans (Figure 1(c)). Positive Alcian blue staining was absent in unstimulated cASCs (Figure 1(a)).

3.5. Adipogenic Differentiation. Adipogenic induction of cASCs was completed after 23 days of cultivation in adipogenic induction medium. Adipogenic cells showed a larger cell morphology with an accumulation of red intracellular

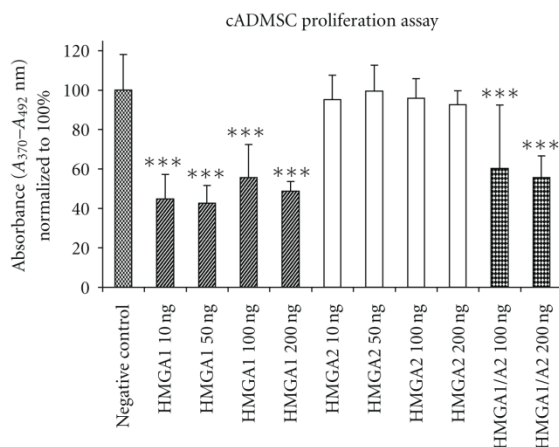


FIGURE 2: Proliferation test of cASCs stimulated with HMGA proteins. Absorbance values were normalized to 100% in the negative control condition, significance levels are given for comparisons versus negative control condition. HMGA1 at all used levels has significant suppressive effects on cell proliferation ($P < 0.001$). In contrast, cell proliferation in the HMGA2-treated groups resulted in no significant differences in comparison to the control group at all chosen concentrations. The combined protein application of 100 ng and 200 ng/mL shows a significant suppressive effect on cASCs proliferation ($P < 0.001$). For statistical comparisons a one-way analysis of variance and a Tukey posttest was carried out (significance levels: * $P < 0.05$; ** $P < 0.01$; *** $P < 0.001$).

lipid droplets after Oil Red O staining (Figure 1(d)). Positive Oil Red O staining and changed cell morphology were absent in unstimulated cASCs (Figure 1(a)).

3.6. Effect of HMGA Proteins on Proliferation Rate of cASCs.

To evaluate whether HMGA proteins have an effect on proliferation of cASCs, cells were cocultured for 48 hours in presence of HMGA1 and HMGA2 proteins at different concentrations and in combination with each other. HMGA1 and HMGA2 related effects on cASC proliferation were compared with proliferation rates of non-HMGA-treated cASCs (Figure 2). No significant enhancement of cASC proliferation after HMGA2 protein application at concentrations of 10 ($94.99 \pm 12.44\%$ (mean \pm standard deviation)), 50 ($99.46 \pm 13.07\%$), 100 ($95.79 \pm 9.95\%$), and 200 ($92.55 \pm 6.95\%$) ng/mL could be detected in comparison to the proliferation rate of unstimulated cASCs ($100 \pm 18.04\%$). In contrast, HMGA1 protein application at concentrations of 10 ($44.73 \pm 12.37\%$), 50 ($42.5 \pm 9.05\%$), 100 ($55.49 \pm 16.83\%$), and 200 ($48.7 \pm 4.81\%$) ng/mL had a significant inhibitory effect on cASC proliferation ($P < 0.001$). Moreover, the combined application of HMGA1 and HMGA2 protein at respective concentrations of 100 ($60.82 \pm 32.04\%$) and 200 ($55.62 \pm 10.93\%$) ng/mL also resulted in a significant decrease of the cell proliferation rate ($P < 0.001$), when compared with untreated cells. Furthermore the proliferation rate of combined HMGA1- and HMGA2-treated cASCs was found to be on the same level as in HMGA1 stimulated cells in all used concentrations.

Expression levels of marker genes in relation to unstimulated ADMSCs (1). Internal control: HPRT

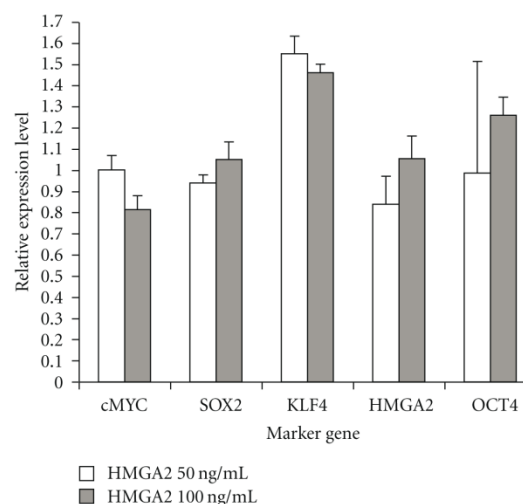


FIGURE 3: Marker gene expression in HMGA2 protein-stimulated (50, 100 ng/mL) and -unstimulated cASCs (relative expression = 1) after RT-qPCR. HPRT was used as endogenous control. All analysed genes (cMYC, SOX2, KLF4, HMGA2, and OCT4) are expressed in cASCs. No significant marker gene regulation could be detected after HMGA2 application in both concentrations.

3.7. Expression Analyzes of Multipotency Marker Genes in HMGA2-Stimulated cASCs.

Relative expression of all analyzed marker genes in unstimulated cASCs was normalized to 1 (Figures 3 and 4) and gene expression in the 50 and 100 ng/mL stimulated cASC condition was normalized accordingly. In case of the experiments in which HPRT1 (Figure 3) was used as endogenous control, KLF4 expression higher in 50 (1.55 ± 0.09) and 100 ng/mL (1.46 ± 0.04 ; $P < 0.05$) HMGA2-treated cASCs than in unstimulated cASCs. However, these differences were not significant. OCT4 expression in relation to HPRT1 in stimulated cASCs was measured on the same level as in unstimulated cASCs after 50 (0.99 ± 0.53 ; $P > 0.05$) and 100 ng/mL (1.26 ± 0.09 ; $P > 0.05$) HMGA2 treatment. No significant differences were found for SOX2, cMYC, and HMGA2 expression in relation to HPRT1 in cASCs after 50 (SOX2: 0.94 ± 0.04 , $P > 0.05$; cMYC: 1.00 ± 0.07 , $P > 0.05$; HMGA2: 0.83 ± 0.13 , $P > 0.05$) and 100 ng/mL (SOX2: 1.05 ± 0.09 , $P > 0.05$; cMYC: 0.81 ± 0.07 , $P > 0.05$; HMGA2: 1.05 ± 0.11 , $P > 0.05$) HMGA2 stimulation in comparison to unstimulated cASCs.

In case of GUSB (Figure 4) as endogenous control no significant differences with regard to KLF4 expression could be detected in cASCs after 50 (1.06 ± 0.09 ; $P > 0.05$) and 100 ng/mL (1.22 ± 0.04 ; $P > 0.05$) HMGA2 stimulation in comparison to unstimulated cells. OCT4 expression in relation to GUSB was slightly but not significantly lower in 50 (0.61 ± 0.07 ; $P > 0.05$) and 100 ng/mL (0.78 ± 0.56 ; $P > 0.05$) HMGA2-treated cASCs in comparison to unstimulated cells. No significant differences were found for SOX2, cMYC

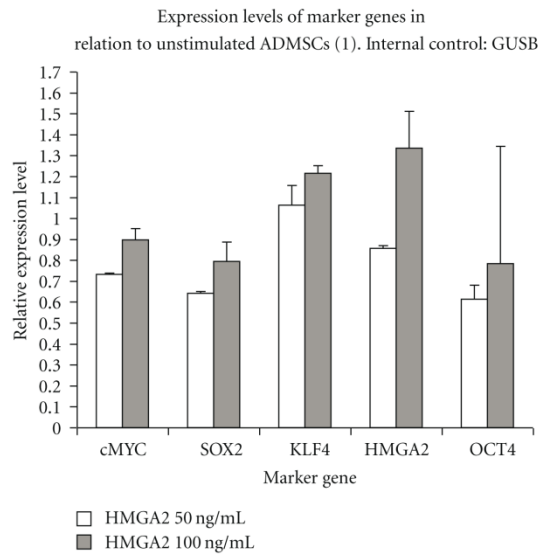


FIGURE 4: Marker gene expression in HMGA2 protein-stimulated (50, 100 ng/mL) and -unstimulated cASCs (1) after RT-qPCR. GUSB was used as endogenous control. All analysed genes (cMYC, SOX2, KLF4, HMGA2, and OCT4) are expressed in cASCs. No significant marker gene regulation could be detected after HMGA2 application in both concentrations.

and HMGA2 expression in relation to HPRT1 in cASCs after 50 (SOX2: 0.64 ± 0.01 , $P > 0.05$; cMYC: 0.73 ± 0.01 , $P > 0.05$; HMGA2: 0.86 ± 0.02 , $P > 0.05$) and 100 ng/mL (SOX2: 0.79 ± 0.09 , $P > 0.05$; cMYC: 0.90 ± 0.05 , $P > 0.05$; HMGA2: 1.33 ± 0.18 , $P > 0.05$) HMGA2 stimulation in comparison to unstimulated cASCs.

4. Discussion

In the field of tissue engineering, a setup of well-defined and reproducible culture conditions that will allow for large-scale expansion of stem cells while providing efficient self-renewal and maintenance of multipotency is critical. The key factor in terms of multipotency and self-renewal characteristics of stem cells is the control by the expression of several unique multipotency-associated marker genes as for example, KLF4, cMYC, SOX2, HMGA2, and OCT4 [13–16, 40].

The present study was focused on the characterization of multipotent effects of HMGA protein application on cultivated cASCs. These adipose-tissue-derived cells have several benefits for clinical applications, providing an autologous source of adult stem cells for therapeutic approaches [41]. In general the isolation of these cells from mammalian tissues is well established as well as the possibility to expand the cells *in vitro*. Thereby, the potential of cASCs to differentiate into osteogenic, adipogenic, and chondrogenic lineages is preserved confirming the stem-cell-like character of the cells kept *in vitro*. Multilineage differentiation capacity could also be demonstrated by histologic analyses for cASCs used in this

study. As the differentiation procedure is a well-established technique [36, 37] further negative controls using, for example, Alcian blue stained undifferentiated cASCs are not presented, which is, however a shortcoming of the here presented study. Recently it could be shown, that adult cASCs do not lose their stem cell features after cryopreservation [42]. Besides ASCs [5, 6], these facts are also valid for mammalian BMSCs [43]. Previous studies demonstrated that the HMGA proteins HMGA1 and HMGA2 are involved in various cellular processes such as proliferation [24] and senescence [44]. In addition, they are highly expressed in undifferentiated cells during embryogenesis and downregulated in differentiated cells [28]. Consequently, in the presented study proliferative effects as well as effects on regulation on stem cell marker genes of cASCs were characterized *in vitro*. Our data indicated that HMGA1 protein at concentrations of 10 ng to 200 ng/mL culture medium as well as a combined protein application of HMGA1 and HMGA2 (100 and 200 ng/mL) resulted in significant suppressive effects on cASCs proliferation after 48 hours of cocultivation. These findings are contrary to an earlier study which reported a reduced cell growth and proliferation due to a decreased HMGA1 expression in gastric cancer cell lines [31]. An explanation for the different response of cASCs to ectopic HMGA1 application might be that functional pathways in cancer cell lines are often not comparable to the pathways of physiological somatic cells or stem cells. In the present study no significant difference of cASC proliferation in comparison to untreated cASCs could be found after HMGA2 protein application at all used concentrations. In contrast, Richter et al. [34] were able to demonstrate that HMGA1a, HMGA1b, and HMGA2 proteins have a significant positive effect on the proliferation rate of chondrocyte monolayers *in vitro* after 24 hours of incubation. In another recently published study, Richter et al. found positive proliferative effects of HMGA2-derived fragments on proliferation of cultured porcine chondrocytes and canine ASCs [34, 45]. However, higher doses of HMG proteins ranging from 1 μg to over 100 $\mu\text{g}/\text{mL}$ were used in the studies of Richter et al. [34, 45]. In the here presented study lower doses of HMG protein were used according to the studies performed with the HMGA sister protein HMGB1 demonstrating biologic effects at concentrations of 10–200 ng/mL protein application [46, 47]. However, in this context it has to be kept in mind that HMGB1 extracellular signaling is well characterised being mediated by TLR and RAGE receptors. In contrast to this, a detailed characterisation of extracellular HMGA receptors is still missing. To our knowledge, only few studies have been carried out to verify how HMGA proteins affect multipotency maintenance and proliferation in adult stem cells. Recently, Nishino et al. [19] have reported that HMGA2 protein knockdown led to inhibition of neural stem cell proliferation and self-renewal of fetal and young-adult mice but not old-adult mice. These findings indicate that HMGA2 might have a proliferative effect only on stem cells at early stages. This hypothesis is supported by the results of our *in vitro* study in which also no proliferative effects of HMGA2 could be found. Nevertheless it has to be stated that in our study an extracellular protein application

was used, whereas in the study of Nishino et al., HMGA2 expression was knocked out [19]. In addition, microRNA let-7b has been reported to regulate self-renewal of neural stem cells through targeting on HMGA2 protein and TLX receptor [19, 48]. Our results reported here using real-time qPCR revealed that HMGA2 protein can contribute to maintain self-renewal and multipotency of cASCs as no significant effects on gene regulation of multipotency marker genes could be found. HMGA2 protein-stimulated and -unstimulated cASCs showed no significant differences in relative expression levels of the marker genes KLF4, SOX2, OCT4, cMYC, and HMGA2 in cASCs. In this context it has to be stated that the OCT4 signal was detectable only at late PCR cycles. Thus, results for this gene have to be looked at critically. However, for reasons of a complete description of the gene panel the OCT4 data is presented. A major limitation of the study is the missing data of marker gene expressions in cASCs after HMGA1 protein application. Therefore, future studies will have to investigate whether the inhibitory effect on cASC proliferation is accompanied by a changed or unaltered expression of multipotency marker genes. As another result, it could be demonstrated that the suppressive effects of HMGA1 protein application on cASC proliferation cannot be blocked by additional HMGA2 application. In case of the combined HMGA1 and HMGA2 application in a concentration of 100 ng/mL each, a high-standard deviation of the measurement values is evident. However, it would be interesting to investigate the effects of HMGA1 protein application on gene expression of the mentioned marker genes and to check for HMGA1 specific receptors on cASCs. Also, multilineage differentiation capacity of HMGA protein-stimulated ASCs remains to be investigated in further studies.

5. Conclusions

In conclusion, HMGA proteins remain interesting candidate proteins for influencing ASC proliferation without altering multipotency gene expression. Further studies focussing on higher concentrations of HMGA protein application on cultured ASCs are needed to fully study the effects on proliferation and marker gene expression. Characterizing the role of HMGA protein on self-renewal and multipotency of ASCs might be providing novel insights for a controlled and efficient application of these cells in regenerative approaches. Especially the possibility to control proliferation of tumour stem cells would be of great advantage in this context.

Authors' Contribution

A. A. Ismail and S. Wagner contributed equally to the development of the paper.

Acknowledgments

This work was supported by the Excellence Cluster REBIRTH (from Regenerative Biology to Reconstructive Therapy, Hannover) within the Excellence Initiative of the German Federal

Ministry of Education and Research and the German Research Foundation (DFG).

References

- [1] E. Leonardi, V. Devescovi, F. Perut, G. Ciapetti, and A. Giunti, "Isolation, characterisation and osteogenic potential of human bone marrow stromal cells derived from the medullary cavity of the femur," *La Chirurgia Degli Organi di Movimento*, vol. 92, no. 2, pp. 97–103, 2008.
- [2] B. Puissant, C. Barreau, P. Bourin et al., "Immunomodulatory effect of human adipose tissue-derived adult stem cells: comparison with bone marrow mesenchymal stem cells," *British Journal of Haematology*, vol. 129, no. 1, pp. 118–129, 2005.
- [3] H. Hattori, M. Sato, K. Masuoka et al., "Osteogenic potential of human adipose tissue-derived stromal cells as an alternative stem cell source," *Cells Tissues Organs*, vol. 178, no. 1, pp. 2–12, 2004.
- [4] Y. A. Romanov, A. N. Darevskaya, N. V. Merzlikina, and L. B. Buravkova, "Mesenchymal stem cells from human bone marrow and adipose tissue: isolation, characterization, and differentiation potentialities," *Bulletin of Experimental Biology and Medicine*, vol. 140, no. 1, pp. 138–143, 2005.
- [5] M. Neupane, C. C. Chang, M. Kiupel, and V. Yuzbasiyan-Gurkan, "Isolation and characterization of canine adipose-derived mesenchymal stem cells," *Tissue Engineering—Part A*, vol. 14, no. 6, pp. 1007–1015, 2008.
- [6] P. A. Zuk, M. Zhu, H. Mizuno et al., "Multilineage cells from human adipose tissue: implications for cell-based therapies," *Tissue Engineering*, vol. 7, no. 2, pp. 211–228, 2001.
- [7] Y. Y. Shi, R. P. Nacamuli, A. Salim, and M. T. Longaker, "The osteogenic potential of adipose-derived mesenchymal cells is maintained with aging," *Plastic and Reconstructive Surgery*, vol. 116, no. 6, pp. 1686–1696, 2005.
- [8] Y. Lin, X. Chen, Z. Yan et al., "Multilineage differentiation of adipose-derived stromal cells from GFP transgenic mice," *Molecular and Cellular Biochemistry*, vol. 285, no. 1–2, pp. 69–78, 2006.
- [9] K. M. Safford, K. C. Hicok, S. D. Safford et al., "Neurogenic differentiation of murine and human adipose-derived stromal cells," *Biochemical and Biophysical Research Communications*, vol. 294, no. 2, pp. 371–379, 2002.
- [10] Y. Zhu, T. Liu, K. Song, X. Fan, X. Ma, and Z. Cui, "Adipose-derived stem cell: a better stem cell than BMSC," *Cell Biochemistry and Function*, vol. 26, no. 6, pp. 664–675, 2008.
- [11] Y. L. Tang, Q. Zhao, Y. C. Zhang et al., "Autologous mesenchymal stem cell transplantation induce VEGF and neovascularization in ischemic myocardium," *Regulatory Peptides*, vol. 117, no. 1, pp. 3–10, 2004.
- [12] M. L. Tong, M. Martina, D. W. Huttmacher, J. H. P. O. Hui, H. L. Eng, and B. Lim, "Identification of common pathways mediating differentiation of bone marrow- and adipose tissue-derived human mesenchymal stem cells into three mesenchymal lineages," *Stem Cells*, vol. 25, no. 3, pp. 750–760, 2007.
- [13] A. Rizzino, "Sox2 and Oct-3/4: a versatile pair of master regulators that orchestrate the self-renewal and pluripotency of embryonic stem cells," *Wiley Interdisciplinary Reviews*, vol. 1, no. 2, pp. 228–236, 2009.
- [14] K. N. Smith, A. M. Singh, and S. Dalton, "Myc represses primitive endoderm differentiation in pluripotent stem cells," *Cell Stem Cell*, vol. 7, no. 3, pp. 343–354, 2010.

- [15] K. K. K. Chan, J. Zhang, N. Y. Chia et al., "KLF4 and PBX1 directly regulate NANOG expression in human embryonic stem cells," *Stem Cells*, vol. 27, no. 9, pp. 2114–2125, 2009.
- [16] M. B. Jones, C. H. Chu, J. C. Pendleton et al., "Proliferation and pluripotency of human embryonic stem cells maintained on type I collagen," *Stem Cells and Development*, vol. 19, no. 12, pp. 1923–1935, 2010.
- [17] S. M. Kooistra, V. van den Boom, R. P. Thummer et al., "Undifferentiated embryonic cell transcription factor 1 regulates ESC chromatin organization and gene expression," *Stem Cells*, vol. 28, no. 10, pp. 1703–1714, 2010.
- [18] M. Richards, S. P. Tan, J. H. Tan, W. K. Chan, and A. Bongso, "The transcriptome profile of human embryonic stem cells as defined by SAGE," *Stem Cells*, vol. 22, no. 1, pp. 51–64, 2004.
- [19] J. Nishino, I. Kim, K. Chada, and S. J. Morrison, "Hmga2 promotes neural stem cell self-renewal in young but not old mice by reducing p16Ink4a and p19Arf expression," *Cell*, vol. 135, no. 2, pp. 227–239, 2008.
- [20] K. Monzen, Y. Ito, A. T. Naito et al., "A crucial role of a high mobility group protein HMGA2 in cardiogenesis," *Nature Cell Biology*, vol. 10, no. 5, pp. 567–574, 2008.
- [21] S. Sanna, A. U. Jackson, R. Nagaraja et al., "Common variants in the GDF5-UQCC region are associated with variation in human height," *Nature Genetics*, vol. 40, no. 2, pp. 198–203, 2008.
- [22] M. Bustin, "Revised nomenclature for high mobility group (HMG) chromosomal proteins," *Trends in Biochemical Sciences*, vol. 26, no. 3, pp. 152–153, 2001.
- [23] R. Grosschedl, K. Giese, and J. Pagel, "HMG domain proteins: architectural elements in the assembly of nucleoprotein structures," *Trends in Genetics*, vol. 10, no. 3, pp. 94–100, 1994.
- [24] R. Reeves, D. D. Edberg, and Y. Li, "Architectural transcription factor HMGI(Y) promotes tumor progression and mesenchymal transition of human epithelial cells," *Molecular and Cellular Biology*, vol. 21, no. 2, pp. 575–594, 2001.
- [25] R. Sgarra, A. Rustighi, M. A. Tessari et al., "Nuclear phosphoproteins HMGA and their relationship with chromatin structure and cancer," *FEBS Letters*, vol. 574, no. 1–3, pp. 1–8, 2004.
- [26] Y. Tay, S. Peter, I. Rigoutsos, P. Barahona, S. Ahmed, and P. Dröge, "Insights into the regulation of a common variant of HMGA2 associated with human height during embryonic development," *Stem Cell Reviews and Reports*, vol. 5, no. 4, pp. 328–333, 2010.
- [27] E. Vartiainen, J. Palvimo, A. Mahonen, A. Linnala-Kankkunen, and P. H. Maenpää, "Selective decrease in low-M(r) HMG proteins HMG I and HMG Y during differentiation of mouse teratocarcinoma cells," *FEBS Letters*, vol. 228, no. 1, pp. 45–48, 1988.
- [28] X. Zhou, K. F. Benson, H. R. Ashar, and K. Chada, "Mutation responsible for the mouse pygmy phenotype in the developmentally regulated factor HMGI-C," *Nature*, vol. 376, no. 6543, pp. 771–774, 1995.
- [29] O. Li, J. Li, and P. Dröge, "DNA architectural factor and proto-oncogene HMGA2 regulates key developmental genes in pluripotent human embryonic stem cells," *FEBS Letters*, vol. 581, no. 18, pp. 3533–3537, 2007.
- [30] A. Eda, Y. Tamura, M. Yoshida, and H. Hohjoh, "Systematic gene regulation involving miRNAs during neuronal differentiation of mouse P19 embryonic carcinoma cell," *Biochemical and Biophysical Research Communications*, vol. 388, no. 4, pp. 648–653, 2009.
- [31] S. I. Akaboshi, S. Watanabe, Y. Hino et al., "HMGA1 is induced by Wnt/ β -catenin pathway and maintains cell proliferation in gastric cancer," *American Journal of Pathology*, vol. 175, no. 4, pp. 1675–1685, 2009.
- [32] G. M. Pierantoni, S. Battista, F. Pentimalli et al., "A truncated HMGA1 gene induces proliferation of the 3T3-L1 pre-adipocytic cells: a model of human lipomas," *Carcinogenesis*, vol. 24, no. 12, pp. 1861–1869, 2003.
- [33] L. Caron, F. Bost, M. Prot, P. Hofman, and B. Binétruy, "A new role for the oncogenic high-mobility group A2 transcription factor in myogenesis of embryonic stem cells," *Oncogene*, vol. 24, no. 41, pp. 6281–6291, 2005.
- [34] A. Richter, G. Hauschild, H. M. Escobar, I. Nolte, and J. Bullerdiek, "Application of high-mobility-group-a proteins increases the proliferative activity of chondrocytes in vitro," *Tissue Engineering—Part A*, vol. 15, no. 3, pp. 473–477, 2009.
- [35] E. K. Karlsson and K. Lindblad-Toh, "Leader of the pack: gene mapping in dogs and other model organisms," *Nature Reviews Genetics*, vol. 9, no. 9, pp. 713–725, 2008.
- [36] M. F. Pittenger, A. M. Mackay, S. C. Beck et al., "Multilineage potential of adult human mesenchymal stem cells," *Science*, vol. 284, no. 5411, pp. 143–147, 1999.
- [37] M. Solorsh, "Cartilage stem cells: regulation of differentiation," *Connective Tissue Research*, vol. 20, no. 1–4, pp. 81–89, 1989.
- [38] M. Fischer, M. Skowron, and F. Berthold, "Reliable transcript quantification by real-time reverse transcriptase-polymerase chain reaction in primary neuroblastoma using normalization to averaged expression levels of the control genes HPRT1 and SDHA," *Journal of Molecular Diagnostics*, vol. 7, no. 1, pp. 89–96, 2005.
- [39] B. Brinkhof, B. Spee, J. Rothuizen, and L. C. Penning, "Development and evaluation of canine reference genes for accurate quantification of gene expression," *Analytical Biochemistry*, vol. 356, no. 1, pp. 36–43, 2006.
- [40] S. M. Hammond and N. E. Sharpless, "HMGA2, MicroRNAs, and stem cell aging," *Cell*, vol. 135, no. 6, pp. 1013–1016, 2008.
- [41] B. M. Strem, K. C. Hicok, M. Zhu et al., "Multipotential differentiation of adipose tissue-derived stem cells," *Keio Journal of Medicine*, vol. 54, no. 3, pp. 132–141, 2005.
- [42] T. Martinello, I. Bronzini, L. Maccatrozzo et al., "Canine adipose-derived-mesenchymal stem cells do not lose stem features after a long-term cryopreservation," *Research in Veterinary Science*, vol. 91, no. 1, pp. 18–24, 2010.
- [43] C. Csaki, U. Matis, A. Mobasheri, H. Ye, and M. Shakibaei, "Chondrogenesis, osteogenesis and adipogenesis of canine mesenchymal stem cells: a biochemical, morphological and ultrastructural study," *Histochemistry and Cell Biology*, vol. 128, no. 6, pp. 507–520, 2007.
- [44] M. Narita, M. Narita, V. Krizhanovsky et al., "A novel role for high-mobility group a proteins in cellular senescence and heterochromatin formation," *Cell*, vol. 126, no. 3, pp. 503–514, 2006.
- [45] A. Richter, M. Lübbling, H. G. Frank, I. Nolte, J. C. Bullerdiek, and I. von Ahsen, "High-mobility group protein HMGA2-derived fragments stimulate the proliferation of chondrocytes and adipose tissue-derived stem cells," *European Cells & Materials*, vol. 21, pp. 355–363, 2011.
- [46] R. Palumbo, M. Sampaoli, F. De Marchis et al., "Extracellular HMGB1, a signal of tissue damage, induces mesoangioblast migration and proliferation," *Journal of Cell Biology*, vol. 164, no. 3, pp. 441–449, 2004.
- [47] E. Meng, Z. Guo, H. Wang et al., "High mobility group box 1 protein inhibits the proliferation of human mesenchymal stem cells and promotes their migration and differentiation along

osteoblastic pathway,” *Stem Cells and Development*, vol. 17, no. 4, pp. 805–813, 2008.

- [48] C. Zhao, G. Sun, S. Li et al., “MicroRNA let-7b regulates neural stem cell proliferation and differentiation by targeting nuclear receptor TLX signaling,” *Proceedings of the National Academy of Sciences of the United States of America*, vol. 107, no. 5, pp. 1876–1881, 2010.

4.3. Tools for modification and detection of gene expression

Following cancer diagnosis and identification of deregulated genes, gene therapeutic approaches can be harnessed to reconstitute or suppress the targets of interest. For that purpose several *let-7* encoding expression vectors were constructed herein.

The successful treatment with gene constructs or products depend highly on the efficient transfer of the corresponding molecules into the cell of interest and additionally on exact titer.

As the commonly used transduction and transfection techniques have to be further optimized a new gold nanoparticle based transfection method was evaluated. Additionally, for the accurate quantification of adeno-associated viruses (AAV) a novel viral genome purification protocol for the subsequent analyses by real-time PCR was established.

Finally, following gene expression modification it is necessary to have appropriated tools to monitor the target protein expression, thus cross-reactivity of a PSMA antibody was evaluated with the canine PSMA protein.

4.3.1. Generation of miRNA *let-7* constructs

For coming analyses of the canine miRNA *let-7* family members *let-7a1*, *let-7a2*, *let-7b*, *let-7c*, *let-7d*, *let-7e*, *let-7f*, *let-7g* and *let-7i* the precursor encoding sequences of were successfully amplified and cloned into the commercially available pGEM-T-Easy vector (Tab. 1).

Additionally the *let-7a1*, *let-7a2* and *let-7b* variants were cloned into the multiple-cloning site of a commercially available pAAV-MCS vector. The expression cassette of these vectors is flanked by inverted-terminal repeats (ITRs). When using this vector for AAV production the part between the ITRs will be packaged into the viral particles (Tab. 1).

Moreover the canine *let-7a1*, *let-7a2* variants as well as a non-sense “scrambled” control sequence and an artificial *let-7a* encoding construct were cloned into the commercially available pEP-has-*let-7a2* vector replacing the intrinsic human *let-7a2* precursor. The expression cassette of this plasmid has an EF1 α -promoter and carries additionally a puromycin resistance gene, enabling stable transfection of

Results

cells. In the following these expression cassettes were used to replace the part between the ITR of the pAAV-MCS vector (Tab. 1).

Table 1 let-7 encoding vectors

Vector name	Insert
pGEM-T-Easy-cfa-let-7a1	Canine let-7a1
pGEM-T-Easy-cfa-let-7a2	Canine let-7a2
pGEM-T-Easy-cfa-let-7b	Canine let-7b
pGEM-T-Easy-cfa-let-7c	Canine let-7c
pGEM-T-Easy-cfa-let-7d	Canine let-7d
pGEM-T-Easy-cfa-let-7e	Canine let-7e
pGEM-T-Easy-cfa-let-7f	Canine let-7f
pGEM-T-Easy-cfa-let-7g	Canine let-7g
pGEM-T-Easy-cfa-let-7i	Canine let-7i
pAAV-CMV-let-7a1	Canine let-7a1
pAAV-CMV-let-7a2	Canine let-7a2
pAAV-CMV-let-7b	Canine let-7b
pEP-cfa-let-7a1	Canine let-7a1
pEP-cfa-let-7a2	Canine let-7a2
pEP-scrambled	Non-sense DNA
pEP-AMPM-let-7a	Artificial let-7a construct
pAAV-EF1 α -cfa-let-7a1	Canine let-7a1
pAAV-EF1 α -cfa-let-7a2	Canine let-7a2
pAAV-EF1 α -scrambled	Non-sense DNA
pAAV-EF1 α -AMPM-let-7a	Artificial let-7a construct

4.3.2. AAV genome isolation for quantification by absolute real-time PCR

Successful gene therapy approaches depend highly on the efficient transfer of the gene of interest into a cell.

One of the commonly harnessed viral vectors is the adeno-associated virus (AAV) family, which bears many advantages like a broad tropism, the disability of self-replication and especially a low immune response (Berns and Bohenzky, 1987; Snyder and Flotte, 2002; Nathwani *et al.*, 2011; Shin *et al.*, 2013). Although the maximal size of the AAV genome is limited (~ 4.7 kilo bases) (Srivastava *et al.*, 1983) it is sufficient for the therapeutic delivery of small genes such as miRNAs (Kota *et al.*, 2009; Mueller *et al.*, 2012).

Accordingly, major steps were taken aiming to optimize the recombinant AAV generation, purification and titration methods. However, these protocols need still further optimization, especially the quantification techniques should not be overlooked as the correct viral titer is prerequisite for the reproducibility of an experiment and a safe application in therapy.

X. Improved rAAV genome isolation for quantification by absolute real-time PCR.

Wagner *et al.*, in preparation for submission.

In the following technical note a novel AAV genome purification protocol is presented. For that purpose recombinant serotype 2 AAVs carrying the *beta-galactosidase* gene, were produced. In the next step the AAV genomes were isolated according to the novel protocol and to two commonly used procedures. Finally, all AAV genomes were quantified by absolute quantitative-real time PCR as previously described by Dr. Jan Soller (doctoral thesis entitled “Strukturelle und funktionelle Analyse ausgewählter High Mobility Group Gene des Haushundes”).

It could be demonstrated, that the novel protocol is less prone to errors and most importantly the measured AAV genome titers are more accurate compared to the other two tested protocols.

X.

Improved rAAV genome isolation for quantification by absolute real-time PCR

Siegfried Wagner, Anacllet Ngezahayo, Hugo Murua Escobar, Ingo Nolte

In preparation for submission.

Own contribution:

- Genomic adeno-associated virus DNA isolation
- Quantitative real-time PCR
- Statistical analyses of real-time PCR results
- Figure preparation (real-time PCR results)
- Partial manuscript drafting

Improved rAAV genome isolation for quantification by absolute real-time PCR

Siegfried Wagner^{1,3}, Anaclet Ngezahayo², Hugo Murua Escobar^{1,3#}, Ingo Nolte^{1§}

¹Small Animal Clinic, University of Veterinary Medicine Hannover, 30559 Hannover, Germany

²Institute of Biophysics, University Hannover, 30419 Hannover, Germany

³Division of Medicine, Dept. of Haematology/Oncology, University of Rostock, 18057 Rostock, Germany

[§]Corresponding author

Email addresses:

SW: siegfried.wagner@tiho-hannover.de

AN: ngezahayo@biophysik.uni-hannover.de

HME: hugo.murua.escobar@med.uni-rostock.de

IN: ingo.nolte@tiho-hannover.de

Abstract

Adeno-associated virus derived vectors are constantly being evaluated in model organisms and humans as gene delivery-based therapeutics. Due to low immune response, broad tropism, and the disability of self-replication these vectors are considered as a promising tool for human and animal gene therapeutic approaches.

Key for the evaluation of these therapeutic or experimental approaches is the availability of pure, recombinant adeno-associated viruses of high quality, and further the possibility to accurately and reliably quantify the respective vector-genomes.

Herein we describe a novel silica-based adeno-associated viral genome isolation protocol allowing the generation of highly pure, DNase resistant viral genomes. Further, we performed a comparison of this new method with two commonly used viral sample preparation protocols for subsequent quantification by absolute real-time PCR.

The new modified silica-based method described in the present study allows a more accurate and highly reproducible adeno-associated virus genome purification for the following quantification via real-time PCR in comparison to the other tested, commonly used methods.

Introduction

The recombinant adeno-associated virus (rAAV) is an icosahedral parvovirus with a diameter of ~ 20 nm [1]. It contains a single stranded DNA (ssDNA) genome of ~ 4.7 kilo bases either in positive- or negative-sense orientation in non-enveloped protein capsids [1,2]. After cell infection the ssDNA is delivered to the nucleus [3] and converted into a double-stranded, transcriptionally active form [4]. It has been shown that rAAVs are able to infect dividing as well as quiescent cells [5] highlighting its importance as therapeutic vector. Due to weak immune response, the disability of self-replication, and a broad tropism this nonpathogenic virus type is considered as a promising vehicle for human and animal gene therapeutic approaches [6-9].

In the last decade, major steps were successfully taken aiming at an optimization of rAAV generation protocols. Despite of the generation itself, the determination of the exact viral titer is crucial not only for accurate and reproducible *in vitro* and *in vivo* applications but also for comparing results between laboratories [10]. Consequently a reliable method for rAAV quantification would be of great value. For this purpose various techniques have been used, such as ELISAs allowing the titration of

assembled viral particles [10], southern blot analysis [11], dot blot hybridization [12], or quantitative real-time PCR [13]. Quantification by real-time PCR has been proven to be the most accurate of these techniques by showing a broad dynamic range. However, a prerequisite for quantification by absolute real-time PCR is the accessibility of highly pure viral genomes (VG).

A direct utilization of a rAAV immersion as template in a real-time PCR is possible, but not very accurate. This can be explained by the fact that not all viral capsids denature at once in the first denaturation step and subsequently not all VGs are accessible as template for the polymerase. Furthermore the non-packaged VGs (VG-containing plasmid DNA and not-packaged VGs from the rAAV production step) also function as template in the reaction. These problems were addressed by incubating the viral suspension in NaOH to degrade all non-packaged VGs and predenature the rAAV capsids to enable the VG release more easily and simultaneously in the first denaturing step of the following real-time PCR [14].

Up to now several techniques have been described for viral genome preparation/isolation. The commonly employed NaOH pretreatment of the viral particles bears some disadvantages: NaOH must be neutralized accurately by applying HCl and the duration of the rAAV pretreatment has to be defined exactly, otherwise the VGs will be released too early and degraded by the NaOH. If the pretreatment is too short, many capsids stay intact during the first denaturation step in the PCR instead of releasing their load. In both cases the measured VG titer appears to be lower than the actual present titer.

In the second commonly used method viral particles are initially pretreated with DNase to digest all non-packaged VGs. After DNase heat-inactivation proteinase K is added to digest the remaining DNase and the viral capsids. Finally proteinase K is also heat-inactivated and the VGs employed directly as template for quantification via real-time PCR. In a modified variant of this method the VGs are purified by phenol/chloroform extraction prior to the quantification.

In general a reliable real-time PCR is dependent on the use of purified VGs. Phenol/chloroform extraction is often used for VG purification from residual enzymes and salts which could interfere with the PCR or have an influence on the VGs. However, this purification method shows also some disadvantages. First of all the procedure is toxic and the phase with the DNA remains difficult to be removed

completely being still contaminated with phenol/chloroform which could interfere with the PCR itself.

To address these obstacles we evaluated a novel, non-toxic, accurate, and easy silica-based protocol for the VG isolation. Herein we used a silica-based 'NucleoSpin RNA Virus' kit purchased from Macherey & Nagel company (Düren, Germany) further termed as M&N. This kit was originally developed for the viral genome isolation of HCV, HBV, HAV, HIV, HSV, HPV, VZV, EBV, parvovirus B19, H5N1 and H1N1 ('NucleoSpin RNA Virus' manual (March 2012/Rev. 10)). Our modifications of the 'Support protocol: Isolation of viral RNA and DNA from cell-free biological fluids with NucleoSpin RNA Virus' protocol enable the purification of rAAV genomes. Compared to the other previously mentioned protocols for viral genome quantification, our new silica-based rAAV genome isolation is less prone to errors and the whole procedure needs less time in comparison to the DNase/proteinase K method. Additionally, we show that the following quantification by absolute real-time PCR displays the lowest inter-assay variability and more accurate titers when using the VGs as template purified according to the new protocol.

Materials and Methods

rAAV-LacZ generation and purification

Eukaryotic AAV-293 cells were taken into culture from a frozen stock in an early passage according to the 'AAV Helper free system' instruction manual, revision A.01 (Stratagene, La Jolla, USA) until reaching 70-80 % confluence. For the production of recombinant AAVs containing the *beta-galactosidase* gene under a CMV promoter (rAAV-LacZ) the cells were co-transfected with three DNA plasmids (pHelper, pAAV-RC and pAAV-LacZ) and harvested 72 h later according to the 'AAV Helper free system' protocol. Following, the AAV-293 host cells were exposed to three freeze & thaw cycles by alternating the immersion in a dry ice/ethanol bath and a 37 °C water bath. In the next step the rAAV-LacZ viral particles were purified from the cell lysate by one-step affinity chromatography according to Smith *et al.* [15] using prepacked 1 ml HiTrap AVB Sepharose columns (GE Healthcare Europe GmbH, Freiburg, Germany).

Sample preparation

Results

For viral genome preparation purified rAAV-LacZ aliquots were diluted 1:20 with Nuclease-Free water (Qiagen Hamburg GmbH, Hamburg, Germany) (sample 1). For the simulation of VG isolation from unpurified viral particles an additional purified virus aliquot was diluted 1:20 with a cell lysate from native, untreated AAV-293 cells (1×10^7 cell/ml x1 PBS) which were treated as described above according to the freeze & thaw procedure (sample 2). The sample 1 and sample 2 were prepared with well-defined compositions of purified virus to enable an easy comparison between the processing of pure and crude viral samples (Figure 1). Additionally, the untreated AAV-293 cell-lysate was diluted 20:1 with Nuclease-Free water as a negative control for an unspecific PCR (sample 3) (Figure 1).

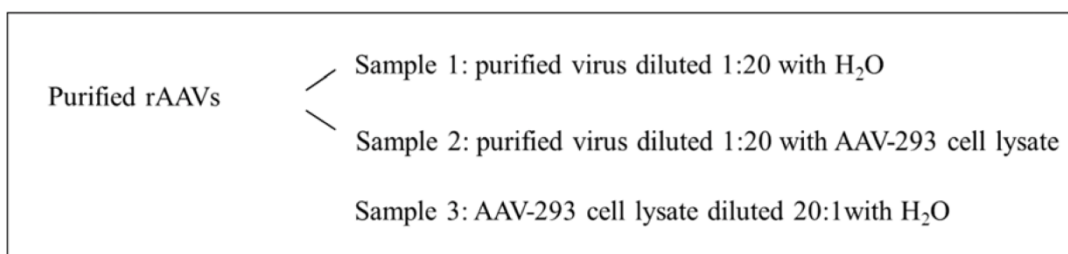


Figure 1. Overview: Sample preparation

The sample 3 contains the same amounts of cell lysate as sample 2. Aliquots of the samples 1-3 were further processed according to three protocols: the silica membrane-based (S), the DNase/preteinase K (D) and NaOH (N) protocol. An overview of the sample processing is shown in table 1.

Table 1. Flow chart: Sample processing

S	D	N
5 µl virus containing aliquot, 10 µl DNase (1U/µl), 2 µl DNase buffer (x10), ad 20 µl H ₂ O	5 µl virus containing aliquot, 10 µl DNase (1U/µl), 2 µl DNase buffer (x10), ad 20 µl H ₂ O	5 µl virus containing aliquot, 20 µl NaOH (2 M), ad 40 µl H ₂ O
↓	↓	↓
1 h incubation, 37 °C	1 h incubation, 37 °C	30 min incubation, 56 °C
↓	↓	↓
5 min incubation, 65 °C, chilling on ice for 1 min	10 min incubation, 65 °C, chilling on ice for 1 min	Neutralisation with HCl (2 M)
↓	↓	↓
20 µg proteinase K, H ₂ O ad 150 µl, 600 µl RAV1 buffer	30 µg proteinase K, 6 µl CaCl ₂ (100 mM), H ₂ O ad 60 µl	Adjust VG suspension volume to 200 µl with H ₂ O
↓	↓	
5 min incubation, 70 °C	30 min incubation, 50 °C	
↓	↓	
VG purification according to the M&N protocol	20 min incubation, 95 °C, chilling on ice for 1 min	
↓	↓	
Adjust VG eluate volume to 200 µl with H ₂ O	Adjust VG suspension volume to 200 µl with H ₂ O	

Flow chart of the sample processing performed according to the three used protocols

S = Silica membrane-based protocol

D = DNase/proteinase K protocol

N = NaOH protocol

To compare the inter assay variability of the three protocols, the complete pretreatment/isolation and quantification processes were repeated three times for each sample and protocol.

Silica membrane-based protocol

The sample incubation with DNase and proteinase K was based on the protocols from Zolotukhin *et al.* and Duffy *et al.* [16,17]. Herein we describe our modifications of the 'Support protocol: Isolation of viral RNA and DNA from cell-free biological fluids with NucleoSpin RNA Virus' protocol (M&N, Düren, Germany).

Aliquots of five µl from sample 1, sample 2 and sample 3 (Table 1) were mixed with RQ1 DNase 10x Reaction Buffer (Promega GmbH, Mannheim, Germany), 10 µl (1 U/µl) RQ1 RNase-Free DNase (Promega GmbH, Mannheim, Germany) and Nuclease-Free water (Qiagen Hamburg GmbH, Hamburg, Germany) in a final volume of 20 µl, respectively. After sample incubation for 60 min at 37 °C, and 5 min

at 65 °C for DNase inactivation, the samples were chilled for ~ 1 min on ice. Afterwards the sample volume was adjusted with Nuclease-Free water to 150 µl, additionally 20 µg proteinase K (Promega GmbH, Mannheim, Germany) and 600 µl Buffer RAV1 (included in the 'NucleoSpin RNA Virus' kit, M&N, Düren, Germany) were added and further proceeded as instructed in the 'Support protocol: Isolation of viral RNA and DNA from cell-free biological fluids with NucleoSpin RNA Virus' protocol (M&N, Düren, Germany). The suspension was applied on the mini spin columns (M&N, Düren, Germany), washed and finally the viral genomes (VG) were twice eluted with 100 µl RNase-free H₂O. The last centrifugation step was carried out at 11,000 x g for 5 min. In the following these samples are named S1, S2 and S3 according to the used type of protocol (S) and the source of the aliquots (sample 1-3, Figure 1).

DNase/proteinase K protocol

Five µl aliquots of sample 1, sample 2 and sample 3 were initially pretreated with DNase as described in the improved 'silica membrane-based protocol'. After the sample chilling on ice for ~ 1 min 30 µg proteinase K (Promega GmbH, Mannheim, Germany) and 6 µl 100 mM CaCl₂ (Applichem GmbH, Darmstadt, Germany) in Nuclease-Free water (Qiagen Hamburg GmbH, Hamburg, Germany) were added and the volume adjusted with Nuclease-Free water to 60 µl. The samples were additionally incubated at 50 °C for 1 h followed by a proteinase K inactivation step at 95 °C for 20 min and ~ 1 min chilling on ice. Finally the sample volume was adjusted to 200 µl with Nuclease-Free water. In the following those samples are named D1, D2 and D3.

NaOH protocol

In the third commonly used protocol, five µl aliquots of the sample 1, sample 2 and sample 3 were pretreated with NaOH (Applichem GmbH, Darmstadt, Germany). At this point it is important to note that in this method the viral particles must not crack open otherwise the enclosed VGs would be degraded; the viral capsids are only partially denaturated and should release their load in the initial denaturation step of the quantitative real-time PCR where it serves as a template. Aliquots were mixed with 15 µl Nuclease-Free water (Qiagen Hamburg GmbH, Hamburg, Germany), 20 µl NaOH (2 M) and incubated for 30 min at 56 °C. Finally, the reactions were

neutralized with an adequate volume of 2 M HCl (Applichem GmbH, Darmstadt, Germany) and the volume adjusted to 200 μ l with Nuclease-Free water. In the following those samples are named N1, N2 and N3.

VG quantification via absolute quantitative real-time PCR

The undiluted VGs were quantified via an absolute quantitative real-time PCR. Measurements were performed in a Master Cycler ep realplex cycler (Eppendorf AG, Hamburg, Germany). In the following all ordered oligonucleotides, synthesized by the Biomerns.net GmbH (Ulm, Germany) are listed, all of which were previously reported by Jan T. Soller. Forward primer: 5'-GAGGTCTATATAAGCAGAGCTCGTTTAGT-3', reverse primer: 5'-GGTGTCTTCTATGGAGGTCAAACA-3', TaqMan probe: FAM-5'-CAGATCGCCTGGAGACGCCATCC3'-TAMRA and standard molecule: 5'-GGTGGGAGGTCTATATAAGCAGAGCTCGTTTAGT-3'.

The CMV (promoter in the rAAV genome) promoter-specific quantitative real-time PCR was performed as described by Jan T. Soller (doctoral thesis: <http://elib.suub.uni-bremen.de/edocs/00101803-1.pdf>) using a TaqMan Universal PCR Master Mix (2X) (Life Technologies Corporation, Germany). To generate a standard curve the oligonucleotide standard was diluted from 10^9 - 10^0 molecules/ μ l in 10-fold dilution steps. The master mix was prepared according to the manufacturer's instructions with a total reaction volume of 25 μ l. Thermal cycler conditions were in accordance with the instructions of the manufacturer. In each reaction 2 μ l template was added, all samples were measured in triplicate. The measured mean threshold (Ct) values were used to calculate the titer of the viral stock solution summarized in column 2 of Table 2 and shown in Figure 2. Standard deviations calculated by the used realplex 2.2 quantitative real-time PCR software (Eppendorf AG, Hamburg, Germany) were converted in percent and finally used for the determination of the standard deviations of the calculated viral stock titers.

Statistical analysis

For statistical analysis of the calculated viral stock titers an ordinary one-way ANOVA analysis with multiple comparisons of the mean values (results are shown in table 3) was performed using the software GraphPad Prism (version 6.0.2 (San Diego, USA)).

Results

For comparative VG preparation and the following quantification by absolute quantitative real-time PCR aliquots, from the three different samples 1-3 (Figure 1) were processed each according to three different protocols (S, D and N) (Table 1). Each sample preparation and quantification was repeated three times. The quantification of VGs isolated according to our improved silica membrane-based protocol revealed for the rAAV-LacZ samples S1 and S2 a mean of $2.0 \cdot 10^{12}$ VG/ml and $3.3 \cdot 10^{12}$ VG/ml in the stock suspension (Figure 2 and Table 2). The samples D1 and D2 pretreated according to the DNase/proteinase K protocol had mean titers of $4.3 \cdot 10^{11}$ VG/ml and $9.9 \cdot 10^{11}$ VG/ml (Figure 2 and Table 2).

The samples N1 and N2 pretreated according to the NaOH protocol had both a mean titer of $6.4 \cdot 10^{11}$ VG/ml (Figure 2 and Table 2).

In the negative controls (sample S3, D3 and N3) with the native AAV-293 cell lysates no rAAV-LacZ genomes were detectable independent of the used pretreatment/isolation protocol (Figure 2 and Table 2).

Table 2. Overview of calculated VG titers in viral stock suspensions

Sample	Titer [VG/ml]	Mean Titer [VG/ml]
S1	1.9E+12	2.0E+12
S1	2.0E+12	
S1	2.0E+12	
S2	3.4E+12	3.3E+12
S2	3.3E+12	
S2	3.2E+12	
S3	-	-
S3	-	
S3	-	
D1	5.0E+11	4.3E+11
D1	5.4E+11	
D1	2.6E+11	
D2	9.4E+11	9.9E+11
D2	9.4E+11	
D2	1.1E+12	
D3	-	-
D3	-	
D3	-	
N1	6.4E+11	6.4E+11
N1	8.8E+11	
N1	3.9E+11	
N2	6.4E+11	6.4E+11
N2	6.7E+11	
N2	6.2E+11	
N3	-	-
N3	-	
N3	-	

Results

In the first column are the samples listed. The first letter indicates according to which of the three methods the samples were processed. In the second column are the calculated viral stock titer (measured in triplicate) shown. The mean viral stock titers are written in the third column.

- No values

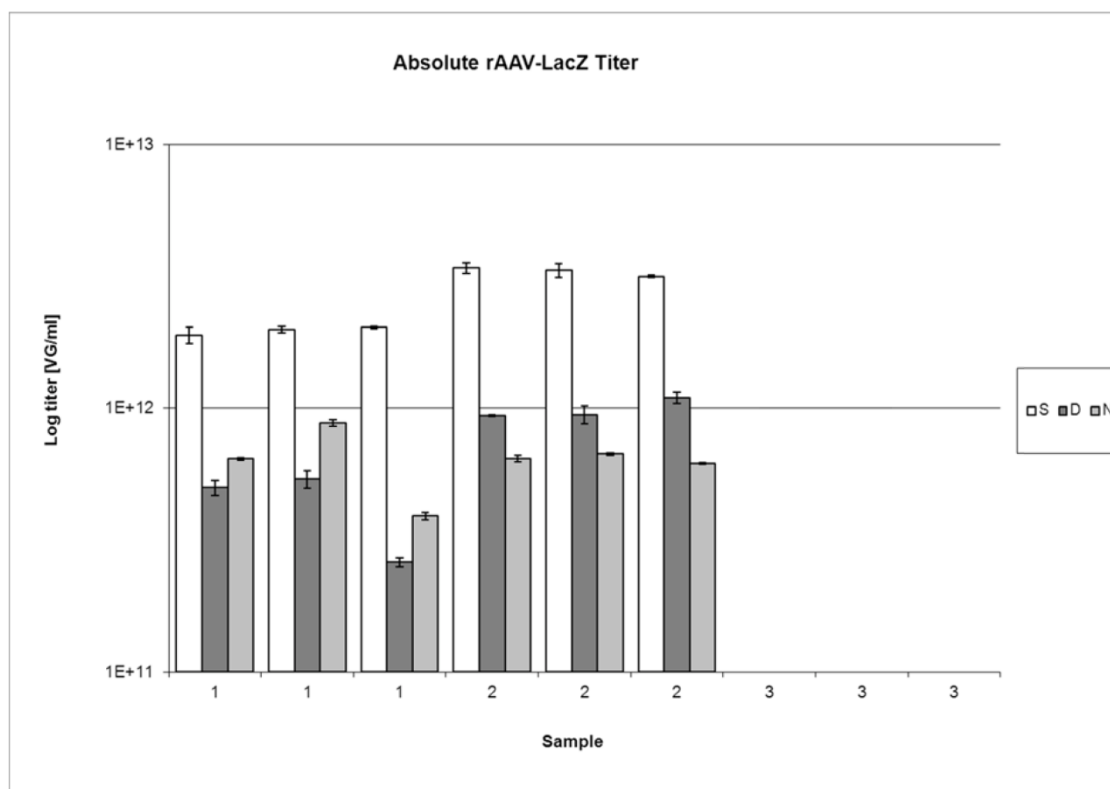


Figure 2. Absolute rAAV-LacZ titer

All viral sample aliquots were processed and quantified in triplicate. Calculated rAAV-LacZ titer in stock suspensions of samples 1-3 pretreated according to the silica membrane-based (S), DNase/proteinase K (D) and NaOH (N) protocols are plotted logarithmic versus x-axis. Error bars are standard deviations. Samples S3, D3 and N3 do not contain viral genomes.

Statistical analysis

The VG titers of the: S1-2, D1-2 and N1-2 (Table 2) were used for the ANOVA analysis. It could be shown that the samples S1 and D1 show statistically significant differences to the mean titers of the samples S2 and D2 respectively. No statistically

Results

significant difference could be observed for the VG titers of samples N1 and N2. The samples S1 and S2 are statistically different from the samples D1, D2, N1 and N2. The measured VG titers of the samples N1, N2 and D1 are statistically similar. The results of the ANOVA analysis are summarized in table 3.

Table 3. Summary of statistical analysis results

Tukey's multiple comparisons test	Significant?	Summary
S1 vs. S2	Yes	****
S1 vs. D1	Yes	****
S1 vs. D2	Yes	****
S1 vs. N1	Yes	****
S1 vs. N2	Yes	****
S2 vs. D1	Yes	****
S2 vs. D2	Yes	****
S2 vs. N1	Yes	****
S2 vs. N2	Yes	****
D1 vs. D2	Yes	**
D1 vs. N2	No	ns
D1 vs. N1	No	ns
D2 vs. N1	No	ns
D2 vs. N2	No	ns
N1 vs. N2	No	ns

Results of the one-way ANOVA analysis.

****: $p \leq 0.0001$

** : $p \leq 0.01$

ns: $p > 0.05$

Discussion

In the last decades, several techniques were evaluated for rAAV quantification, but many of these show considerable limitations. Commercially available kits based on antibodies for fixing the assembled viral particles, followed by capsid digestion and viral DNA detection show to be not very sensitive and are in general expensive. Many alternative quantification techniques such as dot blot, southern blot and ELISA are also not sensitive enough for a variety of downstream applications. Titration of the assembled viral particles with ELISAs has also revealed to miss accuracy due to the fact that not all capsids actually contain a genome [18]. DNase resistant viral genome quantification by absolute real-time PCR appears to be the method of choice but depends on highly pure viral genomes. However this technique is convenient and has a broad dynamic range.

Herein we tested three different protocols for VG preparation and quantified the samples via an absolute quantitative real-time PCR. Our hypothesis was that samples prepared according to the silica membrane-based protocol would better reflect in comparison to the other two commonly used methods the actual titer of a given virus suspension, as the isolated VGs are free of any enzymes and detergents which could digest/degrade them.

Our comparative analyses revealed much lower titers for the samples D1 in comparison to S1 and D2 in comparison to S2 (Table 2 and Figure 2) although the DNase digestion step is identical between the silica membrane-based (S) and DNase/proteinase K (D) protocols. It appears that the DNase kept a residual activity after thermal inactivation and digested many of the VGs in the following 30 min incubation of the samples D1 and D2 with proteinase K. Contrary to this the samples processed according to the silica membrane-based protocol (S) were incubated only for 5 min at 70 °C with proteinase K directly followed by the isolation of the VGs.

Although the sample pairs S1 and S2 as well as D1 and D2 were processed in the same way the final VG quantification revealed statistically significantly higher titers of S2 in comparison to S1 and as well between D2 in comparison to D1 (Table 3). It is likely that these titer differences are caused by the presence of genomic DNA (gDNA) from the AAV-293 host cell lysate, which was included into the samples S2 and D2. The gDNA functioned as DNase substrate competitor so that the DNase digested a smaller part of non-packaged viral genomes in the viral suspension. This could be avoided by increased DNase amounts, longer DNase incubation duration or higher dilution of the viral samples. Due to the high dynamic range of the real-time PCR technique the quantification of higher diluted VGs would not be limited by lower template amounts allowing an accurate VG titer determination.

However processing of highly diluted viral suspensions prepared according to the DNase/proteinase K protocol would negatively influence titer determination as the ratio between present DNA and DNase would be changed significantly and the impact of the residual activity of the DNase would rise.

The titers of the samples N1 and N2 showed to be statistically not different. This was expected as the NaOH is unspecific and degrades all non-packaged nucleotides at once and not step by step like in the case of a single DNase molecule.

During our comparative experiments we observed very high inter assay variability when using the NaOH or the DNase/proteinase K protocol for VG preparation. Our

results demonstrate that the residual DNase activity or the application of NaOH remains problematic resulting in lower VG titer inaccurately reporting the actual titer.

Conclusions

Despite of the lower titer reproducibility of the samples pretreated according to the DNase/proteinase K (D) and NaOH (N) protocol these two methods are still useful to get an estimation of the VG titer in a viral suspension. However, it is better to process the pure as well as crude viral samples according to the herein reported silica-membrane based (S) protocol as this method showed to be less prone to errors, is more accurate, fast and highly reproducible.

Due to similar physical and chemical structures of different rAAV serotypes this novel sample processing protocol may also be suitable for VG preparation from other serotypes as the herein used serotype 2 rAAVs.

Conflict of interests

There is no conflict of interests.

Acknowledgements

We acknowledge Dr. Saskia Willenbrock for scientific discussions and proofreading.

References

1. Srivastava A, Lusby EW, Berns KI. Nucleotide sequence and organization of the adeno-associated virus 2 genome. *Journal of virology* 1983;45(2):555-564.
2. Berns KI, Rose JA. Evidence for a single-stranded adenovirus-associated virus genome: isolation and separation of complementary single strands. *Journal of virology* 1970;5(6):693-699.
3. Leopold PL, Pfister KK. Viral strategies for intracellular trafficking: motors and microtubules. *Traffic (Copenhagen, Denmark)* 2006;7(5):516-523.
4. Fisher KJ, Gao GP, Weitzman MD, DeMatteo R, Burda JF, Wilson JM. Transduction with recombinant adeno-associated virus for gene therapy is limited by leading-strand synthesis. *Journal of virology* 1996;70(1):520-532.
5. Podsakoff G, Wong KK, Jr., Chatterjee S. Efficient gene transfer into nondividing cells by adeno-associated virus-based vectors. *Journal of virology* 1994;68(9):5656-5666.
6. Berns KI, Bohenzky RA. Adeno-associated viruses: an update. *Advances in virus research* 1987;32:243-306.
7. Snyder RO, Flotte TR. Production of clinical-grade recombinant adeno-associated virus vectors. *Current opinion in biotechnology* 2002;13(5):418-423.
8. Nathwani AC, Tuddenham EG, Rangarajan S, Rosales C, McIntosh J, Linch DC, Chowdary P, Riddell A, Pie AJ, Harrington C, O'Beirne J, Smith K, Pasi J, Glader B, Rustagi P, Ng CY, Kay MA, Zhou J, Spence Y, Morton CL, Allay J, Coleman J, Sleep S, Cunningham JM, Srivastava D, Basner-Tschakarjan E, Mingozzi F, High KA, Gray JT, Reiss UM, Nienhuis AW, Davidoff AM. Adenovirus-associated virus vector-mediated gene transfer in hemophilia B. *The New England journal of medicine* 2011;365(25):2357-2365.
9. Shin JH, Pan X, Hakim CH, Yang HT, Yue Y, Zhang K, Terjung RL, Duan D. Microdystrophin Ameliorates Muscular Dystrophy in the Canine Model of Duchenne Muscular Dystrophy. *Mol Ther* 2013.
10. Grimm D, Kern A, Pawlita M, Ferrari F, Samulski R, Kleinschmidt J. Titration of AAV-2 particles via a novel capsid ELISA: packaging of genomes can limit production of recombinant AAV-2. *Gene therapy* 1999;6(7):1322-1330.
11. Halbert CL, Standaert TA, Aitken ML, Alexander IE, Russell DW, Miller AD. Transduction by adeno-associated virus vectors in the rabbit airway: efficiency, persistence, and readministration. *Journal of virology* 1997;71(8):5932-5941.
12. Samulski RJ, Chang LS, Shenk T. Helper-free stocks of recombinant adeno-associated viruses: normal integration does not require viral gene expression. *Journal of virology* 1989;63(9):3822-3828.
13. Clark KR, Liu X, McGrath JP, Johnson PR. Highly purified recombinant adeno-associated virus vectors are biologically active and free of detectable helper and wild-type viruses. *Human gene therapy* 1999;10(6):1031-1039.
14. Veldwijk MR, Topaly J, Laufs S, Hengge UR, Wenz F, Zeller WJ, Fruehauf S. Development and optimization of a real-time quantitative PCR-based method for the titration of AAV-2 vector stocks. *Mol Ther* 2002;6(2):272-278.
15. Smith RH, Levy JR, Kotin RM. A simplified baculovirus-AAV expression vector system coupled with one-step affinity purification yields high-titer rAAV stocks from insect cells. *Mol Ther* 2009;17(11):1888-1896.
16. Duffy AM, O'Doherty AM, O'Brien T, Strappe PM. Purification of adenovirus and adeno-associated virus: comparison of novel membrane-based

- technology to conventional techniques. *Gene therapy* 2005;12 Suppl 1:S62-72.
17. Zolotukhin S, Potter M, Zolotukhin I, Sakai Y, Loiler S, Fraites TJ, Jr., Chiodo VA, Phillipsberg T, Muzyczka N, Hauswirth WW, Flotte TR, Byrne BJ, Snyder RO. Production and purification of serotype 1, 2, and 5 recombinant adeno-associated viral vectors. *Methods (San Diego, Calif)* 2002;28(2):158-167.
 18. Grimm D, Kern A, Rittner K, Kleinschmidt JA. Novel tools for production and purification of recombinant adenoassociated virus vectors. *Human gene therapy* 1998;9(18):2745-2760.

4.3.3. AuNP based laser-transfection

Biotechnological advances in the last decades enabled the use of genes as drugs and targets, and the manipulation of eukaryotic cells for therapeutic approaches. Nevertheless, the efficiency, safety, and toxicity of the commonly used transduction and transfection techniques have to be further optimized especially for sensitive cell types.

VII. Characterization of Nanoparticle Mediated Lasertransfection by Femtosecond Laser Pulses for Applications in Molecular Medicine.

Schomaker *et al.*, Journal of Nanobiotechnology, 2015.

In the following research article the evaluation of an alternative gold nanoparticle mediated laser transfection protocol was described, offering a novel procedure for a highly efficient, minimally cell-toxic and up scalable *in vitro* manipulation of mammalian cells.

Basically, the inflow of extracellular molecules into cells was achieved by fs-laser excitation of cell-membrane-adhered spherical gold nanoparticles inducing a localized membrane permeabilization. To explore the initial mechanism of membrane perforation theoretical simulations and laser induced effects were experimentally investigated by spectrometric and microscopic analysis. The obtained results indicate that near field effects are the initial mechanisms of membrane permeabilization.

For proof of principle the canine prostatic adenocarcinoma derived cell line CT1258, which highly overexpresses the oncogene *HMGA2*, was transfected with fluorophore-labeled short interfering RNAs (siRNAs). The intake of the siRNAs was controlled by flow cytometry revealing a transfection efficacy of about 90 % and a cell viability of 93 %. Finally, siRNA functionality was analyzed by transfection of the same cell line with anti-*HMGA2* short interfering RNAs (siRNAs). A target mRNA down regulation of approximately 40 % could be detected by quantitative real-time PCR.

VII.

Characterization of Nanoparticle Mediated Lasertransfection by Femtosecond Laser Pulses for Applications in Molecular Medicine

Markus Schomaker, Dag Heinemann, Stefan Kalies, Saskia Willenbrock, Siegfried Wagner, Ingo Nolte, Tammo Ripken, Hugo Murua Escobar, Heiko Meyer, Alexander Heisterkamp

Journal of Nanobiotechnology, 2015.

Own contribution:

- RNA isolation and cDNA synthesis
- Quantitative real-time PCR
- Statistical analyses of real-time PCR results
- Figure preparation (real-time PCR results)
- Partial manuscript drafting

RESEARCH

Open Access

Characterization of nanoparticle mediated laser transfection by femtosecond laser pulses for applications in molecular medicine

Markus Schomaker^{1*}, Dag Heinemann¹, Stefan Kalies¹, Saskia Willenbrock², Siegfried Wagner², Ingo Nolte², Tammo Ripken¹, Hugo Murua Escobar^{2,3}, Heiko Meyer^{1,4} and Alexander Heisterkamp^{1,5}

Abstract

Background: In molecular medicine, the manipulation of cells is prerequisite to evaluate genes as therapeutic targets or to transfect cells to develop cell therapeutic strategies. To achieve these purposes it is essential that given transfection techniques are capable of handling high cell numbers in reasonable time spans. To fulfill this demand, an alternative nanoparticle mediated laser transfection method is presented herein. The fs-laser excitation of cell-adhered gold nanoparticles evokes localized membrane permeabilization and enables an inflow of extracellular molecules into cells.

Results: The parameters for an efficient and gentle cell manipulation are evaluated in detail. Efficiencies of 90% with a cell viability of 93% were achieved for siRNA transfection. The proof for a molecular medical approach is demonstrated by highly efficient knock down of the oncogene HMGA2 in a rapidly proliferating prostate carcinoma *in vitro* model using siRNA. Additionally, investigations concerning the initial perforation mechanism are conducted. Next to theoretical simulations, the laser induced effects are experimentally investigated by spectrometric and microscopic analysis. The results indicate that near field effects are the initial mechanism of membrane permeabilization.

Conclusion: This methodical approach combined with an automated setup, allows a high throughput targeting of several 100,000 cells within seconds, providing an excellent tool for *in vitro* applications in molecular medicine. NIR fs lasers are characterized by specific advantages when compared to lasers employing longer (ps/ns) pulses in the visible regime. The NIR fs pulses generate low thermal impact while allowing high penetration depths into tissue. Therefore fs lasers could be used for prospective *in vivo* applications.

Keywords: Laser transfection, Plasmonics, Nanoparticles, Permeabilization mechanisms, siRNA, Gene delivery

Background

The direct modulation of gene expression is essential to establish therapeutic approaches in molecular medicine. Additionally to the development of therapies on the molecular level, the evaluation of target genes as therapeutic agents by combining the technology of RNAi and high throughput screenings is of major interest [1-3].

A major challenge in molecular medicine is the efficient, non-toxic and cell type independent transfection of cells in high throughput. In general a very effective manipulation strategy to achieve this is the transduction

of cells via viral vectors. However, despite of the high efficiency this method bears high biological risk as integrational mutagenesis [4]. Alternative existing non-viral transfection methods show specific advantages and disadvantages. Transfection with lipid based reagents is often applied in high throughput assays but this method is cell type dependent and occasionally inefficient, especially for primary- and stem cell transfection [5]. Due to the difficulties in transfection of these cells, the commonly employed manipulation methods are either electroporation or nucleofection [6,7]. Unfortunately, these methods affect cell viability which is crucial when handling sensitive cells. Consequently in this manipulation it is essential to achieve a balance between transfection efficiency and methodical toxicity. Electroporation and

* Correspondence: m.schomaker@lzh.de

¹Department of Biomedical Optics, Laser Zentrum Hannover, Hollerithallee 8, 30419 Hannover, Germany

Full list of author information is available at the end of the article

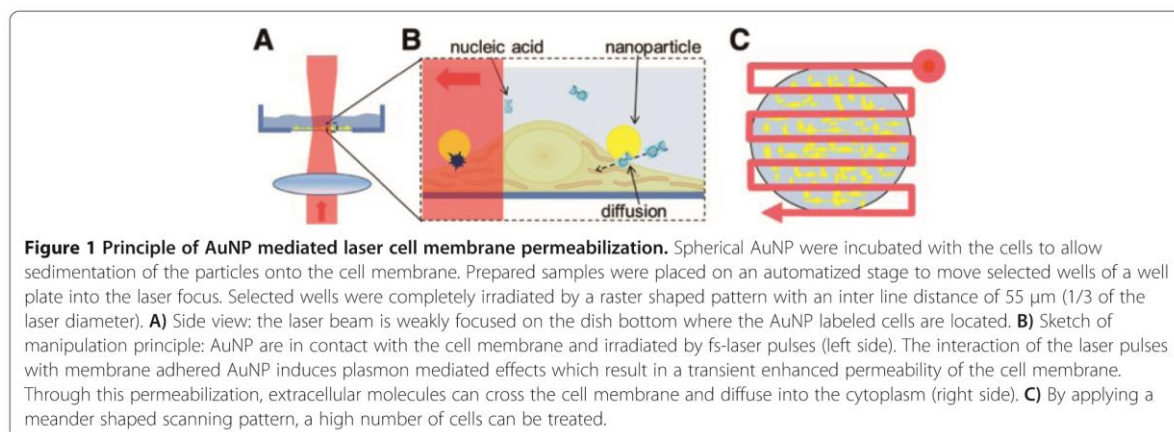
nucleofection can also be utilized for high throughput assays, but these physical techniques remain usually limited to well plates with low well numbers being additionally cost ineffective [8].

In order to address these challenges methodically, a variety of optical transfection techniques have been developed based on pulsed as well as continuously emitting lasers [9-13]. None of these techniques fulfills the requirements of an efficient and low-toxic transfection method combined with high throughput. Accordingly, there is no laser based technique currently established, that allows routinely laboratory or clinical use. A promising tool for molecular medical applications is the nanoparticle mediated laser transfection using a microchip laser emitting ps laser pulses with a resonant wavelength of 532 nm [14,15]. Herein, gold nanoparticle (AuNP) labeled cells are irradiated with a weakly focused laser beam. This method allows targeting many cells simultaneously, ensuring high throughput while maintaining a high spatial selectivity. Additionally, this physical method using resonant laser pulses is very promising for the manipulation of a variety of cell types.

By applying off-resonant fs laser pulses, the transfection of hematopoietic stem cells (CD34+) can be achieved [16]. Here, the excitation of the membrane adhered AuNP with the incident laser light leads to plasmon resonances which increase the absorption and scattering cross section of the AuNP by several orders of magnitude. When the AuNP is irradiated at a resonant wavelength, the laser energy is absorbed leading predominantly to thermal effects and changes in the particles morphology [15,17]. Using near infrared (NIR) femtosecond (fs) laser systems, off-resonant AuNP excitation can be achieved [18]. At this wavelength the absorption and therefore the thermal impact is reduced and the incident light is scattered into the near field of the particle. Due to this "nanolens" effect, an enhancement of the electric field in the near field takes place [19]. If the AuNP is adhered to the cell membrane, the field enhancement can initiate a spatially confined membrane

permeabilization [18]. In proof of principle experiments we could show the possibility to perforate the cell membrane using off resonant 800 nm fs laser pulses to deliver fluorescent labeled small interfering RNA (siRNA) and plasmid DNA (pDNA) into cells [20,21]. In another fs based study, a DNA-transfection rate of 23% using a melanoma cell line was stated and plasma induced nanocavitation is supposed as the membrane permeabilization effect [22]. The advantage of NIR wavelengths located in the "diagnostic window" regime of the electromagnetic spectrum results in higher penetration depths into biological tissue which might allow *in vivo* applications [23]. Furthermore, the low absorption cross section in the NIR reduces the risk of thermal induced AuNP fragmentation.

Within this work, microscopic analyses were performed to visualize the nanoparticle-cell membrane interaction, such that the co-incubation time for membrane permeabilization and the fundamental binding mechanism could be evaluated. To achieve an efficient uptake of extracellular molecules at high cell viabilities, a detailed parameter evaluation for a transient cell membrane permeabilization was performed. Different radiant exposures, scanning velocities of the laser spot, particle concentrations and particle sizes were applied to determine optimized permeabilization parameters. Additionally, the cell viability on a time scale up to 72 h after laser exposure and AuNP incubation was evaluated. The optimized parameters were used to evaluate the siRNA transfection efficiency, cell viability and functional oncogene knockdown in a cancer cell line. Due to the scanning method (Figure 1) and the automated setup, a high throughput is achieved and thus it is possible to handle all kinds of well plates within several minutes. Additionally to the manipulation experiments, the effects involved in the permeabilization process are investigated by temperature and near field simulations and a particle fragmentation study to further analyze the excitation of AuNP and the perforation mechanisms. The results indicate that both, near field and



heating effects contribute to the mechanism of nanoparticle mediated membrane permeabilization in the fs regime.

Results

Interaction of cells with gold nanoparticles

Time lapse multiphoton microscopy was employed to monitor the incubation process. As shown in Figure 2A, bright spots, identified as the luminescence of the AuNP, are visible at the cell membrane after 3 h of incubation. Images which were taken at shorter incubation times show no spots or marginal changes in the background brightness. Increasing the incubation time from 3 to 5 h resulted slightly brighter luminescence. Within 5 to 7 h of co-incubation, the number and brightness of the AuNP signal saturated. The AuNP luminescence was still visible after washing, indicating that the particles remained adhered to the cell membrane.

Scanning electron microscopy (SEM) and environmental scanning electron microscopy (ESEM) provided detailed information about the attachment and distribution of the AuNP at the cell membrane after co-incubation and several washing steps (Figure 2B, C). The results show a loose dispersion of AuNP after 1 h of incubation. The particles were located at the culture dish bottom and on the cell membrane. By increasing the incubation time to more than 3 hours, the particles started to aggregate at the cell membrane. After an incubation time of 5 h, no further increase could be observed. Depending on the location of the particles, some of the particles appeared brighter than others. At higher magnifications, as visible in Figure 2C, some particles were located on the cell membrane (solid ellipse Figure 2C) and some were started to be endocytosed (dashed ellipse Figure 2C), which is demonstrated by the cell membrane covered

particles. Based on this we defined an incubation time of 3 h for our gold nanoparticle mediated laser transfection. Within this time a sufficient number of particles adhere to the cell membrane to induce membrane permeabilization. The number of particles at the cell membrane was counted using ESEM images of ZMTH3 cells taken after 3 h of incubation. An incubation concentration of 11 $\mu\text{g}/\text{ml}$ was applied which represents the optimal concentration for cell manipulation. On average 164 ± 50 particles at the membrane of a single cell were counted.

Evaluation of efficient and gentle cell manipulation parameters

To evaluate the optimal process parameters for an efficient and gentle cell manipulation, the cells were treated with different parameters in the presence of 10 kDa FITC labeled dextran and the corresponding fluorescence level was determined. As an indicator for viability, the respective metabolic activities of the manipulated cells were measured after laser treatment using a fluorescence based assay (Qblue). An efficiency ratio of the used parameters was evaluated as the normalized ratio of FITC fluorescent level and viability. The purpose was to optimize the parameters for later transfection experiments and to get an overview of the influence of the different parameters. It was not intended to determine absolute transfection efficiencies.

The influence of the scanning velocity on the molecular uptake targeting ZMTH3 cells is shown in Figure 3A. At a fixed scanning velocity, AuNP size and AuNP concentration of 11 $\mu\text{g}/\text{ml}$, the FITC fluorescence level increased with increasing radiant exposure. The highest efficiency ratio was found at 80 mJ/cm^2 for a scanning velocity of 50 mm/s. With higher radiant exposures, the

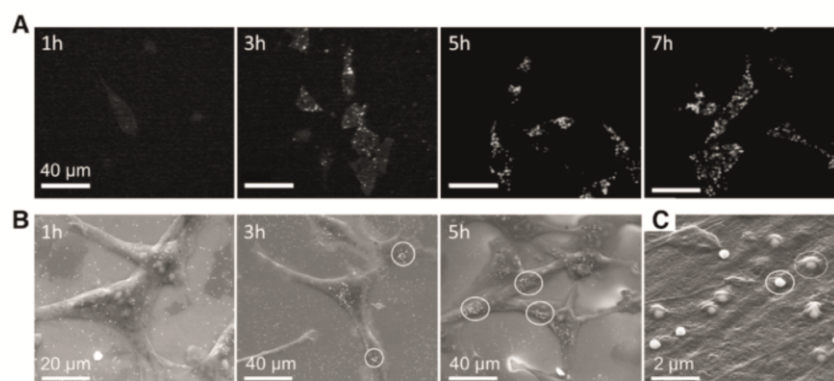
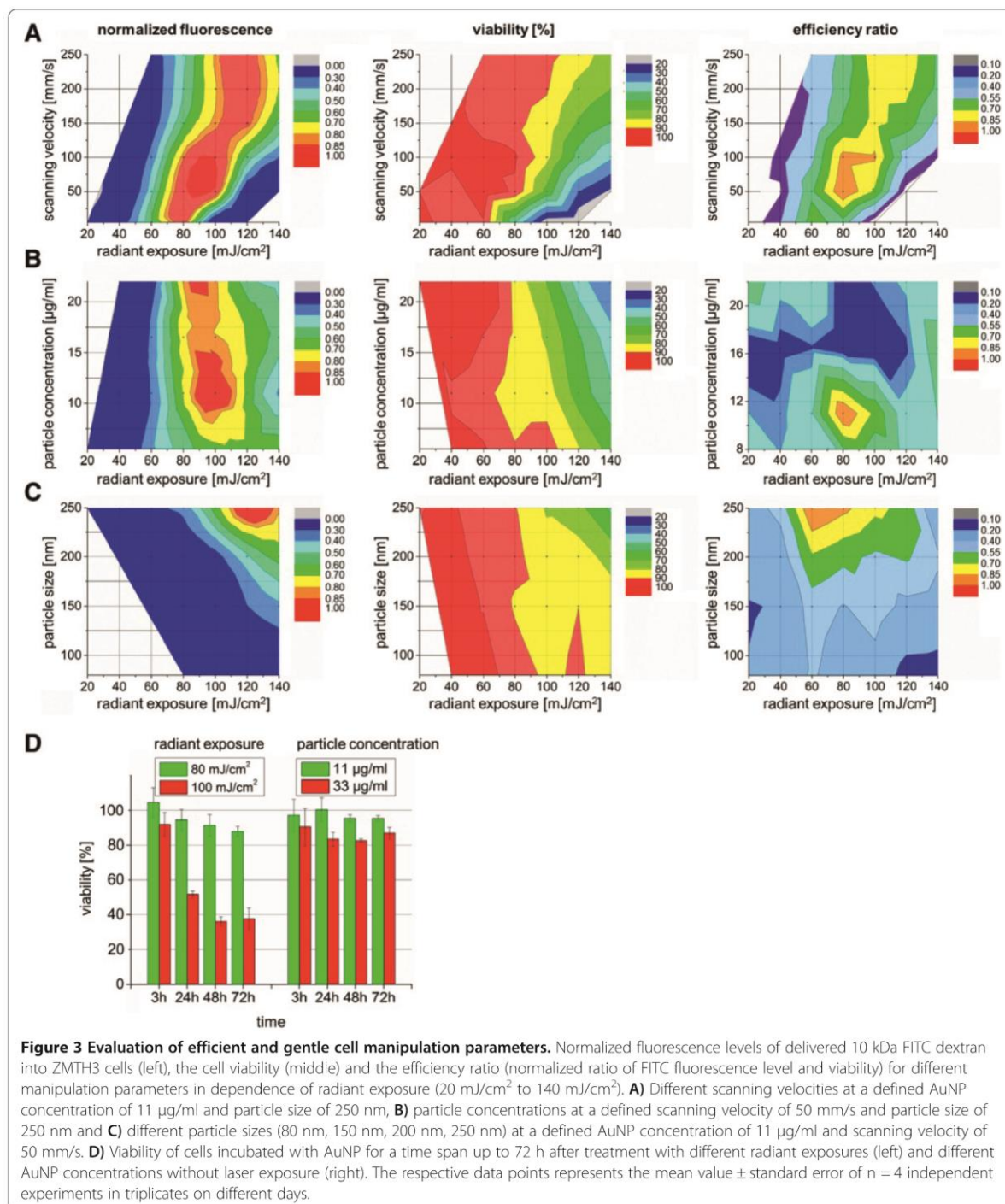


Figure 2 Nanoparticle - cell interaction. A) Time lapse multiphoton microscopy of granulosa cells with 150 nm particles after 1 h, 3 h, 5 h and 7 h of co-incubation. **B)** ESEM and **C)** SEM images of ZMTH3 cells after different incubation times with 200 nm gold particles. **B)** ESEM images: After 1 h a loose dispersion of particles is visible. After 3 h the AuNP started to aggregate (ellipse). The formation of particle clusters at the membrane can be observed after 5 h. **C)** SEM image in a higher magnification: After an incubation time of 3 h, particles are either on the cell membrane (solid ellipse) or covered by the membrane (dashed ellipse) [24].



efficiency ratio decreased due to a loss in cell viability as a consequence of an irreversible damage of the cell membrane and/or the ablation of the cells from the glass bottom. Varying the AuNP concentration (Figure 3B), the highest efficiency ratio was reached at a concentration of

11 µg/ml (6.3 µg/cm²) and a radiant exposure of 80 mJ/cm². When exceeding the threshold of 11 µg/ml the efficiency ratio dropped most likely due to many induced pores which consequently results in irreversible cell damage.

A further parameter impacting the efficiency ratio is the particle size (Figure 3C). A higher efficiency ratio was reached with an increase of particle size. Up to a particle size of 150 nm no efficient permeabilization occurred. Using larger particle sizes, the efficiency ratio peaked at a radiant exposure of 60 mJ/cm² for 200 nm and 60–80 mJ/cm² for 250 nm particles before the efficiency ratio dropped due to laser induced cell damage.

Monitoring of the exposure effects on cell viability

The cell viability after performing permeabilization experiments at different radiant exposures and a fixed AuNP concentration of 11 µg/ml was followed up to 72 h. As presented in Figure 3D (left), the cell viability remained above 80% using radiant exposures up to 80 mJ/cm². For a higher radiant exposure of 100 mJ/cm² the cell viability strongly decreased to 40%.

The incubation of cells with AuNP at a concentration of 11 µg/ml for three hours without laser treatment did not show any pronounced effect on the viability for a time period of 72 h. Even the tripling of the AuNP incubation concentration to 33 µg/ml leads only to a slight decrease to 80–85% in cell viability. This negative effect on cell viability is likely to be caused by the residues of chloroauric acid used while particle manufacture.

Based on the presented results in Figure 3, the optimal parameter for an efficient cell permeabilization and tolerable cell loss is to a radiant exposure of 80 mJ/cm², a particle size of 250 nm and an AuNP concentration of 11 µg/ml.

Nanoparticle mediated laser transfection

The evaluated parameters allowing an efficient and gentle cell permeabilization were used for cell transfection experiments. In Figure 4A the cell density is visualized by Hoechst 33342 nuclei staining. The successful transfection of CT1258 and ZMTH3 cells with an Alexa Fluor 488 labeled siRNA was performed using the optimized parameter (Figure 4B). Neither in the negative control (with siRNA, no laser treatment (Figure 4C)) nor in the AuNP control (with siRNA and AuNP incubation (Figure 4D)) a fluorescent signal was detected. Within the laser control (with siRNA and laser treatment, no AuNP) a weak fluorescence in individual cells was detected (Figure 4E). For CT1258 cells, a transfection efficiency of 85% ± 9 was evaluated using fluorescence microscopy. Here the fraction of necrotic cells was 3%. Flow cytometry analysis of ZMTH3 cells revealed a transfection efficiency of 90% and a cell viability of 93.5%. A significant difference (* p ≤ 0.05) was found between the siRNA samples and the native cells. The percentage of apoptotic cells was 2.15% and 5% for necrotic cells (Figure 4F).

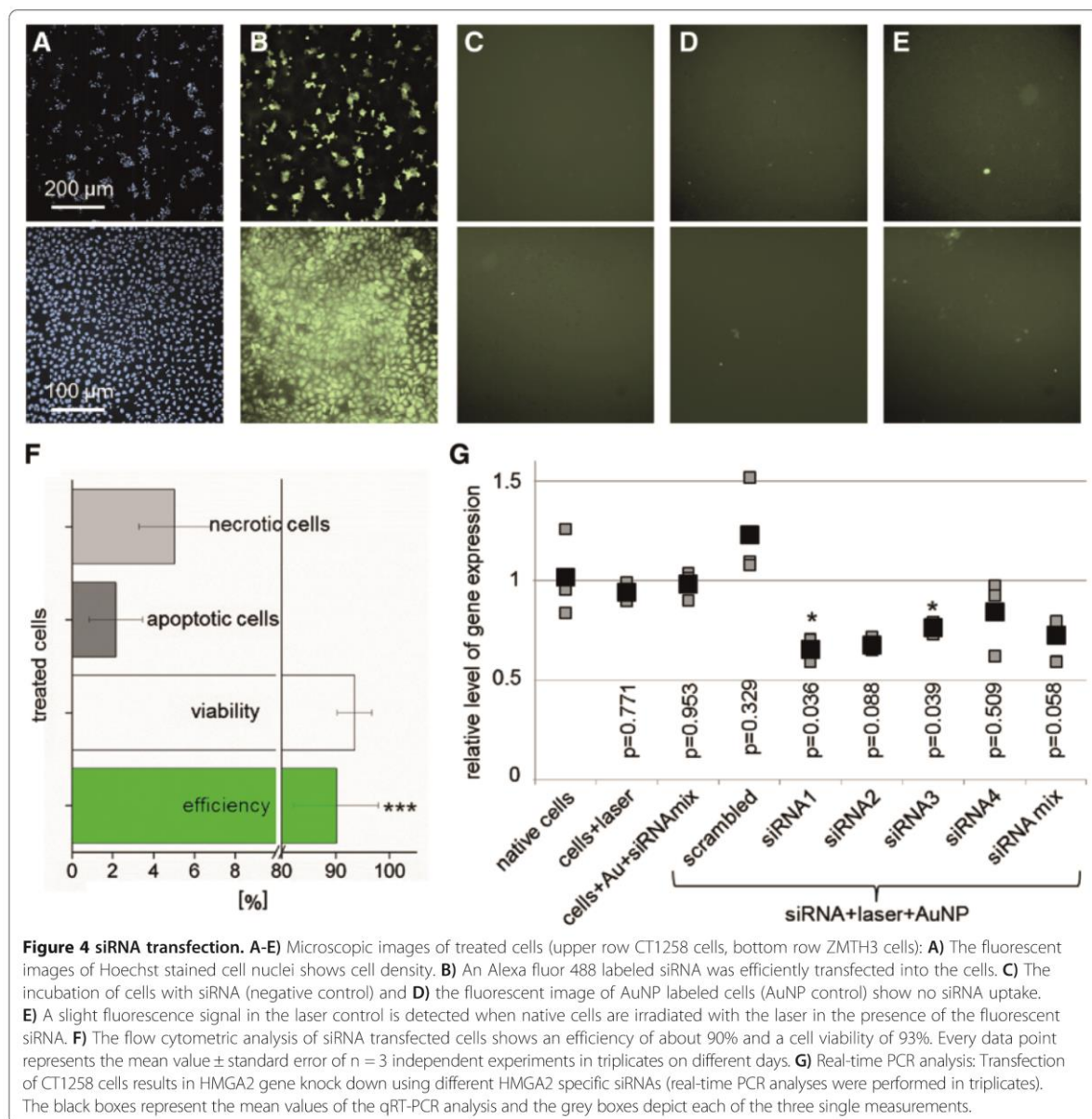
In order to evaluate a potential gene therapeutic approach, functional siRNAs were used in a proof of principle experiment using high cell numbers. For HMGA2 (high mobility group AT-hook 2) gene knock down experiments the canine HMGA2 overexpressing cell line CT1258 [25] was transfected with four different anti-HMGA2 siRNAs complementary to the 3'-untranslated region of the HMGA2 mRNA and one non-sense scrambled siRNA. Due to the lack of reliable evaluated canine antibodies against the protein and thus potential unspecific cross reactions we opted for quantitative real-time PCR as detection method. This technique allows to measure the canine HMGA2 mRNA expression quantitatively.

The relative HMGA2 mRNA expression was analyzed 48 h after treatment via one step quantitative real time PCR (qRT-PCR) analysis (Figure 4G). The HMGA2 expression was quantified relative to the housekeeping gene *Beta-actin* (*ACTB*), the non-treated cells were used for calibration (reference value = 1). In all samples treated with HMGA2 specific siRNAs in combination with the laser manipulation suppression of HMGA2 could be observed. The highest suppression was induced by using the siRNA 1 and 2. For the siRNA 1 and 3, the gene knock down was significant compared to native cells (p-values < 0.05). In the control samples, no HMGA2 gene knock down could be observed. A slight increase was found for the scrambled siRNA, potentially resulting from off-target effects. No significant difference between the control samples and native cells was observed.

Characterization of the nanoparticle mediated membrane permeabilization mechanism

In this section we describe different experiments to address the mechanisms involved in membrane permeabilization focusing on the parameters allowing an efficient and gentle cell manipulation.

Simulations of the near field distribution of the electric field at an incident wavelength of 796 nm for 80 nm and 250 nm particles are shown in Figure 5A and B, mapping the field-enhancement at the particles. For larger particles the dipole emission is distorted due to multipole oscillations within the sphere [17]. The enhancement factors of the different AuNP sizes are presented in Figure 5C (left y axis). For the used particles the highest field enhancement is reached for 150 nm particles. Here the near field is about 10 times higher than the incident field. For the 200 nm and 250 nm particles, the average enhancement is at 6.6 and 4.9, respectively. Furthermore, the near field volume is increasing with an increasing particle size (Table 1) and thereby the interaction zone of the near field with the membrane. This could be a reason for the increasing permeabilization efficiency at larger particle sizes shown in Figure 3C.

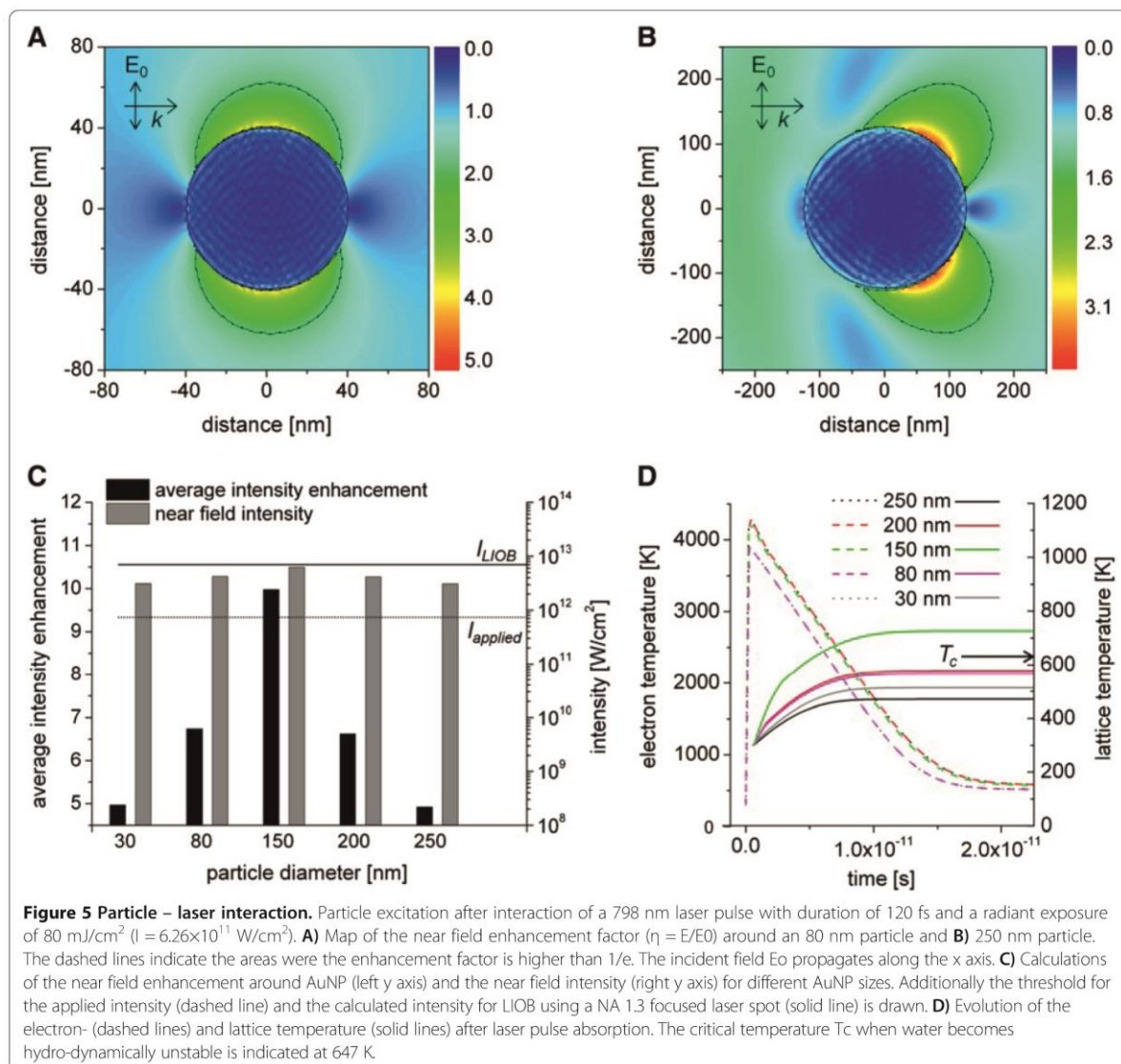


The evaluated enhancement factors and the applied intensity were used to calculate the near field intensity (Figure 5C (right y axis)). The values of the near field intensities of all particle sizes are below the threshold of an optical breakdown (LIOB) in water, which is 6×10^{12} W/cm² for the used wavelength and pulse duration [26]. The highest near field intensity is reached for 150 nm particles which is close to the LIOB threshold. Intensities below the LIOB threshold in the low density plasma regime can lead to nonlinear effects like multiphoton ionization and avalanche-ionization. This might lead to the permeabilization of the cell membrane [14,22,27].

The accumulation of single pulses can induce the dissociation of biological molecules by forming reactive oxygen species (ROS) which results in membrane permeabilization [27]. Here, the threshold pulse energy E_N depends on the number of pulses (Equation (1)) [14,27].

$$E_N = E_1 \cdot N^{-1/k} \tag{1}$$

Where E_1 describes the threshold energy of a single pulse, N is the number of pulses and k the accumulation strength [28].



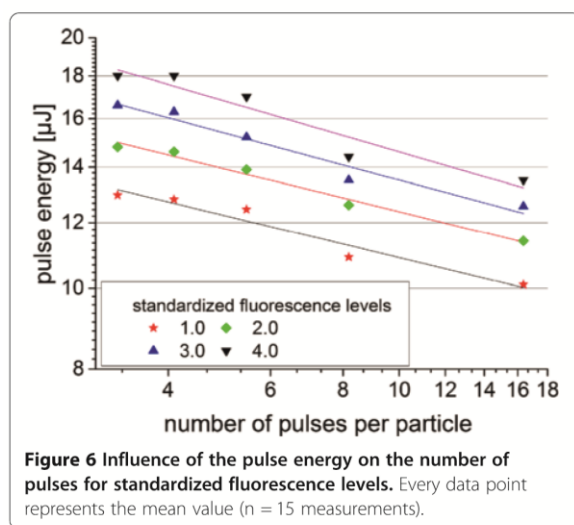
The dependence of the pulse energy on the number of pulses for standardized fluorescence levels (“fluorescence brightness”) is shown in Figure 6. A given fluorescence level corresponds to a specific amount of fluorescence molecules in the cells per well. We analyzed the number

of laser pulses and pulse energy to yield four different fluorescence levels.

With an increasing number of pulses, less pulse energy is needed for an efficient permeabilization. An average accumulation strength of $k = 5.57 \pm 0.02$ was evaluated

Table 1 Near field and temperature related values for AuNP irradiated with 796 nm and 6.26 W/cm²

	30 nm	80 nm	150 nm	200 nm	250 nm
Near field volume [nm ³] (I_{max}/e^2)	7×10^3	1.2×10^5	7.1×10^5	1.6×10^6	2.8×10^6
Average near field intensity [W/cm ²]	3.8×10^{12}	2.5×10^{12}	1.7×10^{12}	2.5×10^{12}	3.3×10^{12}
Absorption efficiency Q_{abs}	0.025	0.05	0.145	0.125	0.08
Particle temperature [K]	541	561	726	578	471



by a power-law fit (Table 2). This indicates that 5 photons with a photon energy of 1.55 eV at the applied wavelength of 796 nm are absorbed simultaneously to reach the ionization threshold of 6.6 eV for water [26].

When laser radiation is absorbed by the electrons of the AuNP the energy is transferred from the electrons to the particle lattice due to electron phonon coupling within a time span of a few ps and the particle temperature increases [29,30]. The temperature of the electrons and the lattice can be calculated with a two-temperature model (Figure 5D) [31]. The lattice temperature reaches the highest temperature of 726 K for 150 nm particles. This temperature is above the critical temperature (T_c) for phase transformation in water. For all other particles sizes this critical temperature is not reached. This reflects the different values for absorption efficiencies Q_{abs} listed in Table 1.

The influence of the laser irradiation and possible changes in the particle morphology due to melting or fragmentation were analyzed by absorbance spectra of irradiated and non-irradiated particles (Figure 7A). After irradiation of 250 nm particles with radiant exposures of 60 mJ/cm² and 100 mJ/cm² a blue shift of the peak of 0.5 nm and 1.75 nm, occurred respectively (Table 3). These shifts were in the SEM range of the untreated control. A reason for small changes can be polishing

Table 2 Power-law fit

	Threshold energy E_1 [μ J]	k	R^2
1.0	16.06 \pm 0.7	5.88 \pm 0.02	0.93
2.0	18.36 \pm 0.7	5.88 \pm 0.01	0.98
3.0	20.79 \pm 0.7	5.55 \pm 0.02	0.94
4.0	23.27 \pm 0.7	5.00 \pm 0.03	0.90

Dependence of the pulse energy on the number of pulses for standardized permeabilization efficiencies.

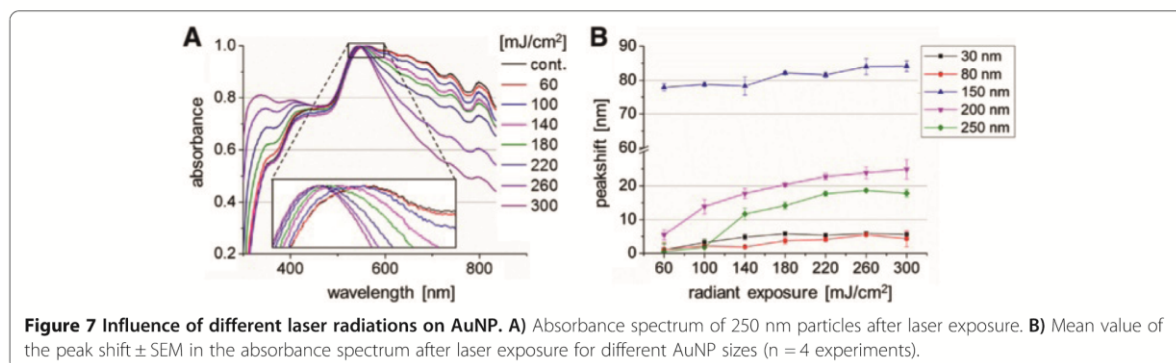
effects due to surface melting of the particle, which occurs below the melting point of bulk gold [17]. At radiant exposures of 140 mJ/cm² and higher values the spectrum were broadly blue shifted (Table 3) and a narrowing of the spectrum occurred (Figure 7A). The spectrum of a 250 nm particle exposed to a radiant exposure of 300 mJ/cm² is broadly similar to the spectrum of 80 nm particles [32]. This clearly indicates a change in particle size due to laser exposure which can be induced by particle evaporation or near field ablation [17].

The value of the peak shift for different particle sizes after laser radiation in dependence of the radiant exposure is shown in Figure 7B. The highest peak shift of 80 nm was measured for 150 nm particles and barley changes with increasing radiant exposures. Relating to the AuNP size of 250 nm used for transfection a peak shift occurred at radiant exposures \geq 140 mJ/cm². Furthermore, the amount of the peak shift for all radiant exposures is lower than for 150 nm particles which correlate with the calculated temperatures and near field enhancement in Figure 5.

Discussion

In our study, we characterized the underlying mechanism and the potential of nanoparticle mediated cell membrane perforation in combination with fs-laser pulses as an alternative optical transfection method. Therefore the influencing parameters on the achieved perforation rate and cell viability were systematically determined and the successful transfection of cells with a fluorescent siRNA as well as the knock down of the oncogene *HMG2* in tumor cells with specific siRNAs was demonstrated. Furthermore, the passive binding of AuNP to the cell membrane was studied.

Multiphoton and scanning electron microscopy images show the localization of AuNP near the cell membrane. Depending on the incubation time of the AuNP, single particles or clusters are located near, or associated with, the membrane. After an incubation time of 3 h the AuNP are clearly visible near the cell membrane. Within this time the particles form clusters with enhanced scattering of the laser light proved by multiphoton microscopy [33]. The agglomeration of particles after 3 hours is also visible in the ESEM images. This is in agreement with findings from Chithrani et al. who determined the uptake half-life at 2.24 h for 74 nm AuNP [33]. Furthermore, they evaluated the uptake of the number of particles per cell and also showed that the number of particles per cell saturated after 5 h. In the present study a particle number of approx. 160 was estimated at the membrane of a single cell for an incubation concentration of 11 μ g/ml. Baumgart et al. [22] counted per cell 90 ± 23 AuNP with a diameter of 100 nm at an incubation concentration of 8 μ g/ml after an incubation time



of 6 h using SEM images. Taking into account that in this work a higher particle concentration and a larger diameter was used (and therefore a faster sedimentation of the particles takes place) the results are in a very good agreement.

In addition, Chithrani et al. evaluated the number of AuNP per vesicle and found an average number of 3 AuNP per vesicle for 100 nm particles. In comparison to our SEM images (see Figure 2B) we assume that one 200 nm particle per vesicle get endocytosed by the cell. As bare AuNP are used, a serum protein corona is formed at the particles surface and no specific binding at the cell membrane is likely to occur. Therefore, we suggested the receptor-mediated endocytosis (RME) to be the acting uptake mechanism [34].

The initial mechanism of plasmon mediated cell membrane permeabilization is still a current matter in research. Depending on the parameters, different mechanisms and effects are assumed. These are thermal (“nanoheater effect”) [19,35], or near field enhancement effects (“nanolens effect”) [18,35]. In addition, the generation of a low density plasma induced by multiphoton ionization combined with thermal effects can possibly lead to membrane permeabilization [14,15]. For short laser pulses in the nanosecond-picosecond regime, where the energy is mainly absorbed by the particle, thermal effects could be the main mechanism for membrane permeabilization [36-38]. After AuNP heating, the water evaporates followed by a shockwave and forming a cavitation bubble around the exposed particles as reported by Pitsillides et al. and Zharov et al. and enabling membrane perforation [39,40]. Using fs laser pulses, nanocavitation bubbles can be formed by the induced field enhancement. This enhancement can lead to an optical breakdown near the

particle and to the generation of a shockwave [18,36]. In this work, the evaluated intensities at the surface of single AuNP are near the threshold for an optical breakdown in the low density plasma regime. In existing studies, different concentrations of AuNP were required to achieve cell membrane perforation [15]. Higher numbers of particles are necessary to manipulate the cells with fs laser pulses [22,41]. Due to the formation of AuNP clusters the near field is further enhanced in comparison to single particles. The neighboring particles interact via the scattered waves and due to plasmon coupling “hot spots” are formed [42,43]. Taking into account that the field enhancement is higher for AuNP clusters compared to single particles, the intensities could be above the optical breakdown threshold [42].

Our assumption herein, that clusters of AuNP at the cell membrane are necessary to induce a field enhancement by fs laser pulses which is high enough to perforate the cell membrane. This is supported by the presented microscopic images and the number of AuNP utilized in this and other studies using fs laser pulses for membrane perforation [22,41]. Within the performed experiments we showed the efficient and transient permeabilization of the cell membrane due to an expected enhancement of the near field at the AuNP clusters. Based on this and the evaluated simultaneous absorption of 5 photons in the pulse number dependent experiments (Figure 6) we understand the near field enhancement followed by the multiphoton ionization of the surrounding medium as the initial perforation mechanism.

The fs laser pulses are enhanced in the near-field of the particle for membrane permeabilization by surface plasmon resonances. NIR fs laser pulses benefit from a

Table 3 Mean values \pm SEM for the peak shift in the absorbance spectrum

Radiant exposure [mJ/cm ²]	0	60	100	140	180	220	260	300
Shift [nm]	0	0.5	1.75	11.68	14.18	17.68	18.62	17.81
SEM [nm]	± 2.98	± 2.68	± 2.21	± 1.71	± 1.01	± 0.66	± 0.13	± 1.06

Irradiation of 250 nm particles with different radiant exposures (n = 4 experiments).

low thermal impact and a high penetration depth into tissue which is important for *in vivo* experiments. Furthermore, laser irradiation mediated fragmentation of nanoparticles is especially for *in vivo* settings an important issue. Fragmentation in small nanoparticles under 5 nm can lead to toxicity by intercalation into the DNA [44]. The comparison of fs pulses and ns pulses reveal a more pronounced change in particle morphology for longer (850 ps, 532 nm) pulses. In absorbance measurements, no pronounced peak shift (as indicator for particle morphology and size change) was detected for a fluence of 100 mJ/cm², which exceeds the optimal fluence for cell manipulation (80 mJ/cm²) using NIR fs pulses (Table 3). In comparison to this, for 850 ps (≈ 1 ns) pulses a peak shift of 15.4 nm was determined using the optimal manipulation fluence of 20 mJ/cm². The change in particle morphology was caused due to thermal effects and the strong linear absorption at 532 nm. Nevertheless, the cell viability stayed above 80% in all the performed experiments suggesting the use of visible ns pulses for *in vitro* experiments [15]. For fs pulses, the cell viability was determined to be above 90%. The presented results and the advantages of NIR fs laser pulses (e.g. a high penetration depth and the avoidance of photo thermal effects) indicate the great potential of fs laser for *in vivo* manipulation. Furthermore the development of endoscopic systems for ultrafast laser microsurgery [45] or fiber based approaches [46] makes the application of ultrashort laser pulses potentially suitable for fs laser *in vivo* cell manipulation. Additionally, first *in vivo* experiments showed the generation of nanobubbles around AuNP clusters for selective cancer cell killing using short, 780 nm laser pulses [47]. Next to the properties of the fs laser pulses, an advantage of the presented method is the double selectivity by the spatial confined radiation (Figure 8A) and the possibility of specific cell targeting by antibody conjugated AuNPs. The latter can be used to induce selective cell manipulation or ablation in both, *in vitro* and *in vivo* models. For example, the treatment of squamous carcinoma cells in the buccal mucosa or at the tongue. Further in tumor scenarios where minimal invasive tissue ablation is essential as malignant glioblastoma, it is crucial to sustain non-target (healthy) tissue. Here the presented method can be a powerful tool. Exemplarily for primary cell manipulation a membrane impermeable fluorescent dye was delivered into a human embryonic stem cell (ES) cell line hES3 and a human induced pluripotent stem cell (iPSC) line hCBiPS2 (Figure 8B).” The results of the siRNA experiments show that fs nanoparticle mediated laser transfection is suitable for high throughput functional gene assays due to the short processing time of approximately 10 min per 96 well plate. As the applied AuNP were shown to be non-toxic, this method is excellent

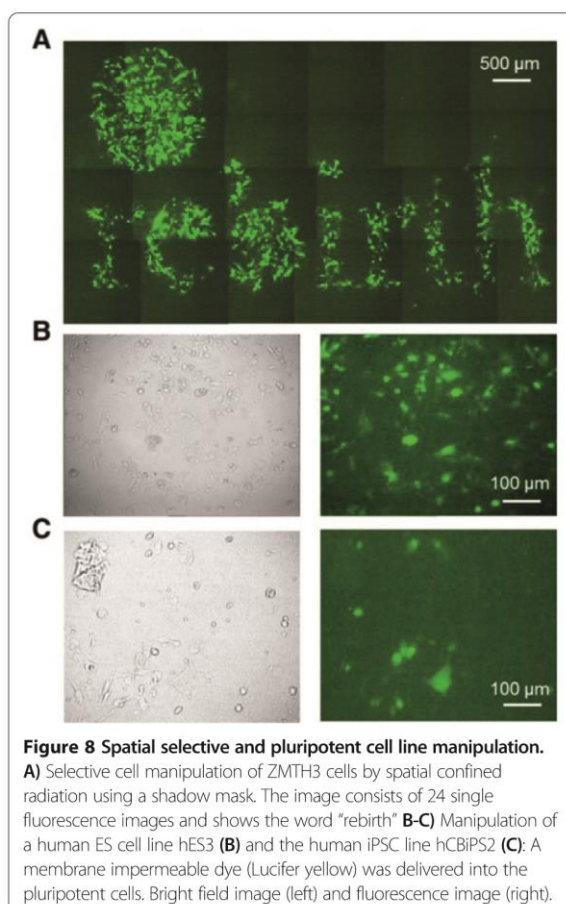


Figure 8 Spatial selective and pluripotent cell line manipulation. **A)** Selective cell manipulation of ZMTH3 cells by spatial confined radiation using a shadow mask. The image consists of 24 single fluorescence images and shows the word "rebirth" **B-C)** Manipulation of a human ES cell line hES3 (**B**) and the human iPSC line hCBiPS2 (**C**): A membrane impermeable dye (Lucifer yellow) was delivered into the pluripotent cells. Bright field image (left) and fluorescence image (right).

suitable for *in vitro* application but also for other applications in molecular medicine. Furthermore, it can be applied for the manipulation of various cell types as shown in our previous work and by Baumgart et al. [16,22]. Additional applications as gene or cell therapeutic approaches can be served by this technique. As an example, it is possible to manipulate high cell numbers required for e.g. tumor vaccination strategies in an appropriate time. The knock down of the oncogene HMGA2 in canine prostate carcinoma cells was carried out successfully as shown by real time PCR expression analyses (Figure 4G). Due to the extraordinary high HMGA2 expression in the CT1258 cell line a incomplete siRNA mediated HMGA2 knock down within the treated cells was to be expected. Conventional HMBA2 knock down in less aggressive human pancreatic cell lines by Watanabe et al. [48] resulted in higher efficiencies. However, we opted to target the canine prostate cancer derived cell line CT1258 as canine prostate cancer represents the only spontaneously arising model for human prostate cancer with considerable incidence. This includes several tumor relevant aspects as biological

behavior, marker gene expression and histological presentation [49]. Thus, a successful establishment of a therapeutic approach in dogs will offers high transfer potential to a human clinical setting. Consequently, prior to human clinical trials, a valid clinical trial in dogs as naturally occurring model is of major interest allowing to monitor the therapeutic intervention in an genetic outbreed model with unmanipulated immune system.

Conclusion

Our studies on nanoparticle mediated fs laser cell perforation show, that this method is suitable for high throughput siRNA transfection with high efficiency and low cell toxicity. To establish this method as an alternative transfection technique, the manipulation of different cell types will be continued in further studies. However, due to the underlying physical mechanism the permeabilization should be cell type independent. Based on the mechanistic investigations, we assume that an enhancement of the near field occurs at AuNP clusters. This leads to the generation of a low density plasma with multiphoton ionization of the surrounding liquid, which in turn perforates the cell membrane. The uptake mechanism of extracellular molecules remains to be investigated in further experiments [50]. The presented method is an alternative transfection method to deliver molecules into living cells being particularly well suited for standardized processes like high throughput or high content screening assays for fundamental and pharmaceutical research.

Methods

Cell culture

The canine pleomorphic mammary adenoma cell line ZMTH3 [51] was cultured routinely in RPMI 1640 supplemented with 10% fetal calf serum (FCS) and 1% penicillin/streptomycin (Biochrom AG, Berlin, Germany). Rat granulosa cells (GFSHR-17) were cultivated in DMEM (Dulbecco's Modified Eagle Medium) supplemented with 5% FCS, 1% penicillin/streptomycin (Biochrom AG, Berlin, Germany). The canine prostate adenocarcinoma cell line CT1258 was derived from an extremely aggressive canine prostate carcinoma [52] and cultured in Medium 199 (Life Technologies GmbH, Darmstadt, Germany) supplemented with 10% FCS and 2% penicillin/streptomycin (Biochrom AG, Berlin, Germany). The human ES cell line hES3 and the human iPSC line hCBiPS2 [53] were cultured and expanded on irradiated mouse embryonic fibroblasts (MEF) in knockout DMEM supplemented with 20% knockout serum replacement, 1mM L-glutamine, 0.1mM β -mercaptoethanol, 1% nonessential amino acid stock (all from Life Technologies) and 10ng/ml bFGF (supplied by the Institute for Technical Chemistry, Leibniz University Hannover). One day before laser transfection cells were

detached from the feeder layer by 0.2% collagenase IV (Life Technologies) followed by an incubation step with TrypLE (Life Technologies) for single-cell dissociation and plated onto Matrigel™ (BD Biosciences) coated dishes in MEF-conditioned medium.

Laser setup

The used automated setup for cell manipulation is operating with a fs amplifier laser system (Spitfire Pro, Newport Corporation, Irvine, USA). The generated laser pulses have a pulse duration of 120 fs at a fixed wavelength of 796 nm. The output power of the system is 2.1 W at a repetition rate of 5 kHz. To irradiate the biological tissue, the laser pulses were guided through an automatized attenuator consisting of a $\lambda/2$ -plate and a polarizing beam splitter and reflected by two scanning mirrors (Littrack, JMLaser, Müller Elektronik, Spaiching, Germany). A convex lens with a focal length of 800 mm was used to focus the laser pulses onto the sample, located on the automatized stage (OptiScan, Prior, Jena, Germany), resulting in a spot diameter of 164 μ m.

Nanoparticle incubation

Prior to the laser cell manipulation experiments and to investigate the interaction of AuNP with the cell membrane, the cells were co-incubated with the AuNP at 37°C in a 5% CO₂ atmosphere. The AuNP were chemically manufactured in presence of chloroauric acid (PGO, Kisker Biotech, Steinfurt, Germany). Uncoated AuNP of 80 nm, 150 nm, 200 nm, 250 nm were used.

Multiphoton microscopy

Images were obtained to evaluate the incubation time for AuNP mediated cell permeabilization and the possibility of a passive binding of the particles. Briefly, granulosa cells were incubated with 150 nm gold particles and imaged after different incubation times. After a PBS wash, the cells were observed with a custom built multiphoton microscope which is based on a fs-laser system tunable from $\lambda = 690$ nm to 1040 nm (Chameleon ultra II, Coherent, Göttingen, Germany) [27]. The images were recorded through a 100 \times oil immersion objective (Carl Zeiss AG, "Plan-Neofluar", NA = 1.3) at an excitation wavelength of $\lambda_{exc} = 700$ nm.

Scanning electron microscopy (SEM) and environmental scanning electron microscopy (ESEM)

To investigate the interaction of cells and AuNP images of ZMTH3 cells were generated after different times of co-incubation with 200 nm particles. The cells were washed after co-incubation with AuNP and fixed by adding a 4% paraformaldehyde (PFA) solution with 0.2% glutaraldehyde at 4°C. For ESEM imaging the cells were washed after 20 min with distilled water. For SEM, the cells were further treated at room temperature for 20

min with a 2% osmium tetroxide solution. Subsequently, the cells were washed 3 times with water for 5 min before incubation with different ethanol concentrations for 10 min each (30%, 50%, 70%, 90%, 95%, 95% and 3 × 100%). Before sputtering the cells with a 5 nm gold layer, the cells were dried for 30 min under laminar air flow conditions. For counting AuNP at the cell membrane after incubation, ImageJ was used [54]. Values represent the mean of $n = 6$ images \pm SEM.

Plate reader measurements

To evaluate the optimal parameters of an efficient and gentle transfection, 2.5×10^4 canine ZMTH3 cells per well were seeded in a black wall/clear bottom 96 well plate (BD Bioscience, Heidelberg, Germany) 24 h before laser treatment. As an indicator of membrane permeabilization, fresh medium with 2 mg/ml of 10 kDa FITC-dextran (Sigma-Aldrich, Steinheim, Germany) was added to the cells. After laser treatment, the cells were incubated for 30 min followed by several washing steps until the background fluorescence from the permeabilization indicator (10 kDa FITC dextran) was eliminated. To measure the metabolic activity of the cells, 10% (v/v) of the resazurin based, fluorometric QBlue viability assay kit (BioCat GmbH, Heidelberg, Germany) was added to the medium. During an incubation time of 1 h, viable cells converted resazurin into the fluorescent form resorufin. The fluorescence levels of the delivered FITC dextran (EX488/EM520 nm) for molecular delivery and the resorufin (EX570/EM600 nm) as an indicator for viability were measured by the Infinite 200 Pro plate reader (Tecan, Männedorf, Switzerland). The value for FITC dextran delivery was calculated by subtracting the fluorescent background from each sample and afterwards the highest FITC fluorescence level was normalized to 1. The cell viability (V) was determined by the QBlue fluorescence level of the sample (F_S), the fluorescence of the untreated control (F_C) and the background (F_B) (Equation(2)).

$$V = \frac{F_S - F_B}{F_C - F_B} \cdot 100 \quad (2)$$

The efficiency ratio (E) was calculated by correlating the fluorescence level for molecular delivery (F_{FITC}) and viability (V) using equation (3). Afterwards the values were normalized to 1.

$$E = F_{FITC} \cdot V \quad (3)$$

Simulation of the particle temperature and near field

For a deeper insight into the mechanisms involved in membrane permeabilization using fs laser pulses, the particle temperature and the near field were analyzed. The temperature of the AuNP during fs irradiation was

calculated based on a two temperature model, employing data for the specific heat capacity of the electrons and the electron phonon coupling constant from Lin et al. [55]. Temperature loss due to interaction with the surrounding medium was not considered due to the short timescales used. The field strength and intensity as well as the near field volume were simulated by the discrete dipole approximation, using the software DDSCAT [56,57]. A dipole separation of less than 3.5 nm was used for the largest sphere with a diameter of 250 nm. Modeling of the optical breakdown intensities in the near field was performed according to the Keldysh theory following the approach used by Vogel et al. [26,58]. The maximum intensity divided by the square of e was considered as near field volume and the enhancement in the modeling of the optical breakdown as well as the near field volume were averaged in the according area.

UV-Vis spectroscopy

Particle spectra were monitored to evaluate a possible peakshift (as an indicator for a change in particle size/shape) of laser irradiated particles compare to untreated particles. Therefore an UV/Vis spectroscope (UV 1650-PC, Shimadzu, Duisburg, Germany) was used. The particles were diluted in culture media (RPMI as described before) without phenol red at a concentration of 50 μ g/ml. Using a 96 well plate, the samples with a total volume of 200 μ l per well were irradiated in a meander pattern.

Fluorescence microscopy

In order to evaluate the transfection efficiency of the CT1258 cells, fluorescence microscopy was applied. 24 h before laser treatment, 1×10^4 cells were seeded in each well of a 24 well plate (PAA Laboratories, Cölbe, Germany). For siRNA transfection, 10 μ M of a fluorescently labeled (AlexaFluor488) siRNA (Qiagen, Hilden, Germany) was added to the extracellular medium before laser treatment. The samples were treated with the optimized parameters as evaluated within the plate reader measurements. After laser treatment, the cells were incubated for 30 min followed by several washing steps until the background fluorescence from the fluorescent siRNA was eliminated. Three independent experiments in duplicates were performed on different days. Three images of each well were analyzed using Image J. By counting the cell nuclei (ca. 546 per image, stained with HOECHST33342) and transfected cells (Alexafluor488 siRNA positive cells) the transfection efficiency was determined. Propidium Iodide was used as an indicator for necrotic cells.

Flow cytometry analysis

Flow cytometric analysis was performed to evaluate the transfection efficiencies and the necrotic- and apoptotic rate. 24 h before laser treatment, 1.5×10^5 cells were

seeded in each well of a 24 well plate. For siRNA transfection, 10 μ M of a fluorescently labeled (AlexaFluor488) siRNA was added to the extracellular medium before laser treatment. The samples were treated with optimized parameters as evaluated within the plate reader measurements. Three hours after laser treatment the samples were prepared for flow cytometric analysis. Therefore, the cells were washed and trypsinized (TrypLE™, Life Technologies (LT), Darmstadt, Germany). A viability staining with Annexin V (V-PE-Cy5 Apoptosis Detection Kit, BioCat, Heidelberg, Germany) to detect the apoptotic cells, and with 1.5 μ M Propidium Iodide (Invitrogen, Darmstadt, Germany) to identify necrotic cells, was performed. The positivity of siRNA transfected cells was determined by comparing the AlexaFluor488 fluorescence intensity to native cells, both measured in the FL1-H channel using a FACSCalibur flow cytometer (BD Bioscience, Heidelberg, Germany). Within the native cell population, a gate was set determining 98% of the native cells as non-transfected using the software Cell Quest (BD Bioscience, Heidelberg, Germany). This gate was subsequently applied on the siRNA transfected cell population resulting in the percentage of positive and non-transfected cells. To determine the ratio of apoptotic and necrotic cells within the siRNA transfected samples, the Annexin V and PI labelled cells were analyzed for PE-Cy5 fluorescence in the FL4-H channel and for PI in the FL2-H channel. Within the native cells a gate was set at which a cell population of 2% was identified as Annexin and PI positive and transferred to the sample with siRNA transfected cells to discriminate living from apoptotic and necrotic cells. For statistical analyses, the student's t-test was used. The significance is given as * for $p < 0.05$, ** for $p < 0.01$ and *** for $p < 0.001$.

HMGA2 suppression analysis

As a proof of principle, that the presented method is suitable for molecular medicine approaches a functional gene knock down experiment was performed. We used the tumor cell line CT1258 which is characterized by over-expression of endogenous HMGA2 [25]. 24 h prior to transfection 3×10^5 cells were seeded per well into a 6 well plate (Greiner Bio-One GmbH, Frickenhausen, Germany). Cells were laser-transfected with 10 nM of different anti-HMGA2 siRNAs, a scrambled siRNA and a siRNA mix consisting of 10 nM of each of the four anti-HMGA2 siRNAs (Ribox, Radebeul, Germany). The corresponding siRNA sequences are listed in Table 4. After a time span of 48 h the growth medium was removed from the CT1258 cells and 1 ml Tryp LE Express (Life Technologies GmbH, Darmstadt, Germany) was applied on cells. Once the cells were detached 1 ml cultivation medium was added to stop the reaction. Cell suspension was pelleted at $300 \times g$ for 5 min. The supernatant was discarded and the pellet stored at -80°C until further processing.

Table 4 Name and sequence of the used siRNAs for HMGA2 knock down

siRNA name	sequence
A2-3UTR 1	5'-UUAAUUCUCUCCGUAGCUCCCC-3'
A2-3UTR 2	5'-UCUUACUGUCCAUUGGCCCCC-3'
A2-3UTR 3	5'-AUUAUCCUUAAGAACCUAGCCCC-3'
A2-3UTR 4	5'-UUCUUACUGUCCAUUGGCCCCC-3'
scrambled siRNA	5'-UAAGCACGAAGCUAGAGUCCCC-3'

RNA extraction

For PCR analysis total RNA was isolated according to the "NucleoSpin miRNA" protocol (Macherey & Nagel, Düren, Germany). Small and large RNAs were finally eluted in 30 μ l nuclease free water. Total RNA concentration was measured with the Synergy 2 reader (BioTek Instruments GmbH, Bad Friedrichshall, Germany).

Quantitative one step real-time PCR analysis

For the relative *HMGA2* / *ACTB* quantification 25 ng total RNA were mixed with SYBR Green, *HMGA2* or *ACTB* specific primers, nuclease free water (Qiagen, Hilden, Germany) and reverse transcriptase according to the "QuantiTect SYBR Green RT-PCR" protocol (Qiagen, Hilden, Germany). The fluorescence of each sample was analyzed in triplicates. As negative controls a non-template and a no-reverse transcriptase control were included. The experiments were performed using the Mastercycler ep realplex (Eppendorf AG, Hamburg, Germany). qRT-PCR conditions were as follows: 30 min at 50°C and 15 s at 95°C , followed by 40 cycles with 15 s at 94°C , 30s at 60°C and 30 s at 72°C . Finally a melting curve analysis was performed to verify specificity and identity of the qRT-PCR products according to the Eppendorf Mastercycler ep realplex instrument instructions. For the comparison of the relative gene expression levels based on the $\Delta\Delta\text{CT}$ method the gene expression level of the untreated CT1258 cells was used as calibrator (calibrator expression level was set as 1). Statistical analysis of the qRT-PCR results was done by using the software tool REST 2009, version 2.0.13. A p-value of ≤ 0.05 was considered as statistically significant.

Competing interests

The authors declare that they have no competing interests.

Authors' contributions

MS: Conceived and designed the experiments, performed the laser perforation and transfection experiments. Performed multi photon imaging and laser-particle interaction experiments, manuscript drafting and wrote the paper. DH: Conceived and designed the experiments, performance of the SEM imaging experiments, participated in the perforation experiments. SK: Carried out the simulation for the particle temperature and near field enhancement. Wrote parts of the paper. SWi: Performed flow cytometry analysis and analyzed the data. Participated in drafting the transfection experiments, wrote parts of the paper. SWa: Performance of PCR analysis and data processing. IN: Contributed reagents/materials/analysis tools and participation at biological study design. TR: Manuscript drafting, Contributed reagents/materials/analysis tools. HME: Donated cell line, partial study design. HM:

Drafting and wrote parts of the manuscript. AH: Conceptual design of the study, reagents/materials/analysis tools, manuscript drafting and finalization. All authors read and approved the final manuscript.

Acknowledgments

The authors thank Regina Carlson for technical support in flow cytometry and the German Research Foundation DFG (within the Transregio 37 and the excellence cluster REBIRTH) for the financial support. We thank Ulrich Martin (Leibnitz Research Laboratories for Biotechnology and Artificial Organs (LEBAO), Hannover Medical School) for providing the hES3 and hCBiPS2 cells.

Author details

¹Department of Biomedical Optics, Laser Zentrum Hannover, Hollerithallee 8, 30419 Hannover, Germany. ²Small Animal Clinic, University of Veterinary Medicine Hannover, Bünteweg 9, 30559 Hannover, Germany. ³Department of Hematology, Oncology, and Palliative Medicine, University of Rostock, Ernst- Heydemann-Str. 6, 18057 Rostock, Germany. ⁴Department of Cardiothoracic Transplantation and Vascular Surgery, Hannover Medical School, Carl-Neuberg-Str. 1, 30625 Hannover, Germany. ⁵Institut für Quantenoptik Leibniz Universität Hannover Welfengarten 1, 30167 Hannover, Germany.

Received: 10 September 2014 Accepted: 1 December 2014

Published online: 03 February 2015

References

- Roth JA, Cristiano RJ: **Gene therapy for cancer: what have we done and where are we going?** *J Natl Cancer Inst* 1997, **89**:21–39.
- Selkirk S: **Gene therapy in clinical medicine.** *Postgrad Med J* 2004, **80**:560–570.
- Dorsett Y, Tuschl T: **siRNAs: applications in functional genomics and potential as therapeutics.** *Nat Rev Drug Discov* 2004, **3**:318–329.
- Hacein-Bey-Abina S, Von Kalle C, Schmidt M, McCormack MP, Wulffraat N, Leboulch P, Lim A, Osborne CS, Pawliuk R, Morillon E, Sorensen R, Forster A, Fraser P, Cohen JL, de Saint Basile G, Alexander I, Wintergerst U, Frebourg T, Aurias A, Stoppa-Lyonnet D, Romana S, Radford-Weiss I, Gross F, Valensi F, Delabesse E, Macintyre E, Sigaux F, Soulier J, Leiva LE, Wissler M, et al: **LMO2-associated clonal T cell proliferation in two patients after gene therapy for SCID-X1.** *Science* 2003, **302**:415–419.
- Uchida E, Mizuguchi H, Ishii-Watabe A, Hayakawa T: **Comparison of the efficiency and safety of non-viral vector-mediated gene transfer into a wide range of human cells.** *Biol Pharm Bull* 2002, **25**:891–897.
- Karra D, Dahm R: **Transfection techniques for neuronal cells.** *J Neurosci* 2010, **30**:6171–6177.
- Papapetrou EP, Zoumbos NC, Athanassiadou A: **Genetic modification of hematopoietic stem cells with nonviral systems: past progress and future prospects.** *Gene Ther* 2005, **12**(Suppl 1):118–130.
- Krausz E: **High-content siRNA screening.** *Mol Biosyst* 2007, **3**:232–240.
- Tsukakoshi M, Kurata S, Nomiya Y, Ikawa Y, Kasuya T: **A novel method of DNA transfection by laser microbeam cell surgery.** *App Phys B* 1984, **35**:135–140.
- Terakawa M, Ogura M, Sato S, Wakisaka H, Ashida H, Uenoyama M, Masaki Y, Obara M: **Gene transfer into mammalian cells by use of a nanosecond pulsed laser-induced stress wave.** *Opt Lett* 2004, **29**:1227–1229.
- Tirlapur UK, König K: **Targeted transfection by femtosecond laser.** *Nature* 2002, **418**:290–291.
- Soughayer JS, Krasieva T, Jacobson SC, Ramsey JM, Tromberg BJ, Allbritton NL: **Characterization of cellular optoporation with distance.** *Anal Chem* 2000, **72**:1342–1347.
- Stevenson DJ, Gunn-Moore FJ, Campbell P, Dholakia K: **Transfection by Optical Injection.** In *Handbook of Photonics for Biomedical science*. Edited by Tuchin VV. Boca Raton: CRC Press, Taylor and Francis Group; 2010:87–118.
- Kalies S, Heinemann D, Schomaker M, Escobar HM, Heisterkamp A, Ripken T, Meyer H: **Plasmonic laser treatment for Morpholino oligomer delivery in antisense applications.** *J Biophotonics* 2013, doi:10.1002/jbio.201300056
- Heinemann D, Schomaker M, Kalies S, Schieck M, Carlson R, Murua Escobar H, Ripken T, Meyer H, Heisterkamp A: **Gold nanoparticle mediated laser transfection for efficient siRNA mediated gene knock down.** *PLoS One* 2013, **8**: doi:10.1371.
- Schomaker M, Killian D, Willenbrock S, Heinemann D, Kalies S, Ngezhahayo A, Nolte I, Ripken T, Junghans C, Meyer H, Murua Escobar H, Heisterkamp A: **Biophysical effects in off-resonant gold nanoparticle mediated (GNOME) laser transfection of cell lines, primary- and stem cells using fs laser pulses.** *J Biophotonics* 2014, doi:10.1002/jbio.201400065.
- Hashimoto S, Werner D, Uwada T: **Studies on the interaction of pulsed lasers with plasmonic gold nanoparticles toward light manipulation, heat management, and nanofabrication.** *J Photoch Photobiol C* 2012, **13**:28–54.
- Boulais E, Lachaine R, Meunier M: **Plasma mediated off-resonance plasmonic enhanced ultrafast laser-induced nanocavitation.** *Nano Lett* 2012, **12**:4763–4769.
- Nedyalkov NN, Imamova S, Atanasov PA, Tanaka Y, Obara M: **Interaction between ultrashort laser pulses and gold nanoparticles: nanoheater and nanolens effect.** *J Nanopart Res* 2011, **13**:2181–2193.
- Schomaker M, Fehlauer H, Binting W, Ngezhahayo A, Nolte I, Murua Escobar H, Lubatschowski H, Heisterkamp A: **Fs-laser cell perforation using gold nanoparticles of different shapes.** *Proc SPIE* 2010, **7589**:75890C.
- Schomaker M, Killian D, Willenbrock S, Diebold E, Mazur E, Binting W, Ngezhahayo A, Nolte I, Murua Escobar H, Junghans C, Lubatschowski H, Heisterkamp A: **Ultrashort laser pulse cell manipulation using nano- and micro- materials.** *Proc SPIE* 2010, **7762**:77623G.
- Baumgart J, Humbert L, Boulais E, Lachaine R, Lebrun JJ, Meunier M: **Off-resonance plasmonic enhanced femtosecond laser optoporation and transfection of cancer cells.** *Biomaterials* 2012, **33**:2345–2350.
- König K: **Multiphoton microscopy in life sciences.** *J Microsc* 2000, **200**:83–104.
- Schomaker M: **Plasmonenbasierte Zelltransfektion im Hochdurchsatz mittels ultrakurzer Laserpulse.** Garbsen, Germany: Degree Thesis, University Hannover, PZH Verlag; 2013.
- Winkler S, Murua Escobar H, Meyer B, Simon D, Eberle N, Baumgartner W, Loeschke S, Nolte I, Bullerdiek J: **HMG2 expression in a canine model of prostate cancer.** *Cancer Genet Cytogenet* 2007, **177**:98–102.
- Vogel A, Noack J, Hüttman G, Paltauf G: **Mechanisms of femtosecond laser nanosurgery of cells and tissues.** *Appl Phys B* 2005, **81**:1015–1047.
- Kuete Meyer K, Rezgui R, Lubatschowski H, Heisterkamp A: **Influence of laser parameters and staining on femtosecond laser-based intracellular nanosurgery.** *Biomed Opt Express* 2010, **1**:587597.
- Jee Y, Becker MF, Walsler RM: **Laser-induced damage on single-crystal metal surfaces.** *J Opt Soc Am B* 1988, **5**:648–659.
- Ekici O, Harrison RK, Durr NJ, Eversole DS, Lee M, Ben-Yakar A: **Thermal analysis of gold nanorods heated with femtosecond laser pulses.** *J App Phys D* 2008, **41**:1–11.
- Pelton M, Aizpuruja J, Bryant G: **Metal-nanoparticle plasmonics.** *Laser Photon Rev* 2008, **2**:136–159.
- Anisimov SI, Kapeliovich BL, Perelman TL: **Electron emission from metal surfaces exposed to ultrashort laser pulses.** *Soviet Physics JETP* 1974, **39**:375–377.
- Jain PK, Lee KS, El-Sayed IH, El-Sayed MA: **Calculated absorption and scattering properties of gold nanoparticles of different size, shape, and composition: applications in biological imaging and biomedicine.** *J Phys Chem B* 2006, **110**:7238–7248.
- Chithrani BD, Ghazani AA, Chan WC: **Determining the size and shape dependence of gold nanoparticle uptake into mammalian cells.** *Nano Lett* 2006, **6**:662–668.
- Nel AE, Mädler L, Velegol D, Xia T, Hoek EM, Somasundaran P, Klaessig F, Castranova V, Thompson M: **Understanding biophysicochemical interactions at the nano-bio interface.** *Nat Mater* 2009, **8**:543–557.
- Pustovalov VK, Smetannikov AS, Zharov VP: **Photothermal and accompanied phenomena of selective nanophotothermolysis with gold nanoparticles and laser pulses.** *Laser Phys Lett* 2008, **5**:775–792.
- Bisker G, Yelin D: **Noble-metal nanoparticles and short pulses for nanomanipulations: theoretical analysis.** *JOSA B* 2012, **29**:1383–1393.
- Lukianova-Hleb E, Hu Y, Latterini L, Tarpani L, Lee S, Drezek RA, Hafner JH, Lapotko DO: **Plasmonic nanobubbles as transient vapor nanobubbles generated around plasmonic nanoparticles.** *ACS Nano* 2010, **4**:2109–2123.
- Lukianova-Hleb EY, Ren X, Constantinou PE, Danysh BP, Shenfeldt DL, Carson DD, Farach-Carson MC, Kulchitsky VA, Wu X, Wagner DS, Lapotko DO: **Improved cellular specificity of plasmonic nanobubbles versus nanoparticles in heterogeneous cell systems.** *PLoS one* 2012, **7**:e34537.
- Pitsillides CM, Joe EK, Wei X, Anderson RR, Lin CP: **Selective cell targeting with light-absorbing microparticles and nanoparticles.** *Biophys J* 2003, **84**:4023–4032.
- Zharov VP, Galitovskiy V, Viegas M: **Photothermal detection of local thermal effects during selective nanophotothermolysis.** *Appl Phys Lett* 2003, **83**:4897–4899.
- Minai L, Yeheksely-Hayon D, Golan L, Bisker G, Dann EJ, Yelin D: **Optical nanomanipulations of malignant cells: controlled cell damage and fusion.** *Small* 2012, **8**:1732–1739.

42. Quinten M: **Local fields close to the surface of nanoparticles and aggregates of nanoparticles.** *Appl Phys B* 2001, **73**:245–255.
43. Nedyalkov NN, Atanasov PA, Obara M: **Near-field properties of a gold nanoparticle array on different substrates excited by a femtosecond laser.** *Nanotechnology* 2007, **18**:305703.
44. Skuridin SG, Dubinskaya VA, Rudoy VM, Dement'eva OV, Zakhidov ST, Marshak TL, Kuz'min VA, Popenko VI, Evdokimov YM: **Effect of gold nanoparticles on DNA package in model systems.** *Dokl Biochem Biophys* 2010, **432**:141–143.
45. Ferhanoglu O, Yildirim M, Subramanian K, Ben-Yakar A: **A 5-mm piezo-scanning fiber device for high speed ultrafast laser microsurgery.** *Biomed Opt Express* 2014, **5**:2023–2036.
46. Ma N, Gunn-Moore F, Dholakia K: **Optical transfection using an endoscope-like system.** *J Biomed Opt* 2011, **16**:028002.
47. Lukianova-Hleb EY, Ren X, Sawant RR, Wu X, Torchilin VP, Lapotko DO: **On-demand intracellular amplification of chemoradiation with cancer-specific plasmonic nanobubbles.** *Nat Med* 2014, **20**:778–784.
48. Watanabe S, Ueda Y, Akaboshi S, Hino Y, Sekita Y, Nakao M: **HMG2 maintains oncogenic RAS-induced epithelial-mesenchymal transition in human pancreatic cancer cells.** *Am J Pathol* 2009, **174**:854–868.
49. Withrow JS, Vail DM: *Withrow and MacEwen's Small Animal Clinical Oncology*. 5th ed. St Louis Missouri: Saunders Company; 2012.
50. Davis AA, Farrar MJ, Nishimura N, Jin MM, Schaffer CB: **Optoporation and genetic manipulation of cells using femtosecond laser pulses.** *Biophys J* 2013, **105**:862–871.
51. Murua Escobar H, Meyer B, Richter A, Becker K, Flohr AM, Bullerdiek J, Nolte I: **Molecular characterization of the canine HMGB1.** *Cytogenet Genome Res* 2003, **101**:33–38.
52. Winkler S, Murua Escobar H, Eberle N, Reimann-Berg N, Nolte I, Bullerdiek J: **Establishment of a cell line derived from a canine prostate carcinoma with a highly rearranged karyotype.** *J Hered* 2005, **96**:782–785.
53. Haase A, Olmer R, Schwanke K, Wunderlich S, Merkert S, Hess C, Zweigerdt R, Gruh I, Meyer J, Wagner S, Maier LS, Han DW, Glage S, Miller K, Fischer P, Schöler HR, Martin U: **Generation of induced pluripotent stem cells from human cord blood.** *Cell stem cell* 2009, **5**:434–441.
54. Schneider CA, Rasband WS, Eliceiri KW: **NIH Image to ImageJ: 25 years of image analysis.** *Nat Methods* 2012, **9**:671–675.
55. Lin Z, Zhigilei LV, Celli V: **Electron-phonon coupling and electron heat capacity of metals under conditions of strong electron-phonon nonequilibrium.** *Phys Rev B* 2008, **77**:075133.
56. Draine BT, Flatau PJ: **Discrete-dipole approximation for scattering calculations.** *J Opt Soc Am A* 1994, **11**:1491–1499.
57. Draine, BT, Flatau PJ: *User Guide to the Discrete Dipole Approximation Code DDSCAT 7.2*. 2012.
58. Keldysh LV: **Ionization in the field of a strong electromagnetic wave.** *J Exptl Theoret Phys (USSR)* 1964, **47**:1945–1957. translation: *Soviet Physics JETP* 1965, **20**: 1307–1314.

Submit your next manuscript to BioMed Central and take full advantage of:

- Convenient online submission
- Thorough peer review
- No space constraints or color figure charges
- Immediate publication on acceptance
- Inclusion in PubMed, CAS, Scopus and Google Scholar
- Research which is freely available for redistribution

Submit your manuscript at
www.biomedcentral.com/submit



4.3.4. Verification of a canine PSMA (FolH1) antibody

Prostate cancer is a highly aggressive malignancy in pet dogs. In contrast to man currently neither standard screening strategies nor curative therapeutic options are available for dogs. In human medicine PSMA is successfully used as therapeutic target for human prostate cancer (Ikegami *et al.*, 2006; Milowsky *et al.*, 2007). However, in dogs the studies on PSMA expression in prostatic tissues are contradictory (Aggarwal *et al.*, 2006; Lai *et al.*, 2008) concerning their specificity for PSMA detection.

Despite the high amino acid homology of 91 % between the human and canine PSMA (Schmidt *et al.*, 2013), validated data on cross-reactive antibodies are still missing.

VIII. Verification of a canine PSMA (FolH1) antibody.

Wagner et al., Anticancer Research, 2015.

By this reason in the following manuscript a monoclonal antibody, reactive with human PSMA protein was evaluated for cross-reactivity with the canine counterpart in Western Blot (WB) analysis. Antibody cross-reactivity with the canine protein in WB was confirmed by mass spectrometry proofing the YPSMA-1 antibody clone specificity for canine PSMA. This antibody represents a reliable tool for coming comparative PSMA studies.

VIII.

Verification of a canine PSMA (FolH1) antibody

Siegfried Wagner, Denise Maibaum, Andreas Pich, Ingo Nolte, Hugo Murua Escobar

Anticancer Research, 2015.

Own contribution:

- Planning of experiments
- Figure preparation (WBs)
- Partial manuscript drafting

ANTICANCER RESEARCH

International Journal of Cancer Research and Treatment

ISSN: 0250-7005

Verification of a Canine PSMA (FolH1) Antibody

SIEGFRIED WAGNER¹, DENISE MAIBAUM¹, ANDREAS PICH²,
INGO NOLTE¹ and HUGO MURUA ESCOBAR^{1,3*}

¹*Small Animal Clinic, University of Veterinary Medicine Hannover, Hannover, Germany;*

²*Core Facility Proteomics, Hannover Medical School, Hannover, Germany;*

³*Division of Medicine, Department of Haematology/Oncology, University of Rostock, Rostock, Germany*

Reprinted from

ANTICANCER RESEARCH 35: 145-148 (2015)

Verification of a Canine PSMA (FolH1) Antibody

SIEGFRIED WAGNER¹, DENISE MAIBAUM¹, ANDREAS PICH²,
INGO NOLTE¹ and HUGO MURUA ESCOBAR^{1,3*}

¹Small Animal Clinic, University of Veterinary Medicine Hannover, Hannover, Germany;

²Core Facility Proteomics, Hannover Medical School, Hannover, Germany;

³Division of Medicine, Department of Haematology/Oncology, University of Rostock, Rostock, Germany

Abstract. *Background: Canine prostate cancer (PC) is a highly aggressive malignancy. However, in contrast to man, neither standard screening strategies nor curative therapeutic options exist for the companion animal. A prostate-specific membrane antigen (PSMA) screening as molecular marker akin to human PC is currently not available for dogs as data on specific canine PSMA detection are contradictory. Materials and Methods: To evaluate an antibody for specific canine PSMA detection by western blotting (WB), lysates of three canine prostatic cell lines (CT1258, DT08/40, DT08/46) were comparatively analyzed by WB and mass spectrometry (MS) to the human cell lines VCaP, LnCaP and PC-3. Results: MS analyses of the detected canine proteins confirmed cross reactivity of the antibody clone YPSMA-1 with canine PSMA. Conclusion: The MS analyses of the extracted canine protein bands proved that the YPSMA-1 clone is as well specific for canine PSMA in WB and, thus, represents a reliable tool for comparative PSMA studies.*

contrast to the situation in human medicine (6, 7), no screening methods are currently available for dogs.

As the canine prostate-specific membrane antigen (PSMA) protein presents a high sequence homology to the human homolog (8) and data on specific PSMA detection in pet dogs are contradictory (5, 9), we evaluated a monoclonal antibody raised against human PSMA for detection of the canine PSMA by western blot (WB) analysis and verified the detected proteins by mass spectrometry (MS).

Prostate cancer (PC) occurs spontaneously in man and dog. Although the incidence rate for the canine malignancy is less than 1% (1) it is often diagnosed at a very late stage (2). Canine PC is highly aggressive and metastasizes rapidly to other body parts, such as lymph nodes, lungs, liver, spleen and bones (3-5).

Consequently, reliable canine molecular markers for diagnosis and early detection are of need. However, in

*These Authors contributed equally to this study.

Correspondence to: Ingo Nolte, Small Animal Clinic, University of Veterinary Medicine Hannover, Buenteweg 9, 30559 Hannover, Germany. Tel: +49 5119536202, Fax: +49 05119536204, e-mail: ingo.nolte@tiho-hannover.de

Key Words: Prostate cancer, PSMA, antibody cross-reactivity, molecular marker, diagnosis, dog.

5. Discussion

Cancer is a group of malignant diseases spontaneously occurring in human and animals. Except hereditary an unhealthy life style, poor nutrition and environmental risk factors are favoring molecular deregulations and mutations, which contribute to the malfunction of genes (American Cancer Society. Cancer Facts & Figures 2013). In the last decades a huge number of genes were identified with many of them being frequently deregulated in malignant neoplasias. On this basis various molecular diagnostic, prognostic and therapeutic approaches for cancer treatment were developed. Nevertheless, a large percentage of patients still die after developing cancer despite of an aggressive treatment regimen (Goldblatt and Lee, 2010), highlighting the need for better therapeutic agents and for biomarkers enabling early diagnosis.

The development of novel, more effective cancer treatment strategies relies on a better knowledge of the genetic and epigenetic changes contributing to this kind of malignancy. In this regard model organisms play a great role.

As pet dogs meet many of the criteria constituting a good model for different human cancer entities, the aim of the present thesis was the analysis of several canine orthologous genes in the context of canine malignant neoplasias.

5.1. Gene expression analyses

5.1.1. Prostate cancer

Although the knowledge of the molecular changes in PC has significantly increased in the last decades, its diagnosis and therapy are still challenging. Additionally, actually no reliable molecular marker for treatment of canine PC exist thus the treatment is mostly palliative (Leroy and Northrup, 2009) similarly to the human hormone refractory PC (Divrik *et al.*, 2012).

Within the first review article presented within this thesis it was highlighted that the miRNA *let-7* family, the directly by *let-7* regulated protein-encoding genes *CCND2*, *HMGA1*, *HMGA2*, *IL6*, *RAS* as well as the downstream targets *AR* and *HMGB1*, all of which are commonly deregulated in human prostate cancer and other neoplasias, are not acting in solitude but are closely interwoven with each other. Additionally, it is of special interest that the miRNA *let-7* family members are major players in the

regulation of these genes and appear to contribute greatly to the maintenance of the “Ying and Yang” in non-neoplastic cells. For that reason the complex intra- and intercellular genetic interactions of the *let-7* family and associated genes must be further investigated.

Owing to that the second presented study deals with the expression analysis of *HMGA1*, *HMGA2*, their regulator the miRNA *let-7a*, additionally the other above mentioned *let-7* targets and the associated genes *FoIH1*, *Klf4*, *MAPK1*, *PI3KCA*, and *PTEN* in canine PC. The expression of the canine *AR* was not quantified as the transcripts encoded by this gene were not adequately characterized.

In accordance with a previous study from Winkler and colleagues (Winkler *et al.*, 2007), *HMGA2* was statistically significantly over expressed in all herein analyzed adenocarcinoma derived tissues of the canine prostate gland and in the adenocarcinoma derived prostatic cell lines CT1258 and DT08/46. On the other hand low *HMGA2* levels were measured in all non-neoplastic samples. This is in accordance with the previous observation that in humans *HMGA2* expression is low or barely detectable in most adult tissues (Rommel *et al.*, 1997).

Compared to non-neoplastic tissue specimens elevated levels of the *HMGA2* regulator *let-7a* were present in the hyperplastic and malignant tissues as well as in the three cell lines CT1258, DT08/40 and DT08/46. Remarkably, a similar observation, previously made by our group, was that in canine oral squamous cell carcinomas *HMGA2* and *let-7a* expression was as well up regulated (Sterenczak *et al.*, 2014). This are interesting similarities, as the regulator and target gene do not show a reciprocal correlation as described in human lung cancer (Lee and Dutta, 2007).

However if the elevated *let-7a* levels are a cellular response to elevated oncogene levels, which are regulated by *let-7a* or if cancer develops as a consequence of the *let-7a* up regulation needs to be clarified.

Human PC-3 cells were previously reported to exhibit a defective *MAPK* pathway. Reconstitution of this pathway by expression of a constitutively active, recombinant *MAPK1* effectively reversed the neoplastic phenotype and prevented aberrant cell proliferation (Moro *et al.*, 2007). In accordance, lowest *MAPK1* levels were found in all malignant canine PC samples. On the other hand *MAPK1* up regulation was

monitored to be associated with survival of castrate-resistant human PC (Mukherjee *et al.*, 2011).

Similarly to *MAPK1*, *HMGB1* expression was statistically significantly lower in the malignant tissues as well as in two of three cell lines. In contrast to the expression in the herein analyzed canine PC samples, previous studies reported elevated *HMGB1* levels among others in human PC (Ishiguro *et al.*, 2005; Tang *et al.*, 2010). The expression analyses of the other protein-encoding genes did not present a correlation with canine PC. However, as the total number of prostatic samples used in this study was very low (n=14) and tumors are often an accumulation of heterogenic cells, it cannot be excluded that analysis of additional samples or cellular sub-fractions would produce more obvious results.

Additionally, another limitation of this study is that the obtained results do not give any information about the presence of mutations within the analyzed transcripts. These changes might destroy or change the function of the gene products thus having dramatic impact on the cell equilibrium without being visible in quantitative real-time PCR (qRT-PCR) analyses. Nevertheless, the obtained data are encouraging further studies with the canine model.

5.1.2. Lymphoma

The canine *HMGA2* gene appears to be associated with cancer of the prostate gland as reported by Winkler *et al.* (Winkler *et al.*, 2007) and as confirmed herein. Owing to that the expression of this promising molecular target as well of its sister gene *HMGA1* was investigated in canine hematopoietic cancer.

In the herein presented study from Joetzke *et al.* 2010 a statistically significant *HMGA1* up regulation was observed in lymph nodes from dogs with B-cell but not T-cell lymphomas. It is notable that *HMGA2* presented a reciprocal expression pattern to *HMGA1*, with low transcript levels in specimen with B-cell but elevated levels in T-cell lymphomas. Also the increased *HMGA2* levels in T-cell lymphomas were not statistically significant (possibly due to low T-cell lymphomas sample number, n=3) these two architectural transcription factors bear great potential as molecular therapeutic targets for the respective lymphoma subgroup but may as well be valuable differentiation markers for canine lymphomas. Additionally, owing to the fact that the *HMGA1* as well as the *HMGA2* genes are direct *let-7* targets,

these canine cancer entities could be potentially treated with *let-7* based therapeutics.

However, as the sample number in this study was very low the potency of the *HMGAs* as molecular marker for canine lymphoma has to be proofed using a greater set of tissue specimen.

5.1.3. Comparison of non-coding RNAs in human and canine cancer

Once dismissed as genomic refuse as transcribed from “junk DNA”, micro RNAs (miRNAs) were discovered to regulate gene expression at post-transcriptional level (Tomari and Zamore, 2005; Schubert *et al.*, 2013) and are furthermore discussed to be involved in the transcriptional regulation of genes (Chen *et al.*, 2012).

The discovery of the post-transcriptional gene silencing (PTGS) mediated by miRNAs is considered as a major breakthrough in biology. Nevertheless, the precise role of this mechanism in cell biology is still poorly understood. Thus comparative studies between different species are essential for cancer research.

As described in Wagner *et al.* 2012 more than 200 canine mature miRNAs (approximately 2/3) were found to present full sequence homology to the published human miRNAs (Sanger Institute, version 16.0) (Kozomara and Griffiths-Jones, 2011) enabling the use of human miRNA assays for research on canine cells.

As a great number of human and canine miRNAs are evolutionary conserved and many of these are involved in similar diseases of both species, it is likely that the expression patterns are also similar. Nevertheless, homologous miRNAs presenting similar expression pattern in different species, should be considered with care as their functions could still deviate strongly depending on other factors. Even individual miRNAs in the same species can have oncogene suppressive functions or act oncogenic depending on diverse tissues and different time points in development (Boggs *et al.*, 2008).

However, an aberrant miRNA expression is partially postulated to be an early event in human tumorigenesis (Cortez *et al.*, 2012). Thus many miRNAs bear great potential as non-invasive biomarkers for different clinically relevant types of human (Hao *et al.*, 2011; Cortez *et al.*, 2012; Shore *et al.*, 2012) and as well canine cancers (von Deetzen *et al.*, 2013). Additionally, they present a potent target for gene manipulation in therapeutic approaches.

5.2. Structural and functional *HMGA* analyses

Chromosomal alterations of the *HMGAs* are as well discussed to be an early event in tumor development (Ingraham *et al.*, 2006; Fusco and Fedele, 2007). Rearrangements of the human chromosome 6 (6p21) and 12 (12q15), which harbor the *HMGA1* and *HMGA2* gene respectively (Manfioletti *et al.*, 1991) were associated with benign human lipomas (Italiano *et al.*, 2007), pulmonary chondroid hamartomas (Tallini *et al.*, 2000), uterine leiomyoma (Kazmierczak *et al.*, 1996; Nezhad *et al.*, 2010) and myeloid malignancies (Odero *et al.*, 2005). Remarkably, *HMGA* re-expression is as well associated with a variety of human malignant neoplasias such pancreatic cancer (Watanabe *et al.*, 2009), breast cancer (Shah *et al.*, 2013), lung cancer (Di Cello *et al.*, 2008), retinoblastomas (Mu *et al.*, 2010) and lymphomas (Wood *et al.*, 2000; Baldassarre *et al.*, 2001). Additionally, Winkler *et al.* described a correlation between *HMGA2* and canine prostate cancer (Winkler *et al.*, 2007).

HMGA1 expression was reported to be post-transcriptionally regulated in a negative way by members of the *let-7* family (Rahman *et al.*, 2009; Schubert *et al.*, 2013). Its sister gene *HMGA2* is as well a *let-7* target (Mayr *et al.*, 2007). Interestingly, the *HMGA2* mRNA bears seven *let-7* miRNA binding sites in its 3'-untranslated region (3'-UTR) enabling efficient translational repression (Mayr *et al.*, 2007).

As abnormal *HMGA* gene expression appears to play a role in the investigated canine epithelial and hematopoietic cancer entities, the knowledge of their gene structure is of great value for ongoing studies. Thus the canine *HMGA1* gene structure, which was not completely known until the year 2008, was investigated herein.

Structural analysis of the canine *HMGA1* gene as described in Beuing *et al.* 2008 revealed the lack of the equivalent to the human exon 4 similarly to the mouse genome, which additionally lacks the equivalent to the human exon 3 (Pedulla *et al.*, 2001). Accordingly, the canine *HMGA1*, which is located on chromosome 12 (CFA12q11), consists of seven exons and six introns spanning in total 9524 bp. These specification induced evolutionary changes appear not to have altered the translation and function of the protein potentially owing to the fact that the absent exons are not part of the protein coding sequence (Friedmann *et al.*, 1993).

However, a context dependent impact on transcriptional or post-transcriptional regulation in the dog cannot be excluded.

Interestingly, the canine *HMGA1* gene was previously reported to map a region, which is not frequently affected by chromosomal alterations (Becker *et al.*, 2003) thus uncontrolled expression of the canine homolog is likely triggered by other mechanisms such as point mutations, post-transcriptional or post-translational modifications.

In this context a small nucleotide polymorphism was previously found in the exon 6 of the *HMGA1* gene of a Dachshund (Murua Escobar *et al.*, 2004). Therefore herein 55 Dachshund samples were screened for *HMGA1* point mutations in the respective exon. A breed specific predisposition was not found. However, while the presented study focused on mutations lying within the exon 6, breed specific mutations in other regions of the gene cannot be excluded.

Another possible mode of HMGA deregulation was indicated by a study from Dement and colleagues, who observed a cell cycle dependent translocation of the HMGA1 protein from the nucleus to the cytoplasm and mitochondria in the mouse embryonic fibroblast cells NIH3T3 and the human transgenic MCF7 cell line (Dement *et al.*, 2005). These findings demonstrate a highly dynamic cellular HMGA1 protein function, the spatially aberrant expression of which is potentially able to trigger cancer development.

Thus the cellular localization of the canine HMGA1 and HMGA2 proteins was analyzed in the herein presented studies from Beuing *et al.* 2008 and Willenbrock *et al.* 2014.

Recombinant HMGA1 and HMGA2 proteins were found to be localized in the nucleus of canine cells, similarly to the human (Disney *et al.*, 1989; Hristov *et al.*, 2009; Chiefari *et al.*, 2012) and murine orthologs (Disney *et al.*, 1989) presenting as well an irregular distribution (Harrer *et al.*, 2004; Henriksen *et al.*, 2010). The HMGA proteins are highly conserved among species (Reeves and Beckerbauer, 2001), owing to that it is likely that they have as well very similar roles in different organisms. Accordingly, the nuclear localization of the canine HMGA proteins implies an identical role as architectural transcription factors as reported for other mammalia (Narita *et al.*, 2006; Henriksen *et al.*, 2010).

According to the above presented results *HMGA2* and its regulator the miRNA *let-7a*

seem to play an important role in neoplasias of the prostate gland thus their relationship in PC etiology is of special interest. For more detailed analyses of the *HMGA/let-7* axis, the canine PC derived cell line CT1258 was used to establish the stably transfected cell line CT1258-EGFP-HMGA2 and the control cell line CT1258-EGFP as described in Willenbrock *et al.* 2014.

CT1258-EGFP-HMGA2 cells present an *in vitro* model system, which highly overexpresses an EGFP-HMGA2 fusion protein. Notably, the recombinant *HMGA2* transcript lacks the 3'-UTR. This is an interesting feature as native *HMGA2* mRNAs bear seven *let-7* binding sites in its 3'-UTR (Mayr *et al.*, 2007). In accordance, native *HMGA2* transcripts were previously reported to be negatively regulated by several members of the *let-7* family (Park *et al.*, 2007; Shi *et al.*, 2009), which were described to be deregulated in human PC (Dong *et al.*, 2010; Nadiminty *et al.*, 2012a; Nadiminty *et al.*, 2012b). A truncated *HMGA2* transcript lacking the 3'-UTR escapes the negative regulation by *let-7* resulting in elevated *HMGA2* levels (Lee and Dutta, 2007; Mayr *et al.*, 2007; Young and Narita, 2007).

As well of interest is the fact that *HMGA2* transcripts were recently reported to modulate the *let-7* impact on the global gene expression by acting as competing endogenous RNAs (ceRNA) (Kumar *et al.*, 2014) potentially favoring over expression of other direct *let-7* targets such as *CCND2* (Dong *et al.*, 2010), *c-Myc* (Sampson *et al.*, 2007), and *NRAS* (Johnson *et al.*, 2005). Furthermore, *HMGA2* suppression was previously suggested to impact the down regulation of its sister gene *HMGA1* (Berlingieri *et al.*, 1995), which in turn is as well negatively regulated by *let-7* (Schubert *et al.*, 2013) and was additionally found to be aberrantly expressed in human PC (Takaha *et al.*, 2004; Takeuchi *et al.*, 2012).

Herein a positive influence on *HMGA1* levels by ectopic *EGFP-HMGA2* expression in CT1258-EGFP-HMGA2 cells was observed. In addition, *HMGA2* over expression appears to positively impact mature *let-7a* miRNA levels, but not the transcript quantity of the analyzed *HMGA2* controlled targets *SNAI1*, *SNAI2* and *CDH1*. These results are remarkable as they demonstrate the complexity of the *HMGA2/let-7* axis. A possible explanation for the increase of the mature *let-7a* levels following recombinant *HMGA2* expression could be a response of the cells trying to down regulate *HMGA2*. Another plausible explanation could be that the endogenous *HMGA2* was down regulated upon ectopic *HMGA2* over expression. Consequently

there would be less native *HMGA2* transcripts able to act as ceRNAs resulting in increased mature *let-7a* levels.

In the performed qRT-PCR the total *HMGA2* levels were shown to be elevated in the cell line CT1258-EGFP-*HMGA2* according to the over expression of the *EGFP-HMGA2* transcripts when compared to CT1258. However, the total *HMGA2* levels do not reflect the percentage of endogenous to ectopic transcripts as the used assay was not able to discriminate between these two transcript variants.

Moreover, a positive EGFP-*HMGA2* effect on growth of canine cells was detected as previously described for HMGA proteins in other species (Di Cello *et al.*, 2013; Keane and de Magalhaes, 2013). This is remarkable as the positive effect on cell proliferation could be further stimulated by ectopic *HMGA2* over expression regardless of the already very high *HMGA2* levels in the native CT1258 cells.

Furthermore, cytogenetic analyses of both fluorescent cell lines CT1258-EGFP-*HMGA2* and CT1258-EGFP were performed as stable transfection might change the chromosomal structure. In addition exogenous *HMGA2* over expression was reported to induce chromosomal aberrations following DNA damage (Li *et al.*, 2009).

The herein presented study revealed a comparable hyperdiploid karyotype for both derived fluorescent cell lines as described for the native CT1258 cells (Winkler *et al.*, 2005). These results indicate two things: First of all the observed effects on cells are not triggered by global chromosomal rearrangements but likely induced by ectopic *HMGA2* over expression. Secondly, the ectopically highly over expressed *HMGA2* did not induce chromosomal aberrations as reported by Li *et al.* (Li *et al.*, 2009). Though, the difference to the experiments done by Li and colleagues is that in the presented study no DNA damage was induced in cells ectopically over expressing *HMGA2*. Finally, the native CT1258 cells are potentially adapted to elevated *HMGA2* levels as this protein was already highly expressed in this cell line. As the spatial HMGA expression appears to be a dynamic process and the *HMGA2* related HMGB1 protein was described to have a cytokine like function (Muller *et al.*, 2001) it is tempting to hypothesize an extracellular role for the HMGAs as well. In fact, the extracellular HMGA protein application on porcine chondrocytes was found to have a positive effect on cell growth *in vitro* (Richter *et al.*, 2009). Thus extracellular HMGA proteins actively or passively secreted by cancer cells could

potentially stimulate tumor growth *in vivo*. On the other hand due to the fact that the HMGA proteins are highly expressed during embryogenesis (Chiappetta *et al.*, 1996) but are barely detectable in most adult tissues (Manfioletti *et al.*, 1991; Chiappetta *et al.*, 1996; Rommel *et al.*, 1997) they might be a valuable tool for cell modification when expressed in the correct context.

To investigate if the HMGA proteins hold potential to preserve multi-potent cells from differentiation in cell culture, and to evaluate their potential extracellular role, recombinant HMGA proteins were applied onto canine adipose-tissue derived mesenchymal stem cells (ADMSCs). Subsequently, the impact of the HMGA1 and HMGA2 proteins on the phenotype, multipotency factors and proliferation rate of canine ADMSCs was analyzed.

Multi-potency and self-renewal are the most important characteristics of stem cells and several factors such as the HMGA protein family were described to impact these features (Shah *et al.*, 2012).

Within the herein presented study from Ismail *et al.* 2012 it could be shown that recombinant HMGA1 protein application alone or in combination with HMGA2 had a positive effect on the proliferation of multi-potent canine ADMSCs. In contrast to HMGA1, the HMGA2 application alone had no effect, neither on cell growth nor on stem cell marker expression. This is astonishing as Richter *et al.* reported a growth-promoting effect of synthetic HMGA2 peptides on canine ADMSCs (Richter *et al.*, 2011). One possible explanation for these controversial results is that the peptides used by Richter and colleagues were much smaller and had no post-translational modifications as the herein used recombinant proteins. Thus, these could potentially be easier taken up by the cells. The assumption that the molecule size contributes to this discrepancy is probable as the HMGA proteins are architectural transcription factors (Narita *et al.*, 2006; Henriksen *et al.*, 2010) and were not found yet to act as extracellular signal mediators. Owing to that it is unlikely that HMGA2 specific receptors on the cell surface exist. Another aspect is the cell identity due to the fact that the ADMSCs used by Richter *et al.* 2011 were not proofed to be able to differentiate into other lineages as it was described in the herein discussed study from Ismail *et al.* 2012. The passage number of the cells could influence the protein impact on cells as well. An additional explanation could be that Richter *et al.* 2011 used lower concentrations of fetal calf serum (FCS) in the

used growth medium, which potentially contains bovine HMGA2. The bovine protein homolog might have competed with the used recombinant HMGA2 proteins. However, when accepting that HMGA2 is unspecifically taken up by the cells and the bovine HMGA2, which is potentially present in the used FCS, can abolish the effects of recombinant HMGA2 the following doubt still remains. As described in the study from Willenbrock *et al.* 2014 ectopic EGFP-HMGA2 over expression in CT1258 cells, which were as well cultivated in growth medium containing 10 % FCS, could still enhance the proliferation rate of the prostatic cells despite the endogenous HMGA2 over expression. However, this was another cell type thus additional studies are necessary to investigate these discrepancies in results.

Concerning HMGA1, the observed results indicate that it can be taken up by the ADMSCs as an enhanced growth rate could be observed. This offers the possibility to modify ADMSC proliferation by extracellular HMGA1 application without introduction of genetic material into cells and avoiding the associated side effects such as the biological risk of insertional mutagenesis.

However, although the exact mechanisms of HMGA uptake in ADMSCs or other cell types need further clarification, it could offer new opportunities for regenerative medicine. Additionally the knowledge of the HMGA biogenesis and function in stem cells could provide valuable information in the context of cancer as cancer stem cells (CSC) are hypothesized to contribute to cancer aggressiveness (Adams and Strasser, 2008). In addition, as this type of cells represent as few as 1 in 10^4 to 10^7 of the tumor cells, depending on the type and advancement of the tumor (Adams and Strasser, 2008) and is often difficult to enrich in adequate quantities, basic research in this field relies as well on alternative stem cell sources such as ADMSCs.

5.3. Tools for modification and detection of gene expression

Ectopically expressed naturally occurring miRNAs or protein-encoding genes have the capability to act therapeutically in an organism. Therefore adequate vehicles are needed to efficiently transport the gene products or the molecules encoding the respective gene into the cell of interest. For that reason it is of major interest to further optimize or evaluate techniques enabling therapeutic approaches *in vitro* and *in vivo* and to establish tools enabling the monitoring of the target expression.

5.3.1. Generation of miRNA *let-7* constructs

As presented herein the miRNA family *let-7* might be a powerful tool for the modification of the global gene expression and therapeutic approaches. Thus several expression vectors encoding different members of the *let-7* family were constructed.

As shown in the gene expression studies with the canine prostate cancer and lymphomas at least one of the direct *let-7* targets *HMGA1* or *HMGA2* was over expressed. Thus these cancer entities potentially represent valuable candidates for the evaluation of *let-7* based therapeutic approaches in future.

5.3.2. rAAV genome isolation for quantification by absolute real-time PCR

Adeno-associated viruses (AAV) are commonly harnessed as vehicles for the efficient delivery of genetic material.

As the success and reproducibility of AAV mediated therapies depend among others on exact viral titers, a novel viral genome (VG) purification protocol was evaluated for the following sensitive and highly reproducible quantification by absolute real-time PCR.

The novel protocol for VG isolation proved to be superior compared to the commonly used NaOH or DNaseI/proteinase K protocols.

The NaOH pretreatment of the viral particles and the following neutralization with HCl have to be seen critically. As it could be observed in our previous experiments, the measured titers varied greatly in the triplica analyses. The explanation for the inter- and intra-experimental titer variances are likely caused by incomplete "digestion" of the AAV particles, which should release the viral genomes during the first denaturation step of the following qRT-PCR. Additionally, often very low titers were measured, which could be explained by "over digestion" with NaOH. Previous non presented experiments confirmed that naked plasmid DNA degrades completely when incubated in 1 M NaOH for a short time. However, to long or to short NaOH pretreatment leads to inaccurate titers, which appear to be lower than they really are.

The other commonly used method for AAV genome isolation is basically similar to the herein presented protocol but lacks the final on-column VG purification, which

may as well result in lower titers as the VGs are degraded by the residual DNaseI activity or the qRT-PCR inhibited by residual proteinase K activity.

5.3.3. AuNP based laser-transfection

Transfection techniques represent a good, up-scalable tool for *in vitro* applications as they enable direct modification of gene expression, which is crucial to establish therapeutic approaches in oncology and other areas of biomedical research.

The herein presented AuNP based laser transfection technique proves to be a very good alternative, when transferring small molecules, to conventional transfection techniques as it is theoretically cell type independent, non-toxic and up-scalable.

For proof of principle this novel method was harnessed to transfect anti-HMGA2 short interfering RNAs (siRNAs) into the canine prostatic cell line CT1258. As this cell line expresses extremely high *HMGA2* levels compared to healthy tissue it is remarkable that it was possible to down regulate the *HMGA2* mRNA-levels by up to ≈ 40 %. It is notable that previous transfection experiments (not presented herein) with the same siRNAs and a chemical transfection reagent were less effective concerning target down regulation despite a transfection efficiency of over 60 %.

The so far achieved results indicate great potential for *in vitro* applications of siRNAs or miRNAs.

5.3.4. Verification of a canine PSMA (FolH1) antibody

After manipulating gene expression in cells it is necessary to monitor the expression of the ectopically expressed gene or the regulated target. This can be easily done by different PCR techniques but as mRNA-levels are not always proportional to the translated protein product it is often necessary to analyze the protein expression.

In this regard biotechnologically produced antibodies must always be tested for their specific reactivity.

Owing to the lack of a specific canine PSMA (FOLH1) antibody and the still not entirely clear situation of the PSMA expression in canine prostate cancer, the antibody clone YPSMA-1, which was raised against a human peptide, was tested herein.

In detail, the specific reaction of the monoclonal antibody was demonstrated with the canine ortholog in western blot (WB) analysis using lysates of the previously

described canine prostatic cell lines CT1258, DT08/40 and DT08/46. Additionally the human prostatic cell lines VCaP, LnCaP, and PC-3 were used as positive controls.

The expected size of the human FolH1 homodimer in a SDS-PAG separation has a size of ≈ 100 kDa (Schulke *et al.*, 2003). The WB analysis of the human control samples revealed two prominent PSMA bands of ≈ 50 kDa and ≈ 100 kDa in size. The analysis of the canine CT1258 and DT08/40 lysates showed as well two protein bands matching the size of the human counterparts. In the DT08/46 cell lysates no protein bands were detected.

In conclusion to previous studies the PSMA expression was lowest in the cell line PC-3 among the human cell lines. In the canine cell lines CT1258 and DT08/40 the PSMA levels were low similarly to PC-3. The low protein levels in the canine cell lines reflect the very low *FolH1* mRNA levels with a C_T over 35 measured by qRT-PCR in the presented manuscript "Let-7 and associated genes in canine prostate cancer".

However, regardless of the target levels in the cell lines the evaluated antibody was shown to react in WB with the canine PSMA. Cross-reactivity with canine PSMA was exemplarily confirmed by mass spectrometric analyses of the recovered CT1258 protein bands. In conclusion, the previous immunohistochemistry evaluation (Lai *et al.*, 2008) and especially the herein presented WB as well as mass spectrometric analyses prove that the YPSMA-1 clone represents a reliable tool for coming PSMA studies in the dog.

6. Outlook

Tumors are believed to evolve through the gradual accumulation of genetic and epigenetic alterations. Chromosomal aberrations and nucleotide mutations account to the genetic changes and contribute, beside the genetic and epigenetic constitution of individuals, to the diversity of cancer cells. This heterogeneity makes it difficult or even impossible to identify omnipotent molecular cancer markers and is responsible for often confusing and contradictory results as well as for unpredictable disease outcome following therapy.

However, although the influence of a single molecular disease marker on cancer etiology in individuals can vary greatly due to the mentioned variability and stage of organismal development, this knowledge is crucial for the understanding of molecular processes. Moreover, as in future whole genome and transcriptome sequencing will provide information on individual molecular changes for lower costs, harnessing this technique for cancer research and especially for medical routine will highly depend on the knowledge where to look at in the obtained huge datasets. Owing to the described similarities between species and due to ethical reasons comparative studies as presented herein are very important for the development of successful cancer treatment strategies.

7. References

- Adams J M, and Strasser A. (2008). Is tumor growth sustained by rare cancer stem cells or dominant clones? *Cancer research* **68**, 4018-4021.
- Aggarwal S, Ricklis R M, Williams S A, and Denmeade S R. (2006). Comparative study of PSMA expression in the prostate of mouse, dog, monkey, and human. *The Prostate* **66**, 903-910.
- Alexander D D, Mink P J, Adami H O, Chang E T, Cole P, Mandel J S, and Trichopoulos D. (2007). The non-Hodgkin lymphomas: a review of the epidemiologic literature. *International journal of cancer* **120 Suppl 12**, 1-39.
- Attard G, Cooper C S, and De Bono J S. (2009). Steroid hormone receptors in prostate cancer: a hard habit to break? *Cancer cell* **16**, 458-462.
- Baldassarre G, Fedele M, Battista S, Vecchione A, Klein-Szanto a J, Santoro M, Waldmann T A, Azimi N, Croce C M, and Fusco A. (2001). Onset of natural killer cell lymphomas in transgenic mice carrying a truncated HMGI-C gene by the chronic stimulation of the IL-2 and IL-15 pathway. *Proceedings of the National Academy of Sciences of the United States of America* **98**, 7970-7975.
- Becker K, Murua Escobar H, Richter A, Meyer B, Nolte I, and Bullerdiek J. (2003). The canine HMGA1 gene maps to CFA 23. *Animal genetics* **34**, 68-69.
- Berlingieri M T, Manfioletti G, Santoro M, Bandiera A, Visconti R, Giancotti V, and Fusco A. (1995). Inhibition of HMGI-C protein synthesis suppresses retrovirally induced neoplastic transformation of rat thyroid cells. *Molecular and cellular biology* **15**, 1545-1553.
- Berns K I, and Bohenzky R A. (1987). Adeno-associated viruses: an update. *Advances in virus research* **32**, 243-306.
- Boffetta P. (2011). I. Epidemiology of adult non-Hodgkin lymphoma. *Ann Oncol* **22**.
- Boggs R M, Wright Z M, Stickney M J, Porter W W, and Murphy K E. (2008). MicroRNA expression in canine mammary cancer. *Mamm Genome* **19**, 561-569.
- Boonyaratanakornkit V, Melvin V, Prendergast P, Altmann M, Ronfani L, Bianchi M E, Taraseviciene L, Nordeen S K, Allegretto E A, and Edwards D P. (1998). High-mobility group chromatin proteins 1 and 2 functionally interact with steroid hormone receptors to enhance their DNA binding in vitro and transcriptional activity in mammalian cells. *Molecular and cellular biology* **18**, 4471-4487.
- Bouchelouche K, Choyke P L, and Capala J. (2010). Prostate specific membrane antigen- a target for imaging and therapy with radionuclides. *Discovery medicine* **9**, 55-61.
- Boyerinas B, Park S M, Hau A, Murmann a E, and Peter M E. (2010). The role of let-7 in cell differentiation and cancer. *Endocrine-related cancer* **17**, F19-36.
- Brase J C, Wuttig D, Kuner R, and Sultmann H. (2010). Serum microRNAs as non-invasive biomarkers for cancer. *Molecular cancer* **9**, 306.
- Cacchiarelli D, Martone J, Girardi E, Cesana M, Incitti T, Morlando M, Nicoletti C, Santini T, Sthandier O, Barberi L, Auricchio A, Musaro A, and Bozzoni I. (2010). MicroRNAs involved in molecular circuitries relevant for the Duchenne muscular dystrophy pathogenesis are controlled by the dystrophin/nNOS pathway. *Cell metabolism* **12**, 341-351.

- Castellano E, and Downward J. (2011). RAS Interaction with PI3K: More Than Just Another Effector Pathway. *Genes & cancer* **2**, 261-274.
- Chen B, Zhang B, Luo H, Yuan J, Skogerbo G, and Chen R. (2012). Distinct MicroRNA Subcellular Size and Expression Patterns in Human Cancer Cells. *International journal of cell biology* **2012**, 672462.
- Chen P S, Su J L, Cha S T, Tarn W Y, Wang M Y, Hsu H C, Lin M T, Chu C Y, Hua K T, Chen C N, Kuo T C, Chang K J, Hsiao M, Chang Y W, Chen J S, Yang P C, and Kuo M L. (2011). miR-107 promotes tumor progression by targeting the let-7 microRNA in mice and humans. *The Journal of clinical investigation* **121**, 3442-3455.
- Chiappetta G, Avantaggiato V, Visconti R, Fedele M, Battista S, Trapasso F, Merciai B M, Fidanza V, Giancotti V, Santoro M, Simeone A, and Fusco A. (1996). High level expression of the HMGI (Y) gene during embryonic development. *Oncogene* **13**, 2439-2446.
- Chiefari E, Nevolo M T, Arcidiacono B, Maurizio E, Nocera A, Iiritano S, Sgarra R, Possidente K, Palmieri C, Paonessa F, Brunetti G, Manfioletti G, Foti D, and Brunetti A. (2012). HMGA1 is a novel downstream nuclear target of the insulin receptor signaling pathway. *Scientific reports* **2**, 251.
- Cho S Y, and Szabo Z. (2013). Molecular imaging of urogenital diseases. *Seminars in nuclear medicine* **44**, 93-109.
- Cimmino A, Calin G A, Fabbri M, Iorio M V, Ferracin M, Shimizu M, Wojcik S E, Aqeilan R I, Zupo S, Dono M, Rassenti L, Alder H, Volinia S, Liu C G, Kipps T J, Negrini M, and Croce C M. (2005). miR-15 and miR-16 induce apoptosis by targeting BCL2. *Proceedings of the National Academy of Sciences of the United States of America* **102**, 13944-13949.
- Coffey D S, and Walsh P C. (1990). Clinical and experimental studies of benign prostatic hyperplasia. *The Urologic clinics of North America* **17**, 461-475.
- Colombatti M, Grasso S, Porzia A, Fracasso G, Scupoli M T, Cingarlini S, Poffe O, Naim H Y, Heine M, Tridente G, Mainiero F, and Ramarli D. (2009). The prostate specific membrane antigen regulates the expression of IL-6 and CCL5 in prostate tumour cells by activating the MAPK pathways. *PloS one* **4**, e4608.
- Cornell K K, Bostwick D G, Cooley D M, Hall G, Harvey H J, Hendrick M J, Pauli B U, Render J A, Stoica G, Sweet D C, and Waters D J. (2000). Clinical and pathologic aspects of spontaneous canine prostate carcinoma: a retrospective analysis of 76 cases. *The Prostate* **45**, 173-183.
- Cortez M A, Welsh J W, and Calin G A. (2012). Circulating microRNAs as noninvasive biomarkers in breast cancer. *Recent results in cancer research. Fortschritte der Krebsforschung* **195**, 151-161.
- Creemers E E, Tijssen a J, and Pinto Y M. (2010). Circulating microRNAs: novel biomarkers and extracellular communicators in cardiovascular disease? *Circulation research* **110**, 483-495.
- Croce C M, and Calin G A. (2005). miRNAs, cancer, and stem cell division. *Cell* **122**, 6-7.
- Dement G A, Treff N R, Magnuson N S, Franceschi V, and Reeves R. (2005). Dynamic mitochondrial localization of nuclear transcription factor HMGA1. *Experimental cell research* **307**, 388-401.
- Dhillon a S, Hagan S, Rath O, and Kolch W. (2007). MAP kinase signalling pathways in cancer. *Oncogene* **26**, 3279-3290.

- Di Cello F, Hillion J, Hristov A, Wood L J, Mukherjee M, Schuldenfrei A, Kowalski J, Bhattacharya R, Ashfaq R, and Resar L M. (2008). HMGA2 participates in transformation in human lung cancer. *Mol Cancer Res* **6**, 743-750.
- Di Cello F, Shin J, Harbom K, and Brayton C. (2013). Knockdown of HMGA1 inhibits human breast cancer cell growth and metastasis in immunodeficient mice. *Biochemical and biophysical research communications* **434**, 70-74.
- Di Lisio L, Sanchez-Beato M, Gomez-Lopez G, Rodriguez M E, Montes-Moreno S, Mollejo M, Menarguez J, Martinez M A, Alves F J, Pisano D G, Piris M A, and Martinez N. (2012). MicroRNA signatures in B-cell lymphomas. *Blood cancer journal* **2**, e57.
- Disney J E, Johnson K R, Magnuson N S, Sylvester S R, and Reeves R. (1989). High-mobility group protein HMG-I localizes to G/Q- and C-bands of human and mouse chromosomes. *The Journal of cell biology* **109**, 1975-1982.
- Divrik R T, Turkeri L, Sahin a F, Akdogan B, Ates F, Cal C, and Baltaci S. (2012). Prediction of response to androgen deprivation therapy and castration resistance in primary metastatic prostate cancer. *Urologia internationalis* **88**, 25-33.
- Dong Q, Meng P, Wang T, Qin W, Qin W, Wang F, Yuan J, Chen Z, Yang A, and Wang H. (2010). MicroRNA let-7a inhibits proliferation of human prostate cancer cells in vitro and in vivo by targeting E2F2 and CCND2. *PloS one* **5**, e10147.
- Eaton G M, Cody R J, Nunziata E, and Binkley P F. (1995). Early left ventricular dysfunction elicits activation of sympathetic drive and attenuation of parasympathetic tone in the paced canine model of congestive heart failure. *Circulation* **92**, 555-561.
- Engelman J A, Luo J, and Cantley L C. (2006). The evolution of phosphatidylinositol 3-kinases as regulators of growth and metabolism. *Nat Rev Genet* **7**, 606-619.
- Evans L S, and Hancock B W. (2003). Non-Hodgkin lymphoma. *Lancet* **362**, 139-146.
- Ferlay J, Shin H R, Bray F, Forman D, Mathers C, and Parkin D M. (2010). Estimates of worldwide burden of cancer in 2008: GLOBOCAN 2008. *International journal of cancer* **127**, 2893-2917.
- Fernandez-Medarde A, and Santos E. (2011). Ras in cancer and developmental diseases. *Genes & cancer* **2**, 344-358.
- Filipowicz W, Bhattacharyya S N, and Sonenberg N. (2008). Mechanisms of post-transcriptional regulation by microRNAs: are the answers in sight? *Nature reviews* **9**, 102-114.
- Friedmann M, Holth L T, Zoghbi H Y, and Reeves R. (1993). Organization, inducible-expression and chromosome localization of the human HMG-I(Y) nonhistone protein gene. *Nucleic acids research* **21**, 4259-4267.
- Fusco A, and Fedele M. (2007). Roles of HMGA proteins in cancer. *Nat Rev Cancer* **7**, 899-910.
- Gerits N, Kostenko S, Shiryaev A, Johannessen M, and Moens U. (2008). Relations between the mitogen-activated protein kinase and the cAMP-dependent protein kinase pathways: comradeship and hostility. *Cellular signalling* **20**, 1592-1607.
- Gideon P, John J, Frech M, Lautwein A, Clark R, Scheffler J E, and Wittinghofer A. (1992). Mutational and kinetic analyses of the GTPase-activating protein

- (GAP)-p21 interaction: the C-terminal domain of GAP is not sufficient for full activity. *Molecular and cellular biology* **12**, 2050-2056.
- Goldblatt E M, and Lee W H. (2010). From bench to bedside: the growing use of translational research in cancer medicine. *American journal of translational research* **2**, 1-18.
- Hao Y, Zhao Y, Zhao X, He C, Pang X, Wu T C, Califano J A, and Gu X. (2011). Improvement of prostate cancer detection by integrating the PSA test with miRNA expression profiling. *Cancer investigation* **29**, 318-324.
- Harrer M, Luhrs H, Bustin M, Scheer U, and Hock R. (2004). Dynamic interaction of HMGA1a proteins with chromatin. *Journal of cell science* **117**, 3459-3471.
- Henriksen J, Stabell M, Meza-Zepeda L A, Lauvrak S A, Kassem M, and Myklebost O. (2010). Identification of target genes for wild type and truncated HMGA2 in mesenchymal stem-like cells. *BMC cancer* **10**, 329.
- Hristov a C, Cope L, Reyes M D, Singh M, Iacobuzio-Donahue C, Maitra A, and Resar L M. (2009). HMGA2 protein expression correlates with lymph node metastasis and increased tumor grade in pancreatic ductal adenocarcinoma. *Mod Pathol* **22**, 43-49.
- Ikegami S, Yamakami K, Ono T, Sato M, Suzuki S, Yoshimura I, Asano T, Hayakawa M, and Tadakuma T. (2006). Targeting gene therapy for prostate cancer cells by liposomes complexed with anti-prostate-specific membrane antigen monoclonal antibody. *Human gene therapy* **17**, 997-1005.
- Iliopoulos D, Hirsch H A, and Struhl K. (2009). An epigenetic switch involving NF-kappaB, Lin28, Let-7 MicroRNA, and IL6 links inflammation to cell transformation. *Cell* **139**, 693-706.
- Ingraham S E, Lynch R A, Surti U, Rutter J L, Buckler a J, Khan S A, Menon a G, and Lepont P. (2006). Identification and characterization of novel human transcripts embedded within HMGA2 in t(12;14)(q15;q24.1) uterine leiomyoma. *Mutation research* **602**, 43-53.
- Ionut V, Liu H, Mooradian V, Castro a V, Kabir M, Stefanovski D, Zheng D, Kirkman E L, and Bergman R N. (2008). Novel canine models of obese prediabetes and mild type 2 diabetes. *American journal of physiology* **298**, E38-48.
- Ishiguro H, Nakaigawa N, Miyoshi Y, Fujinami K, Kubota Y, and Uemura H. (2005). Receptor for advanced glycation end products (RAGE) and its ligand, amphoterin are overexpressed and associated with prostate cancer development. *The Prostate* **64**, 92-100.
- Italiano A, Cardot N, Dupre F, Monticelli I, Keslair F, Piche M, Mainguene C, Coindre J M, and Pedeutour F. (2007). Gains and complex rearrangements of the 12q13-15 chromosomal region in ordinary lipomas: the "missing link" between lipomas and liposarcomas? *International journal of cancer* **121**, 308-315.
- Jemal A, Bray F, Center M M, Ferlay J, Ward E, and Forman D. (2011). Global cancer statistics. *CA: a cancer journal for clinicians* **61**, 69-90.
- Joetzke a E, Sterenczak K A, Eberle N, Wagner S, Soller J T, Nolte I, Bullerdiek J, Murua Escobar H, and Simon D. (2010). Expression of the high mobility group A1 (HMGA1) and A2 (HMGA2) genes in canine lymphoma: analysis of 23 cases and comparison to control cases. *Veterinary and comparative oncology* **8**, 87-95.
- Johnson C D, Esquela-Kerscher A, Stefani G, Byrom M, Kelnar K, Ovcharenko D, Wilson M, Wang X, Shelton J, Shingara J, Chin L, Brown D, and Slack F J.

- (2007). The let-7 microRNA represses cell proliferation pathways in human cells. *Cancer research* **67**, 7713-7722.
- Johnson S M, Grosshans H, Shingara J, Byrom M, Jarvis R, Cheng A, Labourier E, Reinert K L, Brown D, and Slack F J. (2005). RAS is regulated by the let-7 microRNA family. *Cell* **120**, 635-647.
- Kantharidis P, Wang B, Carew R M, and Lan H Y. (2011). Diabetes complications: the microRNA perspective. *Diabetes* **60**, 1832-1837.
- Kawasaki H, and Taira K. (2003). Retraction: Hes1 is a target of microRNA-23 during retinoic-acid-induced neuronal differentiation of NT2 cells. *Nature* **426**, 100.
- Kazmierczak B, Bol S, Wanschura S, Bartnitzke S, and Bullerdiek J. (1996). PAC clone containing the HMGI(Y) gene spans the breakpoint of a 6p21 translocation in a uterine leiomyoma cell line. *Genes, chromosomes & cancer* **17**, 191-193.
- Keane M, and De Magalhaes J P. (2013). MYCN/LIN28B/Let-7/HMGA2 pathway implicated by meta-analysis of GWAS in suppression of post-natal proliferation thereby potentially contributing to aging. *Mechanisms of ageing and development* **134**, 346-348.
- Klaewsongkram J, Yang Y, Golech S, Katz J, Kaestner K H, and Weng N P. (2007). Kruppel-like factor 4 regulates B cell number and activation-induced B cell proliferation. *J Immunol* **179**, 4679-4684.
- Kong D, Heath E, Chen W, Cher M L, Powell I, Heilbrun L, Li Y, Ali S, Sethi S, Hassan O, Hwang C, Gupta N, Chitale D, Sakr W A, Menon M, and Sarkar F H. (2012). Loss of let-7 up-regulates EZH2 in prostate cancer consistent with the acquisition of cancer stem cell signatures that are attenuated by BR-DIM. *PloS one* **7**, e33729.
- Kopper L, and Timar J. (2005). Genomics of prostate cancer: is there anything to "translate"? *Pathol Oncol Res* **11**, 197-203.
- Kota J, Chivukula R R, O'donnell K A, Wentzel E A, Montgomery C L, Hwang H W, Chang T C, Vivekanandan P, Torbenson M, Clark K R, Mendell J R, and Mendell J T. (2009). Therapeutic microRNA delivery suppresses tumorigenesis in a murine liver cancer model. *Cell* **137**, 1005-1017.
- Kozomara A, and Griffiths-Jones S. (2011). miRBase: integrating microRNA annotation and deep-sequencing data. *Nucleic acids research* **39**, D152-157.
- Kumar M S, Armenteros-Monterroso E, East P, Chakravorty P, Matthews N, Winslow M M, and Downward J. (2014). HMGA2 functions as a competing endogenous RNA to promote lung cancer progression. *Nature* **505**, 212-217.
- Lai C L, Van Den Ham R, Van Leenders G, Van Der Lugt J, Mol J A, and Teske E. (2008). Histopathological and immunohistochemical characterization of canine prostate cancer. *The Prostate* **68**, 477-488.
- Le Magnen C, Bubendorf L, Ruiz C, Zlobec I, Bachmann A, Heberer M, Spagnoli G C, Wyler S, and Mengus C. (2012). Klf4 transcription factor is expressed in the cytoplasm of prostate cancer cells. *Eur J Cancer* **49**, 955-963.
- Leav I, and Ling G V. (1968). Adenocarcinoma of the canine prostate. *Cancer* **22**, 1329-1345.
- Lee Y S, and Dutta A. (2007). The tumor suppressor microRNA let-7 represses the HMGA2 oncogene. *Genes & development* **21**, 1025-1030.
- Leroy B E, and Northrup N. (2009). Prostate cancer in dogs: comparative and clinical aspects. *Vet J* **180**, 149-162.

- Li a Y, Boo L M, Wang S Y, Lin H H, Wang C C, Yen Y, Chen B P, Chen D J, and Ann D K. (2009). Suppression of nonhomologous end joining repair by overexpression of HMGA2. *Cancer research* **69**, 5699-5706.
- Li R, Chung a C, Dong Y, Yang W, Zhong X, and Lan H Y. (2013). The microRNA miR-433 promotes renal fibrosis by amplifying the TGF-beta/Smad3-Azin1 pathway. *Kidney international* **84**, 1129-1144.
- Lin L, Faraco J, Li R, Kadotani H, Rogers W, Lin X, Qiu X, De Jong P J, Nishino S, and Mignot E. (1999). The sleep disorder canine narcolepsy is caused by a mutation in the hypocretin (orexin) receptor 2 gene. *Cell* **98**, 365-376.
- Liu C, Kelnar K, Vlassov a V, Brown D, Wang J, and Tang D G. (2012a). Distinct microRNA expression profiles in prostate cancer stem/progenitor cells and tumor-suppressive functions of let-7. *Cancer research* **72**, 3393-3404.
- Liu Y, Yin B, Zhang C, Zhou L, and Fan J. (2012b). Hsa-let-7a functions as a tumor suppressor in renal cell carcinoma cell lines by targeting c-myc. *Biochemical and biophysical research communications* **417**, 371-375.
- Lohi H, Young E J, Fitzmaurice S N, Rusbridge C, Chan E M, Vervoort M, Turnbull J, Zhao X C, Ianzano L, Paterson a D, Sutter N B, Ostrander E A, Andre C, Shelton G D, Ackerley C A, Scherer S W, and Minassian B A. (2005). Expanded repeat in canine epilepsy. *Science (New York, N.Y)* **307**, 81.
- Lyu S, Yu Q, Ying G, Wang S, Wang Y, Zhang J, and Niu Y. (2013). Androgen receptor decreases CMYC and KRAS expression by upregulating let-7a expression in ER-, PR-, AR+ breast cancer. *International journal of oncology* **44**, 229-237.
- Ma J, Sawai H, Ochi N, Matsuo Y, Xu D, Yasuda A, Takahashi H, Wakasugi T, and Takeyama H. (2009). PTEN regulates angiogenesis through PI3K/Akt/VEGF signaling pathway in human pancreatic cancer cells. *Molecular and cellular biochemistry* **331**, 161-171.
- Manfioletti G, Giancotti V, Bandiera A, Buratti E, Sautiere P, Cary P, Crane-Robinson C, Coles B, and Goodwin G H. (1991). cDNA cloning of the HMGI-C phosphoprotein, a nuclear protein associated with neoplastic and undifferentiated phenotypes. *Nucleic acids research* **19**, 6793-6797.
- Mayr C, Hemann M T, and Bartel D P. (2007). Disrupting the pairing between let-7 and Hmga2 enhances oncogenic transformation. *Science (New York, N.Y)* **315**, 1576-1579.
- Milowsky M I, Nanus D M, Kostakoglu L, Sheehan C E, Vallabhajosula S, Goldsmith S J, Ross J S, and Bander N H. (2007). Vascular targeted therapy with anti-prostate-specific membrane antigen monoclonal antibody J591 in advanced solid tumors. *J Clin Oncol* **25**, 540-547.
- Mitsiades C S, Mitsiades N S, Bronson R T, Chauhan D, Munshi N, Treon S P, Maxwell C A, Pilarski L, Hideshima T, Hoffman R M, and Anderson K C. (2003). Fluorescence imaging of multiple myeloma cells in a clinically relevant SCID/NOD in vivo model: biologic and clinical implications. *Cancer research* **63**, 6689-6696.
- Mizuno H, Nakamura A, Aoki Y, Ito N, Kishi S, Yamamoto K, Sekiguchi M, Takeda S, and Hashido K. (2011). Identification of muscle-specific microRNAs in serum of muscular dystrophy animal models: promising novel blood-based markers for muscular dystrophy. *PloS one* **6**, e18388.
- Mondol V, and Pasquinelli a E. (2012). Let's make it happen: the role of let-7 microRNA in development. *Current topics in developmental biology* **99**, 1-30.

- Moro L, Arbin A, Marra E, and Greco M. (2007). Constitutive activation of MAPK/ERK inhibits prostate cancer cell proliferation through upregulation of BRCA2. *International journal of oncology* **30**, 217-224.
- Mu G, Liu H, Zhou F, Xu X, Jiang H, Wang Y, and Qu Y. (2010). Correlation of overexpression of HMGA1 and HMGA2 with poor tumor differentiation, invasion, and proliferation associated with let-7 down-regulation in retinoblastomas. *Human pathology* **41**, 493-502.
- Mueller C, Tang Q, Gruntman A, Blumenkamp K, Teckman J, Song L, Zamore P D, and Flotte T R. (2012). Sustained miRNA-mediated knockdown of mutant AAT with simultaneous augmentation of wild-type AAT has minimal effect on global liver miRNA profiles. *Mol Ther* **20**, 590-600.
- Mueller F, Fuchs B, and Kaser-Hotz B. (2007). Comparative biology of human and canine osteosarcoma. *Anticancer research* **27**, 155-164.
- Mukherjee R, McGuinness D H, McCall P, Underwood M A, Seywright M, Orange C, and Edwards J. (2011). Upregulation of MAPK pathway is associated with survival in castrate-resistant prostate cancer. *British journal of cancer* **104**, 1920-1928.
- Muller S, Scaffidi P, Degryse B, Bonaldi T, Ronfani L, Agresti A, Beltrame M, and Bianchi M E. (2001). New EMBO members' review: the double life of HMGB1 chromatin protein: architectural factor and extracellular signal. *The EMBO journal* **20**, 4337-4340.
- Murua Escobar H, Soller J T, Richter A, Meyer B, Winkler S, Flohr M, Nolte I, and Bullerdiek J. (2004). The canine HMGA1. *Gene* **330**, 93-99.
- Nadiminty N, Tummala R, Lou W, Zhu Y, Shi X B, Zou J X, Chen H, Zhang J, Chen X, Luo J, Devere White R W, Kung H J, Evans C P, and Gao C. (2012a). MicroRNA let-7c is downregulated in prostate cancer and suppresses prostate cancer growth. *PloS one* **7**, e32832.
- Nadiminty N, Tummala R, Lou W, Zhu Y, Zhang J, Chen X, Devere White R W, Kung H J, Evans C P, and Gao C. (2012b). MicroRNA let-7c suppresses androgen receptor expression and activity via regulation of Myc expression in prostate cancer cells. *The Journal of biological chemistry* **287**, 1527-1537.
- Narita M, Narita M, Krizhanovsky V, Nunez S, Chicas A, Hearn S A, Myers M P, and Lowe S W. (2006). A novel role for high-mobility group A proteins in cellular senescence and heterochromatin formation. *Cell* **126**, 503-514.
- Nathwani C, Tuddenham E G, Rangarajan S, Rosales C, McIntosh J, Lynch D C, Chowdary P, Riddell A, Pie J, Harrington C, O'beirne J, Smith K, Pasi J, Glader B, Rustagi P, Ng C Y, Kay M A, Zhou J, Spence Y, Morton C L, Allay J, Coleman J, Sleep S, Cunningham J M, Srivastava D, Basner-Tschakarjan E, Mingozzi F, High K A, Gray J T, Reiss U M, Nienhuis W, and Davidoff M. (2011). Adenovirus-associated virus vector-mediated gene transfer in hemophilia B. *The New England journal of medicine* **365**, 2357-2365.
- Nezhad M H, Drieschner N, Helms S, Meyer A, Tadayyon M, Klemke M, Belge G, Bartnitzke S, Burchardt K, Frantzen C, Schmidt E H, and Bullerdiek J. (2010). 6p21 rearrangements in uterine leiomyomas targeting HMGA1. *Cancer genetics and cytogenetics* **203**, 247-252.
- Noguchi S, Mori T, Hoshino Y, Yamada N, Maruo K, and Akao Y. (2011). MicroRNAs as tumour suppressors in canine and human melanoma cells and as a prognostic factor in canine melanomas. *Veterinary and comparative oncology* **9**, 1476-5829.

- Noguchi S, Mori T, Hoshino Y, Yamada N, Maruo K, and Akao Y. (2013). MicroRNAs as tumour suppressors in canine and human melanoma cells and as a prognostic factor in canine melanomas. *Veterinary and comparative oncology* **11**, 113-123.
- Odero M D, Grand F H, Iqbal S, Ross F, Roman J P, Vizmanos J L, Andrieux J, Lai J L, Calasanz M J, and Cross N C. (2005). Disruption and aberrant expression of HMGA2 as a consequence of diverse chromosomal translocations in myeloid malignancies. *Leukemia* **19**, 245-252.
- Ostrander E A, Galibert F, and Patterson D F. (2000). Canine genetics comes of age. *Trends Genet* **16**, 117-124.
- Paoloni M, and Khanna C. (2008). Translation of new cancer treatments from pet dogs to humans. *Nature reviews* **8**, 147-156.
- Park S M, Shell S, Radjabi a R, Schickel R, Feig C, Boyerinas B, Dinulescu D M, Lengyel E, and Peter M E. (2007). Let-7 prevents early cancer progression by suppressing expression of the embryonic gene HMGA2. *Cell cycle (Georgetown, Tex)* **6**, 2585-2590.
- Pasquinelli a E, Reinhart B J, Slack F, Martindale M Q, Kuroda M I, Maller B, Hayward D C, Ball E E, Degan B, Muller P, Spring J, Srinivasan A, Fishman M, Finnerty J, Corbo J, Levine M, Leahy P, Davidson E, and Ruvkun G. (2000). Conservation of the sequence and temporal expression of let-7 heterochronic regulatory RNA. *Nature* **408**, 86-89.
- Pedulla M L, Treff N R, Resar L M, and Reeves R. (2001). Sequence and analysis of the murine Hmgiy (Hmga1) gene locus. *Gene* **271**, 51-58.
- Pierantoni G M, Rinaldo C, Mottolese M, Di Benedetto A, Esposito F, Soddu S, and Fusco A. (2007). High-mobility group A1 inhibits p53 by cytoplasmic relocation of its proapoptotic activator HIPK2. *The Journal of clinical investigation* **117**, 693-702.
- Pinho S S, Carvalho S, Cabral J, Reis C A, and Gartner F. (2012). Canine tumors: a spontaneous animal model of human carcinogenesis. *Transl Res* **159**, 165-172.
- Ponce F, Marchal T, Magnol J P, Turinelli V, Ledieu D, Bonnefont C, Pastor M, Delignette M L, and Fournel-Fleury C. (2010). A morphological study of 608 cases of canine malignant lymphoma in France with a focus on comparative similarities between canine and human lymphoma morphology. *Veterinary pathology* **47**, 414-433.
- Rahman M M, Qian Z R, Wang E L, Sultana R, Kudo E, Nakasono M, Hayashi T, Kakiuchi S, and Sano T. (2009). Frequent overexpression of HMGA1 and 2 in gastroenteropancreatic neuroendocrine tumours and its relationship to let-7 downregulation. *British journal of cancer* **100**, 501-510.
- Reeves R, and Beckerbauer L. (2001). HMGI/Y proteins: flexible regulators of transcription and chromatin structure. *Biochimica et biophysica acta* **1519**, 13-29.
- Reinhart B J, Slack F J, Basson M, Pasquinelli a E, Bettinger J C, Rougvi a E, Horvitz H R, and Ruvkun G. (2000). The 21-nucleotide let-7 RNA regulates developmental timing in *Caenorhabditis elegans*. *Nature* **403**, 901-906.
- Richter A, Hauschild G, Murua Escobar H, Nolte I, and Bullerdiek J. (2009). Application of high-mobility-group-A proteins increases the proliferative activity of chondrocytes in vitro. *Tissue engineering* **15**, 473-477.

- Richter A, Lubbing M, Frank H G, Nolte I, Bullerdiek J C, and Von Ahsen I. (2011). High-mobility group protein HMGA2-derived fragments stimulate the proliferation of chondrocytes and adipose tissue-derived stem cells. *European cells & materials* **21**, 355-363.
- Rofina J, Van Andel I, Van Ederen a M, Papaioannou N, Yamaguchi H, and Gruys E. (2003). Canine counterpart of senile dementia of the Alzheimer type: amyloid plaques near capillaries but lack of spatial relationship with activated microglia and macrophages. *Amyloid* **10**, 86-96.
- Rommel B, Rogalla P, Jox A, Kalle C V, Kazmierczak B, Wolf J, and Bullerdiek J. (1997). HMGI-C, a member of the high mobility group family of proteins, is expressed in hematopoietic stem cells and in leukemic cells. *Leukemia & lymphoma* **26**, 603-607.
- Rowell J L, Mccarthy D O, and Alvarez C E. (2011). Dog models of naturally occurring cancer. *Trends in molecular medicine* **17**, 380-388.
- Ru P, Steele R, Newhall P, Phillips N J, Toth K, and Ray R B. (2012). miRNA-29b suppresses prostate cancer metastasis by regulating epithelial-mesenchymal transition signaling. *Molecular cancer therapeutics* **11**, 1166-1173.
- Sampson V B, Rong N H, Han J, Yang Q, Aris V, Soteropoulos P, Petrelli N J, Dunn S P, and Krueger L J. (2007). MicroRNA let-7a down-regulates MYC and reverts MYC-induced growth in Burkitt lymphoma cells. *Cancer research* **67**, 9762-9770.
- Schmidt S, Fracasso G, Colombatti M, and Naim H Y. (2013). Cloning and characterization of canine prostate-specific membrane antigen. *The Prostate* **73**, 642-650.
- Schubert M, Spahn M, Kneitz S, Scholz C J, Joniau S, Stroebel P, Riedmiller H, and Kneitz B. (2013). Distinct microRNA expression profile in prostate cancer patients with early clinical failure and the impact of let-7 as prognostic marker in high-risk prostate cancer. *PloS one* **8**, e65064.
- Schulke N, Varlamova O A, Donovan G P, Ma D, Gardner J P, Morrissey D M, Arrigale R R, Zhan C, Chodera a J, Surowitz K G, Maddon P J, Heston W D, and Olson W C. (2003). The homodimer of prostate-specific membrane antigen is a functional target for cancer therapy. *Proceedings of the National Academy of Sciences of the United States of America* **100**, 12590-12595.
- Shah S N, Cope L, Poh W, Belton A, Roy S, Talbot C C, Jr., Sukumar S, Huso D L, and Resar L M. (2013). HMGA1: a master regulator of tumor progression in triple-negative breast cancer cells. *PloS one* **8**, e63419.
- Shah S N, Kerr C, Cope L, Zambidis E, Liu C, Hillion J, Belton A, Huso D L, and Resar L M. (2012). HMGA1 reprograms somatic cells into pluripotent stem cells by inducing stem cell transcriptional networks. *PloS one* **7**, e48533.
- Shan H, Zhang Y, Lu Y, Zhang Y, Pan Z, Cai B, Wang N, Li X, Feng T, Hong Y, and Yang B. (2009). Downregulation of miR-133 and miR-590 contributes to nicotine-induced atrial remodelling in canines. *Cardiovascular research* **83**, 465-472.
- Shi G, Perle M A, Mittal K, Chen H, Zou X, Narita M, Hernando E, Lee P, and Wei J J. (2009). Let-7 repression leads to HMGA2 overexpression in uterine leiomyosarcoma. *Journal of cellular and molecular medicine* **13**, 3898-3905.

- Shin J H, Pan X, Hakim C H, Yang H T, Yue Y, Zhang K, Terjung R L, and Duan D. (2013). Microdystrophin Ameliorates Muscular Dystrophy in the Canine Model of Duchenne Muscular Dystrophy. *Mol Ther*.
- Shore a N, Herschkowitz J I, and Rosen J M. (2012). Noncoding RNAs involved in mammary gland development and tumorigenesis: there's a long way to go. *Journal of mammary gland biology and neoplasia* **17**, 43-58.
- Snyder R O, and Flotte T R. (2002). Production of clinical-grade recombinant adeno-associated virus vectors. *Current opinion in biotechnology* **13**, 418-423.
- Srivastava A, Lusby E W, and Berns K I. (1983). Nucleotide sequence and organization of the adeno-associated virus 2 genome. *Journal of virology* **45**, 555-564.
- Sterenczak K A, Eckardt A, Kampmann A, Willenbrock S, Eberle N, Langer F, Kleinschmidt S, Hewicker-Trautwein M, Kreipe H, Nolte I, Murua Escobar H, and Gellrich N C. (2014). HMGA1 and HMGA2 expression and comparative analyses of HMGA2, Lin28 and let-7 miRNAs in oral squamous cell carcinoma. *BMC cancer* **14**, 694.
- Sterenczak K A, Joetzke a E, Willenbrock S, Eberle N, Lange S, Junghanss C, Nolte I, Bullerdiek J, Simon D, and Murua Escobar H. (2010). High-mobility group B1 (HMGB1) and receptor for advanced glycation end-products (RAGE) expression in canine lymphoma. *Anticancer research* **30**, 5043-5048.
- Sutter N B, and Ostrander E A. (2004). Dog star rising: the canine genetic system. *Nat Rev Genet* **5**, 900-910.
- Takaha N, Resar L M, Vindivich D, and Coffey D S. (2004). High mobility group protein HMGI(Y) enhances tumor cell growth, invasion, and matrix metalloproteinase-2 expression in prostate cancer cells. *The Prostate* **60**, 160-167.
- Takeuchi I, Takaha N, Nakamura T, Hongo F, Mikami K, Kamoi K, Okihara K, Kawauchi A, and Miki T. (2012). High mobility group protein AT-hook 1 (HMGA1) is associated with the development of androgen independence in prostate cancer cells. *The Prostate* **72**, 1124-1132.
- Tallini G, Vanni R, Manfioletti G, Kazmierczak B, Faa G, Pauwels P, Bullerdiek J, Giancotti V, Van Den Berghe H, and Dal Cin P. (2000). HMGI-C and HMGI(Y) immunoreactivity correlates with cytogenetic abnormalities in lipomas, pulmonary chondroid hamartomas, endometrial polyps, and uterine leiomyomas and is compatible with rearrangement of the HMGI-C and HMGI(Y) genes. *Laboratory investigation; a journal of technical methods and pathology* **80**, 359-369.
- Tang D, Kang R, Zeh H J, 3rd, and Lotze M T. (2010). High-mobility group box 1 and cancer. *Biochimica et biophysica acta* **1799**, 131-140.
- Tay Y, Karreth F A, and Pandolfi P P. (2014). Aberrant ceRNA activity drives lung cancer. *Cell research* **24**, 259-260.
- Teske E, Naan E C, Van Dijk E M, Van Garderen E, and Schalken J A. (2002). Canine prostate carcinoma: epidemiological evidence of an increased risk in castrated dogs. *Molecular and cellular endocrinology* **197**, 251-255.
- Thomson J M, Newman M, Parker J S, Morin-Kensicki E M, Wright T, and Hammond S M. (2006). Extensive post-transcriptional regulation of microRNAs and its implications for cancer. *Genes & development* **20**, 2202-2207.
- Tomari Y, and Zamore P D. (2005). Perspective: machines for RNAi. *Genes & development* **19**, 517-529.

- Ueda T, and Yoshida M. (2010). HMGB proteins and transcriptional regulation. *Biochimica et biophysica acta* **1799**, 114-118.
- Uhl E, Krimer P, Schliekelman P, Tompkins S M, and Suter S. (2011). Identification of altered MicroRNA expression in canine lymphoid cell lines and cases of B- and T-Cell lymphomas. *Genes, chromosomes & cancer* **50**, 950-967.
- Vail D M, and Macewen E G. (2000). Spontaneously occurring tumors of companion animals as models for human cancer. *Cancer investigation* **18**, 781-792.
- Viticchie G, Lena a M, Latina A, Formosa A, Gregersen L H, Lund a H, Bernardini S, Mauriello A, Miano R, Spagnoli L G, Knight R A, Candi E, and Melino G. (2011). MiR-203 controls proliferation, migration and invasive potential of prostate cancer cell lines. *Cell cycle (Georgetown, Tex)* **10**, 1121-1131.
- Von Deetzen M C, Schmeck B, Gruber a D, and Klopffleisch R. (2013). Molecular quantification of canine specific microRNA species. *Research in veterinary science* **95**, 562-568.
- Wagner S, Ngezahayo A, Murua Escobar H, and Nolte I. (2014). Role of miRNA and Its Major Targets in Prostate Cancer. *BioMed research international* **2014**, 376326.
- Wang X, Cao L, Wang Y, Wang X, Liu N, and You Y. (2012). Regulation of let-7 and its target oncogenes (Review). *Oncology letters* **3**, 955-960.
- Watanabe S, Ueda Y, Akaboshi S, Hino Y, Sekita Y, and Nakao M. (2009). HMGA2 maintains oncogenic RAS-induced epithelial-mesenchymal transition in human pancreatic cancer cells. *The American journal of pathology* **174**, 854-868.
- Waters D J, Hayden D W, Bell F W, Klausner J S, Qian J, and Bostwick D G. (1997). Prostatic intraepithelial neoplasia in dogs with spontaneous prostate cancer. *The Prostate* **30**, 92-97.
- Waters D J, Patronek G J, Bostwick D G, and Glickman L T. (1996). Comparing the age at prostate cancer diagnosis in humans and dogs. *Journal of the National Cancer Institute* **88**, 1686-1687.
- Waters D J, Sakr W A, Hayden D W, Lang C M, Mckinney L, Murphy G P, Radinsky R, Ramoner R, Richardson R C, and Tindall D J. (1998). Workgroup 4: spontaneous prostate carcinoma in dogs and nonhuman primates. *The Prostate* **36**, 64-67.
- Winkler S, Murua Escobar H, Eberle N, Reimann-Berg N, Nolte I, and Bullerdiek J. (2005). Establishment of a cell line derived from a canine prostate carcinoma with a highly rearranged karyotype. *The Journal of heredity* **96**, 782-785.
- Winkler S, Murua Escobar H, Meyer B, Simon D, Eberle N, Baumgartner W, Loeschke S, Nolte I, and Bullerdiek J. (2007). HMGA2 expression in a canine model of prostate cancer. *Cancer genetics and cytogenetics* **177**, 98-102.
- Winter J, Jung S, Keller S, Gregory R I, and Diederichs S. (2009). Many roads to maturity: microRNA biogenesis pathways and their regulation. *Nature cell biology* **11**, 228-234.
- Withrow J S, and Vail D M. (2012). *Withrow and MacEwen's Small Animal Clinical Oncology*. Saunders Company, St. Louis Missouri 63146 **Fifth edition**.
- Withrow S J, and Macewen E G. (2001). *Small Animal Clinical Oncology*. (W.B. Saunders Co., Philadelphia (USA)).
- Wood L J, Mukherjee M, Dolde C E, Xu Y, Maher J F, Bunton T E, Williams J B, and Resar L M. (2000). HMG-I/Y, a new c-Myc target gene and potential oncogene. *Molecular and cellular biology* **20**, 5490-5502.

References

- Young a R, and Narita M. (2007). Oncogenic HMGA2: short or small? *Genes & development* **21**, 1005-1009.
- Zhao Y, Samal E, and Srivastava D. (2005). Serum response factor regulates a muscle-specific microRNA that targets Hand2 during cardiogenesis. *Nature* **436**, 214-220.

8. Publications

8.1. All Published manuscripts in reverse chronological order

Characterization of Nanoparticle Mediated Lasertransfection by Femtosecond Laser Pulses for Applications in Molecular Medicine. Schomaker M., Heinemann D., Kalies S., Willenbrock S., Wagner S., Nolte I., Ripken T., Murua Escobar H., Meyer H., Heisterkamp A.. J Nanobiotechnology. 2015; 13: 10. Published online 2015 February 3. doi: 10.1186/s12951-014-0057-1.

Verification of a canine PSMA (FolH1) antibody. Wagner S., Maibaum D., Pich A., Nolte I., Murua Escobar H.. Anticancer Res. 2015 Jan;35(1):145-8.

Role of miRNA let-7 and its major targets in prostate cancer. Wagner S., Ngezahayo A., Murua Escobar H., Nolte I.. Biomed Res Int. 2014;2014:376326. Epub 2014 Sep 3.

Generation and Characterisation of a Canine EGFP-HMGA2 Prostate Cancer In Vitro Model. Willenbrock S., Wagner S., Reimann-Berg N., Moulay M., Hewicker-Trautwein M., Nolte I., Murua Escobar H.. PLoS One. 2014 Jun 10;9(6):e98788. doi: 10.1371/journal.pone.0098788. eCollection 2014.

Evaluation of the reactivity of commercially available monoclonal antibodies with equine cytokines. Schnabel C. L. , Wagner S., Wagner B., Durán M. C., Babasyan S., Nolte I., Pfarrer C., Feige K., Murua Escobar H., Cavalleri J. M.. Vet Immunol Immunopathol. 2013 Nov 15;156(1-2):1-19. doi: 10.1016/j.vetimm.2013.09.012. Epub 2013 Sep 25.

Comparison of non-coding RNAs in human and canine cancer. Wagner S., Willenbrock S., Nolte I., Murua Escobar H.. Front Genet. 2013; 4: 46. Prepublished online 2012 November 4. Published online 2013 April 8. doi: 10.3389/fgene.2013.00046

Authentication of primordial characteristics of the CLBL-1 cell line prove the integrity of a canine B-cell lymphoma in a murine in vivo model. Rütgen B. C., Willenbrock S., Reimann-Berg N., Walter I., Fuchs-Baumgartinger A., Wagner S., Kovacic B., Essler S. E., Schwendenwein I., Nolte I., Saalmüller A., Murua Escobar H.. PLoS One. 2012;7(6):e40078. Epub 2012 Jun 28.

Effects of High-Mobility Group A Protein Application on Canine Adipose-Derived Mesenchymal Stem Cells In Vitro. Ismail A. A., Wagner S., Murua Escobar H., Willenbrock S., Sterenczak K. A., Samy M.T., Abd El-Aal A. M., Nolte I., Wefstaedt P.. Vet Med Int. 2012;2012:752083. doi: 10.1155/2012/752083. Epub 2012 Feb 8.

Expression of the high mobility group A1 (HMGA1) and A2 (HMGA2) genes in canine lymphoma: analysis of 23 cases and comparison to control cases. Joetzke A. E., Sterenczak K. A., Eberle N., Wagner S., Soller J. T., Nolte I., Bullerdiek J., Murua Escobar H., Simon D.. Vet Comp Oncol. 2010 Jun;8(2):87-95. doi: 10.1111/j.1476-5829.2010.00207.x.

Co-transfection of plasmid DNA and laser-generated gold nanoparticles does not disturb the bioactivity of GFP-HMGB1 fusion protein. Petersen S., Soller J. T., Wagner S., Richter A., Bullerdiek J., Nolte I., Barcikowski S., Murua Escobar H.. J Nanobiotechnology. 2009 Oct 24;7:6. doi: 10.1186/1477-3155-7-6.

Genomic characterisation, chromosomal assignment and in vivo localisation of the canine high mobility group A1 (HMGA1) gene. Beuing C., Soller J. T., Muth M., Wagner S., Dolf G., Schelling C., Richter A., Willenbrock S., Reimann-Berg N., Winkler S., Nolte I., Bullerdiek J., Murua Escobar H.. BMC Genet. 2008 Jul 23;9:49. doi: 10.1186/1471-2156-9-49.

8.2. Manuscripts in preparation for submission

Improved rAAV genome isolation for quantification by absolute real-time PCR. Wagner S., Ngezahayo A., Murua Escobar H., Nolte I..

Let-7 and associated genes in canine prostate cancer. Wagner S., Eberle N., Ngezahayo A., Murua Escobar H., Nolte I..

8.3. Oral presentations

Veterinary Cancer Society Annual Conference. 17.10. - 19.10.2013, Minneapolis, Minnesota, USA. Wagner S., Murua Escobar H, Nolte I. Comparative gene expression analyses in canine prostate cancer. In: Proceedings of the Veterinary Cancer Society 2013, p. 83

Veterinary Cancer Society Annual Conference. 18.10. - 21.10.2012, Las Vegas, Nevada, USA. Schnabel C., Wagner S., Duran C., Nolte I., Wagner B., Murua Escobar H., Feige K., Mueller J.. Evaluation of equine cytokine specific antibodies. In: Proceedings of the Veterinary Cancer Society 2012, p. 61.

18. Jahrestagung der FG „Innere Medizin und klinische Labordiagnostik“ der DVG (InnLab). 06. - 07.02.2010, Hannover, Germany. Wagner S., Soller J. T., Sterenczak K., Willenbrock S., Nolte I., Bullerdiek J., Murua Escobar H.. A33, Construction of let-7 miRNA expression-vectors for directed HMGA2 knock down. In: Tierärztliche Praxis

8.4. Poster presentations

22. Jahrestagung der FG „Innere Medizin und klinische Labordiagnostik“ der DVG (InnLab). 31.01.2013 - 02.02.2014, Gießen, Germany. Wagner S., Murua Escobar H., Nolte I.. P07, Vergleichende Genexpressionsanalysen an kaninen Prostataprobe. In: Tierärztliche Praxis, p. 15.

European Society of Veterinary Oncology (ESVONC) Annual Congress 2011. 23.03. - 27.03.2011, Glasgow, Scotland, UK. Wagner S., Willenbrock S., Sterenczak K., Bullerdiek J., Nolte I., Murua Escobar H.. Construction of let-7a expressing vectors for down regulation of the tumour marker HMGA2. In: Proceedings of the European Society of Veterinary Oncology 2011.

9. Schulischer / Wissenschaftlicher Werdegang

- 12/2014 – heute Postdoktorand an der Stiftung Tierärztliche Hochschule Hannover, Klinik für Kleintiere, Hannover
- 12/2014 Promotion an der Gottfried Wilhelm Leibniz Universität Hannover (Note: sehr gut)
- 04/2009 – 12/2014 Wissenschaftlicher Mitarbeiter an der Stiftung Tierärztliche Hochschule Hannover, Klinik für Kleintiere, Hannover
- 03/2007 – 03/2009 Wissenschaftlicher Mitarbeiter am Zentrum für Humangenetik, Bremen

Studium:

- 03/2007 – 06/2008 Durchführung der Diplomarbeit am Zentrum für Humangenetik, Bremen (Etablierung einer molekulargenetischen Methode zur quantitativen Analyse der caninen HMGA1 (HMGA1a/b) Expression und vergleichende HMGA1 Expressions-Analysen zwischen Mensch und Hund)
- 10/2002 – 06/2008 Studium der Biologie im Diplomstudiengang an der Carl von Ossietzky Universität, Oldenburg (Note: sehr gut)
- 10/2004 – 03/2007 Parallelstudium der Chemie im Diplomstudiengang an der Carl von Ossietzky Universität Oldenburg

Schulbildung:

- 08/1999 – 06/2002 Fachgymnasium Wirtschaft Friesoythe
- 09/1995 – 06/1999 Albertus-Magnus-Gymnasium Friesoythe

10. Erklärung zur Dissertation

Hiermit erkläre ich, dass ich die Dissertation mit dem Titel

“Analyses of miRNA let-7 and its targets in canine neoplasias as model for human counterparts”

selbstständig verfasst und die benutzten Hilfsmittel und Quellen sowie gegebenenfalls die zu Hilfeleistungen herangezogenen Institutionen vollständig angegeben habe.

Die Dissertation wurde nicht schon als Masterarbeit, Diplomarbeit oder andere Prüfungsarbeit verwendet.

Ich versichere, dass ich die vorstehenden Angaben nach bestem Wissen vollständig und der Wahrheit entsprechend gemacht habe.

Siegfried Wagner

11. Danksagung

Herrn Privat Dozent Dr. Hugo Murua Escobar danke ich für die hervorragende, durchgehende Betreuung und die Unterstützung während meiner gesamten Promotionsphase. „Fokusieere!“

Herrn Prof. Dr. Ingo Nolte danke ich für die mir an der Klinik für Kleintiere (Tierärztliche Hochschule Hannover) gebotenen Möglichkeiten sowie für das Vertrauen, dass er in mich gesetzt.

Meinem Doktorvater Herrn Prof. Dr. Anaclet Ngezahayo danke ich dafür, dass ich meine Doktorarbeit als sein Doktorand beenden durfte. Insbesondere möchte ich mich bei Ihm dafür bedanken, dass er immer ein offenes Ohr für meine Belange hatte und mir immer mit Rat zur Seite gestanden hat.

Herrn Prof. Dr. Thomas Scheper danke ich für die kurzfristige Übernahme des Prüfungsvorsitzes für meine Disputation.

Bei der Hannoverschen Gesellschaft zur Förderung der Kleintiermedizin e.V. (HGFK) möchte ich mich für die finanzielle Unterstützung, die die Durchführung meiner Doktorarbeit ermöglicht hat, bedanken.

Meiner langjährigen Kollegin Frau Dr. Saskia Willenbrock danke ich für die zahlreichen, fachlichen Diskussionen, das Korrekturlesen und die Unterstützung während meiner Zeit als Doktorand.

Herr Prof. Dr. Ingo Nolte sowie Frau Dr. Martina Nolte danke ich für das Korrekturlesen meiner Dissertationsschrift und die Verbesserungsvorschläge.

Weiter möchte ich Frau Dr. Saskia Willenbrock, meinen ehemaligen Kollegen Frau Dr. Katharina Sterenczak und Herrn Dr. Jan Soller für die Einarbeitung im Labor während meiner Diplomarbeit und in den Anfängen meiner Doktorarbeit danken.

Danksagung

Den „alten Hunden“ danke ich für die vielen tollen gemeinsamen Stunden im Büro aber auch beim Feiern.

Frau Gabriele Bante danke ich vielmals für die Hilfe und Unterstützung im verwaltungstechnischen und organisatorischen Bereich und für ihre ansteckende, stets gute Laune.

Meiner Kollegin Frau Susanne Hammer danke ich für das Korrekturlesen meiner Manuskripte und die fachliche Hilfe. Zusätzlich möchte ich mich auch dafür bedanken, dass sie all die vielen Aufgaben, die im Laboralltag anfallen aber die eigene Arbeit nur peripher tangieren, für mich mit übernommen hat.

Weiter danke ich meiner Kollegin Frau Heike Thiemeyer, denn durch Ihre Aufmerksamkeit und fachliche Kompetenz als Tierärztin war es möglich die Ergebnisse des von uns durchgeführten Prostatascreenings besser interpretieren und Trends erkennen zu können.

Den ehemaligen Masterstudentinnen, Susanne Nagel, Denise Maibaum, Birthe Gerike, Feyza Selcuk, Daira Jilani und Laura Schmidt danke ich für die Unterstützung im Labor.

Bei unseren Kollegen Dr. Markus Schomaker und Dr. Dag Heinemann vom Laser Zentrum Hannover und bei Dr. Nicola Reimann-Berg vom Zentrum für Humangenetik Bremen bedanke ich mich für die tolle Zusammenarbeit.

Nicola Du hattest recht es kristallisiert sich alles am Ende heraus!

Den VMTA Praktikantinnen und Praktikanten Fräulein Annika Schnoor, Herrn Steffen Schmalz, Frau Sari Eberle sowie den Technischen Assistenten, Frau Alexandra Anders, Regina Carlson, Herrn Dirk Menzel sowie Herrn Jan Schwarze danke ich für die Unterstützung im Labor.

Herrn Diplom Biologen Andreas Köppen danke ich vielmals für die Unterstützung im EDV Bereich.

Danksagung

Einen ganz herzlichen Dank möchte ich meiner Familie aussprechen. Meiner Frau, die aufgrund meiner langjährigen Promotion mit auf vieles verzichten musste und mich immer aufgebaut und unterstützt hat. „YEAH“.

Einen besonderen Dank möchte ich meinen Eltern aussprechen, die mir das Studium der Biologie ermöglicht haben und mich stets motiviert und unterstützt haben. Die, wie meine Frau meine oft schlechte Laune und teils harschen Ton ertragen haben.

Meinen Schwiegereltern danke ich ebenfalls für die langjährige Hilfe und Unterstützung.

Bei meinem Opa Viktor bedanke ich mich für die Unterstützung und die Gespräche während des Teetrinkens. Meiner Oma Lidia danke ich, dass Sie für uns Kinder immer Zeit hatte und mir, zusammen mit Opa, den ersten Satz auf Deutsch beigebracht hat. Ich kann ihn immer noch 😊.

Meinen Schwestern und Schwagern danke ich ebenfalls für den langjährigen Beistand.

Bei meinem besten Freund Richard bedanke ich mich für die vielen Jahre in denen wir uns zusammen durch den Schulstoff und das Studium gekämpft haben und dabei einiges erlebt haben.

Zum Schluss möchte ich mich noch einmal bei der gesamten Arbeitsgruppe, meinen Freunden, meiner Familie und all den Menschen die mir in irgendeiner Weise geholfen haben, bedanken. Denn abgesehen von der eigenen Motivation und Anstrengung kommt man nur wirklich voran wenn man mit anderen zusammenarbeiten und sich austauschen kann.